Title
LOCAL CORRELATION MODELS AND APPLICATIONS IN ELECTRONIC STRUCTURE THEORY

Author
Azar, Richard Julian

Publication Date
2015

Peer reviewed|Thesis/dissertation

LOCAL CORRELATION MODELS AND APPLICATIONS IN ELECTRONIC STRUCTURE THEORY

by

RICHARD J AZAR

A dissertation submitted in partial satisfaction of the
requirements for the degree of
Doctor of Philosophy

in

Chemistry

in the

Graduate Division

of the

University of California, Berkeley

Committee in charge:

Professor Martin Head-Gordon, Chair
Professor Phillip Geissler
Professor Alexis T. Bell

Spring 2015

LOCAL CORRELATION MODELS AND APPLICATIONS IN ELECTRONIC STRUCTURE THEORY

Abstract

LOCAL CORRELATION MODELS AND APPLICATIONS IN ELECTRONIC STRUCTURE THEORY

by

RICHARD J AZAR

Doctor of Philosophy in Chemistry

University of California, Berkeley

Professor Martin Head-Gordon, Chair

Dynamic inter-electronic correlations are exquisitely local effects responsible for many interesting phenomena in molecular physics, including much or all of mutual attractions between molecules. The main thrust of this work is the development of high-accuracy, low-scaling models of electron correlation exploiting locality in the context of non-covalent interactions.

Contents

List of Figures

List of Tables

Acknowledgments

This work would not have been possible without the help of Martin Head-Gordon, Leslie Silvers, John Parkhill, Westin Kurlancheek, Eric Sundstrom, Paul Horn, Evgeny Epifanovsky, and Narbe Mardirossian.
Thank you.

Chapter 1

Introduction

1.1 Background

By the middle of the 20th century, it had become clear that classical mechanics represented the macroscopic limit of a new "quantum" theory[1–9] which could treat matter at all scales seamlessly, and, ignoring relativistic effects, exactly. All advances in computation since notwithstanding, however, this exact treatment remains possible for only the smallest applications. Thus, the bread and butter of modern quantum chemistry is development and application of *tractable*, *approximate* descriptions of the quantum mechanical behavior of the electrons in atoms and molecules. This thesis is decidedly in that paradigm.

Mathematically, a quantum state is completely specifiable in an inner-product (Hilbert) space as a "ket" vector and its complex conjugate "bra" vector, collectively, the "wavefunction". A measurement corresponds to the action of a linear operator "collapsing" this state to an eigenvector with a probability proportional to the square of its overlap with the state. In the province of molecular quantum mechanics, the many-body ket describing the motions of electrons and nuclei in a molecular system $|\Psi\rangle = |\Psi(\mathbf{r}, \mathbf{R})\rangle$, and eigenvalue E of the Hamiltonian operator, $\hat{H}(\mathbf{r}, \mathbf{R})$, are obtained by solving the time-independent molecular Schrödinger equation,

$$\hat{H}|\Psi\rangle = E|\Psi\rangle. \tag{1.1}$$

We begin with the assumption that the nuclei are infinitely slow relative to the electrons[10]. This effectively uncouples the nuclear and electronic degrees of freedom in eq. 1.1, allowing a solution, E_{el}, to the electronic Schrödinger equation *parametrized* by static nuclei which contribute to the molecular energy via their mutual repulsions. The problem for the electrons is

$$\hat{H}_{el}|\Phi(\mathbf{r}; \mathbf{R})\rangle = E_{el}|\Phi(\mathbf{r}; \mathbf{R})\rangle, \tag{1.2}$$

and we concern ourselves with its solution for the remainder of this work. The electronic Hamiltonian in atomic units is,

$$\hat{H}_{el} = -\sum_{i}^{n} \frac{1}{2}\nabla_i^2 - \sum_{i,A}^{n,N} \frac{Z_A}{|r_A - R_i|} + \sum_{i,j\neq i}^{n,n'} \frac{1}{|r_i - r_j|}. \tag{1.3}$$

The first term describes the kinetic energy, the second term describes attractions to the nuclei, and the third term describes mutual repulsions.

As a first guess at $|\Phi(\mathbf{r})\rangle$, we might imagine populating a product of one-electron (spin-orbital) states $\{|\phi_p(\mathbf{r},\sigma)\rangle\}$, $|\Phi(\mathbf{r})\rangle = \Pi_p^n|\phi_p\rangle$, where, in the absence of spin-orbital coupling, $|\phi_p\rangle$ is a separable product of a spin eigenfunction and a normalizable spatial function, $|\phi_p(\mathbf{r},\sigma)\rangle = |\psi_p(r)\rangle|\chi_p(\sigma)\rangle$, and $\{|\phi_p\rangle\}$ are orthogonal. Because this "Hartree-product"[11, 12] ansatz does not obey Fermi statistics[9, 13], we take an antisymmetrized product instead, equivalently a "Slater" determinant [9, 14],

$$|\Phi\rangle = (n!)^{-\frac{1}{2}}\det\Big\{|\phi_p\rangle\Big\}. \tag{1.4}$$

By the variational theorem, the "best" one-electron states in eq. 1.4 are those that minimize the expectation value, $E = \langle\Phi|\hat{H}|\Phi\rangle$. The Hartree-Fock (HF)[15, 16] eigenvalue equations for these $\{|\phi_p\rangle\}$ come as a consequence of applying Lagrange's method to this end, constraining the spin-orbitals to be orthogonal,

$$\hat{f}|\phi_p\rangle = \epsilon_p|\phi_p\rangle. \tag{1.5}$$

In the spin-orbital representation using Einstein summation, $f_q^p = h_q^p + v_{qi}^{pi}$ where h_q^p includes the one-electron components of eq. 1.3, and v describes a kind of averaged or "mean-field" exchange-repulsion potential experienced by an electron in $|\phi_p\rangle$ due to an electron in $|\phi_i\rangle$, $v_{pi}^{pi} = \langle\phi_p\phi_i|r_{pi}^{-1}|\phi_p\phi_i\rangle - \langle\phi_p\phi_i|r_{pi}^{-1}|\phi_i\phi_p\rangle$. We'll see shortly that this one-body potential only approximately accounts for the explicit two-body repulsions in $\hat{H}$. The HF equations are typically expanded in a basis of atom-centered Gaussian functions ("atomic orbitals"), or plane-wave functions, $\{|\mu\rangle\}$, $|\phi_p\rangle = C_p^\mu|\mu\rangle$, and the molecular orbital coefficients $\{C_p^\mu\}$ are determined by solving the generalized eigenvalue equation,

$$\mathbf{f}_{\mu\nu}\mathbf{C}_{\mathbf{p}}^{\nu} = \mathbf{S}_{\mu\nu}\mathbf{C}_{\mathbf{p}}^{\nu}\epsilon_p. \tag{1.6}$$

$\mathbf{f}_{\mu\nu}$ is the Fock operator in the AO basis, $S_{\mu\nu}$ is the overlap metric, and ϵ_p is the orbital eigenvalue. The n eigenvectors corresponding to the lowest eigenvalues, typically denoted by the indexes $\{ij...\}$, are the states occupied in the HF determinant. The rest are unoccupied or "virtual" states labeled $\{ab...\}$. Because the equations are nonlinear in the potential, e.g., $\mathbf{f} = \mathbf{f}(\mathbf{C})$, the HF equations must be solved iteratively until self-consistency is reached. In this way, we obtain the best single-determinant (HF) wavefunction and variational energy,

$f_i^i + 0.5v_{ij}^{ij}$.

In the language of second quantization[17, 18], which we use below for its convenience, the HF wavefunction (or any single reference determinant) is equivalently represented by the action of a string of "creation" operators $\{a_p^\dagger\}$ on a fictitious "vacuum" state denoted "$|\rangle$",

$$|\Phi_0\rangle = \Pi_p a_p^\dagger|\rangle, \tag{1.7}$$

Correspondingly, the action of "annihilation" operators $\{a_p\}$ is to destroy electrons in spin-orbitals. Like the wavefunction, they are not themselves observable quantities, but represent a useful short-hand for computing complicated matrix elements. Using antisymmetry and anti-commutation relations, non-zero matrix elements of second-quantized operators are determined by bringing strings or products[19] of strings to "normal-ordered" form, that is, permutation until all creation operators sit to left of all annihilation operators. This is accomplished by successive contractions (denoted by "$\bullet$") of operator pairs,

$$a_p^\dagger \bullet a_q|\rangle = a_p^\dagger a_q - \{a_p^\dagger a_q\}, \tag{1.8}$$

where "{}" is a directive to normal-order, and the labels p and q denote any spin-orbital. For added convenience, we'll assume a Fermi vacuum, e.g., the occupied one-electron states labeled $\{ij...\}$ in the reference determinant are "hole" states and the unoccupied levels $\{ab...\}$ are "particle" states, and application of their second-quantized operators implies a reference determinant. The operators a_i and $a_a^\dagger$ create holes and particles, while $a_i^\dagger$ and a_a destroy holes and particles. Using these definitions, the contraction rules are,

$$\begin{aligned} a_i^\dagger \bullet a_j &= a_i^\dagger a_j - \{a_i^\dagger a_j\} = a_i^\dagger a_j + a_j^\dagger a_i = \delta_{ij}, \text{ and} \\ a_a \bullet a_b^\dagger &= a_a a_b^\dagger - \{a_a a_b^\dagger\} = a_a a_b^\dagger + a_b^\dagger a_a = \delta_{ab}, \end{aligned} \tag{1.9}$$

and imply no non-zero contractions between occupied and virtual subspaces.

The second-quantized form of the electronic Hamiltonian of eq. 1.3 in terms of one- and two-electron operators is

$$\hat{H}_{\text{elec}} = h_q^p a_p^\dagger a_q + g_{rs}^{pq} a_p^\dagger a_q^\dagger a_s a_r, \tag{1.10}$$

where repeated indices imply summation, and general labels run over occupied and virtual subspaces. In normal-ordered form making use of eq. 1.9, the Hamiltonian is

$$\begin{aligned} \hat{H}_{\text{elec}} &= [h_q^p + g_{qi}^{pi}]\{a_p^\dagger a_q\} + 0.25 g_{rs}^{pq}\{a_p^\dagger a_q^\dagger a_s a_r\} + f_i^i + 0.5 v_{ij}^{ij} \\ &= H_n + \langle\Phi_0|\hat{H}|\Phi_0\rangle, \end{aligned} \tag{1.11}$$

where the first two terms are the normal-ordered one- (Fock) and two-body operators (collected together as "H_n" in in the second line), and the sum of the final two terms is the

Fermi vacuum expectation value of the Hamiltonian, or in the case of a HF determinant, the HF energy. Already, we see HF theory is inexact owing simply to the fact that it doesn't depend on the full Hamiltonian. It will become clear in the following section that this is due to a single-determinant ansatz.

1.2 The correlation problem

A HF solution is only exact in the one-electron case where the approximate two-body potential vanishes. This is because interacting charge distributions are effectively uncoupled in a mean-field description, e.g., too big for nearby and too small for faraway electrons, and a single-determinant wavefunction cannot describe these *instantaneous* fluctuations. The difference between the HF and Schrödinger energies is called the "correlation" energy, and is much smaller than the total energy. Owing to the fact that interesting chemistry occurs on the same scale, it's no surprise that a satisfactory, manageable description of correlations remains one of the main goals of modern electronic structure. In what follows, we review strategies designed to recover it.

Configuration interaction

One solution is to build correlation into the trial wavefunction from the outset, e.g., adding in configurations which couple electrons across the correlation (normal-ordered) component of Hamiltonian eq. 1.11 *explicitly*. In the exact full configuration interaction (FCI) limit[20], one takes a trial wavefunction of a linear combination of all possible hole-particle substitutions from the HF reference determinant,

$$|\Psi\rangle = \hat{R}|\rangle = \{1_0 + \hat{r}_s + \hat{r}_d + ... + \hat{r}_n\}|\rangle, \tag{1.12}$$

where $\hat{r}_p = (\frac{1}{p!})^2 r^{ii'...i^p}_{aa'...a^p}\{a^\dagger_{a^p} a^\dagger_{a'}...a^\dagger_a a_{i^p}...a_{i'}a_i\}$. Projecting the Schrödinger equation of this trial function into the full n-electron Hilbert space of "excited" configurations $\{\langle\mathbf{h}|\}$, one obtains the coupled equations for the exact correlation energy and wavefunction,

$$\begin{aligned} \langle|\mathbf{H_{hh'}r_{h'}}|\rangle &= E, \\ \langle\mathbf{h}|\mathbf{H_{hh'}r_{h'}}|\rangle &= E\mathbf{r_h}, \end{aligned} \tag{1.13}$$

typically solved by projection or reformulated as a diagonalization. Because the size of $\mathbf{H_{hh'}}$ grows factorially with n, FCI becomes prohibitively expensive very early on. What's more, truncations to $\hat{R}$ conferring polynomial complexity in 1.13, though they retain variationality, lose the property of "size-consistency". That is, the total correlation energy for a truncated

CI expansion scales incorrectly with n. One has recourse to a host of approximate methods improving on the mean-field description. Of "single-reference" methods, e.g., those beginning from a single determinant, many-body perturbation theory and coupled-cluster theory have enjoyed the most success. These are discussed in detail below.

Approximate correlation methods

In the many-body generalization to Rayleigh-Schrödinger perturbation theory[5], FCI is approximated by expanding the Schrödinger equation in a power series specifying a "zeroth-order" Hamiltonian and its eigenfunction, and treating higher-order contributions as small corrections. Splitting $\mathbf{H} = \mathbf{H^{(0)}} + \mathbf{H^{(1)}}$, $\mathbf{r} = \mathbf{r^{(0)}} + \mathbf{r^{(1)}} + \mathbf{r^{(2)}} + ...$, $E = E^{(0)} + E^{(1)} + E^{(2)} + ...$, and separating by order, one obtains

$$\begin{aligned} \mathbf{H^{(0)}_{hh'} r^{(0)}_{h'}}|\rangle &= E^{(0)}|\rangle, \\ \mathbf{H^{(0)}_{hh'} r^{(1)}_{h'}} + \mathbf{H^{(1)}_{hh'} r^{(0)}_{h'}}|\rangle &= \{E^{(0)}\mathbf{1_{h'} r^{(1)}_{h'}} + E^{(1)}\mathbf{1_{h'} r^{(0)}_{h'}}\}|\rangle, \\ \mathbf{H^{(0)}_{hh'} r^{(2)}_{h'}} + \mathbf{H^{(1)}_{hh'} r^{(1)}_{h'}}|\rangle &= \{E^{(0)}\mathbf{1_{h'} r^{(2)}_{h'}} + E^{(1)}\mathbf{1_{h'} r^{(1)}_{h'}} + E^{(2)}\mathbf{1_{h'} r^{(0)}_{h'}}\}|\rangle \\ &... \end{aligned} \tag{1.14}$$

In Møller-Plesset (MP) theory[21], $\mathbf{H^{(0)}_{hh'}}$ is taken as the one-body Hamiltonian and $\mathbf{r^{(0)}_{h'}}|\rangle$ is the reference determinant, viz., $\mathbf{r^{(0)}_{h'}} = 1$. Left projecting eq. 1.14 by $\langle|$ and making use of these definitions gives $\langle|\mathbf{H^{(0)}_{hh'} r^{(0)}_{h'}}|\rangle = \langle|E^{(0)}\mathbf{r^{(0)}_{h'}}|\rangle = E_{\mathrm{HF}}$ at zeroth-order, and leading corrections

$$\begin{aligned} \langle|\mathbf{H^{(1)}_{hh'} r^{(0)}_{h'}}|\rangle &= \langle|E^{(1)}\mathbf{r^{(0)}_{h'}}|\rangle = 0, \text{ and} \\ \langle|\mathbf{H^{(1)}_{hh'} r^{(1)}_{h'}}|\rangle &= \langle|\{E^{(2)}\mathbf{r^{(0)}_{h'}}\}|\rangle. \end{aligned} \tag{1.15}$$

$E^{(1)}$ vanishes because there are no non-zero contractions. For this reason, HF theory is said to be "complete" to first-order in perturbation theory. Projection by $\{\langle\mathbf{h}|\}$ gives equations for the first-order wavefunction,

$$\langle\mathbf{h}|(E^{(0)} - \mathbf{H^{(0)}_{hh'}})\mathbf{r^{(1)}_{h'}}|\rangle = \langle\mathbf{h}|\mathbf{H^{(1)}_{hh'} r^{(0)}_{h'}}|\rangle, \tag{1.16}$$

in spin-orbital notation,

$$\begin{aligned} D^{(0)}_{ia} r^{(1)}_{ia} &= f^{(1)}_{ia}, \\ D^{(0)}_{ijab} r^{(1)}_{ijab} &= v^{(1)}_{ijab}. \end{aligned} \tag{1.17}$$

For a HF reference, one-body effects are already optimized ($\mathbf{f_{ia}} = \mathbf{0}$ by the Lagrangian), causing single excitations to vanish at first-order. Using these expressions in eq. 1.15,

we obtain the second-order MP correction (MP2) to HF describing simultaneous two-body excitations ($i \rightarrow a$) and ($j \rightarrow b$) out of the reference,

$$E^{(2)} = 0.25 v^{(1)}_{ijab} r^{ijab(1)}. \tag{1.18}$$

Though the MP2 energy is not variational, it is size-consistent and a sufficient PT truncation when the zeroth-order starting point is "well-behaved", e.g., when the coefficient of the reference determinant in the true wavefunction is near unity. This is typically thought of as the "weak" correlation regime. For cases where two or more configurations approach unity in the CI expansion, e.g., for a singlet H_2 molecule dissociating to two H atoms, the σ and σ^* orbitals approach degeneracy causing the MP2 amplitudes to diverge, where for FCI, the variational $\{\mathbf{r_{ijab}}\}$ vector included the degenerate configuration at the outset. Thus, to account for this "strong" correlation properly, the wavefunction must have the flexibility to treat potentially degenerate configurations on an equal footing. To this end, many "multi-reference" approaches, all beyond the scope of this work, have been developed. Their accuracy notwithstanding, a criticism commonly leveled against them is that a user-side specification of even basic variables, in general, precludes a "black-box" prescription.

The choice of an exponential ansatz, $|\Psi\rangle = e^{\hat{T}}|\rangle = (1+\hat{T}+\frac{1}{2!}\hat{T}^2+\frac{1}{3!}\hat{T}^3+...)|\rangle$, where $\hat{T}$ has the same form as the linear $\hat{R}$ defined in eq. 1.12, in principle includes all excitations from a single reference, but in contrast to FCI, guarantees an extensive correlation energy because of incremental contributions from "disconnected" excitations. This defines the enormously successful coupled-cluster (CC) ansatz[22–25]. A similarity-transformation of the Hamiltonian, $\hat{H} \rightarrow \bar{H} \equiv e^{-\hat{T}}\hat{H}e^{\hat{T}}$, preserves the FCI spectrum, implying a FCI-equivalent energy when the rank of $\hat{T}$ is equal to n, though the non-Hermitian problem is non-variational, viz., $e^{-T} \neq e^{T^\dagger}$. Projecting the transformed eigenvalue equation by $\langle|$ and $\{\langle\mathbf{h}|\}$ gives the CC energy and amplitude equations,

$$\begin{aligned} \langle|\bar{H}_{00}|\rangle &= E = f_{ia}t^{ia} + 0.25 v_{ijab}t^{ijab} + 0.5 v_{ijab}t^{ia}t^{jb}, \\ \langle\mathbf{h}|\bar{\mathbf{H}}_{\mathbf{h0}}|\rangle &= 0 \end{aligned} \tag{1.19}$$

for arbitrary $\hat{T}$. All orders of MP theory are exactly recoverable by a perturbative expansion of eq. 1.19 treating the fluctuation potential as first-order. $\hat{T}$ is typically truncated at double excitations, defining the $O(N^6)$-complexity "CCSD" model, exact for two electrons. Connected triples and higher are indispensable when CCSD is inadequate, e.g., for double-bond dissociation where $\hat{T}_4$ dominates the wavefunction, but steep polynomial scaling of the amplitude equations in the rank of the cluster operator makes high-rank CC prohibitive for all but the smallest applications. Sophisticated active-space coupled-cluster variants retain a small subset of higher-order amplitudes describing these static correlations, and owing to the locality of a pair reference, maintaining modest scaling at the same time. The perfect quadruples model[26], for instance, includes the $t^{i^\star\bar{i}^\star j^\star\bar{j}^\star}_{i\bar{i}j\bar{j}}$ component of $\hat{T}_4$ and can correctly

dissociate two bonds. When a single-determinant reference is adequate, dynamic correlations on top of CCSD are adequately treated by perturbation theory. Such approximations as CCSD(T)[27] and CCSD(2)[28] are derivable by a Löwdin-type[29] perturbative partitioning of the similarity-transformed eigenvalue problem whereby triple and higher CC moments enter as second-order corrections to a zeroth-order CCSD energy. Their accuracy does come at the cost of non-iterative $\mathrm{O}(N^7)$ complexity, though certain approximations, some of which are proposed in this work, have allowed for considerable scalability.

Higher roots of the FCI Hamiltonian matrix describing excited states on top of a coupled cluster solution can be approximated in the CC framework by projecting the linear equation

$$[\bar{\mathbf{H}}_{\mathbf{pp'}}, \mathbf{r}^{\mathbf{k}}_{\mathbf{p'}}]|\rangle = \omega_{k0}\mathbf{r}^{\mathbf{k}}_{\mathbf{p}}|\rangle \tag{1.20}$$

into the configuration space where the cluster problem was solved (whereby the ground-state eigenvector $\mathbf{r_0} = \{1_0, \mathbf{0_s}, \mathbf{0_d}\}$ returns the CC solution and $\mathbf{r_k} = \{0_0, \mathbf{r^k_s}, \mathbf{r^k_d}\}$ by construction). This is equivalent to diagonalizing $\bar{\mathbf{H}}$ in the space of singles and doubles. These equation-of-motion (EOM) methods[30] furnish accurate solutions for k dominated by single excitations, though non-Hermiticity of the Hamiltonian potentially complicates the implementation and requires computation of a left-hand problem for expectation values other than the energy. Approximations to eq. 1.20 furnish many named excited-state theories, a testament to the versatility of the CC framework. Retaining only the first term in the Hausdorff expansion of $\bar{H}$ and projecting in the space of singles, $\mathbf{r_k} = \{0_0, \mathbf{r^k_s}\}$, one obtains CIS, for instance; adding in the linear term and treating doubles perturbatively, one obtains CIS(D)[31] on top of an MP2-quality ground-state. Diagonalization after adding in singles amplitudes garners the "CC2"[32] approximation to CCSD.

Density-functional theory

A parallel development alongside wavefunction-based approaches that deserves mention is density-functional theory[33, 34] (DFT). It can afford chemical accuracy within an independent-particle (single Slater determinant) model solvable with low-dimensional linear algebra, though at the cost of systematic improveability and introduction of empirical parametrization. For its cubic scaling and basis set convergence properties, it is the *de facto* quantum mechanical framework for large-scale applications, and no doubt the most the popular.

DFT has its theoretical foundations in the Hohenberg-Kohn[35] theorems, proving the exact three-space electronic density maps *one to one* to an external potential, v_{ext}, and furthermore, the density minimizing the energy functional $E[\rho(\mathbf{r})] = \langle\Psi[\rho(\mathbf{r})]|\hat{H}[v_{ext}(\rho(\mathbf{r}))]\Psi[\rho(\mathbf{r})]\rangle$ is equivalently the exact ground-state density. In the Kohn-Sham[36] formalism, this minimization is recast as an eigenvalue problem of determining the eigenstates of a reference system of non-interacting particles, each moving in an effective (one-body) potential which maps uniquely to the density of the interacting system. The equations for these states

are isomorphic to the HF equations eq. 1.5, except the exchange kernel is replaced by an exchange-correlation (XC) functional, making DFT exact in principle. In practice, this is not the case, because the XC potential cannot be represented analytically but for toy systems, and thus, the parametrization of empirical functional forms is the main thrust of modern density functional theory. The simplest type of XC functional depends only on the local spin-density and is exact for the idealized uniform electron gas, but fails to describe the contoured densities of real charge distributions. Introducing a functional dependence on the gradient of the density, the kinetic energy density, fractional HF exchange, and even unoccupied levels incrementally defines a hierarchy of density functionals called "Jacob's Ladder", though higher-rung functionals aren't guaranteed to perform better than lower-rung functionals. That being said, wavefunction methods have found worthy competition in many state-of-the-art density functionals, and in the context of chemical relevance, the promise of an *ab initio* single-particle framework which includes inter-electronic correlations implicitly cannot be overstated.

1.3 Local correlation methods and intermolecular interactions

For wavefunction-based methods to approach the relevance DFT enjoys in the large-molecule regime, much emphasis has been placed on the development of approximations reducing the formal scaling or the associated computational prefactor without degrading the accuracy relative to the conventional result. In the domain of CC and MP theory, these include RI/density-fitting[37–42], explicitly-correlated schemes [43–51], spin-component-scaled formulations [52, 53], rank-reducing tensor decompositions[54–62], and domain fragmentation approximations, the subject of much of this work.

The promise of domain-based (or local correlation) methods is, given the exquisite locality of dynamic correlations, distant inter-atomic or molecular correlations can be safely neglected without an accuracy penalty to force lower scaling. In practice, this is achieved by partitioning a supersystem into a linearly- or quadratically- scaling collection of minimally or non-interacting subdomains, each defining local correlation problems of manageable size.

Local correlation methods find natural application in the computation of intermolecular interaction energies, given as the difference between the total energy of a complex $AB...Z$ and the energy of its vacuum components A,

$$\Delta E(AB...Z) = E(AB...Z) - \sum_{A}^{Z} E(A). \tag{1.21}$$

ΔE is small on the absolute scale, and typically much weaker than *intra*molecular bond energies, e.g., the water dimer interaction energy is some 20kJ/mol, while the O-H bond is

some 500kJ/mol. Thus, a choice of monomer-centered subdomains is not only chemically-meaningful, but also a black-box starting point for any approximate treatment of the super-system $E(AB...Z)$ truncating interactions on the basis of locality.

There are two issues bearing on the quality of a predicted ΔE. The first deals with the question of the *representation* parametrizing local approximations to the supermolecular term. The second concerns the treatment of *correlation* effects, typically responsible for much or all of attractive ΔE.

- *Representation:* A valid local approximation to ΔE depends critically and delicately on the correspondence between the posited and actual representation of these molecular subdomains, which by their definitions, effectively parametrize the truncation structure. There is an exact correspondence in the second term of eq. 1.21, trivially, but not in the first term if $AB...Z$ is represented in a basis of delocalized HF orbitals, especially if the underlying AO basis includes diffuse functions. A poor approximation to ΔE will reflect this representation imbalance. As such, approaches seeking to impose locality truncations in the canonical or localized orthogonal representation such as divide-expand-consolidate[63–65], natural linear scaling coupled-cluster[66, 67], the clusters in molecules[68, 69] method, and others[70, 71] must treat a very large number of overlapping subdomains typically specified by the user or determined empirically at run-time. *Absolute* locality in the molecule-centered sense is arguably the best way for a non-redundant local correlation method to guarantee the representations in eq. 1.21 are commensurate. One realization of this is achieved by imposing locality constraints on the degrees of freedom entering the cluster SCF problem, e.g., requiring that molecule-tagged orbitals be linear combinations strictly of AO functions centered on that molecule alone. Applying the variational theorem with this constraint, one obtains a set of non-orthogonal SCF MI equations[72, 73] for non-orthogonal absolutely-localized molecular orbital (ALMO) states[74–76] and a total energy which is an upper-bound to the unconstrained SCF energy.

As an aside, we note that the structure of the ALMO wavefunction makes it an unambiguous intermediate wavefunction in the context of energy decomposition analysis (EDA), whereby the components of ΔE are divided into electrostatic, polarization, charge-transfer and dispersion contributions. Much of the early part of this thesis references the ALMOs in this capacity.

- *Correlation*: As already discussed, HF theory lacks correlation altogether, causing it to be invalid when London dispersions dominate interaction energies, e.g., in the case of clusters of non-polar molecules. Moreover, HF predicts inflated dipole moments and polarizabilities. MP2 can improve a description of permanent and induced electrostatics, but typically overestimates dispersion. As a consequence, interaction energies of at least CCSD quality - and preferably CCSD(T) - are desirable.

Much of the latter part of this work is devoted to the development and application of local correlation models of a linear and quadratic number of CCSD-level variables within the ALMO representation.

1.4 Outline

This thesis is organized as follows.

Chapter 2

This "first-year project" was inspired by a then-recent study by the Neumark group of vibrational autodetachment of an excited acetonitrile anion dimer[77]. Potential energy surface scans in coordinates specific to a dissociative normal mode common between the excited and ground states of the valence anion as well as the ground-state neutral dimer species shed light on the proposed vibrational autodetachment mechanism. This Chapter was published as a paper in *Phys. Chem. Chem. Phys.*[78], and was the basis for a follow-up collaboration investigating electron ejection from THF-solvated iodide[79].

Chapter 3

Here, a CCSD-level an energy decomposition analysis (EDA) from an orthogonalized ALMO reference was proposed and applied. Stability of the correlated components with respect to basis set extension hadn't theretofore been afforded by the Kohn-Sham or MP2 ALMO-EDA. This Chapter was published in *J. Chem. Phys.*[80].

Chapter 4

A minimal-basis lower-bound model for SCF-level intermolecular polarization is developed, which, when considered together with upper-bound ALMO polarization, provides an estimate of the range of energy-lowering due to induction. This Chapter was published in *J. Chem. Phys.*[81].

Chapter 5

Local SCF models extending the variational space of the ALMOs to include compact representations of charge-transfer-like excitations are presented here. Quantitative accuracy against reference interaction energies is demonstrated in linear cost. This Chapter has been submitted to *J. Chem. Phys.*

Chapter 6

ALMO-reference perturbation theories describing non-covalent interactions are developed employing a Löwdin partitioning of the similarity-transformed Hamiltonian into a zeroth-order intramonomer piece (taking local CCSD solutions as its zeroth-order eigenfunction) plus a first-order piece coupling the fragments. Different restrictions on the zeroth- and first-order amplitudes in the proposed intermolecular similarity transformed perturbation theory (iSTPT) are explored in the context of large-computation tractability and elucidation of non-local effects in the space of singles and doubles. This Chapter has been accepted by *J. Chem. Phys.*

Chapter 7

Fully-non iterative variants of the local iSTPT models introduced in Chapter 6 are developed by substituting MP2-level amplitudes for CCSD-level ones at zeroth-order. Applications show that errors relative to canonical CCSD depend more on rank-reduction in the amplitude vector than the quality of the amplitudes themselves. A comparison of perturbation theories derived from Löwdin and MP partitioning follows.

Chapter 8

Finally, a hierarchy of "perturb-then-diagonalize" schemes solving an effective Schrödinger equation in the space of singles in doubles, but folding in effects from triples and quadruples, is introduced and compared to conventional post-CCSD corrections.

Chapter 2

Excited states of anionic acetonitrile clusters

2.1 Introduction

Molecular clusters of polar molecules accommodating an excess electron have been studied in great detail, both experimentally and theoretically, with the objective of making sense of fundamental electron-solvent interactions. Spectroscopic properties, attachment and relaxation dynamics, and reactivities of free electrons in host solvents, including water[82–85] and acetonitrile [86–90], in both the condensed and gas phases have been reported extensively in the literature.

Clusters harbor an excess electron in one of three ways; either *i*) the electron interacts electrostatically with the cluster's permanent dipole moment, accommodated in a very diffuse "dipole-bound" orbital, *ii*) the excess electron is confined within an interior spheroidal cavity enclosed by solvent molecules, so-called "solvation-bound," or most interestingly, *iii*) the electron can be fully-localized on one or two solvent molecules, accommodated in a half-filled valence orbital, leading to geometric distortion of the anion relative to the neutral species. Electrons trapped in this way are often termed "valence-bound." Between *i*) and *ii*), the latter binding motif is preferred in larger clusters where significant geometric reorientation of the solvent bonding network to maximize interactions with the excess electron is viable, while dipole-bound conformations are thought to dominate in smaller clusters. The valence-bound motif is fundamentally different from *i*) and *ii*) in the sense that it represents the formation of a solvated molecular radical anion state.

That there exist multiple distinct features in the photoelectron spectra of these anionic clusters lends credence to the conjecture of different solvation motifs, and indeed, the distinction of these motifs has proved useful in the spectroscopy of anionic acetonitrile clusters, the focus of the current study. Solute photoionization of excess electrons into bulk acetonitrile produced two distinct absorption bands, one prevalent at low temperatures in the

visible region between 500 and 600nm (∼2.25eV), and the other at high temperatures in the infrared region with a maximum near 1400nm[88, 89] (∼0.08eV). The visible-region band was attributed with the aid of low-level ab initio calculations to photodetachment from a valence-bound radical anion species, $(CH_3CN)_2^{-1}$, of C_{2h} point group symmetry, with slipped anti-parallel geometry and highly-deformed CCN bond angles. The long-wavelength band was attributed to the absorption of a solvation-bound electronic state [87].

In the gas phase, photoelectron spectra of anionic acetonitrile clusters ranging in size between ten and one hundred molecules, again, exhibited two prominent peaks, one relatively sharp band of vertical detachment energy (VDE) between 0.4 and 0.7eV, ascribed to a solvation-bound electron, and the other broader feature of VDE between 2.4 and 2.8eV, assigned to a valence-bound dimer state [86]. Interestingly, the relative photoelectron intensities of the two features are a function of cluster size, with the lower-VDE motif more prevalent in smaller clusters, and vice versa for the larger-VDE motif. Moreover, the higher-energy feature blue shifts with increasing cluster size, underscoring the importance of solvation on the stability of, putatively, the valence-bound electron.

Thorough *ab initio* studies on ground-state anionic clusters of acetonitrile have corroborated the above assignments [91–94]. Particularly illuminating are VDE calculations on two $(CH_3CN)_6^{-1}$ isomer types, one an O_h-symmetry, solvation-bound structure with the methyl functions of the solvent molecules all oriented toward the cavity center (1.27eV), and the other a C_{2h} dimer core solvated by four acetonitrile molecules (between 3.40 and 3.43eV) [92]. The difference in the calculated VDEs (∼ 2.15eV) as a function of binding motif is similar to the difference in experimental VDEs, supporting the experimental assignments, and the fact that the calculated VDEs are about 1eV higher than their experimental counterparts is not surprising given that the hybrid density functional employed has been observed in anionic water clusters to systematically overestimates VDEs [95]. Also suggesting legitimate correspondence is the apparent increase in calculated VDEs with the size of valence-, but not solvation-bound clusters.

Other interesting variations on the dipole-bound theme explored previously [91, 94] in dimeric species include the "head-to-head" isomer, in which the methyl functions of two solvent molecules bind the excess electron, and the "head-to-tail" isomer, which binds an electron in a diffuse orbital with its whopping ∼8.5D dipole moment. Both are lower in energy than the C_{2h} valence anion, the focus here.

Recent experimental work has explored time-resolved dynamics in anionic clusters between twenty and fifty acetonitrile molecules in size [77]. Photoelectron kinetic energy spectra on $(CH_3CN)_{40}^{-1}$ produced distributions of maxima consistent with the previous gas phase assignments, but a prominent "slow" (near-zero KE) feature upon irradiation with 1.57eV photons had not theretofore been observed, and was attributed to an electronically-excited state of the valence-bound dimer since this photon energy is intermediate between the VDE of the solvation- and valence-bound isomers. Time-resolved photoelectron imaging (TR-PEI) [96] in which a similar-sized cluster was pumped and probed with 1.57 and 3.14eV photons, respectively, lent credence to this speculation, as there was a depletion at small

positive pump-probe delay intervals of the photoelectron kinetic energy intensity associated with detachment from the ground-state valence-bound anion, and a concomitant increase in photoelectron intensity at higher kinetic energies, associated with photoelectrons detached to the continuum from an electronically-excited state. As the distribution of VDEs of a photoelectron ejected from the valence-bound motif overlaps the 1.57eV electronic-excitation energy, the "slow" peak observed in the kinetic energy spectrum was attributed to vibrational autodetachment [97] of the electron from an excited state of valence-bound radical dimer, with lifetimes ranging between 200 and 270 femtoseconds.

Here, we investigate the electronically-excited state of the C_{2h} radical anion dimer computationally, surveying the character of the excitation via both wavefunction- and density-based methods, exploring the effect on this character by explicit solvation with other acetonitrile molecules, and finally, following the vibrational autodetachment of the dimer along a dissociative harmonic mode connecting the vertically-excited anion to the neutral dimer.

2.2 Computational Details and Methods

All electronic structure calculations were performed with the Q-Chem electronic structure package [98].

Ground-state geometry optimizations, single-point calculations, and normal-mode analyses were performed at the ωB97/6-311++G** level of theory for the valence anion. The so-called "long-range-corrected" ωB97 functional [99] guarantees full Hartree-Fock exchange at large inter-electronic distances, necessary to treat charge-transfer excited states and excited states of large molecules and clusters, and so is preferred over the B3LYP functional.

Vertical detachment energies (VDE) from anionic clusters are computed according to

$$\begin{aligned} VDE = E(&\text{neutral at optimized anion geometry}) \\ &- E(\text{anion at optimized anion geometry}), \end{aligned} \tag{2.1}$$

and adiabatic binding energies (BE) according to

$$\begin{aligned} BE = nE(&\text{neutral monomer at optimized neutral geometry}) \\ &- E(\text{anion at optimized anion geometry}), \end{aligned} \tag{2.2}$$

where n is the number of monomers comprising the cluster.

Symmetry-allowed ground- to excited-state transitions of the C_{2h}-constrained valence anion were calculated by the equation-of-motion coupled-cluster electronic-excitation (EOM-EE-CCSD)[30, 100–102], correlated configuration interaction singles (CIS(D)) [31], and time-dependent density functional theory (TDDFT)[103] methods in the 6-311++G** basis. Subsequent calculations on anionic clusters ranging from n=3 to n=10 were performed at the ωB97/6-31++G** level of theory.

The $^2B_u^{-1}$ excited state was optimized by SOS-CIS(D_0)[104] in the 6-311++G** basis, and the adiabatic excitation (AE) was calculated according to

$$\begin{aligned} AE = & E(\text{excited anionic state } (^2B_u^{-1}) \text{ at optimized excited-state geometry}) \\ & -E(\text{ground anionic state } (^2A_g^{-1}) \text{ at optimized ground-state geometry}). \end{aligned} \tag{2.3}$$

Symmetry-adapted orbitals were plotted at a contour value of 0.025 $\mathring{A}^{-\frac{3}{2}}$. Two-dimensional potential energy surface scans were constructed from some eleven thousand ω B97/6-31++G** single-point calculations for each of the $^2A_g^{-1}$, $^2B_u^{-1}$, and $^1A_g^0$ states, and contour plots were constructed by polynomial interpolation using Mathematica 7.0.

2.3 Results and Discussion

Valence anion ground-state calculations.

Both the ground-state, valence-bound $^2A_g^{-1}$ and the slipped antiparallel neutral $^1A_g^0$ dimer species (Fig.2.1) were optimized within C_{2h} point group symmetry (the energy of the C_1-optimized structures differed from their higher-symmetry counterparts by a few tenths of a kcal/mol), the latter only some 21.41kcal/mol more stable, and the lowest-energy acetonitrile dimer species for that matter, and the former only kinetically stable with respect to autodetachment, as indicated by the negative BE calculated for this species (Fig 2.5). The constituent acetonitrile molecules of the valence-bound dimer are far from linear, with $C_{\beta(\prime)}C_{\alpha(\prime)}N$ bond angles of 128.2°, and the 'inter-monomer' $C_\alpha C_{\alpha\prime}$ valence-bond distance contracted almost two-fold relative to the neutral species, from 3.494 to 1.691$\mathring{A}$. However, there are no other gross structural differences between the two species; all other corresponding bond length and bond and dihedral angle parameters are within a few tenths of 1$\mathring{A}$ and between one-half and two degrees from one another, respectively, suggesting a mostly local (albeit severe) structural effect of accommodating an excess valence electron. This idea will be important later on when two-dimensional PES scans in the coordinates Θ and R are considered.

It is interesting to consider how these geometric distortions affect the harmonic vibrational modes of the acetonitrile dimer. Normal mode analysis of the equilibrium structures reveals a red shifting of the majority of the thirty modes of the dimer in the $^2A_g^{-1}$ state relative to the $^1A_g^0$ state. Most dramatically affected are the asymmetric $C_{\beta(\prime)}N$ and $C_{\alpha(\prime)}C_{\beta(\prime)}$ stretching modes ($\Delta\nu$ = -600cm^{-1} and -200cm^{-1}, respectively), and surprisingly, the "hardest" asymmetric and symmetric CH stretching modes ($\sim$-100cm^{-1}). This is readily attributed by NBO analysis[105] to the fractional population of σ^* antibonding orbitals, mediated by donation from the valence $\sigma(C_\alpha C_{\alpha\prime})$ inter-monomer bonding orbital occupied by the excess electron in this basis. MO transformation to the NBO basis gives the Lewis picture

of bonding, and by second-order perturbation theory [106], NBO donation into antibonding orbitals lowers the electronic energy according to

$$\Delta E_{d\to a} = o_d \frac{|f_{da}|^2}{f_{dd} - f_{aa}}, \tag{2.4}$$

where the subscripts d and a correspond to donor and acceptor NBO orbital pairs, respectively, o_d represents the occupancy of the donor NBO, ϕ_d, f_{da} is the matrix element $\langle\phi_d|\hat{F}|\phi_a\rangle$, and $\hat{F}$ is the one-particle Fock operator. The predominant contributions to donor-acceptor stabilization energies are summarized in Table 2.1, and mirror the calculated red shifts in corresponding normal modes. The featured $\sigma \to \sigma^*$ interaction energies are on the order of weak hydrogen bonds, interestingly, comparable to the results obtained in similar studies on anionic water clusters [107].

Despite their limitations, Mulliken populations reveal a lot about the electronic structure of the valence anion. Analysis of spin difference densities indicates a substantial excess of α electrons on each of the nitrogen atoms (0.462), suggesting localization of nearly 95% of the excess electron at those atoms. Moreover, the excess electron decreases the Mulliken charge on each of C_β relative to the neutral species by nearly a half-electron. Indeed, the fractional population of C_β and nitrogen Rydberg orbitals in the donor-acceptor analysis of Table 2.1 can be understood in terms of excess negative charge and α-electron spin-density, respectively. The viability of two resonance hybrids for the valence anion, in both of which the unpaired electron resides in an atomic p-type orbital conferring a formal charge of -1 on one or the other nitrogen, suggests potential multi-reference character typically exhibited by open-shell species. However, inspection of ground-state occupied orbital energy eigenvalues revealed no near-degeneracies, and the largest single- and double-substitution amplitudes contributed just 0.042 and 0.18%, respectively, to the CCSD wavefunction, indicating that the ground-state is adequately described by the HF reference. On the other hand, the LUMO and LUMO+1 a_g and b_u MOs are nearly degenerate, some 2mEh apart (Fig. 2.2), and representing non-bonding orbitals on the nitrogens and $C_{\alpha(')}$. The singly-occupied a_g spin-orbital places electron density in the $\sigma(C_\alpha C_{\alpha'})$ bond along the inter-monomer bond axis and in lone-pair orbitals on either nitrogen, while the HOMO-1 b_u is squarely antibonding with respect to the inter-monomer $\sigma(C_\alpha C_{\alpha'})$ bond.

Valence anion excited-state calculations.

The only allowed excited states of the valence-bound anion consist of transitions between orbitals of symmetry irreducible representations (irreps.) whose direct product transforms as A_u or B_u, given the transformation of the dipole operator in the C_{2h} point group. Accordingly, the first few low-lying electronic transitions of A_u and B_u symmetry were sought in EOM-EE calculations, and transition strengths versus excitation energies for the first few low-lying symmetry-allowed transitions are plotted in Fig. 2.3. Only the lowest-energy,

highest-oscillator strength root of (x, y)-polarized B_u symmetry (2.016eV) is considered subsequently, as the other excitation energies, z- and (x, y)-polarized, are within, or exceed the spectrum of experimental valence-bound anion VDEs (2.4-2.8eV), and are therefore irrelevant. That the calculated excited-state energy is greater than the experimental value ($\sim 1.57eV$) is no huge surprise, since solvation by other acetonitrile molecules, to be considered later, presumably stabilizes the excited state. On the other hand, that *i*) the charge of the ground and excited states of the valence-bound anion are equivalent, and *ii*) the inversion symmetry of the molecule implies no permanent dipole moment both suggests that any electronic state of the dimer is not particularly "wanting" in solvation, and so any further stabilization is due to higher-order terms in the multipole expansion.

The first B_u symmetry excited state is well-described by a linear combination of singly-substituted determinants (Fig. 2.4), and is overwhelmingly single-excitation in character, of norm($\hat{R}_1$)= 0.94. The major contributions account for a very adequate 75% of the excited-state character, with the most significant contribution from the $1b_u \rightarrow 4a_g$ transition (70%).

The difference in second moment between the EOM-EE and ground-state electron density, $\Delta\langle\hat{R}^2\rangle$, is a useful quantitative gauge to assess the spatial extent of the excited state [108]. In valence-type transitions, there is little difference between the ground- and excited-state moments of electron density, whereas in Rydberg transitions, $\Delta\langle\hat{R}^2\rangle$ is on the order of $10\mathring{A}^2$. Between the ${}^2A_g^{-1}$ and ${}^2B_u^{-1}$, $\Delta\langle\hat{R}^2\rangle = 6\mathring{A}^2$, indicative of quasi-Rydberg character, and reflected in the comparatively diffuse nature of the $4a_g$ orbital into which the HOMO-1 excites, although one would be hard-pressed to assert with confidence that this orbital in any way characteristically resembles a hydrogenic orbital. It is curious given the enhanced density of electronic states of open-shell radicals that there is no sizable doubles amplitude corresponding to the concomitant promotion of an electron from the singly-occupied orbital to a valence virtual alongside promotion from a doubly-occupied orbital into the singly-occupied orbital.

n-mer calculations.

To extend these calculations to the realm of experimental relevance, e.g., by exploring cluster properties by incorporating explicit solvent molecules and scanning potential surfaces, cheaper electronic structure methods are required, and in light of the single-excitation character of the ${}^2B_u^{-1}$ state, CIS(D) and TDDFT calculations on the C_{2h} valence anion were deemed appropriate. B_u-symmetry transitions are compiled in Table 2.2.

The first CIS root is identical in character to the EOM-EE root of Fig. 2.4, of similar oscillator strength and incorporating the same orbitals in the excitation, but the correlated root over-shoots the EOM-EE result. The first ωB97 root also shares the character of the EOM-EE root, producing a comparable excitation energy, but evening out contributions from the $(1b_u \rightarrow 4a_g)$ and $(1b_u \rightarrow 2a_g)$ excitations in the wavefunction. Thus, we proceed with confidence that explicit inclusion of doubly-substituted configurations does not

contribute significantly to the description of the excited-state wavefunction, and that the TDDFT/ωB97 eigenvector is sufficient to adequately describe this excited state.

To best approximate the experimental conditions of the electronic excitation, minimum acetonitrile n-mer structures ranging from n=3 to 10 were optimized, with the near-C_{2h}-symmetry valence anion core remaining intact for each n-mer. VDE, excitation energy (EE), and BE as a function of n, tabulated in Fig. 2.5, were calculated by (TD)DFT/ωB97, reliably reproducing the dimer EOM-EE $^2B_u^{-1}$ state. That the valence anion dimer VDE is smaller than the corresponding EE number is a little bit surprising, as it would seem unphysical that the first electronically-excited anionic state is higher in energy than a vertically-detached neutral state. At the high-n end, VDEs are overestimated by about 1eV for reasons discussed earlier. The valence-anion core cluster only becomes thermodynamically stable past n=4, highlighting the relative importance of solvation in spite of the absence of a permanent dipole moment in the C_{2h} core. The cluster BE quickly stabilizes, hovering around 4kcal/mol beginning at n=6, suggesting that it is primarily stabilized by solvation of the core by the first few solvent molecules, whose methyl functions are dipole-oriented toward the core nitrogen atoms (Fig. 2.5, inset), on which the excess α-electron was found to be localized. It is curious that the $^2B_u^{-1}$ EE remains relatively stationary up to n=6, whereupon it drops to $\sim$1.63eV, nearing the experimental value of 1.57eV. At this point, the $1b_u \rightarrow 4a_g$ contribution begins to overtake the $1b_u \rightarrow 2a_g$ substitution in the TDDFT eigenvector, contributing about three-fifths of the norm. By n=10, the two-configurational $^2B_u^{-1}$ state is best described by a single configuration ($\sim 90\%|\Phi_{1b_u}^{4a_g}\rangle$), similar to that obtained by EOM-EE (Fig. 2.4), and the excitation energy has, for the most part, converged on the experimental quantity.

$^2B_u^{-1}$ minimum-energy structure.

The character of the optimized minimum-energy structure of the $^2B_u^{-1}$ excited state is marked by the contraction of the $C_\alpha C_{\alpha'}$ bond by 0.22$\mathring{A}$, protraction of the $C_\beta N$ bonds by 0.022$\mathring{A}$, and a decrease in the $C_\beta C_\alpha N$ bond angle by nearly 7 degrees (Fig. 2.6.). This is consistent with the vertical excited-state wavefunction of Fig. 2.4, wherein the high-amplitude $|\Phi_{1b_u}^{4a_g}\rangle$ contribution has depleted both *i*) antibonding character with respect to the $C_\alpha C_{\alpha'}$ valence bond, and *ii*) bonding character with respect to the $C_{\beta(')}C_{\alpha(')}N$ bonding lobes, *and* introduced inter-monomer $C_\alpha C_{\alpha'}$ bonding character.

On vertical excitation, the unpaired spin density shifts from the nitrogens to the $C_{\alpha(')}$s, while the $C_{\beta(')}$s, with Mulliken populations approaching zero, lose atomic charge density to the $C_{\alpha(')}$ and Hs. On relaxation to the $^2B_u^{-1}$ minimum, the $C_{\alpha(')}$ have each gained about a quarter of an electron, while the $C_{\beta(')}$s have lost about a tenth. Interestingly, the unpaired density finishes up on the $C_{\alpha(')}$s and Hs. The adiabatic $^2A_g^{-1} \rightarrow {}^2B_u^{-1}$ excitation energy is determined as 1.37eV, some 0.2eV and 0.6eV shy of the vertical experimental and calculated

excitation energies, respectively.

PES scans and picture of vibrational autodetachment.

To investigate the putative vibrational autodetachment of the excess electron from the excited state, PES scans along R and Θ, coordinates which most compactly connect the minimum $^2A_g^{-1}$, $^2B_u^{-1}$, and $^1A_g^0$ electronic state geometries (Fig. 2.7a. and b.). The equilibrium ground- and excited-state anion dimer structures share smaller coordinate values (lower left-hand corner), the C_αs of near-"sp^2" hybridization, double-bonded to the nitrogens, whereas the neutral dimer minimum is located at higher coordinate values (upper right-hand corner), with nearly-linear monomers containing "sp"-hybridized C_αs, oriented in an antiparallel fashion in, as discussed previously, the most stable dimer species. Vertical excitation from the $^2A_g^{-1}$ minimum to the $^2B_u^{-1}$ surface places the wavepacket distal to the seam with the $^1A_g^0$ surface. Thus, the wavepacket can cross over to the $^1A_g^0$ surface, the excess electron detaching at the surface-crossing.

One a_g-symmetry, blue-shifted 779.9cm^{-1} harmonic mode of the excited state (henceforth referred to as ν^*), featuring both the concerted elongation of the inter-monomer $C_\alpha C_{\alpha'}$ bond (R), and an increase in the$C_\beta(')C_\alpha(')N(')$ bond angle (Θ), is particularly well-suited for the discussion of vibrational autodetachment since, to a good approximation, one can imagine traveling between the minimum geometries of each electronic state along just this normal-mode coordinate, the ground-state anion minimum intermediate in coordinate values between the excited-state and neutral dimer species. As such, a single linear slice through the scan should intersect each of the three minima, with the topology of the energy landscape around each of the electronic minima determining the force constants for this mode for each electronic state. So this mode can be viewed as the bona fide vibrational dissociation/electron detachment coordinate connecting the excited anion and neutral dimer states.

Vertical excitation from the ground vibrational state with frequency ν on the ground-state electronic surface in this mode places the wavefunction in a superposition of the ground and excited vibrational states in the ν^* mode above the $^2B_u^{-1}$ surface, with contributions weighted by the Franck-Condon overlaps, and evolving according to the time-dependent Schrödinger equation with the "upstairs" Hamiltonian [109]. Within the Franck-Condon approximation however, the highest-probability $(^2A_g^{-1}, \nu_{n=0}) \rightarrow (^2B_u^{-1}, \nu_n^*)$ vibronic transition can be determined by examining the "upstairs" stationary state of the largest vertical overlap with the ground state, or in other words, the state whose turning point lies most closely in the coordinate vertically above the ground-state anion minimum.

The three electronic potentials along the dissociation coordinate are schematically plotted in Fig. 2.8, with the zero-point corrections factored into the reported energies. Not surprisingly, the minimum-energy structures obtained from scanning are very similar in both geometry and absolute energy to those obtained when all other internal coordinates are allowed to relax, so validating the approximation.

If this "dissociative" mode adequately captures the vibrational autodetachment process, the oscillator energy above the $^2B_u^{-1}$ minimum places the wavepacket in a superposition of ν^* states, with the largest contributions from $\nu^*_{n=5}$, of energy eigenvalue ∼0.53eV. There is no barrier to curve-crossing, as the Franck-Condon region is beyond the seam with the $^1A_g^0$, and so the autodetachment process is expected to be very fast. To a rough approximation, we can interpret the probability density of the $\nu^*_{n=5}$ state integrated from the $^2B_u^{-1}$-$^1A_g^0$ seam to $q = \infty$ as the probability that the excited-state has autodetached, or in other words, that the $(^2B_u^{-1}, \nu^*_{n=5})$ state has vibrated into the $(^1A_g^0, \nu_n^{'})$ state, ejecting an electron in the process. The rate of autodetachment, then, is given by this probability multiplied by the mode frequency, calculated to be ∼0.00234/femtosecond. The lifetime, given by the inverse of this rate, is ∼427 femtoseconds, consistent with ten vibrational periods on the $^2B_u^{-1}$ surface. The computed value is on the order of experimental value for clusters of n=39, between 200 and 270 femtoseconds [77]. On the other hand, the positive, near-asymptotic BEs at higher n relative to the negative dimer value from Fig. 2.5 suggest that the valence dimer in the bulk relative to the neutral dimer is stabilized, and so the set of anionic electronic curves in Fig. 2.8 is expected to shift downward relative to the neutral electronic curve in the field of other solvating acetonitriles. Such a downard shifting will increase the $^2B_u^{-1}$-$^1A_g^0$ seam value in q, ultimately increasing the calculated excited-state lifetime.

Conclusions and Future Direction.

We have characterized the experimentally-relevant excited state of molecular acetonitrile anion clusters, determining *i*) that the $^2B_u^{-1}$ state is single-excitation in character, *ii*) two-determinantal at n=2, but *iii*) is dominated by a single configuration ($|\Phi^{4a_g}_{1b_u}\rangle$) for n >6, *iv*) and the $^2A_g^{-1} \rightarrow {}^2B_u^{-1}$ excitation energy approaches the experimental quantity as the number of explicit solvent molecules is increased; also, we have *v*) explored the topologies of the $^2A_g^{-1}$, $^2B_u^{-1}$, and $^1A_g^0$ potential surfaces in the internal coordinates R and Θ, which bear most heavily on a "dissociative" normal mode of the dimer, and *vi*) examined the plausibility of vibrational autodetachment from an excited level of the corresponding ν^* harmonic mode of the excited $^2B_u^{-1}$ state. This is the mechanism of excited-state detachment posited recently[77] to account for the observation of "slow" photoelectrons in experimental spectra. The calculated excited-state lifetime in this work is consistent with experiment.

Future work might include propagating the ν^*-mode vibrational wavepacket on the $^2B_u^{-1}$ surface and plotting Dyson orbitals by EOM-IP[110] to examine the wavefunction of the photodetached electron from both the ground and excited states of the anion dimer at the seam of the $^2B_u^{-1}$ and $^1A_g^0$ potentials to corroborate experimental photoelectron angular distribution data.

$\sigma(C_\alpha C_{\alpha'}) \rightarrow$	$\Delta E_{d\rightarrow a}$ / $kcal/mol$
$\mathrm{Ry}^*(N)$	1.89
$\mathrm{Ry}^*(C_\beta)$	3.78
$\sigma^*(CH)$	2.56
$\sigma^*(C_\alpha C_\beta)$	0.76
$\sigma^*(CN)$	0.68

Table 2.1: $\Delta E_{d\rightarrow a}$ stabilization energy analysis.

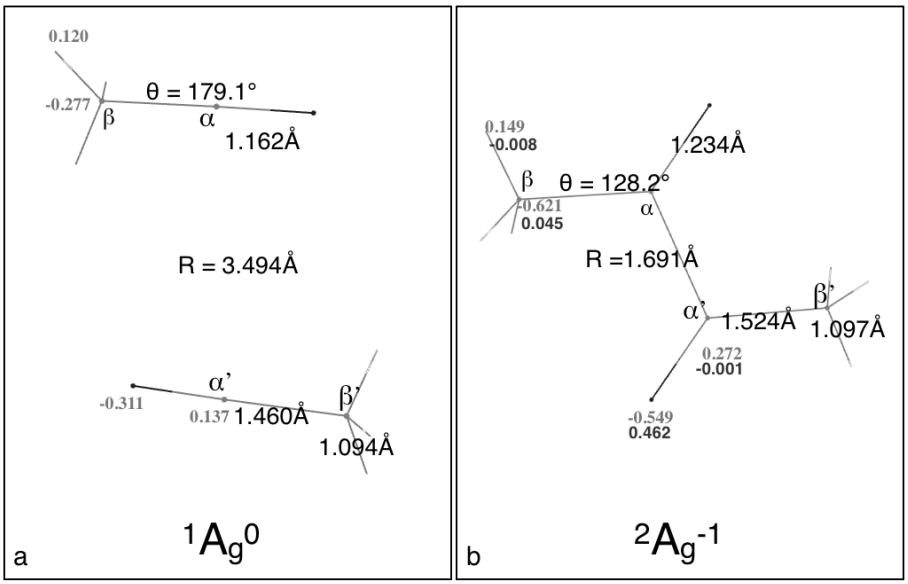

Figure 2.1: Ground-state C_{2h} ${}^1A_g^0$ and ${}^2A_g^{-1}$ states. Mulliken atomic charges and spin-difference densities are reported in grey and black, respectively. R denotes the inter-monomer $C_\alpha C'_\alpha$ inter-monomer distance; Θ denotes the $C_\beta C_\alpha N$ bond angle.

EOM-EE-CCSD	CIS	CIS(D)	TDDFT/B3LYP	/ωB97
2.016	0.807	2.589	2.189	2.068
2.438	2.998	3.259	2.196	3.392
2.602	3.994	4.020	2.378	3.604
2.974	4.078	1.541	2.844	3.729

Table 2.2: C_{2h} valence anion excitation energies/eV.

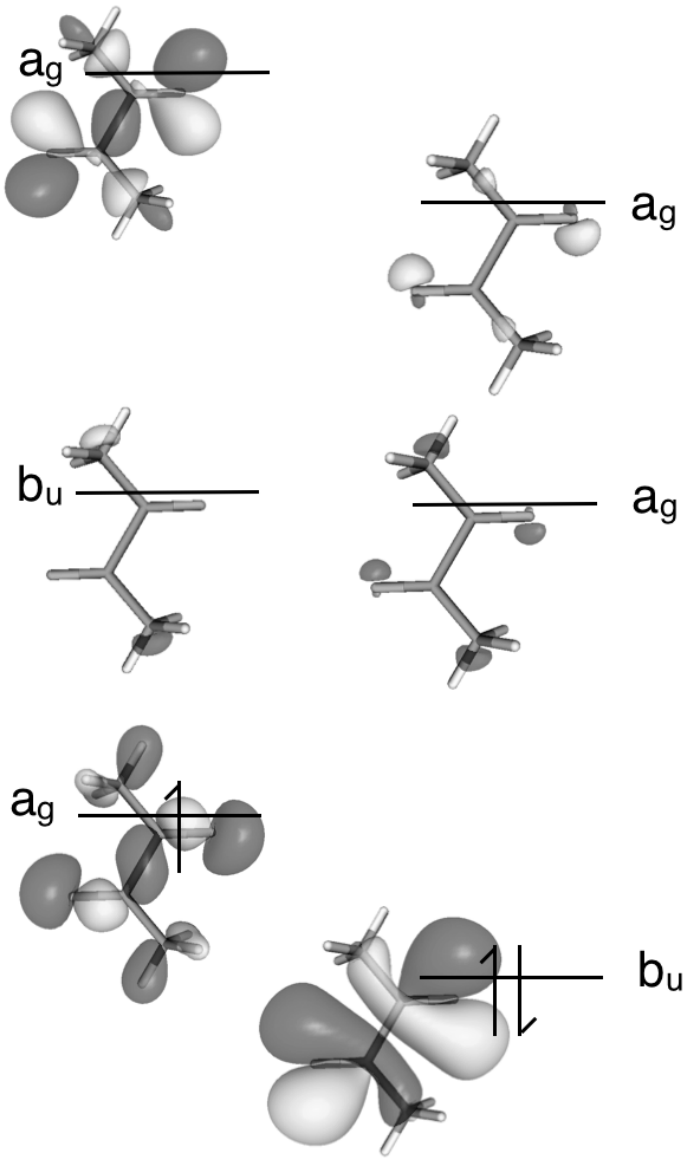

Figure 2.2: ${}^2A_g^{-1}$ frontier orbitals.

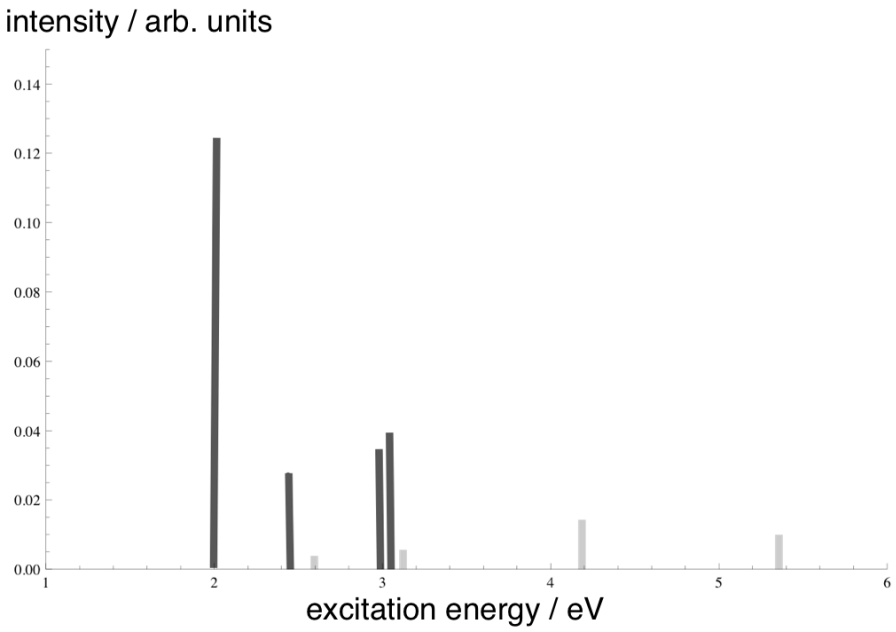

Figure 2.3: Excitation energy spectrum for vertical excitations from the ${}^2A_g^{-1}$ state. B_u and A_u-symmetry transitions are colored black and grey, respectively.

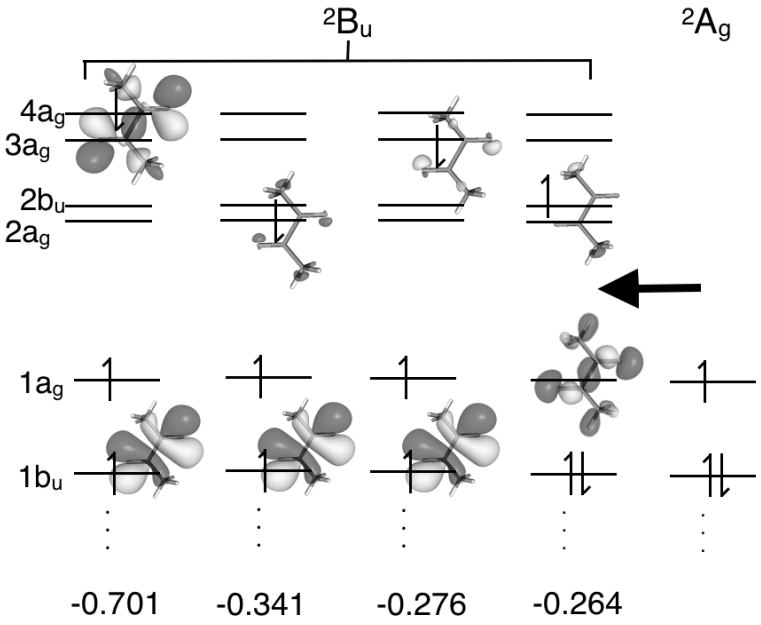

Figure 2.4: $^2B_u^{-1}$ valence anion excited-state wave function.

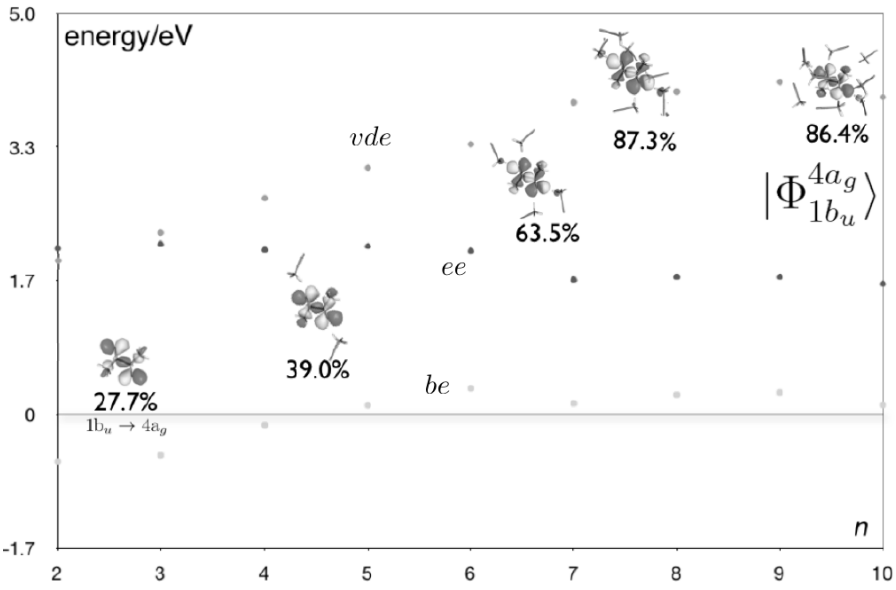

Figure 2.5: VDE (grey),BE(light grey), and EE(black) vs. cluster size n, calculated by (TD)DFT/ωB97 in the 6-31++G** basis; Inset: percent $|\Phi^{4a_g}_{1b_u}\rangle$ vs. n.

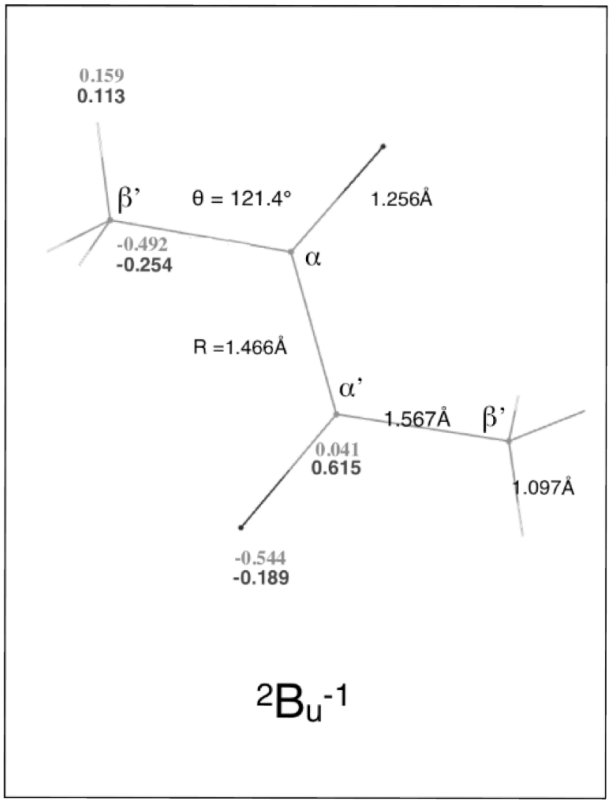

Figure 2.6: Minimum $^2B_u^{-1}$ structure. Mulliken atomic charges and spin-difference densities are reported in grey and black, respectively.

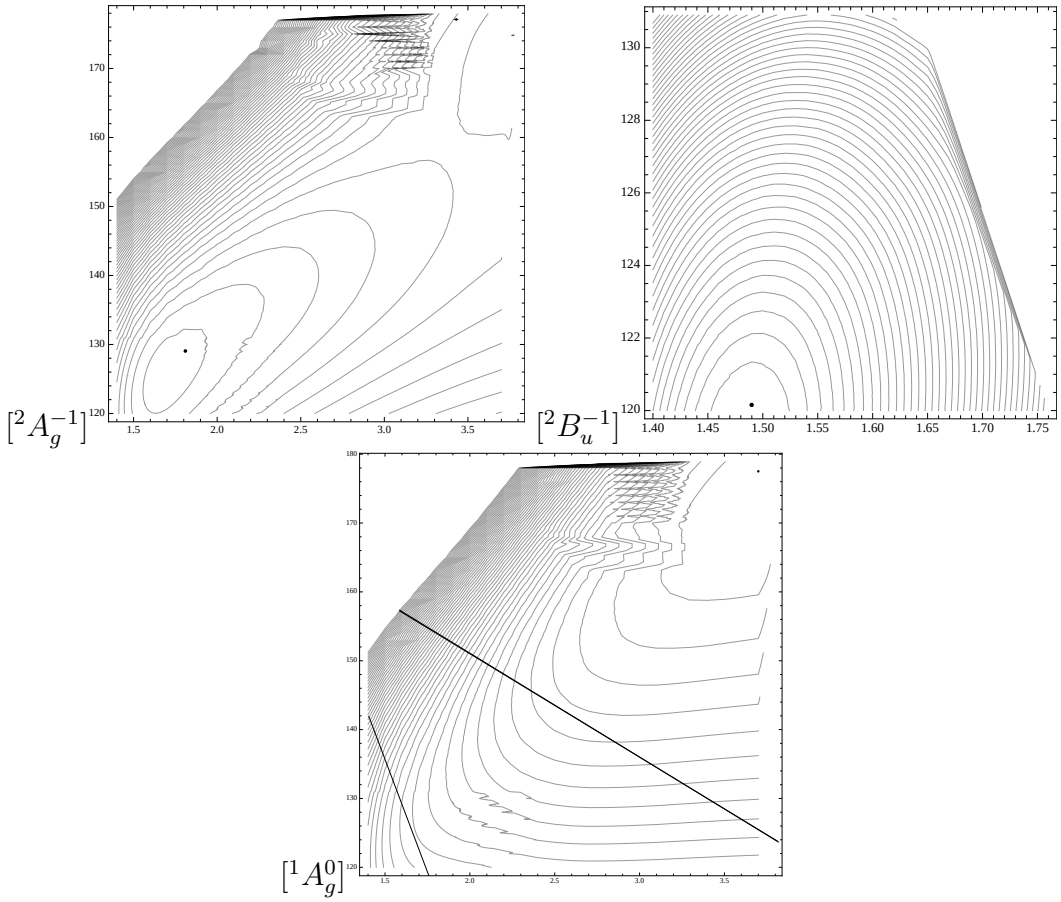

Figure 2.7: PES scans along R (abscissa) and Θ (ordinate) for the ground- and excited-states of the dimer anion, and the neutral dimer, calculated by (TD)DFT/ωB97 in the 6-31++G** basis. Contours are spaced 0.16, 0.03, and 0.22eV apart, respectively. Black dots indicate scanning minima. Relative to the neutral minimum, the ground- and excited-state anion minima are +1.25 and +2.77eV, respectively. The light and dark lines in the neutral surface represent (roughly) the seams with the dimer anion excited- and ground-state potentials.

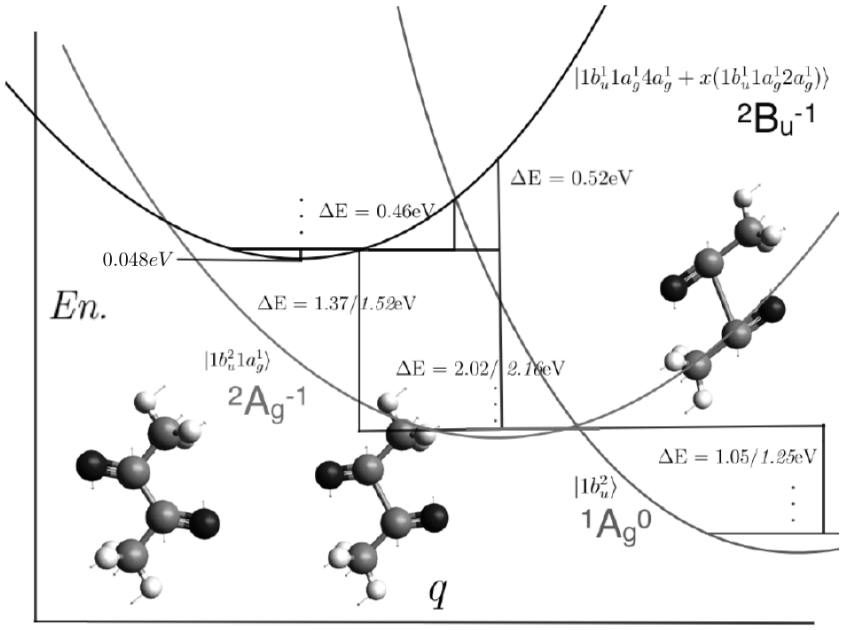

Figure 2.8: Electronic potentials schematically along the a_g-symmetry "dissociative" mode. Where there are paired values, those italicized values were obtained by considering the single point energies derived from the PES scan, whereas the values in roman script were obtained from single-point calculations wherein all internal coordinates were relaxed.

Chapter 3

EDA from orthogonalized ALMOs at the CCSD level

3.1 Introduction

Intermolecular interactions are ubiquitous, fundamental to processes ranging from biochemical signaling mediated by ligand-receptor interactions[111], to interstellar chemistry and atmospheric aerosol nucleation[112], to bulk properties. As such, a thorough understanding of so-called "soft" potentials and the specific contributions comprising them cast within an *ab initio* framework is without a doubt useful, for example, in the training and development of empirical potentials for molecular dynamics simulations, in rational drug design [113], where a medicinal chemist might fine-tune physical properties of pharmacophores of interest as a function of the chemical substituents that bear on the protein docking properties, and in crystal engineering [114] and polymer synthesis [115], where tweaking secondary interactions at the molecular level can affect bulk properties.

The components that make up weak interactions have long been well-characterized. Molecular complexes are stabilized by *i*) electrostatic forces experienced between charges, between permanent or induced multipoles, and between charges and permanent or induced multipoles, by *ii*) weaker dispersive forces resulting from instantaneous multipole interactions, and by *iii*) donor-acceptor interactions between intermolecular occupied-virtual orbital pairs. A slew of energy decomposition analysis (EDA) schemes, of both the wavefunction and density functional theory-based (DFT) persuasion, have been proposed to unravel the nature of such weak interactions, and can be broadly organized into two categories, variational and perturbative. Of the latter category, symmetry-adapted perturbation theory[116] (SAPT), for wavefunction and density-functional approaches [117, 118], has probably enjoyed the most acclaim and successful application. It represents a many-body generalization of London's polarization theory treating intermolecular interactions[119], employing a Rayleigh-Schrodinger perturbative expansion with the fluctuation potential chosen as those coulombic terms cou-

pling monomers treated at infinite separation in zero-order, the zero-order wavefunction and energy chosen as the antisymmetrized Hartree product of the non-interacting fragments and the sum of non-interacting energies, respectively. The SAPT treatment decomposes the energy correction into "electrostatic polarization" and "exchange repulsion" interaction terms, corresponding to classical repulsion of charge distributions and quantum mechanical electron tunneling between fragments, respectively, in first-order, and "multipole induction" and "dispersion" in second-order, with these contributions separated based on partitioning the RS resolvent in the second-order expression for the energy. Other high-level dynamically-correlated approaches have obtained the dispersion contribution from frequency-dependent density susceptibilities at the coupled-cluster (CC) level [120–122].

Some popular variational approaches block-partition the Fock matrix into diagonal intra-fragment and off-diagonal inter-fragment occupied-occupied, occupied-virtual, and virtual-virtual blocks. In the Kitaura-Morokuma (KM) scheme[123], the interaction energy is determined by zeroing certain off-diagonal subspaces of the Fock matrix depending on which component is sought after, with binding energy elements consisting of an "electrostatic" term, which includes inter-fragment, two-particle Coulomb integrals and one-particle contributions and describes classical electrostatics, an occupied-occupied, virtual-virtual mixing inter-fragment "exchange" term, an intra-fragment "polarization" term, which provides for occupied-virtual mixing within a fragment, and finally, an inter-fragment occupied-virtual mixing "charge-transfer" term, accounting for intermolecular delocalization. Despite criticism that the intermediate KM wavefunctions don't satisfy Pauli antisymmetry [124, 125], resulting in divergence of the charge transfer and polarization terms as the atomic orbital (AO) basis set approaches completion, it has been used widely, and with distinction [126–128].

Other approaches have been developed to remediate the problem of violation of antisymmetry, including natural energy decomposition analysis (NEDA) [129] within the natural bond orbital (NBO) framework of Weinhold and coworkers [130], the reduced variational space self-consistent field (RVS SCF) [131] method, and the restricted constrained space orbital variations (CSOV) [132] approach. NEDA decomposes the binding energy into a deformation term, accounting for geometric differences between isolated monomers and their complex geometries, an electrostatic term determined as the difference between the complex wavefunction and the antisymmetrized Hartree product of the deformed monomer wavefunctions, and finally, a charge transfer term defined as the difference between the antisymmetrized product energy and the full complex SCF energy, accounting for inter-fragmental electron delocalization. Because the intermediate antisymmetrized product is not variationally determined, the charge transfer contribution to binding is sometimes overestimated.

RVS SCF and CSOV are similar conceptually, obtaining the polarization energy due to a given molecule in the cluster by solving the variational problem in orthonormalized, reduced subspaces built from the occupied block of the Fock matrix, with the constraint that off-diagonal elements coupling to the molecule of interest's occupied orbitals are zeroed, thus freezing these orbitals and allowing the other occupied orbitals to relax in a frozen field.

This process is repeated for the occupied orbitals belonging to other fragments. Charge transfer terms are computed naturally when the variational subspaces are augmented with intra- and extra-fragment virtual blocks. One drawback is that the polarization energy is not determined self-consistently in either of these schemes, but rather piecemeal variationally.

More recently, Head-Gordon and coworkers have proposed a promising EDA for intermolecular interactions based on localized molecular orbitals [74, 75, 133], obtained from a variational description of molecule-labeled MOs in terms of the AO functions belonging strictly to the molecule itself, determined on solving the nonorthogonal locally-projected SCF equations for molecular interactions (SCF MI) as first proposed by Stoll [72], and later recast in slightly different formalisms by others [73, 134, 135], for a basis of nonorthogonal molecular orbitals. The SCF MI provides for a self-consistent determination of the intermolecular polarization term, constraining the MO coefficient matrix to be block-diagonal in each of the cluster molecules, by definition preventing intermolecular charge transfer, but at the same time allowing for intra-molecular relaxation of each local MO in the field of all other molecules. Moreover, this constraint obviates the problem of basis set superposition error (BSSE)[136] that beleaguers calculations involving complexes. The charge transfer term is determined subtractively from the full counterpoise[137]-corrected binding energy, or can be approximated very accurately using a perturbative expansion of the ALMOs, with a term in the second-order energy term resembling the non-Brilluoin singles in the standard Møller-Plesset second-order (MP2) energy correction for a set of non-canonical orbitals.

Formally, the binding energy in the ALMO EDA is the sum of *i*) *geometric distortion*, defined as the energy required to deform a free molecule's internal coordinates to those consistent with the cluster geometry, and evaluated for each element straightforwardly as the SCF energy difference between the two structures, *ii*) $frozen\ orbital$ (frz) interactions, accounting for both permanent electrostatic contributions and Pauli repulsion between same-spin electrons, corresponding to bringing infinitely-separated distorted molecules together to form an antisymmetrized Hartree product of fragment wavefunctions, and operationally determined from the energy associated with the density matrix formed from the converged MO matrices of the isolated molecules, *iii*) *polarization* (pol), defined as the relaxation of fragment ALMOs in the field of all other ALMOs, but with the block-diagonal constraint on the coefficient matrix still in place, and *iv*) $charge\ transfer$ (ct), stabilization due to intermolecular relaxation of molecular orbitals due to occupied-virtual pair interactions, identical to the unconstrained SCF solution.

The ALMO EDA has been applied to many studies of various molecular complexes with merit [76, 138–141], using both the Hartree-Fock (HF) and Kohn-Sham DFT methods and producing binding components consistent with physical intuition. But total electronic energies are extensive properties, and within the subtractive supermolecule approach to the computation of binding energies, the inclusion of explicit inter-electronic correlations is necessary: the magnitude of error in the mean-field intermolecular potential can dwarf the interaction energy itself. Though it includes exchange correlation, DFT has long been known to furnish inaccurate intermolecular interaction potentials describing van der Waals forces

[142, 143], charge transfer and Rydberg excited states [144], and strongly-correlated systems, and so a wavefunction-based correlated supplement to the mean-field potential is desirable. The simplest post-HF treatment of electron-correlation effects, often touted as the delightful G-major of quantum chemistry, MP2[145] furnishes very accurate interaction energies for hydrogen-bonded complexes [146, 147] and donor-acceptor interactions in DNA base-pair interactions[148, 149], though it can often overestimate dispersive interactions [148, 150].

An EDA for a local approximation of the MP2 correlation energy based on the dimers-in-molecules (DIM) model[151] has recently been implemented in our group, called the fragments-in-molecules (FIM) method [152], correlating the ALMO EDA polarized reference. Among sundry other intermolecular interactions, FIM has successfully described the water dimer complex, ascribing twenty and twelve percent of the binding energy to mean-field polarization and correlated dispersion, respectively, and twenty-two percent between mean-field and correlated charge transfer, with the rest attributed to frozen electrostatics. Although presently practically limited to large applications, the coupled-cluster[153] methods represent some of the most accurate many-body approaches to computing experimental observables, especially if perturbative triples [154] are included. As such, an ALMO EDA correlated at the coupled-cluster level is desirable, and the development of one at the coupled-cluster singles and doubles (CCSD) level is the focus of the present work.

Herein, we develop the formalism of the ALMO EDA at the CCSD level, with applications to the water dimer, rare gas dimers and other van der Waals complexes, and charge transfer-dominated donor-acceptor interactions in borane adducts. The EDA yields correct intermediate and asymptotic behavior of each energy component and highly accurate interaction potentials for weakly interacting systems, all in the language of intermolecular interactions that is at once intuitive and instructive.

3.2 Theory

We use the following notation: $i, j, k, l, ...$ denote MOs spanning the occupied subspace; $a, b, c, d, ...$ denote MOs spanning the virtual subspace; $p, q, r, s, ...$ denote any spin-orbital; $\mu, \nu, \sigma, \lambda, ...$ denote AO basis functions lying in the full one-particle Hilbert space; $X, Y, Z, ...$, are fragment labels; we utilize the tensor algebra formalism described previously [155, 156] to work in the nonorthogonal spin-orbital basis, $\{|\phi_p\rangle\}$, and the Einstein summation convention applies where a co-/contravariant index pair occurs.

Subspaces and strong orthonormality

In line with general many-electron correlation theory, we first partition the underlying Hilbert space into two mutually-orthogonal subspaces, the first consisting of levels occupied in the ALMO reference determinant, and the second of the virtual levels, with the associated

projection equation:

$$\hat{1} = \hat{P} + \hat{Q}, \tag{3.1}$$

in which $\hat{P}$ and $\hat{Q}$ are idempotent projectors onto the occupied and virtual spaces, respectively, and for which $\hat{P}\hat{Q} = 0$. Any valid treatment of correlation must guarantee this condition of so-called *strong orthogonality*, whereby all functions lying in the virtual space are orthogonal to functions lying in the occupied space, thus satisfying $\mathbf{g}_{ia} = \mathbf{0}$, where $\mathbf{g}_{pq}$ is the matrix of MO overlaps, $\langle\phi_p|\phi_q\rangle$. In other words, excited determinants must be strictly orthogonal to the reference.

The eigenvectors of the converged SCF MI Fock matrix are *i*) neither generally orthogonal *within* a Hilbert subspace, *ii*) nor are they orthogonal *amongst each other*. That is, $\mathbf{g}_{pq} \neq \delta_{pq}$. We thus begin by obtaining a new set of virtuals, $\{|\tilde{\phi_a}\rangle\}$, strongly orthogonal to the set of occupied orbitals, viz., satisfying $\mathbf{g}_{\tilde{\mathbf{i}}\tilde{\mathbf{a}}} = \mathbf{0}$, and related to the old set $\{|\phi_a\rangle\}$ by:

$$|\tilde{\phi_a}\rangle = \hat{Q}|\phi_a\rangle = (\hat{1} - \hat{P})|\phi_a\rangle = (\hat{1} - |\phi_i\rangle\langle\phi^i_\bullet|)|\phi_a\rangle, \tag{3.2}$$

and the transformation matrix $\mathbf{Q}$ in the AO representation is given by,

$$\mathbf{Q}_{\mu\nu} = \mathbf{S}_{\mu\nu} - \mathbf{S}_{\mu\lambda}\mathbf{C}^{\dagger\lambda}_{\bullet i}\mathbf{g}^{ij}\mathbf{C}_{j\bullet}{}^{\sigma}\mathbf{S}_{\sigma\nu}, \tag{3.3}$$

where $\mathbf{g}^{ij}$ is an element of the occupied block of the contravariant metric matrix, $\mathbf{g}^{pq}$, $\mathbf{S}$ is the AO overlap matrix, and $\mathbf{C}$ is the MO by AO ALMO coefficient matrix. In projecting out the occupied from the virtual space, we are left with strongly-orthogonal subspaces.

At this point, we orthonormalize the orbitals within each subspace to simplify the otherwise involved nonorthogonal coupled-cluster projection equations, permissible since the SCF MI energy is invariant to nonunitary transformations performed within each orbital subspace separately. We expand the set of new orthonormal functions $\{|\tilde{\phi_p}\rangle\}$ in terms of the nonorthogonal (ALMO) set, $\{|\phi_p\rangle\}$, carrying out the orthonormal transformation for each subspace separately:

$$|\tilde{\phi_q}\rangle = |\phi_p\rangle X^p_{\tilde{q}}, \tag{3.4}$$

where the transformation matrix $\mathbf{X}$ is determined to guarantee $\langle\tilde{\phi_p}|\tilde{\phi_q}\rangle = \delta_{pq}$, and by symmetric orthogonalization, the matrix equation $\mathbf{X}^\dagger\mathbf{g}\mathbf{X} = 1$ is solved for $\mathbf{X} = \mathbf{g}^{-\mathbf{1/2}}$. In this orthogonalization procedure, a small degree of locality is sacrificed, as the freshly-orthogonalized functions extend spatially to other fragments' nuclei, by construction. The story is worse for the virtual functions, as they are generally more delocalized than the occupied functions to begin with, and the problem of "orthogonality tails" is exacerbated by the *necessary* inclusion of diffuse functions in the AO basis set for applications of interest, whereby resultant diffuse virtual MOs become no longer imputable to a specific molecular fragment. This is due to the fact that symmetric orthogonalization treats the AO basis functions democratically,

viz., a tight s-type MO on one fragment unfavorably mixes in some diffuse character from an AO centered on a distant fragment.

To remediate this problem, we localize the virtual space by exploiting the automatic locality of atom-centered AO functions, with the method of Subotnik and Head-Gordon[157]. In their algorithm, the Hilbert space is partitioned into a minimal basis space which includes the ultimately localized occupied ($\mathcal{O}$), a chemically-meaningful valence virtual spaces ($\mathcal{V}$), and a "hard" virtual space ($\mathcal{H}$) that includes all of the diffuse AOs,

$$\mathcal{A} = \mathcal{O} \cup \mathcal{V} \cup \mathcal{H}. \tag{3.5}$$

First, a set of so-called "proto-hard" virtuals specific to each atom is constructed by projecting the atom's minimal STO-3G basis $\{|\chi_q\rangle\}$ onto the eigenvectors of the atomic SCF, $\{|\omega_q\rangle\}$,

$$|\gamma_q\rangle = \left(\sum_p |\omega_p\rangle\langle\omega_p| \right) |\chi_q\rangle, \tag{3.6}$$

producing a minimal atomic basis space $\{|\gamma_q\rangle\}$. The occupied levels are then projected out of this space. Next, projecting the STO-3G basis onto the ALMO basis, $\{|\phi_p\rangle\}$,

$$|\psi_q\rangle = \left(\sum_p |\phi_p\rangle\langle\phi_p| \right) |\chi_q\rangle, \tag{3.7}$$

produces a minimal molecular basis space $\{|\psi_p\rangle\}$, from which the occupied space is then projected out, and the resulting minimal valence virtual space (as well as the occupied space) is localized with the Boys[158] procedure. The hard virtual space is constructed by projecting each atom's AOs onto $\mathcal{H}$, and then maximizing the overlap between this set and the set of proto-hard virtuals constructed earlier. Thus, we expand our ALMO virtuals in a minimal localized valence virtual space, and an atom-localized (and by extension, fragment-localized), hard virtual space. We don't hesitate to mention that the results of the EDA will depend on both the orthogonalization procedure and the localization scheme, though we feel we have straightforwardly provided for strongly-orthogonalized, internally orthogonal orbital subspaces in a natural way.

Coupled-cluster EDA

The above manipulations leave us with a reference determinant $|\Phi_o\rangle$ of strongly-orthogonal subspaces, orthogonal among themselves. We abandon the co- and contravariant distinction at this point, as orthogonalization removes the biorthogonal character of the equations. We

employ the standard exponential ansatz for the CC wavefunction, $|\Psi\rangle = e^{\hat{T}}|\Phi_o\rangle$, and proceed to solve the standard CCSD projection equations,

$$\langle\Phi_o|\bar{\hat{H}}|\Phi_o\rangle = E_{CCSD}, \tag{3.8}$$

$$\langle\Phi_i^a|\bar{\hat{H}}|\Phi_o\rangle = 0, \tag{3.9}$$

and

$$\langle\Phi_{ij}^{ab}|\bar{\hat{H}}|\Phi_o\rangle = 0, \tag{3.10}$$

for $\hat{T}$ and E_{CCSD} , where $\bar{\hat{H}} = e^{-\hat{T}}\hat{H}e^{\hat{T}}$ and $\hat{T} = \hat{T}_1 + \hat{T}_2$, and the CCSD correlation energy is given by:

$$E_{CCSD}^{corr} = \sum_{ia} f_{ia}t_i^a + \frac{1}{4}\sum_{ijab} II_{ijab}t_{ij}^{ab} + \frac{1}{2}\sum_{ijab} II_{ijab}t_i^a t_j^b, \tag{3.11}$$

where f_{ia} represents the fock operator in the orthogonalized ALMO representation, $\langle\phi_i|\hat{f}|\phi_a\rangle$, and II_{ijab} is the two-electron antisymmetrized integral, $\langle\phi_i\phi_j||\phi_a\phi_b\rangle$.

Consider the dimer system $X \circ Y$ composed of fragments X and Y. The binding energy is given in the supermolecule approach as

$$\Delta E_{bind} = E(X \circ Y) - (E(X) + E(Y)), \tag{3.12}$$

where $E(X \circ Y)$ is the energy of the complex, and $E(X)$ and $E(Y)$ are the energies of the free fragments, each in its cluster geometry. Each term in eq. 3.12 includes both mean field- and correlation-level contributions,

$$\Delta E_{bind} = \Delta E_{bind}^{SCF} + \Delta E_{bind}^{corr}, \tag{3.13}$$

and we expand the terms in equation 3.13 by level of theory:

$$\Delta E_{bind} = (E(X \circ Y)_{SCF} - E(X)_{SCF} - E(Y)_{SCF}) + \tag{3.14}$$

$$(E(X \circ Y)_{CCSD}^{corr} - E(X)_{CCSD}^{corr} - E(Y)_{CCSD}^{corr}). \tag{3.15}$$

As in the SCF-level ALMO EDA, we decompose the first (ΔE_{SCF}) term of eq. 3.13 as $\Delta E_{frz} + \Delta E_{pol}$; we don't include the standard SCF-level charge transfer term, ΔE_{ct}, because we haven't allowed for orbital delocalization. Rather, we're concerned with correlating a basis of fragment-localized, self-consistently-polarized spin-orbitals, and so charge transfer effects are thus expected to be captured subsequently as part of the correlation treatment. Specifically, the Fock singles term of eq. 3.11 represents the infinite-order energetic contribution due to occupied-virtual mixings, exactly what is sought in the mean-field charge-transfer term.

As for the correlated portion of the EDA, we take the sum of those terms in eq. 3.11 whose

orbital indices belong to any one fragment and only that fragment as its intra-fragment correlation, the sum of which not surprisingly dominates the correlation energy, as noncovalent interactions are generally weak in comparison. We subtract these from the full $X \circ Y$ correlation energy to give ΔE^{corr}_{CCSD}, the inter-fragmental correlation energy. In our scheme, we decompose the inter-fragmental correlation into dispersive correlations, ΔE_{disp}, and charge transfer components, ΔE_{ct}:

$$\Delta E_{CCSD} = \Delta E_{disp} + \Delta E_{ct}, \tag{3.16}$$

and anticipate that these terms tend to zero smoothly at infinite inter-fragmental separation. We take ΔE_{disp} as those terms in 3.11 that include I) concerted excitations, where each fragment promotes an electron to one of its own virtual levels, and II) charge-conserving inter-fragment exchange, where each fragment promotes an electron to a virtual belonging to the other fragment. The form of the $\hat{T}_2$ operator allows naturally for a mathematical rendering of the above delineations:

$$\begin{aligned} \Delta E_{disp} \leftarrow & I)\ \{ia\} \otimes \{jb\} \mid (i, a \in X) \wedge (j, b \in Y) \oplus \\ & II)\ \{ia\} \otimes \{jb\} \mid (i, b \in X) \wedge (j, a \in Y). \end{aligned} \tag{3.17}$$

We decompose ΔE_{ct} as those excitations producing an uneven number of particle and hole excitations on a given fragment. We include, for example, I) ionic charge transfer, where two occupied orbitals on one fragment are promoted to virtual levels on another fragment, and II) dispersive charge transfer, where a pair of occupied orbitals on separate fragments are promoted to occupy virtual levels on either one of the fragments:

$$\begin{aligned} \Delta E_{ct} \leftarrow & I)\ \{ia\} \otimes \{jb\} \mid (i, j \in X) \wedge (a, b \in Y) \oplus \\ & II)\ \{ia\} \otimes \{jb\} \mid (i, a, b \in X) \wedge (j \in Y) \oplus \\ & III)\ \{ia\} \otimes \{jb\} \mid (i, j, a \in X) \wedge (b \in Y). \end{aligned} \tag{3.18}$$

The reader will note that these statements are symmetric to permutation of fragment labels, that there is only one particle-hole pair in the case of charge transfer contribution due to the Fock term in eq. 3.11, and that two hole-particle pairs are realizable with all the $\hat{T}_2$ terms and the terms quadratic in $\hat{T}_1$. We correct for BSSE in the charge transfer terms by the counterpoise method [137].

Thus, the total ALMO CCSD interaction energy is decomposed as

$$\Delta E_{bind} = \Delta E_{frz} + \Delta E_{pol} + \Delta E_{disp} + \Delta E_{ct}. \tag{3.19}$$

It should be mentioned in passing that the canonical and ALMO CCSD energies are not formally equivalent, as they are not related by a unitary transformation. The energy obtained from the cluster ansatz is non-variational, and so we cannot know which is closer

to the exact answer, even though both the canonical and ALMO references are obtained self-consistently. Canonical CCSD will generally predict a larger well-depth, but the differences are small. This is likely because the orbital reference is locally-constrained (though the effects of the constraint vanishes in the limit where the fragments are non-overlapping). The logic given here can also be extended to triple substitution - a topic we hope to consider in the future.

3.3 Results

All calculations were performed using a modified version of Q-Chem[98]. Basis set and geometry information is given where appropriate.

Water dimer

The water dimer is among the most widely-studied molecular complexes, examined extensively both experimentally and computationally, with a high-level non-zero-point-corrected, BSSE-corrected binding energy $D_e = 5.03$ kcal/mol obtained at the CCSD(T)/CBS-limit level [159], and with an experimental binding energy estimated as 4.91kcal/mol by regression analysis of observables determined from microwave, terahertz, and infrared vibration-rotation-tunneling (VRT) spectroscopy [160].

The global minimum of the dimer is of C_s point-group symmetry, with the intramolecular covalent O-H bond in line with the intermolecular O-H hydrogen bond, and, interestingly, with the molecular dipoles not optimally aligned, but rather considerably offset, suggesting a delicate balance between donor-acceptor orbital interactions and exchange-repulsion. As such, an accurate description of the rich interplay of elements contributing to the water dimer hydrogen bond has become, in a sense, the "holy grail" for researchers developing EDA methods, and the question of what elements are important is not without considerable controversy.

The KM EDA at the HF level produced results consistent with a picture that the hydrogen bond is dominated by permanent electrostatics [123] (a little larger than the total binding energy itself), but the calculated binding energy was woefully chemically inaccurate, highlighting the importance of explicit correlation. RVS SCF and CSOV produced similar results [131, 161]. NEDA, on the other hand, though it produced nearly the same overall binding energy as KM, suggested that the hydrogen bond is fundamentally coordinate-covalent in character, the prevalent contribution being a $n(\mathrm{O}) \rightarrow \sigma^*(\mathrm{O\text{-}H})$ donor-acceptor interaction, obtaining a charge transfer term just shy of two times the total binding energy [129]. It should be mentioned quickly that the DFT/B3LYP flavors of NEDA and CSOV laudably reproduce the water dimer binding energy to within chemical accuracy [161, 162].

Though the fact that different EDAs produce quantitatively different binding energies and

basis set	ΔE_{frz}	ΔE_{pol}	ΔE_{ct}	ΔE_{disp}	ΔE_{bind}
cc-pVDZ	-2.36	-0.780	-0.654	-0.704	-4.52
aug-cc-pVDZ	-1.51	-1.10	-0.817	-1.24	-4.67
cc-pVTZ	-1.98	-0.963	-1.080	-1.043	-5.07
aug-cc-pVTZ	-1.34	-1.34	-0.838	-1.26	-4.78

Table 3.1: Tabulated decomposition elements for the C_s water dimer with basis set extension / kcal/mol.

interaction components for water dimer is somewhat disconcerting, the ALMO EDA scheme stands out because it has the advantage of producing intermediate self-consistent energies that are variationally-optimized, and has enjoyed successful application at the DFT/B3LYP level to the water dimer, where frozen interactions, polarization, and charge transfer were shown to contribute nearly evenly to the chemically-accurate binding energy [76], has recently cleverly been employed to shed light on the effects of charge transfer on vibrational spectra in model hydrogen bonding systems [141], and to medium- to large-sized water clusters, where it was determined that two-body terms were contained primarily in the polarization contribution, whereas charge transfer and frozen interactions were primarily three-body in nature[163], a logical result given the nature of these contributions, lending credence to the validity of the ALMO EDA scheme.

We present the counterpoise-corrected results of our ALMO CCSD EDA for the water dimer in different basis sets (Table 3.1) to demonstrate the stability of the components as the basis set approaches completeness. In our most accurate calculation at the aug-cc-pVTZ basis, the components are fairly balanced, with mean-field level frozen electrostatics slightly larger, and with a binding energy calculated at 4.78 kcal/mol, recovering 95% of the counterpoise-corrected CCSD(T)/CBS binding energy [159]. Charge-transfer interactions are dwarfed by polarization interactions when diffuse functions are included, consistent with the perturbative FIM results [152], and with the ALMO EDA at the DFT/B3LYP level[76], but nearly equivalent otherwise. Overall, the results of the decomposition are consistent with those of the KM and reduced-space methods, emphasizing electrostatics and polarization, but with the advantage of yielding quantitative agreement with high-level benchmarks.

It is necessary on physical grounds that *i*) polarization and dispersion fall off as $\sim R^{-6}$ in the intermolecular distance, the lowest-order term in London's [119] expansion of the fluctuation potential in powers of R^{-1}, and *ii*) that charge transfer terms fall off exponentially, with the inter-fragmental orbital-pair overlap. We follow the hydrogen-bond breaking coordinate to verify their intersection, and the intersection between the mean-field polarization and CCSD-level charge transfer (Fig. 3.1). As R(O-H) is decreased, squishing the donor H and acceptor O electron densities together, Pauli and electrostatic repulsions described in ΔE_{frz} overwhelm all other contributions, and beyond the equilibrium region, frozen electrostatics represent the only sizable contribution to the binding energy, as the dipole-dipole potential

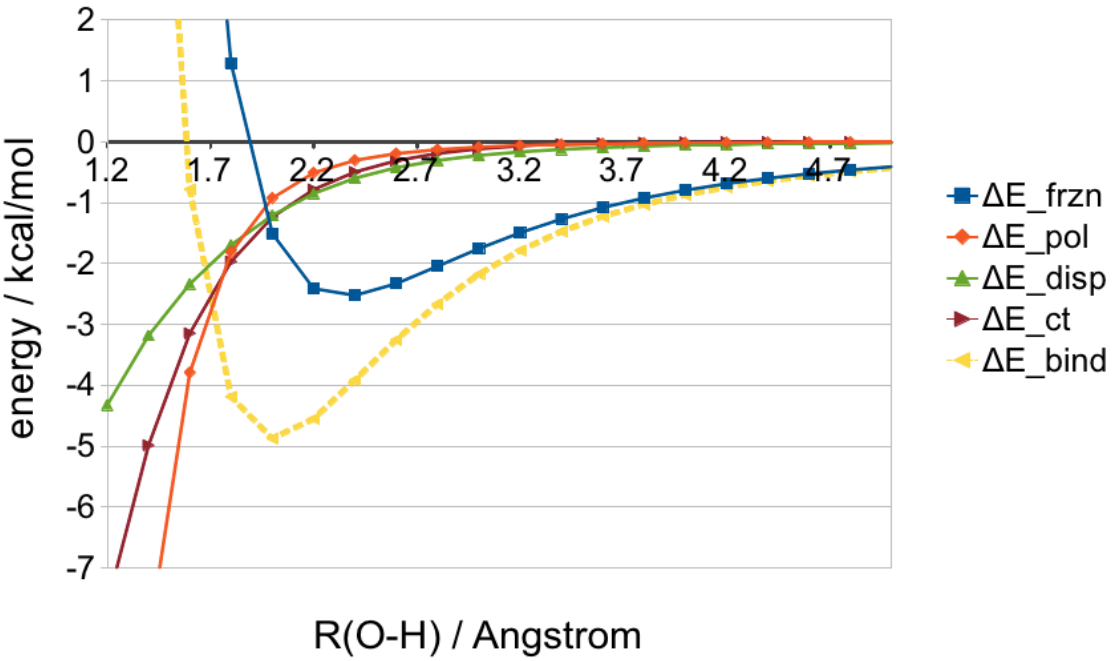

Figure 3.1: Binding energy components for C_s-symmetry water dimer along the hydrogen bond-breaking coordinate performed in the aug-cc-pVDZ basis.

is more shallow, falling off as $\sim R^{-3}$. In the equilibrium region, however, it appears that the components contribute nearly equally to the stabilization of the dimer, underscoring the complex structure of the water dimer hydrogen bond.

Rare gas and other dispersion-bound complexes

Unlike ionic or polar interactions, weak dispersion-dominated interactions due to van der Waals forces can be difficult to characterize, since these forces arise as a direct consequence of electron correlation and thus require high-level theory. Successful efforts have been made recently[164–169] to correct the inadequacies inherent in the DFT and MP2 treatments of long-range dispersion effects. The main source of error in the MP2 interaction energy, for instance, is that the leading contribution to the description of the long-range interaction is dependent on an overestimation of the second-order dispersion coefficients, C_6R^{-6} constructed from the uncoupled (static) HF polarizabilities of the isolated systems[170]. The general strategy employed to repair this has been to add C_6R^{-6} terms determined self-consistently at the coupled HF level to the intermolecular binding energy with the hope that the longe-range C_6 coefficients are consistent with dynamic polarizabilities. These correc-

dimer	ΔE_{frz}	ΔE_{pol}	ΔE_{ct}	ΔE_{disp}	ΔE_{bind}	$\Delta E_{bind,\ ref}$ [173]
He_2	0.0112	-0.000946	-0.00450	-0.0264	-0.0206	-0.022
Ne_2	0.0261	-0.0213	-0.0161	-0.0752	-0.0865	-0.084
Ar_2	0.126	-0.000466	-0.0775	-0.299	-0.251	-0.285

Table 3.2: counterpoise-corrected binding energy components for rare gas dimers performed in the aug-cc-pVTZ basis / kcal/mol. Minimum-energy geometries were taken from counterpoise-corrected CCSD/aug-cc-pVTZ benchmark data [174].

tions have been employed successfully[167, 168], producing smooth potential curves for van der Waals complexes of CCSD(T) quality. Indeed, one could make a case for the immediate improvement of existing DFT/MP2-based EDA schemes for the treatment of van der Waals complexes by adding the empirical correction to the dispersion component, as happens when, e.g., B3LYP-D or ωB97X-D is used.

The coupled-cluster-level wavefunction, which includes disconnected triples, does not suffer as much from these shortcomings, producing more accurate van der Waals potentials, of course at the expense of being an order more costly computationally in the number of molecular orbitals than canonical MP2 (two orders in the case of DFT).

We present the results of our EDA for rare gas dimers in Table 3.2. Not surprisingly, dispersion represents the most substantial contribution to the interaction energy in each case. It should be noted that the mean-field components ΔE_{frz} and ΔE_{pol} considered alone fall short of producing a stable complex, and the addition of readily-computed mean-field charge transfer (not shown), determined subtractively from the full counterpoise-corrected SCF binding energy, still produces a positive ΔE_{bind}, in line with the notion that explicit correlation is required to describe dispersion. Indeed, supplementation with the correlation components results in complex stability and good agreement with the reference calculations at the CCSD(T)/aug-cc-pV5Z level, supplemented with inter-atomic floating bond functions[171] (last column of Table 3.2), and the experimental [172] binding energies for He_2 , Ne_2, and Ar_2 of 0.021, 0.082, and 0.277 kcal/mol, respectively.

We next consider dimers of single-, double-, and triple-bonded organic van der Waals complexes of molecules. Weak forces in this context obviously have important implications in the biochemistry of the lipid bilayer and hydrophobic interactions that bear heavily on protein folding. Accordingly, there has been much recent interest in the accurate computation of van der Waals potentials and vibronic structure for small dispersion-bound organic compounds [175–177]. We decompose the interaction energies of the minimum energy quasi-D_{3d} methane, C_{2h} ethylene, and C_{2v} acetylene dimers in Table 3.3. As in the case of the rare gas dimers, these complexes are not bound at the mean-field level, and dispersive correlation makes up the bulk of the binding energies, competing primarily with the repulsive Pauli contributions. Charge transfer contributions become increasingly important as donor-acceptor bonding-antibonding interactions become spatially feasible and symmetry-allowed with bond

dimer	ΔE_{frz}	ΔE_{pol}	ΔE_{ct}	ΔE_{disp}	ΔE_{bind}	$\Delta E_{bind,\ ref}$
$(CH_4)_2$	0.370	-0.00828	-0.138	-0.726	-0.502	-0.53[159]
$(C_2H_4)_2$	1.09	-0.065	-0.351	-1.82	-1.15	-1.37[179]
$(C_2H_2)_2$	0.401	-0.327	-0.403	-1.02	-1.35	-1.54[178]

Table 3.3: counterpoise-corrected binding energy components for van der Waals complexes performed in the aug-cc-pVDZ basis / kcal/mol. The methane dimer minimum geometry was taken from counterpoise-corrected CCSD(T)/CBS S22 benchmark set [159]. The ethylene and acetylene dimers were optimized at the RI-MP2[180]/aug-cc-pVDZ level of theory. $\Delta E_{bind,ref}$ values for ethylene and acetylene were computed at the CCSD(T)/aug-cc-pVTZ level.

unsaturation, demonstrated here in the shrinking ratio of dispersion to charge transfer in the degree of unsaturation, though dispersion remains, by far, the more important contribution to binding. Quasi-C_{2v} acetylene represents a very interesting case of T-stacking, whereby the electron-rich alkyne bond donates electron density to a terminal σ^*(C-H) bond of the other acetylene, making a "π-type hydrogen bond"[178], albeit a lot weaker than a more traditional hydrogen bond. Total binding energies for the methane, ethylene, and acetylene dimers compare favorably with the reference binding energies in the last column of Table 3.3.

Charge transfer-dominated borane adducts

Dative bonds represent another important class of intermolecular interactions, characterized by the donation of a Lewis base lone electron pair to a vacant orbital of an acceptor Lewis acid [181]. Donor-acceptor complexes of borane adducts represent textbook cases of dative complexes, and have been studied extensively. The promotion of a donor electron pair to to a vacant $2p$ orbital of boron stabilizes such complexes considerably, with interaction energies much stronger than hydrogen bonds, but weaker than formally ionic complexes, and with the repulsive proximity of the electron pair on complex formation severely distorting the trigonal planar D_{3h} borane to the trigonal pyramidal C_{3v} orientation. Ammonia-borane (H_3NBH_3) is an interesting $n(\mathrm{N}) \rightarrow 2p(\mathrm{B})$-stabilized complex, while in the more exotic carbonyl-borane ($OCBH_3$) interaction, CO serves as both a σ donor and a π^* acceptor in back-donation from each of the σ(B-H) bonds. We present the results of our EDA to untangle the binding components of these charge transfer complexes and cyanide-borane (BH_3CN^-) in Table 3.4.

As expected, in all three donor-acceptor complexes, charge transfer is the most substantial component of the correlation-level contribution. Mean-field polarization also represents a sizable portion, particularly in BH_3CN^-, as cyanide is negatively-charged, and has a fairly large dipole moment, and in BH_3CO where the dipole moment points toward C in its most viable resonance form. In line with the previous conclusions regarding these borane adducts

dimer	ΔE_{frz}	ΔE_{pol}	ΔE_{ct}	ΔE_{disp}	ΔE_{bind}	$\Delta E_{bind,ref}$
BH_3NH_3	31.5	-39.5	-14.2	-6.30	-28.5	-28.5[182]
BH_3CO	76.0	-49.48	-34.03	-8.71	-16.2	-14.6[183]
BH_3CN^-	42.1	-70.4	-29.6	-7.98	-65.8	-77.37[a]

Table 3.4: counterpoise-corrected binding energy components for donor-acceptor borane adducts performed in the aug-cc-pVDZ basis / kcal/mol. BH_3NH_3, BH_3CO, and BH_3CN^- minimum structures were optimized at the RI-MP2/aug-cc-pVDZ level of theory. $\Delta E_{bind,ref}$ values for BH_3NH_3 and BH_3CO were computed using CCSD(T)/aug-cc-pVDZ and full CI [184] /general DZ levels, respectively. [a] $\Delta E_{bind,ref}$ for BH_3CN^- was calculated at the CCSD(T)/aug-cc-pVDZ level.

at the ALMO EDA B3LYP/6-31(+,+)G(d,p) level[76], BH_3CO is a better π^* acceptor than BH_3CN^- , likely due to the fact that the π^*(C=O) virtual is lower-lying energetically than π^*(C≡N), and thus closer to the σ(B-H) energy, and so it is a reasonable assertion from the view of perturbative energy-lowering due to occupied-virtual mixings.

The computed binding energies by ALMO CCSD for BH_3NH_3 and BH_3CO are in impressive agreement with the reference values, while BH_3CN^- appears to be slightly underbound, likely for the reason mentioned above that the reference is constrained. Experimental estimates of the binding energy for BH_3CO are highly disparate, ranging between 18.8-27.5kcal/mol[185–188].

3.4 Discussion and Future Direction

We have presented the formalism and applications of the ALMO EDA at the CCSD level, examining various intermolecular complexes and ascribing to binding well-defined interaction components, and with reasonable success for the systems considered. Desirable improvements might include generalization to systems larger than dimers and extension of the correlative treatment to include perturbative or full triples, though both of these hopes would require careful consideration in the definitions of the contributions arising from both the $\hat{T}_3$ terms, and terms in the cluster operator containing indices belonging to more than two fragments, and finally, generalization of the CCSD-level ALMO EDA to open-shell systems to access the rich chemistry of radicals and complexes of high-spin multiplicity states.

Chapter 4

Lower-bound intermolecular polarization

4.1 Introduction

There is no question that interest in intermolecular interactions with an eye toward elucidating the interplay of forces underlying weak potentials has grown in recent years. With it, so has the number of so-called energy decomposition analysis (EDA) schemes, designed to resolve a quantum mechanical (QM) interaction energy into physically-based components. In addition to direct use for insight or interpretive purposes, EDAs can serve as high-level QM tools in applications ranging from guiding drug functionalization [189, 190] to designing force fields for molecular mechanics (MM) simulations [191].

The physical contributions that give rise to weak interactions between distant molecules whose densities do not overlap have long been well-characterized [192]. At a given separation, the magnitude of interactions can be directly evaluated from properties of the individual (isolated) molecules. They include *i*) long-range *permanent* electrostatic interactions coupling the monopole, dipole, quadrupole, and higher-order moments of the isolated species; *ii*) additional *induced* electrostatic interactions, which arise from distortions of the charge densities due to electric fields emanating from nearby molecules. For a given field, induction is determined by static molecular polarizabilities, e.g., dipole, quadrupole, etc.; and *iii*) weaker dispersive forces, or van der Waals interactions, resulting from instantaneous multipole interactions, of strength governed to leading-order by the C_6 coefficients of the molecules.

When the interacting molecules overlap, additional interactions arise. In qualitative terms, these effects are well-known, and are usually described in molecular orbital (MO) language [106]. Specifically, they include *iv*) Pauli repulsions that distort the density due to the overlap between occupied levels on neighboring molecules, and *v*) attractive donor-acceptor (dative) interactions that arise when there is sufficient overlap between occupied

and empty levels of neighboring molecules, leading to partial charge transfer. In quantitative terms, there is no unique prescription for partitioning the observable binding energy in the overlapping regime. For example, in MO terms, when molecular neighbors overlap, there are many ways to infer occupied and empty orbitals of each molecule, which affects the relative values of induction and charge transfer. The task of an EDA is to provide a well-defined procedure for calculating each contribution. Exploring different definitions of these components and resolving differences between different EDAs (provided they are physically-defensible) is a basis for deepening our understanding of intermolecular interactions.

While summarizing the full range of available EDAs is a task for a detailed review, it is useful to identify some of the most widely-used methods, and to distinguish those that *decompose* a given level of calculation (e.g. DFT) from those which also aim to provide a method for efficiently *calculating* the interactions. Considering first the constructive approaches to intermolecular interactions, symmetry-adapted perturbation theory (SAPT) [193, 194] is a many-body generalization of Heitler-London polarization theory that treats the inter-monomer coupling as the fluctuation potential. SAPT has become popular, particularly with the development of inexpensive density functional theory (DFT) approaches for computing previously demanding terms [195, 196]. Direct use of the many-body expansion [197] to separate pairwise, three-body, and higher terms is another strategy in approaches such as the fragment MO method [198, 199]. Finally, it is important to note that results on the form of intermolecular interactions from decomposition methods such as those discussed below have been incorporated into efficient computational approaches such as the effective fragment potential (EFP) method [200, 201], a step towards even more highly-simplified methods such as polarizable MM potentials [202, 203].

Regarding decompositions, the pioneering variational Kitaura-Morokuma (KM) EDA [123] partitions the binding energy into (including, but not limited to) geometric distortion, electrostatic, polarization, and charge-transfer components. The related Ziegler-Rauk procedure was developed essentially at the same time [204, 205]. The natural orbital EDA (NEDA) [129] scheme is used as part of the widely-employed natural bond orbital analysis [106, 206, 207]. A markedly different "density-based" EDA[208] has been proposed recently, which constrains the electrostatic density to remain identical to the superposed density while the electrostatic interaction energy is determined variationally. Many other EDAs have provided useful modifications and improvements to the basic KM framework [131, 132, 209–211]. One class of improvements is the use of block-localized, [212, 213] or, equivalently, absolutely-localized MOs (ALMOs) [76, 138] to variationally describe polarization. The ALMOs are determined by solving nonorthogonal, locally-projected SCF equations for molecular interactions (SCF MI) as first proposed by Stoll [72], and later recast in different ways [214, 215], and then efficiently implemented [75].

The ALMO EDA provides a self-consistent determination of intramolecular polarization as the energy-lowering upon solving the SCF-MI equations with the MO coefficient matrix constrained to be block-diagonal in each of the cluster molecules. The molecule-blocking prevents intermolecular charge transfer while simultaneously allowing for relaxation of each

MO in the field of all other electrons and nuclei. This natural separation of charge transfer and self-consistent polarization is a merit of the approach. Formally, the binding energy in the ALMO EDA is the sum of four terms: *i*) *geometric distortion* (gd), defined as the energy required to deform an isolated molecule's internal coordinates to those consistent with the cluster geometry, and evaluated as the energy difference between the complex in its equilibrium geometry and the sum of its elements', each taken at its vacuum minimum,

$$\Delta E_{gd} = E_{AB}|_{complex} - E_A|_{min.} - E_B|_{min.}; \tag{4.1}$$

ii) *frozen orbital* (frz) interactions, accounting for both permanent electrostatic contributions and Pauli repulsions, corresponding to bringing infinitely-separated, distorted molecules together, and operationally determined from the energy associated with the supermolecular density matrix formed from the converged MO matrices of the isolated molecules, each in its complex geometry,

$$\Delta E_{frz} = E_{AB}\{\mathbf{P_{frz}}(\mathbf{C_A}, \mathbf{C_B}))\}|_{complex} - E_A(\mathbf{C_A})|_{complex} - E_B(\mathbf{C_B})|_{complex}; \tag{4.2}$$

iii) *polarization* (pol), defined as the relaxation of fragment ALMOs in the field of all other ALMOs, but with the block-diagonal constraint in place,

$$\Delta E_{pol} = E_{AB}(\mathbf{P_{pol}}) - E_{AB}(\mathbf{P_{frz}}); \tag{4.3}$$

and *iv*) *charge transfer* (ct), stabilization due to intermolecular relaxation of ALMOs to the canonical orbitals,

$$\Delta E_{ct} = E_{AB}(\mathbf{P_{can.}}) - E_{AB}(\mathbf{P_{pol}}). \tag{4.4}$$

Taken together, these contributions sum to the full binding energy, $\Delta E^{SCF}_{\text{bind}}$,

$$\Delta E^{SCF}_{\text{bind}} = \Delta E_{gd} + \Delta E_{frz} + \Delta E_{pol} + \Delta E_{ct}. \tag{4.5}$$

Though the ALMO EDA in its current form gives a reasonable decomposition and has enjoyed much recent success in application [79, 216–220] and extension to explicit correlation [80], we acknowledge here that the polarization term has no well-defined basis set limit because there is a point of over-completeness of the underlying basis beyond which relaxation of the ALMO constraint can no longer improve the fragment-localized orbitals. In other words, there is enough variational freedom near the basis-set limit in the constrained orbitals to completely describe their delocalized counterparts, thus invaliding the physical insight of the orbital constraint and rendering polarization and charge-transfer no longer separable. While this may seem like a purely formal objection, it has the practical implication that one *cannot* converge the polarization and charge-transfer components of the ALMO EDA to a well-defined basis set limit. While reasonable stability has already been demonstratedin the aug-cc-pVXZ, X=D,T,Q sequence for the water dimer [221], it is worthwhile to emphasize that this is at best metastability.

This paper focuses on exploring several aspects of the definition and stability of the polarization and charge-transfer contributions to intermolecular interaction energies. First, we present a proposal for the definition of polarization that is designed to yield stable contributions across a wide range of basis set sizes by removing near-linear dependencies between the virtual spaces describing polarization on different fragments. This is accomplished by defining small numbers of polarization functions for each fragment based on singular value decomposition (SVD) of the first-order singles amplitudes associated with the frozen MOs, which are then orthogonalized amongst themselves and relocalized. SVD has been useful in defining the most important orbitals in applications ranging from analyzing excited states [222], to donor-acceptor orbitals in EDA [138], to analyzing electron correlation effects [223] and MP2 [224]. Using the resulting minimal polarization basis, we retain the general structure and terms of the ALMO approach, notably the feature of self-consistent polarization, emphasizing that the added benefit of orthogonal MOs allows for trivial extension of the method beyond a mean-field treatment. This procedure is described in detail in Sec. 4.2.

The second main aspect of the paper consists of numerical results that compare the new approach to polarization against the existing fragment-blocked SCF-MI method as a function of basis set size and composition, energy functional, and geometry, for the model system of the water dimer. These comparisons are undertaken in Sec. 4.3. It is interesting to assess the dependence of calculated polarization and charge transfer contributions for different sequences of basis sets: cc-pVXZ, aug-cc-pVXZ and d-aug-cc-pVXZ, as well as to compare the results obtained at the mean-field Hartree-Fock level against the components calculated with various density functionals. Additionally, since the difficulty in disentangling polarization and charge transfer arises directly from the degree of intermolecular overlap, it is interesting to assess the separation dependence of the differences in results between the new approach and polarization evaluated by the SCF-MI procedure. Some results are also given for the Na^+CH_4 complex, where polarization effects are dominant. We summarize our main conclusions in Sec. 4.4.

4.2 Theory

The Einstein summation convention applies where a co- or contravariant index pair occurs, except for fragment labels. O_A and V_A refer to the number of occupied and virtual spin-orbitals on molecule A. N_A is the number of AO functions centered on A. F is the number of fragments. The indices $i, j, k, l, ...$ denote MOs spanning the occupied subspace; $a, b, c, d, ...$ mean virtual MOs; $p, q, r, s, ...$ are any spin-orbitals; and $\mu, \nu, \sigma, \lambda, ...$ are AO basis functions.

We first discuss the behavior of the SCF-MI eigenvectors as the basis approaches completeness, and then detail a procedure for determining the optimal fragment-tagged variational subspaces to obtain polarized molecular states in the supermolecular field, taken as solutions of a set of constrained equations.

Basis set superposition error (BSSE) and the drawbacks of SCF-MI as a basis for EDA.

The term taken as intramolecular polarization in the ALMO scheme has no basis set limit. It is instructive to examine the general BSSE problem [136] to understand why. Consider computing the binding energy ΔE of the molecular complex $X \circ Y$ within the subtractive supermolecule approach, $\Delta E = E(X \circ Y) - E(X) - E(Y)$. Self-consistent diagonalization of the Hamiltonian operator in the full AO basis will yield a set of orthonormal eigenfunctions, each with an associated eigenvalue equation:

$$\hat{f}|\phi_{pX}\rangle = \varepsilon_{pX}|\phi_{pX}\rangle, \tag{4.6}$$

While each MO formally has amplitudes on all fragments, the fact that this is a complex means that, in general, the MOs can be fragment-localized by standard methods such as Boys [225] or Edmiston-Ruedenberg localization [226]. It is the fact that even after localization $\hat{f}|\phi_{pX}\rangle$ can be resolved into projections onto the fragment basis and its orthogonal complement that gives rise to the BSSE that pockmarks such calculations:

$$\hat{f}|\phi_{pX}\rangle = \hat{f}\ \hat{1}\ |\phi_{pX}\rangle = \hat{f}\hat{P}^X|\phi_{pX}\rangle + \hat{f}(\hat{1} - \hat{P}^X)|\phi_{pX}\rangle, \tag{4.7}$$

where $\hat{P}^X = |\omega_{X\mu}\rangle S^{-1}_{X\mu\nu}\langle\omega_{X\nu}|$. Specifically, the second term on the right-hand side of eq. 4.7 allows for variational optimization of $|\phi_{pX}\rangle$ via access to functions that are not centered on that fragment. The consequence is systematic overestimation of binding energies due to inflation of the $E(X \circ Y)$ term.

Of course, at the complete basis set limit, the second term approaches zero, and the basis functions centered on fragment X span a sufficient space to describe X's eigenvectors without any borrowing. Away from this limit, many methods to counteract BSSE have been developed, of which the most popular is probably the counterpoise method [137], where the energy-lowering due to borrowing of extra-fragment functions is explicitly subtracted from the supermolecular result $E(X \circ Y)$. Other approaches include forcible elimination of the BSSE term of eq. 4.7 from the Roothaan equations [227, 228], but at the expense of the Hermiticity of the matrix representation of the Hamiltonian operator.

Another strategy is that employed by the SCF-MI approach, detailed above, which constrains the MO coefficient vectors $\{\mathbf{C_{pX}}\}$ to be block-diagonal (absolutely-localized) in the interacting fragments,

$$|\phi_{pX}\rangle = |\omega_{\mu X}\rangle C^{\mu X}_{\bullet\ pX}, \tag{4.8}$$

By performing variational optimization with fragment-blocking of the MO coefficients, BSSE is prohibited by construction: ALMOs tagged to a given fragment cannot employ basis functions from other fragments.

The use of the SCF-MI procedure within an EDA for describing the energy-lowering due to polarization relies on the physically-intuitive assumption that fragment-blocking the

MO coefficient matrix also prohibits charge transfer from a given fragment to any other. Since an ALMO tagged to a given fragment cannot contain contributions from AOs on other fragments, dative interactions should be prohibited. Thus polarization is any energy-lowering where the trace of the on-fragment density matrix operator is preserved, or in other words, where electrons are not shuttled between molecules. Charge transfer can then be associated with any remaining energy-lowering that is achieved when the ALMO constraint is lifted.

However, separating the energy-lowering associated with polarization and charge transfer based on the SCF MI constraint of eq. 4.8 has deficiencies. It can only be used with one-particle basis sets that are atom- or fragment-tagged, and thus is natural with AO basis sets, but cannot be used directly with a plane wave expansion. Furthermore, even with AO basis sets, at or near the complete basis set limit, a given fragment-tagged MO will already be described optimally and will not benefit from any projection onto the basis functions of a neighboring fragment. Alternatively put, the second term of eq. 4.7 will be reduced to zero (as will the associated charge-transfer term, ΔE_{ct}), and it becomes obvious that the magnitude of the EDA components is basis set-dependent. Thus the success of the ALMO EDA in practice depends upon using a basis set that is not too small (inaccurate total interaction energies), but also not too large (as the ct contribution will progressively be damped away). In practice, the aug-cc-pVTZ basis has appeared to be a reasonable compromise.

General construction.

Our goal is to obtain a small set of linearly-independent functions that are still local (fragment-ascribable) which may be used to described the energy-lowering due to polarization in a way that is stable with respect to basis set extension. Should these functions be non-orthogonal (like AOs), or orthogonal (like MOs)? While either is possible, we shall employ the orthogonal choice here because it ensures zero overlap between the Hilbert spaces associated with different fragments. Furthermore, orthogonalization will generate a basis of fragment-tagged linearly-independent orbitals whose shapes and extents are parametrized by *all* centers, not just a subset, which is appropriate to properly respect antisymmetry between electrons on different fragments [229]. For instance, when two fluorine atoms approach each other to form F_2, the electrons occupying the σ_u^* orbital avoid collapsing into the nuclei by maintaining orthogonality to the mostly unperturbed core $1s$ states, a property that neither of the individual atomic $2p_z$ states exhibited with respect to the core of the other nucleus before the bond was formed. In the same way, the spatial extent and nodal structure of orthogonalized functions centered on one molecule in the field of another should reflect these intermolecular exchange interactions. While orthogonalization will produce delocalization tails extending to other fragments, fragment identity can be maintained via the transformations that we shall detail below. The functions we shall employ are eigenvectors of the intramolecular response density, whose number will be equal to the number of electrons on each fragment.

The starting point for treating intra-fragment polarization is the result of calculations

on individual fragments in the basis of their own AOs, and without any consideration of neighboring molecules, which is the so-called "frozen" orbital calculation. The eigenvectors of the Hamiltonian operator in the frozen orbital representation are *i*) orthogonal *within* a fragment, satisfying $\{p \cup q\} \in X \mid \mathbf{g}^{\mathbf{X}}_{pq} = \delta_{pq}$, where $\mathbf{g}^{\mathbf{X}}_{pq}$ is the matrix of MO overlaps belonging to X, and *ii*) *strongly orthogonal*, whereby all functions lying in the fragment's virtual space are orthogonal to functions lying in its occupied space, $\{i \cup a\} \in X \mid \mathbf{g}^{\mathbf{X}}_{ia} = \mathbf{0}$. These properties are the direct consequence of solving the SCF equations for each fragment independently, guaranteeing a block-diagonal Hamiltonian matrix and idempotent one-particle frozen density. However, any *inter*-fragmental MO pair is neither orthogonal *within* a subspace, nor is it orthogonal *between* subspaces. That is, $\{(p \, \varepsilon \, X) \cup (q \, \varepsilon \, Y)\} \mid \mathbf{g}_{pq} \neq \mathbf{0}$.

As we'd like to unambiguously determine non-overlapping occupied and virtual subspaces, we construct a new set of "projected" virtual orbitals, $\{|\phi'_a\rangle\}$, strongly orthogonal to the global set of occupied orbitals, and related to the old set $\{|\phi_a\rangle\}$ by:

$$|\phi'_a\rangle = \hat{Q}|\phi_a\rangle = (\hat{1} - \hat{P})|\phi_a\rangle = (\hat{1} - |\phi_i\rangle g^{ij} \langle\phi_j|)|\phi_a\rangle, \tag{4.9}$$

and the projection matrix $\mathbf{Q}$ in the AO representation is given by

$$\mathbf{Q}^{\mu}_{\bullet\nu} = \delta^{\mu}_{\bullet\nu} - \mathbf{C}^{\mu}_{\bullet i} \mathbf{g}^{ij} \mathbf{C}^{\dagger\sigma}_{j\bullet} \mathbf{S}_{\sigma\nu}, \tag{4.10}$$

where $\mathbf{S}$ is the AO overlap matrix and $\mathbf{C}$ is the frozen coefficient matrix. The transformation $\mathbf{C'}^{\mu}_{\bullet p} = \mathbf{Q}^{\mu}_{\bullet\nu} \mathbf{C}^{\nu}_{\bullet p}$ smoothly guarantees strong orthogonality, $\mathbf{g}_{ia} = \mathbf{0}$, as $\hat{Q} \to \hat{1}$ in the non-overlapping limit, preserving the original spaces.

We next seek to orthonormalize the orbitals within each subspace separately, noting that the frozen density is invariant to such transformations. performed within each orbital subspace separately. Having already orthogonalized the subspaces, this is sufficient to enforce $\langle\phi_p|\phi_q\rangle = \delta_{pq}$ for all p and q. Generally, we want to transform the nonorthogonal set by

$$|\tilde{\phi_{qY}}\rangle = \sum_{Z} |\phi_{pZ}\rangle X^{pZ}_{\bullet qY}, \tag{4.11}$$

where $\mathbf{X}$ is the orthogonalizer that takes the non-orthogonal set $\{|\phi_p\rangle\}$ to the orthogonal set $\{|\tilde{\phi_q}\rangle\}$. (to keep the notation uncluttered, we have dropped the " $'$ " that denoted the frozen, projected set.)

Schemes rooted in symmetric orthogonalization represent a least-squares minimization of the Hilbert-space distance between a function of the nonorthogonal set $\{|\phi_p\rangle\}$ and the corresponding function of the orthonormal set $\{|\tilde{\phi}_p\rangle\}$. Most generally [230], the sum Z to be minimized is the difference in the vectors pre- and post-orthogonalization,

$$Z = \sum_{p} w_p \int \big|\big| \, |\tilde{\phi}_p\rangle - |\phi_p\rangle \big|\big|^2 d\tau, \tag{4.12}$$

where $\{|\phi_p\rangle\}$ is the non-orthogonal vector set, $\{|\tilde{\phi}_p\rangle\}$ is the orthogonal set, $\{w_p\}$ is a set of weighting scalars, and $d\tau$ represents infinitesimal Hilbert space.

If each non-orthogonal MO contributes equivalently in the construction of the orthogonal spin-orbital (i.e. the matrix of weighting scalars is chosen as $\mathbf{W_p} = 1$) then eq. 4.12 is minimized by choosing $\mathbf{X^p_{\bullet q}} = (\mathbf{g})^{-\frac{1}{2}}_{\mathbf{pq}} \equiv g^p_{\bullet q}$, and we have arrived at the familiar Löwdin (symmetric) prescription for orthogonalization [231]. We transform the occupied space according to

$$|\tilde{\phi_{iA}}\rangle = \sum_B |\phi_{jB}\rangle g^{jB}_{\bullet iA}. \tag{4.13}$$

The "absolute" locality in the AO basis afforded by the ALMO scheme is sacrificed at this point since the freshly orthogonalized functions span the entire occupied space, but they are still imputable to parent fragments because of the relative compactness of the occupied subspace and the least-squares connection, eq. 4.12. The orthonormal occupied set is subsequently tightened by the Boys' localization scheme [225] which, again, leaves the frozen density invariant.

The story is more bleak for the virtual functions since they are more delocalized to begin with, and the problem is only exacerbated by the necessary inclusion of diffuse AOs for applications of interest. Symmetric orthogonalization of this subspace will treat the basis too democratically, mixing on equal footing a relatively tight MO on one fragment with some diffuse MO centered far away, for instance. Consequently, evenly-mixed virtual MOs become hardly imputable to a specific molecule. The crux of the problem is thus the careful delineation of a space belonging to each fragment which a least-squares minimal orthogonalization will not appreciably distort.

More specifically, we want to develop a partitioning of the Hilbert space $\mathcal{H}$ into a minimal valence space (relevant for intramolecular polarization) spanned by the set $\mathcal{M}$ and a "low-impact" space spanned by the more diffuse, Rydberg-like functions $\mathcal{R}$, $\mathcal{H} = \mathcal{M} \oplus \mathcal{R}$, where

$$\mathcal{M} = \bigoplus_A \mathcal{M}_\mathcal{A} \quad \text{and} \quad \mathcal{R} = \bigoplus_A \mathcal{R}_\mathcal{A}, \quad \text{with} \tag{4.14}$$

$$\mathcal{M}_\mathcal{A} = \mathcal{V}_\mathcal{A} \oplus \mathcal{O}_\mathcal{A}, \tag{4.15}$$

and where $\mathcal{O}_\mathcal{A}$ and $\mathcal{V}_A$ are the minimal occupied and virtual spans centered on molecule A and all subspaces are orthogonal, $\mathcal{V}_\mathcal{A} \perp \mathcal{V}_\mathcal{B} \perp \mathcal{R}_\mathcal{B}$. In the subsection below, we develop an approach to obtain the minimal valence space, $\mathcal{M}$, from a perturbation theory of intramolecular polarization in the supermolecular field. Once $\mathcal{M}$ is available, the functions that span it can be orthogonalized via essentially the same scheme described above for the frozen occupied space.

A minimal basis for polarization.

The Fock matrix built from the frozen density will necessarily contain non-zero occupied-virtual coupling elements $\mathbf{f}^{\mathbf{iX}}_{\bullet\mathbf{aY}}$ that arise in response to the perturbation of each isolated fragment by the supermolecular environment. A subspace partitioning for the purpose of variationally determining molecular eigenstates in the supermolecular field can be guided by this fact. Specifically, we can use perturbation theory to examine the on-fragment polarization response, and extract a small set of polarization functions (not exceeding the number of electrons on the fragment) that can *exactly* represent it. Those functions can be used as a basis for a variational treatment of polarization after orthogonalization.

Perturbation theory for either DFT or Hartree-Fock is conveniently cast in terms of the one-particle density matrix, $\mathbf{P}$, and the Fock matrix, $\mathbf{F}$. Given a frozen density, $\mathbf{P}^{(0)}$, we evaluate the Fock matrix as $\mathbf{F} = \mathbf{F}(\mathbf{P}^{(0)})$. Since we are interested only in the intramolecular polarization, we shall consider perturbation theory for a single fragment in the orthonormal space of its frozen occupied orbitals, and its (orthormalized) projected frozen virtuals, defined in eq. 4.9. In other words, each fragment now has its own perturbation problem, and we neglect the interfragment coupling on the grounds that it is charge-transfer-related.

The fragment Fock operator is partitioned into zeroth-order pieces (the OO and VV blocks), and a first-order perturbation (the OV and VO blocks) due solely to the presence of the supermolecular environment: Thus:

$$\mathbf{F} = (\mathbf{F}_{OO} + \mathbf{F}_{VV})^{(0)} + (\mathbf{F}_{OV} + \mathbf{F}_{VO})^{(1)}. \tag{4.16}$$

The problem of minimizing the energy for a perturbed Fock matrix in an orthogonalized basis may be expressed in several equivalent ways: (i) block diagonalization to zero the coupling between the occupied and virtual blocks in the new basis (ii) finding a valid one-particle density matrix that commutes with the Fock matrix, $\mathbf{FP} = \mathbf{PF}$, or (iii) solving the following set of quadratic equations [232, 233]:

$$\mathbf{F}_{VO} + \mathbf{F}_{VV}\mathbf{X}_{VO} - \mathbf{X}_{VO}\mathbf{F}_{OO} - \mathbf{X}_{VO}\mathbf{F}_{OV}\mathbf{X}_{VO} = \mathbf{0}_{VO}, \tag{4.17}$$

and then evaluating the energy-lowering (relative to the unperturbed problem) as

$$\delta E = Tr\left(\mathbf{F}_{OV}\mathbf{X}_{VO}\right). \tag{4.18}$$

This last form is convenient for doing perturbation theory with the partitioning given in eq. 4.16. To zeroth order, it is immediately clear from eq. 4.17 that $\mathbf{X}^{(0)}_{VO} = \mathbf{0}_{VO}$. First-order perturbation theory applied to eq. 4.17 is straightforward assuming that $\mathbf{F}^{(0)}_{VV}$ and $\mathbf{F}^{(0)}_{OO}$ are initially diagonalized such that $F^{(0)}_{ab} = \varepsilon^{(0)}_a \delta_{ab}$ and $F^{(0)}_{ij} = \varepsilon^{(0)}_i \delta_{ij}$. The resulting first-order perturbed amplitudes, $\mathbf{X}^{(1)}_{VO}$, are given as

$$X^{(1)}_{ai} = -F^{(1)}_{ai} \Big/ \left(\varepsilon^{(0)}_a - \varepsilon^{(0)}_i\right) \tag{4.19}$$

with a corresponding second-order energy-lowering obtained by substituting into eq. 4.18. Note that these are exactly of the form obtained when doing Hartree-Fock perturbation theory in the space of single substitutions, but are equally valid for Kohn-Sham DFT.

A solution of the form of eq. 4.19 can be constructed individually for each fragment, say A, describing the first-order polarization effects on that fragment due to the presence of the other components of the complex. On an individual fragment, there are $O_A V_A$ coupling parameters within $\mathbf{X}^{(1)}_{VO}$, so the first-order correction to $|\eta_i\rangle$ will contain V_A components in the orthogonal complement:

$$|\eta^{(1)}_{iA}\rangle = |\eta_{aA}\rangle X^{a(1)}_{\bullet iA}. \tag{4.20}$$

Since typically $O_A << V_A$, it is desirable to condense the information encoded in this sum, by finding a minimal virtual basis sufficient to describe the first-order wavefunction. The first-order result (on a fragment) can be exactly recaptured in this way by performing a singular value (SVD) decomposition of $\mathbf{X}^{(1)}_{VO}$. The SVD is defined as

$$\mathbf{L}_{VV}\mathbf{X}^{(1)}_{VO}\mathbf{R}^{\dagger}_{OO} = \mathbf{x}^{(1)}_{OV}. \tag{4.21}$$

Here $\mathbf{x}^{(1)}_{VO}$ is a rectangular matrix with only O_A non-zero entries lying along the diagonal; these are the singular values. The left eigenvectors, $\mathbf{L}_{VV}$, describe transformations of the original virtual functions into a reduced set of essential virtuals whose number is no greater than O_A.

$$|\gamma_{a'A}\rangle = |\eta_a\rangle L^{aA}_{\bullet a'A}, \quad a' = 1, ..., O_A. \tag{4.22}$$

All other virtual orbitals correspond to zero singular values and retaining only the virtuals above, we are guaranteed to recover the energy-lowering of eq. 4.18 but in a rank-reduced polarization basis. This is our definition of the minimal virtual space, $\mathcal{V}_A$, on fragment A.

This transformation gives an intuitive bond-antibond picture of polarization whereby relaxations through first-order in perturbation theory on a given fragment can be exactly expressed via a minimal polarization basis no larger than the occupied space. The presence of polarization is a direct consequence of violating Brillouin's theorem, ($\mathbf{F}_{VO} = \mathbf{0}$), in the intermolecular environment, as the inhomogeneous term of eq. 4.17 is $\mathbf{F}_{VO}$. The null space of the SVD spanned by the vectors of $\mathbf{L}$ with vanishing singular values will naturally include diffuse molecular states especially as the AO basis set is extended. As the polarization energy of eq. 4.18 is convergent with the basis set provided the perturbation theory is well-behaved, so too will the SVD and minimal polarization orbitals.

The minimal set of virtual functions for the complex can now be defined as the union over fragments of the minimal virtual set, $\{\mathcal{V}_A\}$. However, these functions will not, in general, be orthogonal between fragments, and so we orthogonalize the minimal set of virtual vectors amongst themselves via eq. 4.13, then Boys-localize across the orthonormalized minimal virtual space, paralleling the procedure used for the occupied orbitals to complete

the specification of the functions spanning the minimal basis set for polarization, $\mathcal{M}$. The null space spanning $\mathcal{R}$ is discarded in the minimal scheme because its vectors are extraneous to a description of polarization at the level of perturbation theory, as follows from the SVD, eq. 4.21. However, re-introducing $\mathcal{R}$ after polarization is necessary to guarantee recovery of the full SCF energy and delocalized eigenfunctions.

We note that orthogonalization will reintroduce BSSE into the polarization term, but this is not before the variational subspaces are determined as the span of the minimal eigenset of the first-order orbital response. It is thus assumed that mutual frozen interactions in the approach induce deformations first among a molecule's own electronic distributions, followed by inter-fragment distortions in the interest of orthogonality. We also note that, though we make no explicit reference to the underlying AO basis in the equations determining each molecule's variational space, each's set of response amplitudes $\{X^{aA(1)}_{\bullet iA}\}$ remains ultimately parametrized by fragment-allotted AO functions originating from the frozen set of ALMOs.

Orthogonal SCF for molecular interactions and associated EDA.

We solve the problem of computing the energy-lowering due to intramolecular polarization in a manner similar to the original SCF-MI approach. The polarization energy is taken as the energy-lowering on self-consistently solving subspace-projected fragment-labeled SCF equations constrained to conserve the number of electrons on a fragment, e.g., the trace of the fragment density projector in the fragmental basis remains constant. The charge-transfer stabilization is subsequently determined as the difference between the full SCF energy and the energy of the polarized wavefunction as in the ALMO scheme:

$$\Delta E_{\text{bind}} = \Delta E^{SCF}_{\text{bind}} = \Delta E_{\text{gd}} + \Delta E_{\text{frz}} + \Delta E_{\text{pol}} + \Delta E_{\text{ct}}. \tag{4.23}$$

The above constraint is realized by demanding that the self-consistently polarized set $\{|\psi_{pX}\rangle\}$ – which corresponds to ΔE_{pol} from the energy of the super-system computed with the frozen density (given in eq. 4.2) – simultaneously be described by OV mixings strictly among the vectors of the subsystem X,

$$|\psi_{pX}\rangle = |\gamma_{qX}\rangle U^{qX}_{\bullet pX}, \tag{4.24}$$

and satisfy the variational eigenvalue equation

$$\hat{f}|\psi_{pX}\rangle = |\psi_{pX}\rangle \varepsilon_{pX}, \tag{4.25}$$

where $\hat{f}$ is the standard mean-field or DFT Hamiltonian, and $|\psi_{pX}\rangle$ is what we term a polarized orthogonal local molecular orbital (POLMO) eigenfunction labeled p of the supermolecular Hamiltonian matrix projected into the variational space spanned by fragment X. Developing the working equations, we resolve the identity into properly-idempotent

projectors onto the individual fragment subspaces, $\hat{1} = \sum_X^F \hat{R}_X = \sum_X (\hat{P}_X + \hat{Q}_X)$, with $\hat{P}_X \hat{P}_Y = \hat{P}_X \delta_{XY}$ and $\hat{P}_X \hat{Q}_Y = 0$, and insert above,

$$\sum_Y^F \left(|\gamma_{qY}\rangle \langle {}^{\gamma qY}_{\bullet}| \right) \hat{f} \sum_Z^F \left(|\gamma_{rZ}\rangle \langle {}^{\gamma rZ}_{\bullet}| \right) |\psi_{pX}\rangle \varepsilon_{pX} = |\psi_{pX}\rangle \varepsilon_{pX}. \tag{4.26}$$

Left-multiplying by $\langle {}^{\psi sW}_{\bullet}|$ and expanding $|\psi_{tX}\rangle$ in the minimal basis respecting the local constraint of eq. 4.24, we arrive at

$$U^{sX\dagger}_{\bullet qX} f^{qX}_{\bullet rX} U^{rX}_{\bullet pX} = \delta^s_p \varepsilon_{pX}. \tag{4.27}$$

Thus, we have F projected sets of SCF equations for the polarized eigenvectors and eigenvalues,

$$\mathbf{U}^{\mathbf{X}\dagger}_{\bullet\mathbf{X}} \mathbf{f}^{\mathbf{X}}_{\bullet\mathbf{X}} \mathbf{U}^{\mathbf{X}}_{\bullet\mathbf{X}} = \varepsilon_{\mathbf{X}}. \tag{4.28}$$

Solving these projected equations is equivalent to block-diagonalizing the Hamiltonian matrix in the minimal polarization basis. All remaining orbital mixings (either between fragments in the minimal space, $\mathcal{M}$, or coupling to any member of the Rydberg space, $\mathcal{R}$) account for the remaining energy-lowering necessary to approach the full SCF calculation. Within the minimal polarization space, the utility of initially neglecting interfragment mixings, $\mathbf{U}^{\mathbf{X}}_{\bullet\mathbf{Y}}$, is that it serves to cleanly separate intra- and intermolecular effects. The motivation for neglecting the Rydberg space is that it is not associated with intramolecular polarization to leading-order in perturbation theory. We expect the locally-projected POLMO wavefunction and energy to approach exactness in the limit that the fragments make negligible use of charge-transfer rotations to relax their orbitals, for instance, in the case of very weakly-interacting systems, or for systems near dissociation. We emphasize that the polarized wavefunction is an exact eigenfunction of $\hat{F}^{(0)}$ with energy complete through second-order perturbation theory, as discussed in the previous subsection. Once the POLMOs are obtained self-consistently for the polarization energy, the vectors spanning $\mathcal{R}$ are re-introduced and the full Hamiltonian matrix is diagonalized to self-consistency. the energy-lowering due to charge transfer delocalizations connecting to the observable binding energy. What follows is a sketch of the POLMO-based EDA:

1. Perform F independent self-consistent HF calculations to obtain $\{C^X_{\bullet\, p}\}$.
2. Build $\mathbf{P}$ and $\mathbf{F}(\mathbf{P})$ and compute ΔE_{frz} by eq. 4.2.
3. Project off the occupied space from virtual space following eq. 4.9.
4. Symmetrically-orthogonalize across the occupied space following eq. 4.13, then Boys-localize.

5. Semi-canonicalize the occupied and virtual subspaces by fragment to make the denominator of eq. 4.19 diagonal.
6. Construct and SVD X_{VO} by eq. 4.21, then transform to the natural polarization basis $\mathcal{M}$, discarding $\mathcal{R}$.
7. Symmetrically orthogonalize across the minimal virtual set, then Boys-localize.
8. Solve the locally-projected eqs. 4.28 self-consistently, obtaining ΔE_{pol}.
9. Re-introduce $\mathcal{R}$ and semi-canonicalize across full occupied and virtual subspaces.
10. Relax the constraint of eq. 4.24 to obtain full-space eigenvectors and ΔE_{ct}.

4.3 Results and Discussion

It will, of course, be essential to inspect the results of the EDA when applied to a wide variety of molecular complexes, but for the present purpose of uncovering trends particular to the decomposition methods, we limit our scope to the widely-studied water dimer interaction potential. The C_s-symmetry global minimum places the molecular dipoles at an appreciable offset presumably to enhance the $p(O) \rightarrow \sigma^*(OH)$ interaction, hinting at a delicate balance between dative and electrostatic interactions. So there is no question that a satisfactory description of the water dimer interaction is difficult, and the question of what elements are important is not without considerable controversy [221, 234]. We performed all computations within a development version of Q-Chem [98]. AO basis set parameters for all 5z [235] and doubly-augmented basis sets [236] were obtained from the EMSL Basis Set Exchange with h-angular-momentum functions removed. The C_s-symmetry CCSD(T)/cc-pvqz-level optimized water dimer minimum was taken from the S22 set [159]. The data were not corrected for BSSE.

Stability with respect to basis set extensions.

It is desirable for any EDA scheme that, in the same way that the binding energy is convergent with respect to basis set extension, its resolved components likewise converge on some limiting value. If this weren't the case, there would be no reason to take the components of the EDA in one AO basis versus another as superior. In general, there is good reason to prefer larger- to smaller-basis results (if the former are feasible) simply because increasing the variational degrees of freedom available to the wavefunction leads to a description closer to the complete basis set limit. For well-posed methods, this corresponds to a more precise description of the intermolecular interactions themselves. Within Hartree-Fock theory, we compare the behavior of EDA terms in the minimal POLMO approach and the existing ALMO scheme with respect to enhancements of the AO basis in Table 4.1. We visualize

basis	frz	pol(POLMO)	pol(ALMO)	ct(POLMO)	ct(ALMO)	bind
dz	9.88	2.22	3.34	12.11	11.00	24.21
tz	8.30	2.54	4.03	7.57	6.08	18.41
qz	6.82	2.57	4.49	7.05	5.13	16.44
5z	5.72	2.79	4.84	6.89	4.84	15.40
aug-dz	6.32	2.79	4.62	6.86	5.03	15.96
aug-tz	5.61	2.93	5.60	6.62	3.95	15.16
aug-qz	5.29	2.91	5.75	6.93	4.09	15.13
aug-5z	5.21	2.87	6.03	6.94	3.78	15.01
d-aug-dz	6.07	2.83	4.94	7.30	5.19	16.20
d-aug-tz	5.37	2.96	6.05	6.98	3.89	15.31
d-aug-qz	5.24	3.06	6.82	6.91	3.15	15.21

Table 4.1: HF minimal-basis POLMO and ALMO EDA components of the interaction between equilibrium water dimer in kJ/mol.

the $p(O)$ and $\sigma^*(OH)$ guess orbitals and their mutually-polarized and delocalized versions in Fig. 4.1. The data are grouped according to basis diffusivity. Augmented basis sets add a single diffuse shell of each angular momentum to every atom. For instance, in the case of aug-cc-pVDZ, an extra set of low-ζ s- and p-type functions on hydrogen, and s-, p-, and d-type functions on oxygen. Doubly-augmented sets add a second yet more diffuse shell of each angular momentum. A negative sign in front of a contribution means it will destabilize the complex. The HF limit for binding is estimated at 15.19 kJ/mol from a CBS extrapolation within the doubly-augmented series according to a fitted equation $B(L) = B(CBS)+Xe^{-AL}$, where L is the quantum number of the highest-angular momentum function in the set, e.g., L(dz)=2, L(tz)=3, and L(qz)=4. The magnitude of the favorable frozen contribution (labeled frz in Table 4.1) decreases as the basis set is extended, converging most slowly in the non-augmented set and comprising the biggest contribution to the net change in binding energy beyond the double-zeta level in that series. The frozen interactions include permanent electrostatics, which in the water dimer primarily reflect favorable dipole-dipole interactions and unfavorable exchange repulsions. When the local orbitals have access to increasingly diffuse functions to describe their spatial extents, exchange repulsions are felt more strongly and must distort their densities to respect Pauli exclusion. We find it quite interesting that the frozen contribution converges so slowly with respect to basis set size, as it is still changing slightly when the total binding energy is apparently converged. It follows that if the frozen contribution is unfavorable, e.g., when the molecules are squeezed together, a diffuse basis should only increase its magnitude until convergence. Though the sum of charge transfer and polarization is stable, the individual ALMO quantities are manifestly not, with unacceptably large ranges of ∼3.5 and ∼8 kJ/mol for, respectively, polarization and charge transfer. Even if we exclude the small double-zeta results (which suffer walloping BSSE due

contracted 20%	frz	pol(ALMO)	ct(ALMO)	pol(POLMO)	ct(POLMO)
dz	0.96	4.91	15.51	2.78	17.64
tz	3.49	6.43	10.12	3.89	12.67
qz	5.60	7.18	9.18	4.21	12.15
5z	7.22	8.09	8.68	4.68	12.09
aug-dz	5.38	7.59	8.18	5.25	10.52
aug-tz	7.24	9.06	7.58	4.39	12.25
aug-qz	7.80	9.47	7.58	4.60	12.45
aug-5z	7.78	9.94	6.96	4.57	12.34
d-aug-dz	5.59	7.74	8.42	4.84	11.32
d-aug-tz	7.43	9.81	7.11	4.45	12.47
d-aug-qz	7.80	10.71	6.41	4.94	12.19

Table 4.2: Behavior of polarization in non-equilibrium H-bonds depends strongly on the AO basis when overlaps are large.

to incompleteness), and all results obtained without augmented basis sets, the range remains ∼1.2 kJ/mol for polarization and ∼0.8 kJ/mol for charge transfer, while the range in the total binding energy is only ∼0.1 kJ/mol. The deficiency is especially palpable in the doubly-augmented trend where the largest number of near-linear dependencies exist. These results are consistent with the fact that the ALMO polarization contribution will steadily increase as the basis approaches completeness. The effect becomes larger when the inter-fragment H-bond length is contracted by about 20%, as given in Table 4.2. In the ALMO scheme, polarization continues to increase as the lone-pair on the donor oxygen atom's freedom to infiltrate the core region of the other oxygen increases with the size of the variational space allotted to the donor. By contrast, of course, the instability of the individual ALMO terms diminishes when the bond length is protracted by about 13% (given in Table 4.3). This is because the molecules overlap only weakly, and therefore the extent to which basis functions on one water molecule can mimic charge transfer to the other molecule is greatly reduced. The total interaction energy is similar (∼9kJ/mol) at both displacements. Turning to the behavior of the POLMO treatment of polarization, it is significantly more stable than the ALMO polarization for the water dimer at its equilibrium separation, as shown in Table 4.1. The reduction in the spread of results as the basis set improves is about a factor of four across all basis sets considered. However, if we again exclude the small double-zeta basis, and the non-augmented calculations (which converge slowly), the resulting range in the POLMO polarization is less than 0.2 kJ/mol, a roughly 6-fold reduction over the spread in the corresponding ALMO polarization results. This 0.2 kJ/mol range is very comparable to the range in the total binding energies across the same selection of basis sets. The converged value of POLMO polarization is ∼3 kJ/mol which gives a roughly 35%:20%:45% frz:pol:ct decomposition of the interaction energy in these essentially CBS-limit HF calcu-

protracted 13%	frz	pol(ALMO)	ct(ALMO)	pol(POLMO)	ct(POLMO)
dz	-8.58	0.32	5.57	0.25	5.64
tz	-8.74	0.45	2.68	0.34	2.78
qz	-8.71	0.51	1.30	0.38	1.43
5z	-8.64	0.56	0.48	0.41	0.63
aug-dz	-8.55	0.53	0.70	0.38	0.85
aug-tz	-8.51	0.59	0.46	0.44	0.61
aug-qz	-8.52	0.63	0.28	0.43	0.48
aug-5z	-8.51	0.66	0.21	0.43	0.44
d-aug-dz	-8.62	0.59	0.71	0.38	0.93
d-aug-tz	-8.49	0.64	0.48	0.43	0.70
d-aug-qz	-8.50	0.67	0.30	0.42	0.56

Table 4.3: POLMO polarization is slightly smaller than ALMO polarization at intermediate separation. The "-" sign reads as repulsive.

lations. If the EDA components are normalized to the binding energy and plotted against the basis diffusivity (in the same order as above), then the slope will be a measure of basis set dependence (which we hope will approach zero if the binding energy is converged). Any intersections will suggest a fundamental change in (the assessment of) the character of the interaction. We plot the components in Fig. 4.2 and note the minimal-basis polarization and charge transfer stabilize quickly and never cross, while the ALMO polarization crosses the frozen and charge-transfer contributions well after the binding energy is converged (by the aug-tz level by Table 4.1), though the polarization is quasi-stable in the singly-augmented trend where it is most likely to be used. The impact of the Boys orbital localization steps on the stability of the polarization term is assessed in Table 4.4. Boys localization of the occupied and virtual spaces serves to attenuate the real-space extent of the individual subspace spanned by each fragment's orbitals while, of course, leaving the full span intact. The consequence of this is a considerable improvement in the stability of the method. The dependence is increasingly noticeable in the doubly-diffuse trend since a larger spatial extent allows the converged POLMOs a degree of artificial charge-transfer energy-lowering that the ALMOs enjoy, albeit less dramatic. Both the Boys localization procedure and that the subspaces associated with different fragments have no overlap serves to attenuate the contributions to polarization associated with the POLMO description while still providing the variational flexibility in the full space of virtual functions associated with second-order perturbation theory.

basis	POLMO(Boys)	POLMO(w/o Boys)	ALMO
dz	2.22	2.19	2.78
tz	2.54	2.66	3.69
qz	2.57	2.64	4.49
5z	2.79	2.77	4.97
aug-dz	2.79	2.98	4.15
aug-tz	2.93	3.33	6.19
aug-qz	2.91	3.07	6.63
aug-5z	2.87	3.40	7.11
d-aug-dz	2.83	3.24	4.40
d-aug-tz	2.96	3.74	6.93
d-aug-qz	3.06	3.62	7.81

Table 4.4: POLMO polarization contributions in the basis set extension depend slightly on the localization, increasing gently with diffusivity.

DFT decomposition quantities and exchange effects.

A post-mean-field treatment of intermolecular interactions is vital for any serious application of the EDA, and DFT represents a parsimonious first thrust in this direction. When the exchange contribution is adjusted and inter-electronic correlations are included, the results of the equilibrium decomposition differ from those at the HF level (Table 4.5). Larger polarization and charge transfer effects tend to result from smaller HOMO-LUMO gaps (standard functionals tend to underestimate the gap [237, 238], while HF overestimates it). Of course electron correlation effects generally strengthen intermolecular interactions, so the HF values should not be regarded as true. Frozen interactions are sensitive to the dipole moment, which is overestimated at the HF level. Thus density functionals may typically exhibit less favorable frozen interactions than HF, but based on this criterion, the resulting value should be more reliable. The frozen interactions are also sensitive to the treatment of exchange, but it is difficult to guess the effect of functional approximations on this term. To test the dependence of all EDA terms on the composition of a density functional more carefully, we vary the amount of exact exchange (e.e.) in the three-parameter B3LYP exchange-correlation potential explicitly, keeping Slater exchange at a constant 8% and adjusting %B88 exchange to allow for the desired %HF exchange. Consistent with the general considerations already given, the results of Fig. 4.3 suggest roughly linear behavior of frz and shallow inverse dependence of ct with e.e., and weak-to-zero e.e.-dependence of pol in either scheme. Since the B3LYP functional energy is linear in the HF exchange parameter, we can only expect the total energy to scale linearly with e.e. *a priori*, as observed. That frz and ct clearly depend on e.e. in a way consistent with their definitions demonstrates correspondence between the terms of our decompositions and a totally independent metric describing exchange forces. In other words, these terms appear well-suited to describe the physical phenomena for which

contribution/basis	frz			pol			ct			bind		
XC/ %e.e.	dz	tz	qz	dz	tz	qz	dz	tz	qz	dz	tz	qz
B3LYP/20 [239]	5.92	5.80	5.53	2.49	2.73	2.85	11.02	10.38	10.60	19.43	18.91	18.99
M06L/0 [240]	5.57	6.45	4.96	2.41	2.60	2.77	10.81	10.90	12.37	18.78	19.95	20.09
M06/27 [241]	7.56	7.16	5.67	2.59	2.72	2.74	10.05	10.24	11.51	20.21	20.11	19.92
M06-2X/54 [241]	10.59	10.50	9.87	2.58	2.95	2.90	8.61	8.11	8.59	21.77	21.56	21.36
PBE/0 [242]	3.22	3.11	3.30	2.50	2.86	2.98	12.54	11.66	11.92	11.82	11.41	11.60
PBE0/25 [243]	8.48	7.92	7.60	2.55	2.71	2.82	10.48	10.15	10.40	21.50	20.78	20.82

Table 4.5: KS-DFT POLMO augmented-series components (kJ/mol) in the basis and exact exchange (e.e.). Charge transfer decreases with increasing e.e., while frozen interactions increase.

basis	frz	pol(POLMO)	pol(ALMO)	ct(POLMO)	ct(ALMO)	bind
dz	11.22	2.19	2.78	19.60	19.01	33.01
tz	10.94	2.32	3.69	12.56	11.20	25.83
qz	9.51	2.57	4.49	10.94	9.07	23.02
5z	8.48	2.75	4.97	10.40	8.18	21.63
aug-dz	8.79	2.53	4.15	10.24	8.62	21.56
aug-tz	8.16	2.73	6.19	10.11	6.65	20.99
aug-qz	7.52	2.77	6.63	10.03	6.66	20.81
aug-5z	7.44	2.77	7.11	10.43	6.08	20.64
d-aug-dz	8.61	2.53	4.40	10.11	8.68	21.24
d-aug-tz	7.99	2.72	6.93	10.36	6.15	21.08
d-aug-qz	7.46	2.90	7.81	10.62	5.65	20.98

Table 4.6: ωB97X-D-level decomposition components in kJ/mol. Most of the dispersion is captured in frozen electrostatics.

they were designed. We note that dispersion is not considered explicitly in the energy decomposition, and even if a dispersion-corrected functional is employed, the correction will formally be spread out between the decomposition terms, none of which is alone adequate to entirely capture this force. We might, however, expect the leading effect of dispersion to be contained in the frozen interactions, with smaller, density-dependent corrections contained in the polarization and charge-transfer terms. If the dispersion is not density-dependent at all, such as for "-D" functionals, then it will be entirely contained in the frozen term, As an illustration, we decompose the essentially quantitative interaction energy for water dimer furnished by the range-separated ωB97X-D [244] hybrid functional in Table 4.6. The ωB97X-D binding energy approaches the CCSD(T)/CBS extrapolation of 20.8kJ/mol [159]. With density-independent dispersion, it is no surprise that the frozen interaction is some $\sim$2kJ/mol larger in magnitude than at the B3LYP level. Comparing the most accurate decompositions at ωB97X-D and B3LYP, the "-D" augmentation of the frozen interaction appears to be the principle contributor to the binding energy difference between them.

Breaking the hydrogen bond of the water dimer.

If one goal of the EDA is that it be a true quantum-mechanical basis for force field parameters in molecular mechanics simulations, the EDA components should be well-behaved across the potential energy surface, each weighted in accordance with the true intermolecular force it designates and decaying to zero at the dissociation limit. Thus, when the two molecules of a dimer are squeezed together along some interaction coordinate, Pauli and electrostatic repulsions will begin to trump all other forces. Conversely long-range electrostatic forces should exert their effects long before the wavefunction assumes the equilibrium supermolecular configuration that will be determined on polarization and charge transfer. Polarization gives a sense in which permanent poles are deformed in the supermolecular field and should decay classically as the inverse of some (induced) multipole order in the interaction coordinate R, while charge transfer is contingent on intermolecular overlaps and dies off exponentially, and so at the very least these components must cross. Because the PES is sampled a great deal in the course of thermal fluctuations, an accurate description of the interaction potential along the entire weak-bond-breaking coordinate is indispensable. We plot the potential energy across the H-bond-breaking coordinate of the water dimer in Fig. 4.4, showing the contribution of the POLMO terms for B3LYP calculations on the left-hand side, and a log-log plot showing the R-dependence of the non-ct terms on the right-hand side. From Fig. 4.4(b), we observe the appropriate distance-dependence of all electrostatic terms in the long-range limit (at a separation greater than $1.5R_{eq}$ where this asymptotic analysis becomes valid). Frozen interactions are dominated by dipole-dipole interactions, while the polarization terms are dominated by dipole-induced dipole contributions. It is only in the strictly-non-overlapping regime that we should expect slopes of exactly three and six for frozen and polarization contributions respectively. Inclusion of quantum mechanical exchange in the Hamiltonian will be responsible for slight deviations away from the correct curve. The effective power law behavior for decay of the polarization via the ALMO and POLMO treatments are particularly interesting. Both ALMO and POLMO should be exact (within the chosen basis) in the non-overlapping regime (as the interaction becomes weak enough that the perturbative model for minimal virtual functions in the POLMO method becomes increasingly suitable). At small separations, we have argued that a part of the ALMO polarization is in fact attributable to charge transfer, and this error will increase as the basis set is improved. Since this error diminishes with the overlap of the fragments, its presence should cause the ALMO power law for decay of the polarization contribution to exceed six. The data show a power law with exponent 6.1 for the ALMO model. On the other hand, the POLMO model, with polarization described in a minimal orthogonal space, will likely underestimate the polarization contribution in the strongly-overlapping regime while approaching exactness in the non-overlapping limit. This will result in a power law exponent of less than six (5.9 for the POLMO model). We conclude that the data shown in Fig. 4.4(b) is consistent with POLMO polarization being a lower-limit estimate of the true polarization in the overlapping regime, while the ALMO polarization should be regarded as an upper

limit to polarization in the overlapping regime. Armed with the potential surface, we can read off the story of the gas-phase water dimer interaction from the right in Fig. 4.4(a): Two approaching water molecules in the appropriate orientation first see each other's vacuum dipoles at a separation greater than $3R_{eq}$. As they approach closer along the axis that becomes a hydrogen bond, dipole polarization occurs along the H-bonding axis (in Fig. 4.1, the POLMO $p(O)$ donor has changed its orientation w.r.t. the symmetry axis of its vacuum analogue to better respond to the acceptor σ^*(OH) in its field). As separation of the two water molecules is further decreased, the dative interaction, which decreases the equilibrium H-bond length for the dimer well within the frozen minimum by some 0.5Å begins to rapidly increase. At the equilibrium geometry, all three types of contributions (frozen, polarization, and charge-transfer) are important.

The Na^+CH_4 monopole-induced-dipole polarization.

The case of the water dimer illustrates what we believe is the most common paradigm in complex intermolecular interactions: there is a rich distance-dependent admixture of permanent (frozen), polarization, and charge transfer interactions. It is also useful to briefly examine an interaction in which charge transfer effects are expected on chemical grounds to be negligible, while polarization effects are very important. Such a case will be a potentially difficult challenge for the POLMO approach, because it generally will underestimate polarization, and therefore overestimate CT. In a case where CT is negligible, such a result would be spurious. A specific system that is anticipated to have negligible CT is the Na^+CH_4 interaction, which one may intuitively think of as a problem of describing a Stark-shifted methane molecule. The positive charge resides on Na^+, and its occupied orbitals are very deep in energy, and therefore donation into σ^* orbitals on methane is blocked. For CT in the other direction, methane is a poor donor, and Na^+ does not have low-lying affinity orbitals, so CT is expected to be very small. The POLMO and ALMO decomposition terms for the Na^+CH_4 interaction were obtained from a 6-311++G**/B3LYP-optimized geometry and are given in Table 4.7 for a wide range of basis sets (without counterpoise correction). In both schemes, polarization is the chief contribution to binding with a disparity between the decompositions decreasing steeply on inclusion of higher-angular momentum functions to ∼5 and ∼6 kJ/mol for 5z and aug-5z calculations, respectively. If it is accepted based on the arguments above that there is no "real" charge-transfer in this interaction, then it follows that ALMO polarization should be stable and an adequate estimate of the true polarization. The numerical results support this contention, as the ALMO polarization is converging smoothly in both basis set sequences, and CT is very small. ALMO-based CT is roughly 7% of the polarization value in the largest basis set reported in Table 4.7. The POLMO results improve significantly in the larger basis sets, in the sense that POLMO polarization generally increases in magnitude as the basis set is improved. The gap between ALMO CT and POLMO CT diminishes ranges from 4-12 kJ/mol depending on the basis set, with somewhat smaller differences for the larger basis sets. Relative to the size of the interaction

basis	frz	pol(ALMO)	pol(POLMO)	ct(ALMO)	ct(POLMO)	bind
dz	0.72	20.62	15.30	12.75	18.07	34.09
tz	0.74	26.68	19.08	5.17	12.79	32.59
qz	0.82	29.54	24.74	3.34	8.13	33.70
5z	0.62	30.99	25.48	0.76	7.89	33.99
aug-dz	-0.18	30.74	21.87	1.77	10.64	32.33
aug-tz	0.54	31.58	19.02	1.19	13.75	33.31
aug-qz	0.64	32.08	27.70	2.63	6.96	35.34
aug-5z*	0.53	32.23	25.84	2.19	8.45	34.83

Table 4.7: B3LYP decomposition components of the polarization-dominated Na^+CH_4 interaction in kJ/mol. *Na was treated at the 5z level.

(35 kJ/mol with this density functional), the gap between ALMO and POLMO CT is only about 20% in the larger basis sets, so both treatments give a qualitatively similar picture of a polarization-dominated interaction. These considerations bolster the contention that POLMO polarization represents a lower-limit estimate, while ALMO polarization represents an upper limit. This issue will be discussed further in Sec. 4.3.

Bracketing intrinsic polarization effects.

We understand the POLMO minimal-basis polarization as a lower bound to true polarization since we neglect the vectors in $\mathcal{R}$ during polarization, as well as enforce orthogonality between the variational spaces associated with different fragments. While neglect of $\mathcal{R}$ has zero error at the second-order perturbation level, it must lead to an underestimate relative to the energy-lowering evaluated with a fragment-based partitioning of the orbital space that includes all functions. The magnitude of this difference will depend strongly on the geometry, since the error tends to zero when perturbation theory amplitudes approximate the space of the true polarized wavefunction well (which will be the case when polarization is small). Thus in the POLMO scheme, charge-transfer effects are overestimated, or, from a physical standpoint, they contain some contaminating polarization contributions. By contrast, as we discussed in detail in Sec. 4.2, use of ALMO polarization will tend to be an overestimate, because the non-orthogonal one-particle Hilbert spaces of different fragments have an intersection, and that intersection increases as the basis set is improved. Thus ALMO polarization is contaminated with some energy-lowering that is in fact related to charge transfer. We therefore bracket true polarization as lying between the upper-bound ALMO polarization and the lower-bound minimal-basis POLMO polarization. How large or small is the difference between the upper and lower bounds for the water dimer at the basic Hartree-Fock level of theory, at equilibrium? The tightest upper bound for polarization by the ALMO approach comes from the smallest value of polarization when the sum

of polarization and charge transfer energy is converged. Referring back to Table 4.1, the smallest upper limit might be the cc-pVQZ pol(ALMO), at $\sim$ 4.6kJ/mol. If we take the lower-estimate pol(POLMO) quantity as $\sim$ 3.0kJ/mol, then true polarization is bounded within a 1.6kJ/mol range, (3.0,4.6). We would obtain an essentially identical result with the ωB97X-D functional, as can be seen from Table 4.6. For HF at the compressed geometry shown in Table 4.2, the corresponding bracket for true polarization is (4.9,8.1) kJ/mol, which is necessarily wider because of the increased overlap between the fragments. At the stretched geometry shown in Table 4.3, the estimated bracket for true polarization is narrower, at (0.4,0.6) kJ/mol. Finally, for comparison, we can infer a bracket for polarization of roughly (26,30) kJ/mol for the polarization-dominated Na^+CH_4 interaction using the data from Table 4.7. What are the implications for the overestimation of polarization effects in the ALMO EDA as it is commonly employed? Let us consider the water dimer at the equilibrium geometry again, and assume that a standard application of the ALMO EDA employs the aug-cc-pVTZ basis. In that case, the calculated ALMO polarization is $\sim$5.6 kJ/mol, while our bracket for true polarization is (3.0,4.6) kJ/mol. We therefore conclude that polarization is overestimated by at least 1 kJ/mol, and not more than 2.6 kJ/mol in the ALMO EDA/aug-cc-pVTZ method. Thus the true polarization is no less than 20% smaller than the ALMO value, and it could be as much as 46% smaller. Since the errors depend on the identity of the basis it is likely that they are quite systematic, so trends in the ALMO polarization estimate are likely to be reliable. Nonetheless, it is clear that improved procedures for calculating polarization are important for future work. The POLMO method is one such candidate.

4.4 Conclusions and outlook

In energy decomposition analysis of intermolecular interactions, one important issue is disentangling the separate contributions associated with intramolecular polarization in the field of neighboring molecules and intermolecular charge transfer (dative bonding) between molecules. This issue is challenging because such a separation in all likelihood cannot be uniquely defined in the important regime where the molecular partners overlap significantly. We have studied some aspects of this issue with the aim of attempting to understand strengths and weaknesses of existing EDAs, and introduce a new and complementary approach. Our main results and conclusions are as follows:

1. We have demonstrated that fragment-blocking the molecular orbital coefficient matrix as employed in the ALMO EDA [76, 138] and the related BLW-EDA [212, 213] overestimates the energy-lowering due to polarization effects in intermolecular interactions. In essence, this arises because the one-particle Hilbert spaces of different fragments are allowed to have non-zero intersection, and the extent of the intersection increases with the size of the basis set. Therefore in the ALMO EDA, the energy-lowering due

to polarization becomes contaminated with charge-transfer effects as one improves the basis set.

2. We have developed a new method that uses fragment-blocked variations to obtain a minimal basis of polarized orthogonal local MOs (POLMOs) describing stabilization due to polarization. Only one POLMO is provided per occupied MO of the isolated fragments by SVD of the first-order polarization response on each fragment followed by symmetric orthogonalization and relocalization.

3. The POLMO approach will underestimate polarization because strict orthogonality is maintained between variational subspaces that describe polarization on different fragments, and a large fraction of the virtual orbitals is discarded. Therefore, taken together, the ALMO and POLMO estimates of polarization are expected to bracket the true value.

4. Numerical tests of the ALMO and POLMO polarization energies have been carried out on the water dimer using a large sequence of cc-pVXZ, aug-cc-pVXZ and d-aug-cc-pVXZ (X=D,T,Q,5) basis sets. The POLMO scheme is stable with respect to basis set extensions even in the strongly-overlapping regime. By contrast, the ALMO polarization contribution is not stable with respect to basis set extensions. Analysis of the power law decay of ALMO and POLMO polarization as a function of intermolecular distance is consistent with ALMO overestimating and POLMO underestimating polarization. Results were also calculated for the Na^+CH_4 interaction, which is dominated by polarization in both the ALMO and POLMO approaches.

5. Within the Hartree-Fock method, for the water dimer at the equilibrium geometry, the estimated range within which the true polarization energy-lowering lies is (3.0,4.6) kJ/mol. If an aug-cc-pVTZ basis is taken as typical for the ALMO EDA method, our results suggest that true polarization is at least 20% less than the ALMO result, though not more than 46% less. Accordingly it is important to use the ALMO polarization contributions primarily for comparative purposes, as the absolute values are demonstrably too large. Further work on better separating polarization from charge transfer for EDA purposes is clearly desirable.

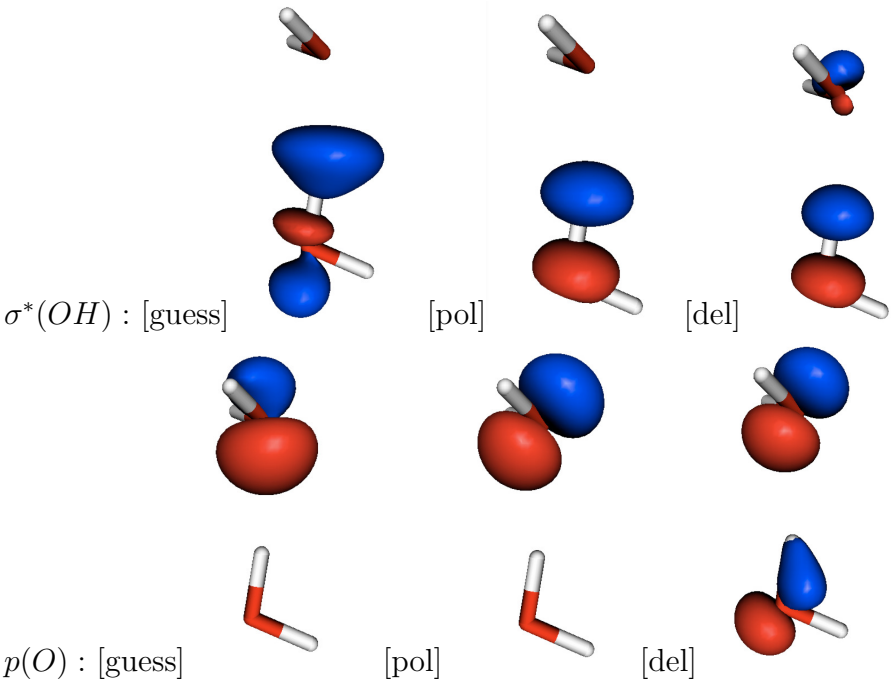

Figure 4.1: $\sigma^*(OH)$ and $p(O)$ guess, POLMO, and delocalized orbital pair set plotted at a contour value of 0.12. Guess and polarized orbitals have mostly local amplitudes in spite of orthogonality.

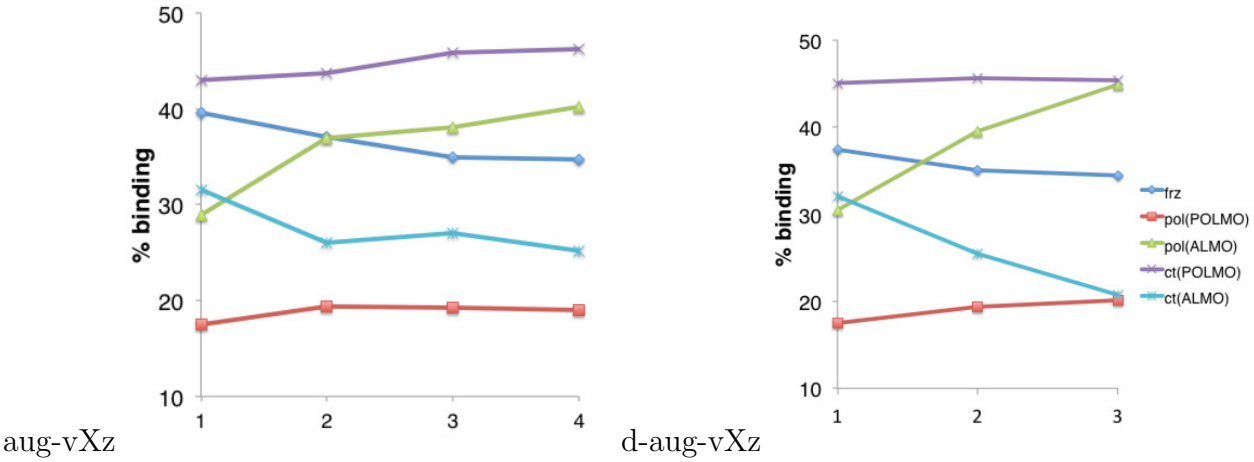

Figure 4.2: The character of the C_s water dimer interaction is basis-set dependent in the SCF MI scheme, but stable in the minimal-basis scheme.

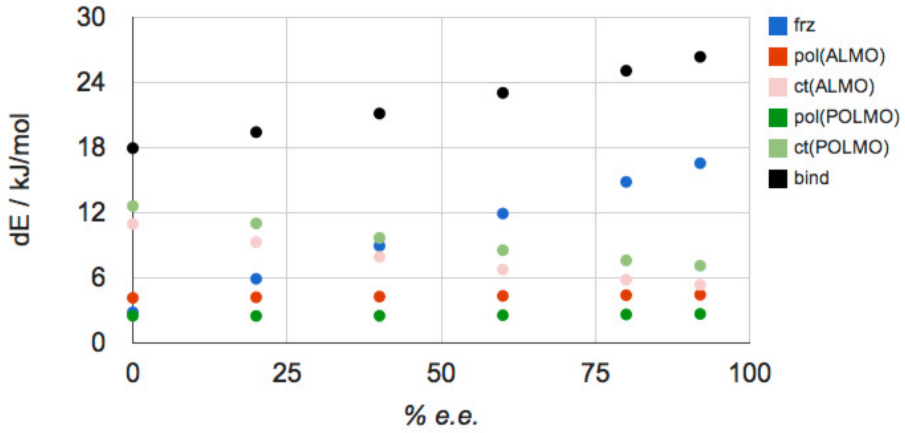

Figure 4.3: Component magnitudes in the aug-dz basis scale with e.e. in accordance with the form of the decomposition term described. The 20% e.e. point corresponds to optimized B3LYP.

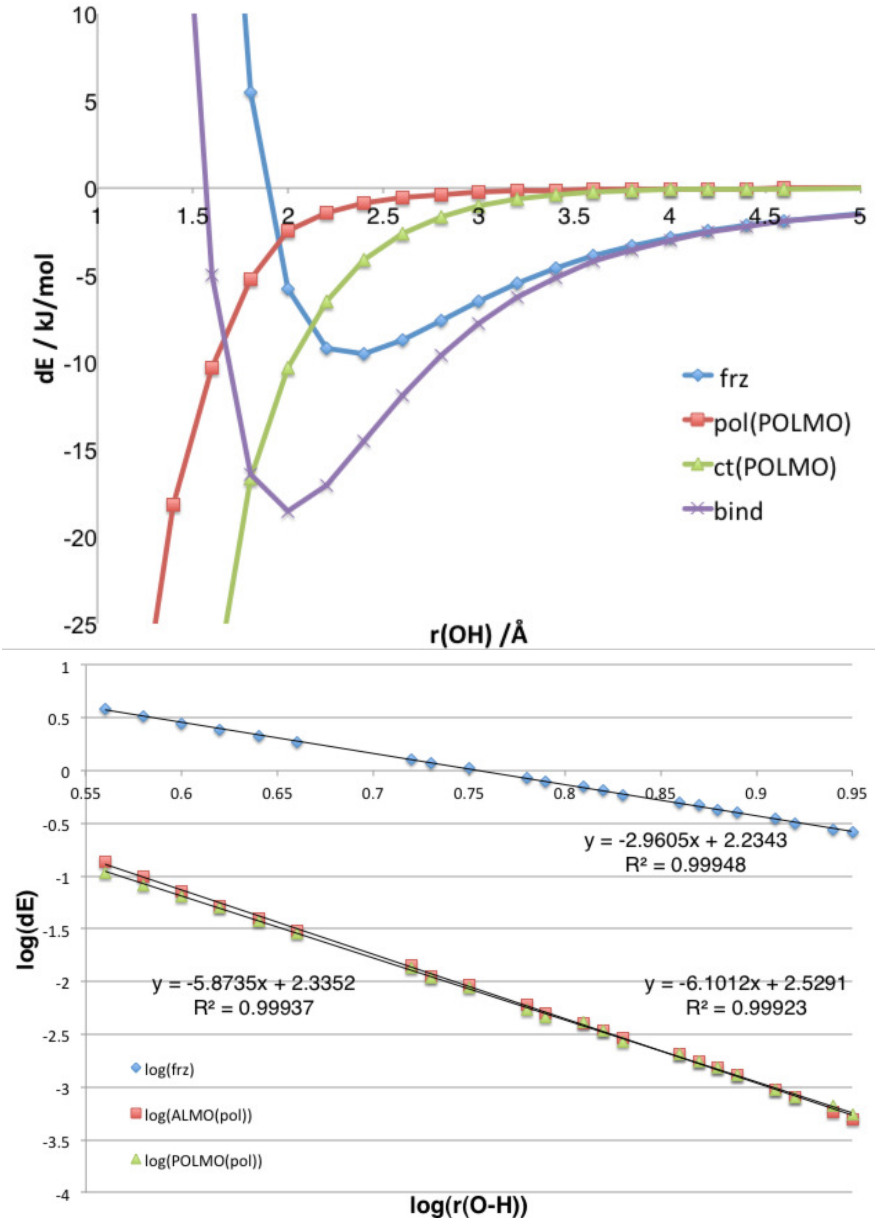

Figure 4.4: (a) POLMO binding components of B3LYP/aug-cc-pvdz C_s water dimer traversing its H-bond-breaking coordinate have the correct limiting behavior and a complicated binding interaction; (b) log(ΔE)-log(r) plot of the frozen and polarization contributions indicate scaling consistent with appropriate classical inverse square-power.

Chapter 5

Frugal supermolecular perturbation theories

5.1 Introduction

Quantum chemistry has undoubtedly emerged as a mature field with considerable predictive power in the past few decades. Ever-increasing improvements in computing power have arguably served to shift its scope of applied focus to large molecular clusters, surfaces, and the condensed phase. Much emphasis has been placed on the development of low-scaling approximations to high-level model chemistries, e.g., resolution-of-the-identity/density-fitting[37–42] for two-electron integrals, explicitly-correlated F12/R12[43, 45–51] formulations for accelerated CBS convergence, spin-component-scaled Laplace-transformed [52, 53], and rank-reducing tensor decompositions[54–62] in Møller-Plesset (MP) and coupled-cluster (CC) methodology, hybrid QM/MM[245, 246] embedding approaches, and domain fragmentation for local correlation methods[63, 68, 247–254]. In view of its lower-order scaling and quicker basis set convergence than traditional wavefunction approaches, density functional theory (DFT)[33, 34] is arguably the most qualified quantum mechanical framework currently available for applications on large systems, and no doubt the most the popular. Modern sophistications in parametrization techniques, e.g., range-separation of the Coulomb operator, inclusion of unoccupied levels, non-local correlation, and empirical dispersion, have produced state-of-the-art functionals competitive with wavefunction methods for a host of problems, all within an independent-particle (single Slater determinant) model solvable with low-dimensional linear algebra.

The SCF procedure that underlies DFT (and Hartree-Fock) methodology typically involves iterative diagonalization of a one-body Hamiltonian that is a function of its eigenvectors until self-consistency is achieved, e.g., until neither it nor its solutions change. Efforts at tractability gains have historically focused on either Hamiltonian construction or diagonalization. Perhaps the most ground-breaking achievement in the former was surmounting

the so-called "Coulomb problem", the unavoidable quadratic growth with system size of the number of important two-center integrals. Linear scaling of Coulomb matrix construction[255–257] was achieved with the introduction of fast-multipole-method (FMM)[258–260]-based schemes partitioning the Coulomb interaction into near- and far-field domains and parametrizing the latter with multipole expansions in tree algorithms. Cost reduction in the computation of exchange followed from capitalizing on the inherent sparsity of density matrix elements for finite-band-gap systems, where judicious screening can reduce the computation of the K matrix to linear complexity[261–263]. The error in these linearizations is machine-double-precision-tunable, and benefits are conferred rigorously in the asymptotic regime though they're realized in practice for calculations of intermediate size, whereupon the crux of the SCF procedure becomes the cubic effort of Hamiltonian diagonalization and quadratic memory cost, the focus of the current work.

Many alternatives to iterative full-space diagonalization have been proposed. So-called "direct" methods forgo any explicit diagonalizations, exploiting or enforcing sparsity in the molecular orbitals[264–266] or density[267–269] and solving constrained optimizations taking advantage of linear-cost sparse matrix multiplication. Projective diagonalization-free approaches such as the variational coupled-cluster singles[270] method solve non-linear projection equations from a Brilluoin-violating guess to obtain corrections to the energy and orbitals equivalent to those obtained by a single Roothaan-Hall step. Non-iterative projected atomic orbital (PAO)[271, 272] and dual-basis methods[273–275] solve a reference problem in an economical basis and compute a second-order correction describing non-Brilluoin couplings in a larger basis from an linearized or untruncated CCS amplitude equation, requiring a single diagonalization step. An atomic orbital representation leaves the matrices of interest sparse and thus amenable to fast matrix operations. Fragmentation schemes partition the large SCF problem into a linearly-growing number of manageable, independent sub-domains, e.g., atomic or molecular, and solve "local" Roothaan-Hall equations, patching together subsystem quantities to approximate the supersystem ones. Used in tandem with the many-body expansion (MBE), approaches such divide-and-conquer [276–280], fragment molecular orbital (FMO) [281–284], XPOL+SAPT[285, 286], and many-overlapping-body[287] have produced encouraging energetics for large systems, and are generally amenable to large-scale parallelization.

Some characteristics any proposed linear-scaling SCF model should possess beyond the property of being formally satisfactory include variationality; formal or at least apparent smoothness on the PES; demonstrated and sustained cost-savings relative to conventional SCF while remaining accurate for *relative* energies; intuitive, physically-motivated domain identification in the case of fractionation; clear limiting behavior; and portability to any single-particle model. In this work, we propose a novel alternative to full-space diagonalization in line with these desiderata, exploiting information garnered from perturbation theory to project the diagonalization problem into a variational space no larger than *twice* the number of electrons. We focus on non-covalent interactions, applying perturbation theory on top of zeroth-order states taken either as eigenfunctions of the vacuum one-particle Hamiltonian,

or as absolutely-localized molecular orbitals (ALMOs)[75, 288–291], the variational solutions to locally-projected non-orthogonal SCF equations[72, 292]. We demonstrate a subsequent SCF performed in aminimal basis space spanned by the perturbative wavefunction recovers the conventional result nearly exactly, with relative errors virtually insensitive to the choice of basis or PT order treated. As shall be seen, these conclusions still apply when the rate-limiting minimal basis construction is linearized by restricting operations to convergent molecular domains.

5.2 Theory

We use the labels $i, j, k, l, ...$ and $a, b, c, d, ...$ to represent occupied and virtual orbitals, while $p, q, r, s...$ are general spin-orbital indices and $A, B, C, ...$ represent fragment labels. Repeated indices imply summation.

Beginning from any guess, $|0\rangle$, at the ground-state eigenfunction of a Hartree-Fock or Kohn-Sham Hamiltonian, one obtains the variational solution by iterative diagonalization of the Hamiltonian matrix in the guess representation until self-consistency is reached. For our purposes, we recast this optimization problem in the language of perturbation theory. Taking $\mathbf{H^{(0)}} = |0\rangle H_{00}\langle 0| + |\mathbf{s}\rangle \mathbf{f_{ss'}} \langle \mathbf{s'}|$, $\mathbf{H}^{(1)} = |0\rangle \mathbf{f_{0s}} \langle \mathbf{s}| + |\mathbf{s}\rangle \mathbf{f_{s0}} \langle 0|$, and a perturbative wavefunction $|0^{(n)}\rangle = e^{t^{s(n)}}|0\rangle$ where $\{t^{s(n)}\}$ describes the nth-order perturbative projection onto the singles manifold, we left-project the Schrödinger equation with $\langle 0|$ and expand the energy in orders of the perturbation obtaining,

$$\begin{aligned} E^{(0)} &= \langle 0|\mathbf{H^{(0)}}|0\rangle = H_{00}, \\ E^{(1)} &= \langle 0|\mathbf{H^{(1)}}|0\rangle = 0, \text{and} \\ E^{(n)} &= \langle 0|\mathbf{H^{(1)}}|0^{(n-1)}\rangle = f_{ia}^{(1)} t^{ai(n-1)}, \end{aligned} \tag{5.1}$$

and amplitude equations complete through $(2n-1)$th order in MP partitioning,

$$t^{ai(n)}\{f_{ii} - f_{aa}\}^{(0)} = f_{ai}^{(1)} - t^{ak(n-1)} f_{kc}^{(1)} t^{ci(n-1)}. \tag{5.2}$$

Truncating the perturbative wavefunction at first-order gives the familiar non-Bruilloin correction linear in the amplitudes, $t^{ai(1)} = f_{ai}^{(1)}\{f_{ii}^{(0)} - f_{aa}^{(0)}\}^{-1}$, while carrying n to infinite-order guarantees a correction equivalent to the energy-lowering on a single Roothaan-Hall diagonalization. One can thus imagine obtaining the variational energy and wavefunction this way by macroiterations, updating the orbitals by the infinite-order solution of eq. 5.2, and repeating until the correction vanishes. Taking this alternative route, one avoids iterative diagonalization in the full AO space, but at the expense of cubic contractions in the non-linear piece of eq. 5.2, and pseudocanonicalization in each subspace to uncouple the denominator at each macroiteration. The cost of such a procedure thus approaches that of standard SCF in the *relevant* limit $N_v >> N_o$. To avoid the pitfalls of macroiterative update, then, one has

to be content that a non-iterative correction to $|0\rangle$ will be useful to approximate conventional SCF. This will, of course, depend critically on the size of the perturbation which is, in turn, parametrized by the zeroth-order wavefunction. In dual-basis methods, for instance, the same PT eqs. 5.1 & 5.2 are employed taking $|0\rangle$ as the canonical solution in a smaller basis and solving for infinite-order amplitudes, with the quality of the single Roothaan step in the larger basis improving with the description in the smaller basis until the correction vanishes in the limit the reference and target basis sets are identical. Our approach here will be to remove some dependence on the guess by adding a degree of self-consistency while eschewing iterative diagonalization in high-rank. A singular value decomposition of $t^{s(n)}$,

$$\mathbf{L}_{a'a}\mathbf{t}^{ai(n)}\mathbf{R}^{\dagger}_{ii'} = \mathbf{T}^{(n)}_{a'i'}, \tag{5.3}$$

and subsequent transformation of the virtual orbitals by the columns of $\mathbf{L}$ with N_o non-vanishing singular values assuming $N_v >> N_o$,

$$|a'\rangle = |a\rangle L^a_{a'}, \quad a' = 1, ..., N_o, \tag{5.4}$$

guarantees that the nth order wavefunction and energy are recovered *exactly*, but in a $2*N_o$-dimensional basis of the most important occupied-virtual pairs, e.g., eigenvectors of the response density. We perform a subsequent SCF in this rank-reduced pair basis, expecting the the variationality of the optimization to afford accuracy gains relative to non-iterative corrections to SCF.

Though the proposed perturb-then-diagonalize minimal-basis SCF detailed above scales with the occupied dimension alone, we'll want to recast the foregoing PT problem in terms of N_A *fragmented* ones giving rise to N_A fragment-optimal minimal basis sets in order to avoid the full virtual-block diagonalization required at the outset. We nevertheless understand this full-rank model as the variational lower bound for our minimal-basis schemes, and because there is no imposed fragmentation of subspaces, we'll refer to it as the "proper" model henceforth. We approach the fractionation problem beginning with a reference of molecule-tagged states, either optimized (ALMO) or unrelaxed (frozen) in the supermolecular field. By construction, a perturbative treatment will be complete to infinite- or first- order in elements of $\mathbf{H^{(1)}}$ confined to a given molecular center, respectively, and we should therefore expect to treat electrostatic and inductive interactions well when higher-order effects are negligible. The reader will recall that rotations zeroing occupied-virtual Fock elements from the ALMO or frozen references correspond to energy-lowering due to charge-transfer and (re-)polarization effects. Accordingly, in the limit that any two fragments are non-interacting, their shared occupied-virtual block of the Fock matrix will vanish, and as they begin to interact, their shared contribution to the perturbative wavefunction grows with the elements in their shared block of $\mathbf{f_{ov}}$. We shall make use of this information to economize the minimal basis construction. Specifically, the rank of a given fragment's perturbative wavefunction $\{t^{s(n)}_A\}$ can be truncated substantially by retaining for each occupied set only those virtual functions giving rise to strong couplings in $\mathbf{f_{ov}}$, e.g., those of magnitude greater than or equal

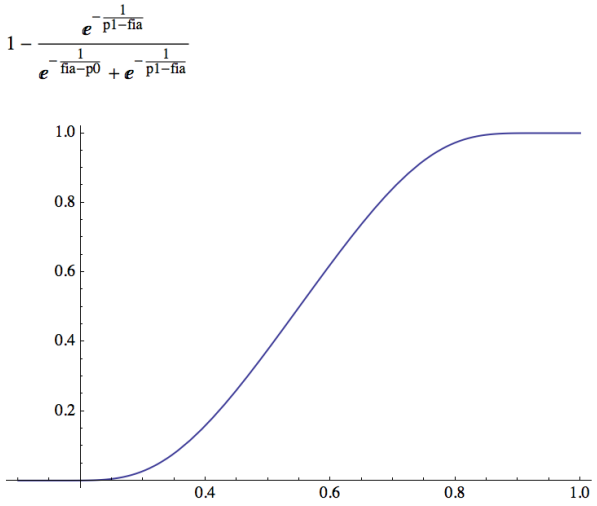

Figure 5.1: Acceptance function K over the coupling interval (p_0=0.1, p_1=1.0).

to some cut-off threshold. Such an approach, though it will guarantee true linear-scaling, will yield PESs not formally smooth because the number of important virtual orbitals taken into consideration by a given fragment will vary along the reaction coordinate. We shall demonstrate, however, that the cut-off can be chosen to cause any discontinuities to vanish. We describe the selection procedure below.

For a given fragment A wanting a virtual space, we submit its occupied-virtual block to an acceptance function K centered on a pre-specified coupling interval (p_1, p_2) which by its output will help us determine an appropriate rank for the virtual dimension in A's amplitude equation. We'll retain for A the union of all virtual functions giving rise to nonzero K. Letting the region around p_0 correspond to a weak interaction limit and the region around p_1 to a strong limit, the choice of the bump function given in Fig. 5.1 guarantees

$$\begin{aligned} |f_{ov}| < p_0,\ K[f_{ov}] = 0, \\ |f_{ov}| > p_1,\ K[f_{ov}] = 1,\ \text{and} \\ p_0 < |f_{ov}| < p_1,\ K[f_{ov}] < 1. \end{aligned} \tag{5.5}$$

In the limit $p_2 = p_1 = h$, K tends to a Heaviside function centered about h. As $h \to p_1$, then each fragment will finish up with amplitudes drawn from the full virtual set, and the difference in error between it and the foregoing "proper" model shall be imputed to non-locality in the occupied space. We'll refer to this case as the "global" variant henceforth, noting it will serve as a bound for models where fragments reference subsets of the virtual space in their PT problems. Considering the other limit where $h \to p_2$, the virtual rank of each fragment-centered problem tends to zero and the error approaches the difference between the exact and zeroth-order energies with no virtual functions to perturb into. Our task will thus be to find a reasonable compromise between the sizes of the individual problems

and the forfeited accuracy against the "global" bound. Models where the minimal basis is constructed in this way shall be referred to as "truncated". We compile our models in Table 5.1 for quick reference and present our algorithm below.

model / PT dimensions	occupied	virtual
"proper"	N_o	N_v
"global"	$N_A * N_{oA}$	N_v
"truncated"	$N_A * N_{oA}$	$N_A * N_{v'A}$

Table 5.1: Model specifics. Both the "proper" and "global" models allow all occupied-virtual rotations and require semicanonicalization in the full virtual rank N_v for construction of the $2 * N_o$-dimensional minimal space. "Truncated" models require a linearly-growing number of $O(N_{v'A})^3$-cost diagonalizations, where $N_{v'A}$ is the number of "important" virtuals required in A's perturbative wavefunction.

1. For $\{A\}$,

   construct K$[(p_0, p_1),\ \mathbf{f_{oAv_{\{B\}}}}]$ and accumulate $\{v_{\{B\}}\}$ for $K > 0$, yielding $\{N_{v'A}\}$: $O(N_{oA} * N_v)$.

   Diagonalize $\mathbf{f_{oAoA}}$ and $\mathbf{f_{v'Av'A}}$, then transform $\{C^{\mu}_{vA}\}$ to the semi-canonical basis: $O(N_{oA})^3$+$O(N_{v'A})^3$.

   Construct and SVD local semicanonical $\mathbf{t^{oAv'A}}$, then transform $\{C^{\mu}_{pA}\}$: $O(N_{oA})^3$+$O(N^A_{v_{min}})^3$.

2. Orthogonalize across the set of minimal basis sets: $O(N_{v_{min}})^3 + O(N_o)^3$.

3. Diagonalize the Fock matrix in the minimal-basis representation to self-consistency: $O(2 * N_o)^3$.

The "global" model requires the same manipulations as above in the occupied space, but full-rank operations in the virtual space, e.g., without thresholding or fragmentation. For the "proper" model, full-rank operations are performed in both subspaces without reference to fragment labels. The cost of these models will therefore be dominated by the unavoidable $O(N_v)^3$ diagonalization step. Nevertheless, should they show promise, either can be recommended on the grounds that it asymptotically represents an *iteration-number*-fold net speedup relative to conventional SCF. This follows from taking a ratio of their costs in the limit $N_v >> N_o$, e.g., as the basis describing a given center approaches completeness, or as the number of molecules approaches some large value. If the net cost of the "proper" model is $\mathcal{O}(N_o)^3 + \mathcal{O}(N_v)^3 + m^{iter}_{min} * (2 * N_o)^3$ and the cost of the conventional algorithm goes as $m^{iter}_{can} * O(N_v + N_o)^3$, then the asymptotic ratio is $1 : m^{iter}_{can}$. For "truncated" models, we replace $\mathcal{O}(N_v)^3$ by $\mathcal{O}(\sum_A (N_{vA})^3) = N_A * \mathcal{O}(N_{vA})^3$ and obtain ${s_{frac}}^3 : ({N_A}^2 * m^{iter}_{can})$, where s_{frac} is the ratio of the number of virtuals incorporated in A's amplitudes to the number native to A, (or the number of virtual spaces appropriated by A, effectively) the cube of which is conveniently understood as the prefactor multiplying the linear-effort truncated virtual-block diagonalizations. We expect formal linear scaling to set in as s_{frac} converges on some

n-independent value and the local environment is minimally perturbed on the addition of a molecule.

In the following section, we benchmark our models on prototypical interactions of dimers and clusters taking the interaction error relative to conventional SCF as our figure of merit. We shall hope to demonstrate the quality of our minimal-basis models is largely invariant to both the choice of basis set and order of the perturbative wavefunction parametrizing them, and moreover that a judicious choice of K can furnish low-prefactor, linear-effort truncation models representing attractive alternatives to conventional SCF for intermolecular interactions. All models were implemented in a developmental version of the Q-Chem 4.0 electronic structure package.

5.3 Applications

We begin by examining the performance of tried-and-true, non-iterative dual basis (DB) and polarized atomic orbital (PAO) corrections to economical SCF references as a baseline for comparison. Interaction errors for these methods relative to the conventional scheme for the C_s-symmetry[293] water dimer interaction are given in Table 5.2. The zeroth-order DB-SCF energy consistently overshoots the exact result due to BSSE, improving roughly two-fold with the cardinal number, while the corresponding PAO-SCF number consistently underbinds and is insensitive to a choice of the underlying basis set. A single Fock matrix construction, and perturbative treatment (infinite-order for DB-SCF and first-order for PAO-SCF) in the secondary basis improves the former by an order of magnitude and the latter by two orders, both garnering quantitative binding energies for an *iteration-number*-fold reduction in cost over the conventional scheme, a true success story for perturbation theory.

error	DB-SCF/racc-pVZ(0)	PAO-SCF(0)	DB-SCF/racc-pVZ$_{t=t^{(\mathrm{inf})}}$	PAO-SCF$_{t=t^{(1)}}$	E$^{bind}_{exact}$
aug-cc-pvdz	-3.07	1.56	-0.12	0.04	19.52
aug-cc-pvtz	-1.18	1.42	-0.08	0.04	19.00
aug-cc-pvqz	-0.68	1.70	-0.04	0.05	19.08

Table 5.2: kJ/mol interaction errors for dual-basis and projected atomic-orbital SCF against vanilla SCF for $(H_2O)_2$ in its C_s equilibrium geometry computed with the B3LYP functional.

How does the choice of reference wavefunction affect performance of the perturbation theory? PAO-SCF and DB-SCF represent opposite extremes of reference localization in a supermolecular binding energy calculation. The PAO-SCF scheme solves a constrained variational problem yielding a reference of strictly-atom-centered non-orthogonal states, while the DB-SCF reference wavefunction is simply the canonical (delocalized) solution in a basis subsumed by the target one. A reference of ALMOs or unrelaxed (FRZ) orbitals represents, in some sense, an intermediate node on an imagined scale of orbital locality, since therein,

molecular orbitals are delocalized on a molecule, but strictly *molecule*-localized. Not-so-intermediate errors against the same reference calculations for both zeroth-order references are presented in the first column of Table 5.3. In stark contrast to DB- or PAO-SCF, the error from either reference - some fifty and thirty percent - respectively, is large, but not staggering, as what we're calling "error" here has been ascribed in the context of energy decomposition analysis (where these references serve as intermediate wavefunctions connecting to the canonical energy and wavefunction) as induction plus charge-transfer energy in the case of the FRZ reference, and charge-transfer energy from an ALMO reference (not to mention that the DB- and PAO-SCF corrections possibly benefit from error cancellation in the supermolecular subtraction). Given the significant dative character of this interaction, we acknowledge perturbation theory from either molecule-centered reference shall thus have to do a lot of work to compete.

We throw away fragment labels for the moment and perform perturbation theory accord-

error	FRZ(0)	ALMO(0)	$\text{FRZ}_{t=t^{(1)}}$	$\text{FRZ}_{t=t^{(\infty)}}$	$\text{ALMO}_{t=t^{(1)}}$	$\text{ALMO}_{t=t^{(\infty)}}$
aug-cc-pvdz	13.04	8.96	0.38 / 0.13	0.40 / 0.13	0.43 / 0.05	0.44 / 0.05
aug-cc-pvtz	12.55	6.93	0.39 / 0.14	0.42 / 0.14	0.30 / 0.04	0.30 / 0.04
aug-cc-pvqz	12.86	6.82	0.41 / 0.15	0.44 / 0.15	0.27 / 0.03	0.28 / 0.03

Table 5.3: interaction error in kJ/mol as as function of basis set against vanilla B3LYP/$(H_2O)_2$ in its C_s equilibrium geometry for *non-iterative/iterative* "proper" models beginning from either FRZ or ALMO reference orbitals and taking first- or infinite-order t^s amplitudes.

ing to the "proper" PT scheme detailed above which, as the reader will recall, takes the same expressions as the DB and PAO methods. The corrections are compiled in the second set of columns of Table 5.3. Glancing at the leading entries there, we conclude the performance of the non-iterative correction does not seem to depend critically on the order (linearized or iterated solution to eq. 5.2 of the perturbative wavefunction, choice of basis set, or choice of reference, though we're still left with interaction errors larger than the foregoing corrections by an order of magnitude. This gap is apparently bridged in the subsequent minimal basis iterations as the trailing columns of Table 5.3 indicate. Again, there's an insensitivity of the relaxed-basis error to perturbative order and basis set, though corrections from an ALMO starting point are slightly better than those from a FRZ reference. Your correspondents emphasize again that the most computationally-demanding part of the proposed methods and DB and PAO schemes alike is the full-rank virtual-virtual block diagonalization of the Fock matrix required to solve the amplitude equations. Because of their isomorphism, we expect that a similar variational optimization in the rank-reduced eigenspace of t_1 obtained from a DB or PAO reference will likely effect significant accuracy gains for those theories, for free.

As discussed previously, we must cause the rank of the virtual dimension in Eq. 5.2 to be

$\|0\rangle$ geometry	FRZ $1{*}R_{eq}$	ALMO $1{*}R_{eq}$	FRZ $1.5{*}R_{eq}$	ALMO $1.5{*}R_{eq}$	FRZ $2{*}R_{eq}$	ALMO $2{*}R_{eq}$
error { K[(1,5)*E-3]}	0.44	0.76	0.30	0.15	0.03	0.01
error {K[(1,5)*E-5]}	0.14	0.25	0.01	0.02	0.00	0.00
error{K[(1,5)*E-7]}	0.14	0.04	0.01	0.01	0.00	0.00
error{K[(1,5)*E-8]}	0.14	0.04	0.01	0.00	0.00	0.00
error(global)	0.14	0.04	0.01	0.00	0.00	0.00
error(proper)	0.14	0.04	0.01	0.00	0.00	0.00
$\langle sfrac\rangle$ { K[(1,5)*E-3]}	0.75	0.32	0.01	0.00	0.00	0.00
$\langle sfrac\rangle$ { K[(1,5)*E-5]}	1.98	1.46	1.68	0.78	1.18	0.48
$\langle sfrac\rangle$ { K[(1,5)*E-7]}	2.00	1.98	1.99	1.53	1.95	1.45
$\langle sfrac\rangle$ { K[(1,5)*E-8]}	2.00	2.00	2.00	1.95	2.00	1.99
$\langle sfrac\rangle$(global)	2.00	2.00	2.00	2.00	2.00	2.00

Table 5.4: binding error in kJ/mol as as function of acceptance function domain against conventional B3LYP in aug-cc-pvtz for $/(H_2O)_2$ in its C_s equilibrium geometry for iterative models beginning from either FRZ or ALMO taking infinite-order t_1 amplitudes to parametrize minimal basis and corresponding $\langle s_{frac}\rangle$.

independent of cluster size to achieve linear scaling. Our solution will be to fractionate the full-rank problem into N_A molecule-centered problems, each including a *convergent* fraction of occupied-virtual excitations in its perturbative wavefunction. In the limit that the acceptance function K defined in Fig. 5.1 is centered in a weak coupling domain, no fragment sees the perturbation and the correction vanishes; In the "global" limit, each fragment's perturbative wavefunction is full-rank and we should expect errors comparable to those of the "proper" scheme at a similar cost. Though we anticipate (*vide infra*) in applications on large clusters that a given fragment shall automatically utilize most or all of its nearest neighbors' virtual functions, we shall investigate in the short-term effects of truncation in the dimer. Choosing an acceptance function K[$p0 = 1.0{*}$E-X, $p1 = 5.0$E-X] for X={3, 5, 7, 8}, (e.g., spanning couplings between one and one one-hundred-thousandth kJ/mol), we compile interaction errors and corresponding $\langle s_{frac}\rangle$ in Table 5.4. We see the FRZ-reference truncation model errors and $\langle s_{frac}\rangle$ approach the intrinsic "global" bound more quickly than their ALMO-reference analogs at all intermonomer separations, though the disparity decreases as the references approach equivalence in the long range. Because non-zero coupling elements in the FRZ representation are larger and more numerous than in the ALMO representation, we should expect $\langle s_{frac}\rangle$ and truncation error to be much less sensitive to the threshold beyond some coupling regime, albeit larger, e.g., at $2 * Req$, unrelaxed fragments require half of the virtual space, while polarized fragments require a quarter.

The adaptive freedom afforded by this approach to truncation implies a varying $\langle s_{frac}\rangle$ along an interaction coordinate, therefore bearing critically on the question of smoothness.

	trunc.(1,5*E-4)	(1,5*E-5)	(1,5*E-6)	(1,5*E-7)	global	proper	DB-SCF	PAO-SCF
total	1.37	0.88	0.15	0.10	0.10	0.10	0.28	0.58
hb	1.35	0.66	0.20	0.17	0.17	0.17	0.42	0.81
disp	1.57	1.18	0.11	0.02	0.02	0.02	0.16	0.45
mix	1.11	0.70	0.10	0.02	0.02	0.02	0.17	0.31

Table 5.5: S66 RMSEs relative to ωB97X-D/aug-cc-pvdz in kJ/mol. Local models use ALMO orbitals and infinite-order t_1 for minimal basis parametrization. $\langle s_{frac} \rangle$ for the truncation models are 0.98, 1.40, 1.89, and 1.99, respectively.

Examining the top panel of Fig. 5.2, we see the slope of $\langle s_{frac} \rangle$ changes more rapidly for more aggressive thresholds as the dimer traverses its H-bond coordinate, though computed potentials and gradients in the second row of panels virtually overlay the "global" plots. A closer look at the truncation errors in the energy and gradient plotted in the third row, however, reveals discontinuities across all thresholds, though they never exceed a hundredth of a kJ/mol (or a tenth of a kJ/mol/Å) for sensible 1- and 0.1-microhartree cut-offs. This needling issue can be easily side-stepped if one enforces a constant $\langle s_{frac} \rangle$ at all intermolecular distances, but this comes at the expense of the adaptability of the selection scheme to both economize the calculation and maintain a constant gauge of the perturbation strength, e.g., we see rapidly decaying $\langle s_{frac} \rangle$ for a stabilized truncation error in the long range. To put it a different way, a rigid $\langle s_{frac} \rangle$ would make the wavefunction either too sparse or include too much information. Though we shouldn't expect any of these acceptance intervals to guarantee the same smoothness gauge or error margin for other interactions *a prior*, simple, automatable scans such as above are instructive for identifying the intrinsically narrow width of important couplings required to produce a satisfactory level of smoothness.

As our initial analysis showed, the ALMO EDA predicts comparable electrostatic/Pauli repulsive, inductive, and dative contributions to the ∼20kJ/mol interaction strength between two waters. Debate about the merits of the decomposition notwithstanding, the intermediate wavefunctions there are, as the reader will recall, the zeroth-order references we've employed in our perturbative models. We should thus expect our methods to perform best for non-dative non-covalent interactions, e.g., those dominated by permanent and/or induced electrostatics and/or dispersion. To quantify any dependence of performance on interaction character, we apply our models to the S66[294] dataset of varied interactions comparing against those obtained from conventional ωB97X-D/aug-cc-pvdz calculations. RMSEs for all schemes and other non-iterative corrections are compiled in Table 5.5. DB-SCF is seen to outperform PAO-SCF two-fold in all categories, but its total RMSE is three-fold larger than the "global" and "proper" methods' from an ALMO starting point. As anticipated, the most substantial gains are in dispersion and mixed interactions. Tracking total RMSEs for schemes truncating the virtual space, we conclude that an acceptance domain minimally in the microhartree regime is required for quantitative accuracy, improving ten-fold over the most aggressive 100-milihartree-scale model. Computed $\langle s_{frac} \rangle$ provided in the headings of Table 5.5 indicate nearly the entire virtual set is chosen by each fragment in the case of the

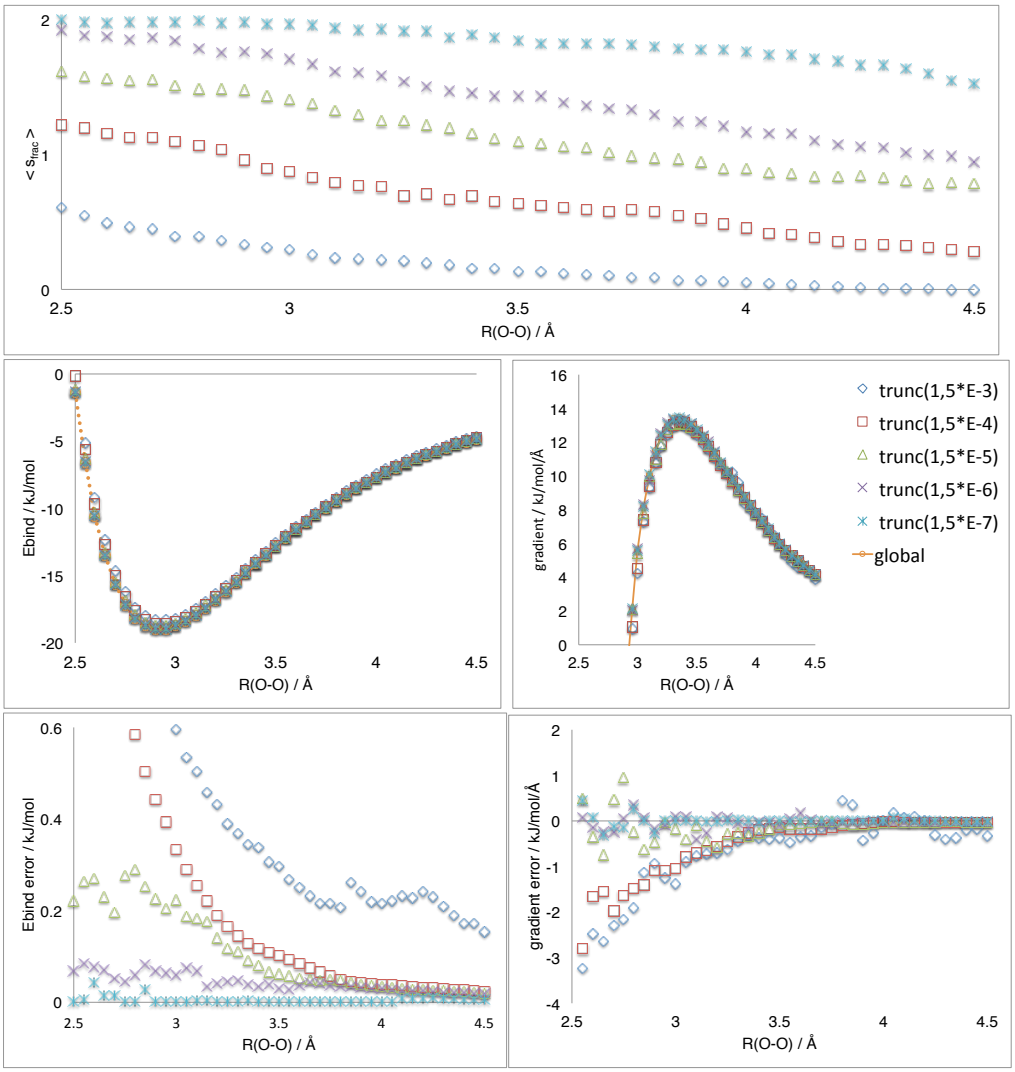

Figure 5.2: Properties of C_s water dimer traversing its H-bond coordinate computed at the B3LYP/aug-cc-pvtz. Models take an ALMO reference and minimal basis parametrized by infinite-order t_1. Top: $\langle s_{frac} \rangle$ as a function of intermonomer separation computed for a range of acceptance functions. Middle: Interaction potential and gradient computed for truncation models and the global bound. Numerical gradients were computed by the central-difference approximation. Bottom: corresponding truncation errors.

n	DB-SCF/6-31G	trunc(1,5*E-3)	(1,5*E-4)	(1,5*E-5)	[a]global	PAO-SCF	E_{exact}^{bind}/kJ*mol^{-1}
2	8.2	1.4	1.1	1.0	0.4	-0.3	25.4
3	8.1	5.5	0.6	0.4	0.4	-0.6	85.0
4	9.3	5.4	0.7	0.6	0.6	-0.2	143.9
5	10.5	5.7	0.7	0.5	0.5	0.0	181.2
6	7.7	5.8	0.7	0.6	0.6	-0.6	246.9
7	8.8	5.8	1.1	0.6	0.6	-0.5	285.8
8	8.8	6.3	1.6	0.6	0.6	-0.3	335.5
9	8.2	6.3	0.9	0.7	0.7	-0.5	387.8
10	7.6	6.8	1.5	0.8	0.8	-0.6	480.8
13	7.7	7.3	1.8	0.8	0.8	-0.7	670.9
17	8.4	7.6	3.1	0.9	0.9	-0.7	880.4
30	9.6	8.1	1.4	1.0	1.0	-0.8	1380.8
46	10.0	8.0	1.2	1.0	1.0	-0.9	2074.1
71	9.8	8.1	1.4	1.0	1.0	-0.9	3428.2
106	13.8	9.2	2.6	1.4	1.4	-4.1	2397.3
127	19.9	13.7	3.3	2.1	2.1	-4.6	2335.3
147	10.6	7.4	1.6	1.1	1.1	-1.8	5946.0
range	12.2	12.3	2.7	1.7	1.7	4.6	

Table 5.6: Binding energy percent error against conventional PBE/6-31G* for $(H_2O)_n$ clusters. Structures were optimized in Avogadro with the MM94 force field. Models use ALMO orbitals and infinite-order t_1 for minimal basis parametrization. [a]The "proper" models produced identical errors on this scale and were not included for brevity.

latter, while nearly half is chosen in the former. We shall expect in studies on large clusters that $\langle s_{frac} \rangle$ should exceed, or at the very least be equivalent to, the first coordination number, and consequently that nearest-neighbor interactions will approach the "global" quality automatically.

For its large interaction-strength-to-size ratio, we return to water to uncover properties of our models when extended to treat clusters. We have chosen a set of seventeen MM94[295]-optimized complexes up to 147 water molecules in size, and bound up to ∼300 times the strength of the dimer interaction. As before, we shall scan a range of acceptance domains to uncover general trends, including convergence of per-monomer error to the global bound as well as saturation onset in $\langle s_{frac} \rangle$. Percent errors in the binding energy relative to conventional PBE/6-31G* are given in Table 5.6. DB methods surprisingly maintain poor performance across all cluster sizes, likely due to an exceedingly poor reference. A choice of the r64G[275] primary basis does nothing to improve its performance (*vide infra*). PAO-SCF overbinds consistently, but only slightly, while the "global" and "proper" models consistently err on the other side by a similar amount for small- to medium- sized clusters, but finish up for clusters larger than n=71 with ∼two-fold smaller percent errors and ranges. At least a 10-microhartree acceptance domain is required to reproduce global model errors, while the 100-microhartree acceptance domain is the most aggressive threshold furnishing acceptable results.

How do the (automated) domain regime choices affect saturation of intensive properties? Since coupling amplitudes are implicitly proportional to orbital overlaps, we expect more ag-

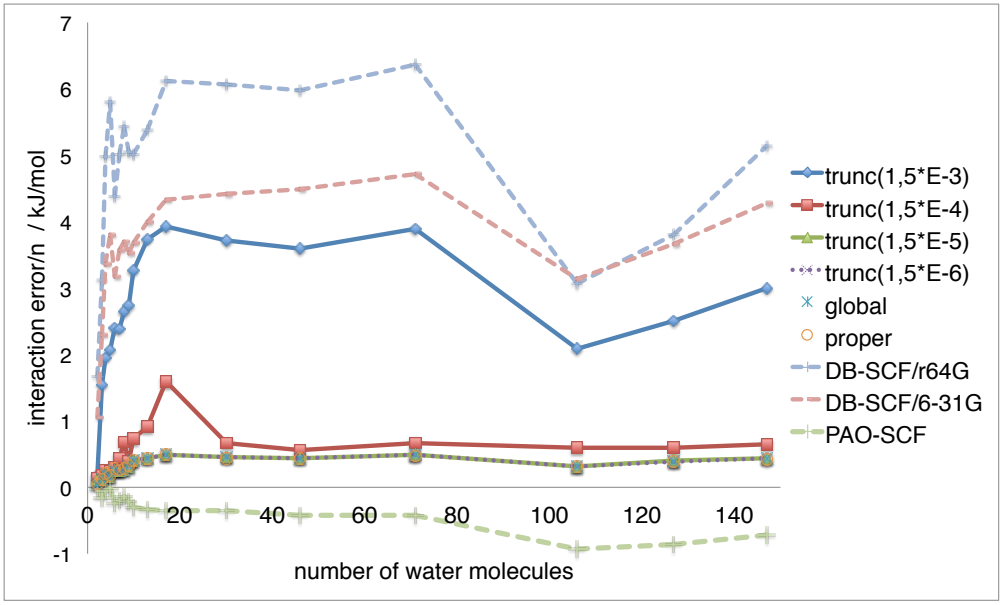

Figure 5.3: Error/n in kJ/mol computed relative to conventional PBE/6-31G*.

gressive thresholds to give rise to more sensitive per-monomer errors, and correspondingly, that $\langle s_{frac} \rangle$ should asymptote more quickly. Examining per-monomer interaction error versus n in Figure 5.3, we see larger initial gradients for more aggressive thresholds, and moreover that the millihartree acceptance domain never reliably compensates the change in local environment an additional of a peripheral fragment effects.

In addition to its computational significance as the linear prefactor for our truncation models, $\langle s_{frac} \rangle$ represents, in a sense, a figure of coordination number whose asymptotic value can not only bear on the error analysis, but also inform acceptance domain selection. We can interpret from the left panel of Figure 5.4 that each fragment in a truncation scheme taking a 1-millihartree domain appropriates the virtual spaces of some 8 surrounding neighbors (and this is still insufficient, as we have seen), each monomer in the 100-microhartree domain requires 18 to produce nearly-converged errors, and 35 per monomer in a 10-microhartree domain is conservative enough to recover the "global" bound. Acknowledging full well the approximate nature of the following analysis, we nevertheless attempt to relate saturated $\langle s_{frac} \rangle$ to coordination numbers computed by integrating center-of-mass radial distributions over putative solvation shell domains given in the column headings of Table 5.7. Sample radial distributions for surface and solvated configurations extracted from the n=147 cluster are plotted in the right panel of Fig. 5.4 for calibration. Average coordination numbers are compiled in Table 5.7. Focusing on the first coordination shell, we see a rough correspondence between the average coordination number and the asymptotic $\langle s_{frac} \rangle = 8$ obtained by the 1-millihartree-domain truncation model above. We conclude that this truncation model has, on average, included in each monomer's perturbation problem the virtual spaces of monomers

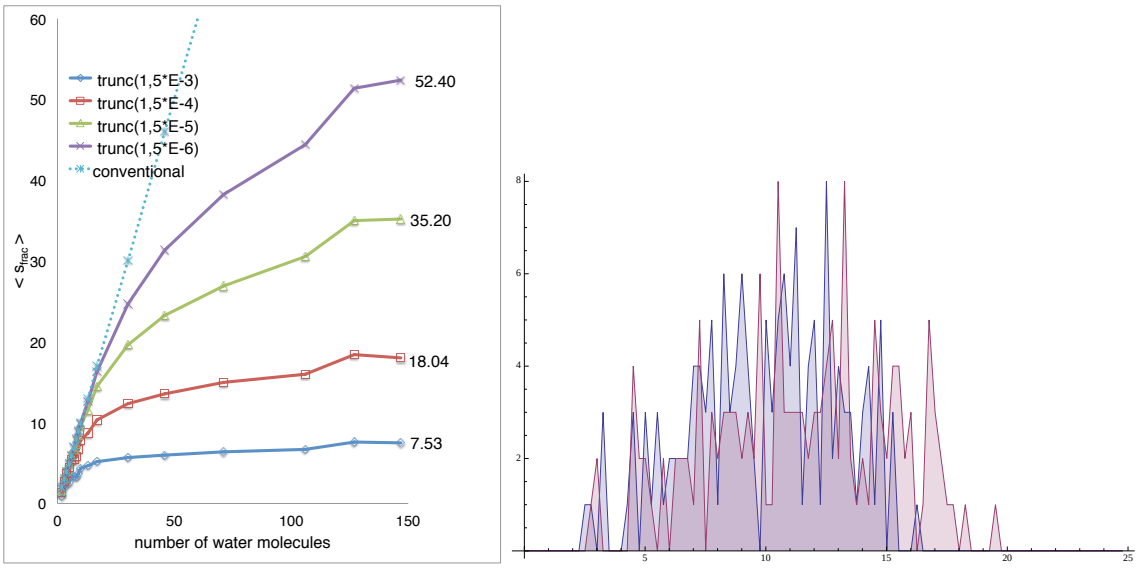

Figure 5.4: Left: $\langle s_{frac} \rangle$ as a function of acceptance domains converges by n =∼127. Right: Integrated radial distribution as a function of center-of-mass displacement in angstrom for peripheral (red) and interior (blue) monomers in the n =147 cluster.

$\lvert \mathbf{r}_{\text{c.o.m.}} - \mathbf{r}' \rvert$ domain / Å	0.00-3.49	3.50-5.49	5.50-7.49	7.50-9.99	10.00-∞
putative solv. shell no.	1	2	3	4	5
$\langle n \rangle$	7.4 ± 3.7	14.6 ± 5.5	23.1 ± 7.9	35± 8.1	65.5± 21.9
cumulative	7.4	22.0	45.1	80.5	146.0

Table 5.7: Putative coordination numbers by shell for the $(H_2O)_{147}$ cluster. Computed $\langle n \rangle$ for the first three shells roughly mirror the number of virtual spaces appropriated per fragment by truncation models taking the acceptance functions K[$(1, 5)E$-X] for X={3, 4, 5}, respectively.

in its first solvation shell. That the per-monomer error there is unstable suggests the second solvation shell perturbs the core monomer substantially. Summing the first and second coordinations, we see a correspondence between the total number coordinated through two shells and the asymptotic $\langle s_{frac} \rangle = 18$ of the 100-microhartree-domain model, suggesting that including some two coordination spheres about each center is minimally required to stabilize the per-monomer error. It follows that the dramatic increase in per-monomer error at n=17 for the 100-microhartree-domain model seen in Fig. 5.3 is attributable to a yet *unsaturated* $\langle s_{frac} \rangle \sim 10$. The 10-microhartree-domain model of $\langle s_{frac} \rangle = 35$ corresponds to including some fraction of the third shell on top of the first two shells. The most conservative 1-microhartree model yields $\langle s_{frac} \rangle = 52$ corresponds here to a little more than three solvation shells of virtual functions per monomer. As we've seen, this augmentation mini-

mally affects the truncation error, suggesting an optimal domain size is somewhere between the second and third shells.

The above analysis has served to highlight the merits (and attendant complications) inherent to a selection algorithm informed by coupling strengths rather than by a real-space metric such as center-of-mass displacements or van der Waals overlaps. Increased adaptability in domain breadth due to a consideration of $N_o * N_v$ coupling variables instead of N_A^2 inter-fragment distances effectively smears monomeric perturbative wavefunctions over non-integer coordination domains, allowing for more precise convergence on the optimal domain size, but at the cost of intuitive appeal the real-space metric affords. That being said, the generalizability of either metric is questionable at the least. One would have been hard-pressed to intuit that greater than two solvation shells' worth of virtual functions per monomer would be required to reduce the truncation error to noise in the water cluster interactions above. This number unequivocally depends on the character of the cluster, too, e.g., less-structured interactions between non-polar solvents are expected to require fewer solvation shells, while heterogeneous interactions likely require variable domain sizes. The problem of generalizability notwithstanding, we have demonstrated that truncation according to unrelaxed coupling strengths can hierarchically approach the full-rank "global" bound at low-prefactor linear cost.

5.4 Conclusions

We have developed and applied a suite of non-Brilluoin perturbation theories from molecule-centered references to approximate supermolecular interactions. Large-scale accuracy and tractability gains are obtained by projecting the full-rank SCF problem into a $2*N_o$-rank representation (which exactly recovers the perturbative wavefunction), and then performing an SCF optimization in the minimal space. Like DB and PAO corrections to SCF, models detailed here taking full-virtual-rank perturbative wavefunctions afford an *iteration-number*-fold speedup against conventional SCF. In contrast, they benefit from variational relaxation in a subsequent minimal-basis SCF. Fragmentation of the full-rank perturbative problem into N_A molecule-centered sub-problems provides a tunable trade-off between accuracy and the onset of linear scaling, but at the cost of formal smoothness in the PES and facile generalizability in domain selection. (We want to emphasize, however, that generalizability is the crux of any linear-scaling algorithm forcing sparsity by truncation.) Thus, we recommend our full-rank models in cases where a single $O(N_v^3)$ diagonalization is affordable. Otherwise, we recommend truncation minimally in an acceptance regime of the same order as the calculation's convergence threshold and caution that more aggressive truncation will require thorough benchmarking of acceptance domains.

Chapter 6

Local transformed perturbation theory

6.1 Introduction

With the formal foundations well-established for the routine computation of a host of molecular properties in density-functional and wavefunction frameworks, quantum chemistry has undoubtedly emerged as a mature field with considerable predictive power in the past few decades. These advances coupled to ever-increasing improvements in computing power have arguably served to shift its scope of applied focus to larger systems of molecular clusters, extended surfaces, and even solvated biomolecules. To this end, much emphasis has been placed on the development of low-scaling approximations to high-level model chemistries, e.g., RI/density-fitting[37–42] for two-electron integrals, explicitly-correlated F12/R12[43–51] formulations, spin-component-scaled Laplace-transformed [52, 53], and rank-reducing tensor decompositions[54–62] in Møller-Plesset (MP) and coupled-cluster (CC) methodology, hybrid QM/MM[245, 246] embedding approaches, and domain fragmentation for low-scaling local correlation methods.

Chief among the observables for which these efforts at economization have proved essential are binding energies. Perhaps the most popular of non-supermolecular schemes is symmetry-adapted perturbation theory (SAPT),[296, 297] a many-body generalization of Heitler-London theory that treats the two-body Hamiltonian as a perturbation to monomer wavefunctions complete to some order in MP theory, and furnishes decomposable interaction energies directly, that is, without subtraction. It has seen immense development in wavefunction and DFT[298, 299] flavors, and even extended to the realm of molecular clusters with the use of pairwise-additive many-body techniques[286, 300, 301]. Among the most sophisticated coupled-cluster level variants are the CCD+ST(CCD)[302, 303] and SAPT(CCSD)[304–307] methods. The former computes dispersion by solving intermonomer ring-CCD equations on top of CCD monomers and treats singles and triples perturbatively, and has recently

been treated in a reduced "natural" orbital representation[308]. The latter computes dispersion from frequency-dependent polarizabilities of CCSD-level monomer wavefunctions and adds non-iterative triples and quadruples. These methods have shown themselves to be very accurate when applied to two-body interactions, but extending SAPT in its purest form to non-pairwise-additive interactions has proved far from straightforward[286, 300, 301]. Other direct methods tackle the problem via application of the many-body expansion (MBE) separating pairwise, three-body, and higher terms. The fragment MO method [281–284], many-overlapping-body[287], and divide-and-conquer[276–280] approaches have produced encouraging energetics for calculations on large clusters, and are generally amenable to large-scale parallelization. Moreover, low-order truncations can furnish surprisingly accurate results while obviously conferring huge computational savings.

Non-constructive/supermolecular techniques generally seek to recover a given level of canonical treatment of the supersystem by carving out domains defining individual correlation problems, oftentimes in localized orbital representations. Such approaches are motivated by the inherent locality of dynamical correlations, and thus neglecting distant correlations should effect lower scaling of the supermolecular computation without forfeiting accuracy. Pulay[309] and Saebø[247, 248, 310, 311] did the first seminal work in this field, developing an iterative MP2 scheme retaining only a *quadratic* number of domain-pair amplitudes but recovering of more than 98% of the canonical correlation energy in a basis of localized occupied orbitals and a non-orthogonal, redundant set of atomic orbitals projected into the virtual space (termed PAOs). Their approach has since inspired the non-iterative fixed-domain dimers- (DIM) and triatomics-in-molecules (TRIM)[249] models for MP2-level correlation and a fourth-order triples model[312], the local coupled cluster methods[250–252, 313–315] introduced by Werner and Schutz and developed by others, purely AO-based algorithms[253, 254, 316, 317], and mixed CC-MPBT approaches[318–320]. Other local correlation methods similar in spirit to the MBE approaches eschew non-orthogonality and its attendant complications, e.g., linear-dependence, rank dilation, and retention of overlap integrals in the spin-orbital equations, opting instead for localized orthogonal orbitals and domain specification based on the relative locality of the occupied subspace, allowing straightforward use of standard-package codes and facile parallelization of completely independent (albeit sometimes overlapping) subdomain calculations. These include the divide-expand-consolidate approach[63–65], natural linear scaling coupled-cluster[66, 67], the clusters in molecules[68, 69] method, and other higher-order methods [70, 71].

Some qualities a local correlation model should possess beyond the property of being formally satisfactory arguably include simple, physically-motivated domain identification; monotonic convergence to the (upper-bound) untruncated/canonical correlation energy as the model space is augmented to full-rank; consistent treatment of occupied and virtual subspaces; free of empirical or tunable parameters; demonstrated and sustained cost-savings relative to the canonical result while remaining accurate for *relative* energies; extension to arbitrary correlation rank; well-defined limiting behavior; and guaranteed smoothness on the potential energy surface. In this work, we introduce a hierarchy of elegant local correlation

theories which we feel satisfies all of the above criteria. Guided by the ethos of perturbation theory, we assume outright that the interaction energy is *substantially* smaller than the total energy. Making use of Löwdin partitioning[29, 321–324], we define a zeroth-order wavefunction as the solution of truncated, non-orthogonal, molecule-centered coupled cluster equations of at most a quadratic number of variables, and treat non-local excitations at second-order. Our reference determinant shall be built from absolutely-localized molecular orbitals (ALMOs)[75, 288–290], determined as the variational solution of locally-projected (SCF-MI) equations[72, 292] constraining the coefficient matrix to be block-diagonal in the molecules. Such a reference has treated induction effects to infinite-order (or satisfied Brillouin's condition on-site), but remains an upper bound to canonical Hartree-Fock (HF), increasingly accurate as inter-site Brillouin matrix elements vanish, e.g., for interactions between insulators or interactions approaching the long range.

We hope to demonstrate that our models represent attractive non-iterative alternatives to canonical MP2 where an absence of higher-order terms is responsible for a poor description of dispersion. Moreover, in the regime where a perturbative treatment is valid, models of locally-projected solutions with a linear or quadratic number of variables will not only effect immense tractability gains, but also serve as useful alternatives to the canonical formulation.

6.2 Theory

An exact solution $|R_k\rangle = \sum_h r_h^k |h\rangle$ of the Schrodinger equation in the full Hilbert space of n-electron Slater determinants, $|\mathbf{h}\rangle = |0\rangle + |\mathbf{s}\rangle + |\mathbf{d}\rangle + |\mathbf{t}\rangle + |\mathbf{q}\rangle + ...$, is obtained by solving

$$\hat{H}|R_k\rangle = E^k|R_k\rangle \tag{6.1}$$

for $\{\mathbf{r_h^k}\}$, the components of $|R_k\rangle$ in $|\mathbf{h}\rangle$. Similarity transformation of the molecular Hamiltonian leaves the eigenvalue spectrum of $\hat{H}$ unchanged implying a coupled cluster solution of rank n will be equivalent to full configuration interaction. Such a limit is obviously infeasible, so eq. 6.1 is generally treated in a small fraction of $|\mathbf{h}\rangle$, call it $|\mathbf{p}\rangle$, where one solves $\mathbf{\bar{H}_{p0} = 0}$ for $\mathbf{t_p}$, neglecting projections onto the complementary space, call it $|\mathbf{q}\rangle$. Viewing a solution to a standard low-rank CC problem in $|\mathbf{p}\rangle$ as a well-defined zeroth-order wavefunction, we can account for q-space components non-iteratively, couching eq. 6.1 in the language of perturbation theory.

Shifting to a matrix representation with $\mathbf{\bar{H}_{pq}} = |\mathbf{p}\rangle\langle\mathbf{p}|\bar{H}|\mathbf{q}\rangle\langle\mathbf{q}|$, projecting with the left eigenfunction $\langle 0|\mathbf{l^k}$ and $\langle\mathbf{h}|$, we obtain expressions for the energy E^k and amplitudes $\{\mathbf{r_h^k}\}$,

$$\langle 0|\sum_{\mathbf{h}\ \mathbf{h'}} \mathbf{l_{h'}^k \bar{H}_{h'h} r_h^k}|0\rangle = E^k, \Big\{\mathbf{E_k 1} - \mathbf{\bar{H}_{hh}}\Big\}\mathbf{r_h^k}|0\rangle = \sum_{\mathbf{h'}\neq\mathbf{h}} \mathbf{\bar{H}_{hh'} r_{h'}^k}|0\rangle, \tag{6.2}$$

Splitting $\mathbf{H} = \mathbf{H^{(0)}} + \mathbf{H^{(1)}}$, $\mathbf{r} = \mathbf{r^{(0)}} + \mathbf{r^{(1)}}$+..., and $\mathbf{l} = \mathbf{l^{(0)}} + \mathbf{l^{(1)}}$+..., and expanding eqs. 6.2 and henceforth dropping the state level k for brevity, we obtain corrections to the energy

through second order:

$$\begin{aligned} E^{(0)} &= \langle|\mathbf{l^{(0)}H^{(0)}r^{(0)}}|\rangle, \\ E^{(1)} &= \langle|\mathbf{l^{(0)}H^{(1)}r^{(0)}}|\rangle, \quad \text{and} \\ E^{(2)} &= \langle|\mathbf{l^{(0)}H^{(1)}r^{(1)}}|\rangle. \end{aligned} \tag{6.3}$$

Choosing $\mathbf{H^{(0)}} = \bar{\mathbf{H}}_{\mathbf{pp}} + \mathbf{F}_{\mathbf{qq}}$, $\mathbf{H^{(1)}} = \bar{\mathbf{H}}_{\mathbf{pq}} + \bar{\mathbf{H}}_{\mathbf{qp}} + \bar{\mathbf{V}}_{\mathbf{qq}} + \bar{\mathbf{F}}_{\mathbf{qq}} - \mathbf{F}_{\mathbf{qq}}$, $\mathbf{r^{(0)}} = \mathbf{1_{pp}}$, and $\mathbf{l^{(0)}} = (\mathbf{1_{pp}} + \mathbf{\Lambda_{pp}})$, where Lambda is the de-excitation operator from the coupled-cluster pseudo-Lagrangian[325–327], we're guaranteed i) a zeroth-order eigenfunction of the transformed Hamiltonian equivalent to the coupled cluster energy,

$$E^{(0)} = \langle|(\mathbf{1} + \mathbf{\Lambda})_{\mathbf{pp}}\bar{\mathbf{H}}^{\mathbf{(0)}}_{\mathbf{pp}}\mathbf{1}|\rangle = E^{\mathrm{CC}}, \tag{6.4}$$

ii) $E^{(1)} = 0$ since q- and p-space determinants cannot connect across the first-order Hamiltonian, and iii) first-order amplitude equations that uncoupled the left-hand side of eq. 6.2 following a transformation of basis that diagonalizes the energy difference. Identifying the scope of $|\mathbf{p}\rangle$ determines the correlation model. Taking $|\mathbf{p}\rangle = |\mathbf{0}\rangle + |\mathbf{s}\rangle + |\mathbf{d}\rangle$, $|\mathbf{h}\rangle = |\mathbf{t}\rangle + |\mathbf{q}\rangle$, and $\mathbf{H^{(0)}_{qq}} = \bar{\mathbf{F}}_{\mathbf{qq}}$, for example, one obtains the "(2)" correction to CCSD[328] of Gwaltney *et. al.* A choice of bare $\mathbf{F_{qq}}$ instead gives the "$(2)_{TQ}$"[329–331] corrections of Hirata and crew. Neglecting quadruples and approximating $\mathbf{\Lambda} = \mathbf{t}^\dagger$, one obtains CCSD(T). Though all are orbitally-invariant, a transformed one-body operator in the q space requires a fifth-order transformation to a set of biorthogonal eigenstates to diagonalize the amplitude equations. We take the untransformed operator in the q-space here.

After a change of basis and expansion of eq. 6.2, the equations for the first-order wavefunction are

$$\begin{aligned} \mathbf{D^{(0)}_{ss}r^{s(1)}} &= \bar{\mathbf{H}}^{(1)}_{\mathbf{s0}} + \bar{\mathbf{H}}^{(1)}_{\mathbf{ss'}}\mathbf{r^{s'(0)}} + \bar{\mathbf{H}}^{(1)}_{\mathbf{sd}}\mathbf{r^{d(0)}} + \bar{\mathbf{H}}^{(1)}_{\mathbf{st}}\mathbf{r^{t(0)}}, \\ \mathbf{D_{dd}r^{d(1)}} &= \bar{\mathbf{H}}^{(1)}_{\mathbf{d0}} + \bar{\mathbf{H}}^{(1)}_{\mathbf{ds}}\mathbf{r^{s(0)}} + \bar{\mathbf{H}}^{(1)}_{\mathbf{dd'}}\mathbf{r^{d'(0)}} + \bar{\mathbf{H}}^{(1)}_{\mathbf{dt}}\mathbf{r^{t(0)}} + \bar{\mathbf{H}}^{(1)}_{\mathbf{dq}}\mathbf{r^{q(0)}}, \\ \mathbf{D_{tt}r^{t(1)}} &= \bar{\mathbf{H}}^{(1)}_{\mathbf{t0}} + \bar{\mathbf{H}}^{(1)}_{\mathbf{ts}}\mathbf{r^{s(0)}} + \bar{\mathbf{H}}^{(1)}_{\mathbf{td}}\mathbf{r^{d(0)}} + \bar{\mathbf{H}}^{(1)}_{\mathbf{tt'}}\mathbf{r^{t'(0)}} + \bar{\mathbf{H}}^{(1)}_{\mathbf{tq}}\mathbf{r^{q(0)}}, \quad \text{and} \\ \mathbf{D_{qq}r^{q(1)}} &= \bar{\mathbf{H}}^{(1)}_{\mathbf{q0}} + \bar{\mathbf{H}}^{(1)}_{\mathbf{qd}}\mathbf{r^{d(0)}} + \bar{\mathbf{H}}^{(1)}_{\mathbf{qt}}\mathbf{r^{t(0)}} + \bar{\mathbf{H}}^{(1)}_{\mathbf{qq'}}\mathbf{r^{q'(0)}}. \end{aligned} \tag{6.5}$$

where $\mathbf{D^{(0)}_{qq}} \equiv \{E^{(0)}\mathbf{1}_{qq} - \bar{\mathbf{H}}^{(0)}_{\mathbf{qq}}\}$, and repeated indices imply summation. Applying these to the expression for the second-order energy above, we obtain

$$\begin{aligned} E^{(2)} = \bar{\mathbf{H}}^{(1)}_{\mathbf{0s}}\mathbf{r^{s(1)}} + \bar{\mathbf{H}}^{(1)}_{\mathbf{0s}}\mathbf{r^{d(1)}} + \\ \mathbf{\Lambda^{s(0)}}\bar{\mathbf{H}}^{(1)}_{\mathbf{ss'}}\mathbf{r^{s'(1)}} + \mathbf{\Lambda^{d(0)}}\bar{\mathbf{H}}^{(1)}_{\mathbf{ds}}\mathbf{r^{s(1)}} + \mathbf{\Lambda^{s(0)}}\bar{\mathbf{H}}^{(1)}_{\mathbf{sd}}\mathbf{r^{d(1)}} + \mathbf{\Lambda^{d'(0)}}\bar{\mathbf{H}}^{(1)}_{\mathbf{dd'}}\mathbf{r^{d'(1)}} + \\ \mathbf{\Lambda^{s(0)}}\bar{\mathbf{H}}^{(1)}_{\mathbf{st}}\mathbf{r^{t(1)}} + \mathbf{\Lambda^{d(0)}}\bar{\mathbf{H}}^{(1)}_{\mathbf{dt}}\mathbf{r^{t(1)}} + \mathbf{\Lambda^{d(0)}}\bar{\mathbf{H}}^{(1)}_{\mathbf{dq}}\mathbf{r^{q(1)}}. \end{aligned} \tag{6.6}$$

The generality of a similarity-transformed perturbation theory (STPT) no doubt affords one a flexible framework within which various correlation models can be dreamt up and, as

has been discussed, where others can be subsumed under. It has proven itself a natural framework for extending active-space correlation to the external domains of orbital-optimized[332, 333] and pair references[334, 335], excited-state theories [329, 330, 336–338], and other formulations. Below, we couch a description of intermolecular interactions in a (2)-type model partitioning the configuration space to obtain molecule-centered coupled-cluster states as zeroth-order wavefunctions.

Beginning with a solution to a locally-projected SCF problem, call it $|0\rangle$, we restrict the primary space to include $|0\rangle$ and the set of singly- and doubly-substituted determinants where excitations are *confined to one molecular site*,

$$|\mathbf{p}\rangle = |0\rangle + |\mathbf{s}_{\{ia\}}\rangle + |\mathbf{d}_{\{iajb\}}\rangle, \tag{6.7}$$

with the braces restricting indices to obtain from one center. Its complement includes two-center single excitations through four-center double excitations, as well as full-rank triples, quadruples, etc., though in the present work we choose to restrict our attention singles and doubles in order to benchmark non-locality error against standard CCSD,

$$|\mathbf{q}\rangle = |\mathbf{s}_{\{i\}\{a\}}\rangle + |\mathbf{d}_{\{ia\}\{jb\}}\rangle + |\mathbf{d}_{\{i\}\{a\}\{jb\}}\rangle + ... + |\mathbf{d}_{\{i\}\{a\}\{j\}\{b\}}\rangle. \tag{6.8}$$

Applying this Hilbert-space partitioning and the same definitions as above for the Hamiltonian and the left and right zeroth-order states to eqs. 6.3, we obtain a coupled-cluster-quality description of local excitations, and a non-iterative treatment of the interaction complete to fourth order in MP theory. Because the number of p-space variables scales linearly with the number of molecules, we refer to this theory henceforth as the "linear" model. Its instructive value notwithstanding, we shall expect to find this model wanting when higher-order correlations become significant.

Given free rein to specify $|\mathbf{p}\rangle$, one can imagine developing a hierarchy of schemes augmenting it to completeness in the space of singles and doubles, whereby the zeroth-order solution would be exact and there would be no perturbative correction to the energy and wavefunction. A first logical step is to include a quadratic number of dispersion-type configurations confining hole-particle excitations to a given center, e.g., $\{|\mathbf{d}_{\{ia\}\{jb\}}\rangle\}$, in the reference space. Such an ansatz is reminiscent of the DIM-MP2 model for atom-centered local correlations, and an evaluation of the zeroth-order energy with first-order amplitudes should produce exactly that model. Promoting this class of excitations from a fourth- to an infinite-order treatment, we should expect to recover the bulk of the truncation error in dispersion interactions, where inductive and dative and effects are vanishing and repulsions dominate the mean-field interaction.

Further augmentation of the p space with a quadratic number of non-local singles, e.g. $\{|\mathbf{s}_{\{i\}\{a\}}\rangle\}$, is expected to relax the local-orbital reference with respect to inter-site occupied-virtual rotations, recovering the bulk of the truncation error in cases where charge-transfer effects - which remain unaddressed at the locally-projected mean-field level - are substantial.

Still better, adding in the remaining non-local doubles defines a quartic model with the

same number of variables as canonical CCSD and equivalent if $|0\rangle = |\mathrm{HF}\rangle$. This model shall thus serve as a useful Hylleraas bound to assess the performance of our upper-bound truncation models. We summarize their properties in Table 6.1.

model	$\|\mathbf{d}\rangle$	$\|\mathbf{s}\rangle$
linear	$\{iajb\}$	$\{ia\}$
linear+nls	$\{iajb\}$	$\{i\}\{a\}$
quadratic	$\{ia\}\{jb\}$	$\{i\}\{a\}$
quartic	$\{i\}\{a\}\{j\}\{b\}$	$\{i\}\{a\}$

Table 6.1: Model specifics. Enclosed indices obtain from individual molecular subspaces.

Seeing as our models are defined in a Hilbert space describing excitations from a non-orthogonal reference, we shall derive fully non-orthogonal spin-orbital equations for matrix elements of the transformed Hamiltonian for consistency. We emphasize that the following equations are appropriate in any representation and reduce exactly to the conventional expressions with orthogonal orbitals diagonalizing the Fock matrix in the occupied and virtual sub-blocks. We begin in the biorthogonal [339, 340] representation where local quantities are covariant. Repeated indices imply Einstein summation and contra- and covariant indices may be inter-converted by multiplication with the overlap g_{pq} or the inverse overlap g^{pq}, e.g., $C^{ij}_{ab} = g^{ik}g^{jl}C_{klab}$. Given any choice of $|\mathbf{p}\rangle$, the symmetric component of the zeroth-order energy and amplitude equations in the natural representation are

$$\begin{aligned} E^{(0)} = E^{\mathrm{CCSD}} &= f^i_a t^a_i + 0.25 v^{ij}_{ab} t^{ab}_{ij} + 0.5 v^{ij}_{ab} t^a_i t^b_j, \\ \langle^a_{i\in\mathbf{p}}|\bar{H}|0\rangle &= f^a_b t^b_i - t^a_j f^j_i + A^a_i(t_1,t_2) = 0, \text{ and} \\ \langle^{ab}_{ij\in\mathbf{p}}|\bar{H}|0\rangle &= f^a_c t^{cb}_{ij} + f^b_d t^{ad}_{ij} - t^{ab}_{kj} f^k_i - t^{ab}_{il} f^l_j + B^{ab}_{ij}(t_1,t_2) = 0. \end{aligned} \tag{6.9}$$

A and B in the *covariant* integral representation in Appendix A.1.

Applying the virtual-block metric to eliminate the left-hand inverses and the occupied metric to bring the amplitudes to contravariance, we recast the above equations in the covariant integral representation and regroup terms obtaining,

$$\begin{aligned} E^{\mathrm{CCSD}} &= f_{ia} t^{ai} + 0.5 v_{ijab} t^{ai} t^{bj} + 0.25 v_{ijab} t^{abij}, \\ \{f_{ji} g_{ab} - f_{ab} g_{ij}\} t^{bj} &= A_{ai}(\bar{t}), \\ \Big\{\{f_{lj} g_{bd} - f_{bd} g_{jl}\} g_{ki} g_{ac} + \{f_{ik} g_{ac} - f_{ac} g_{ik}\} g_{bd} g_{jl}\Big\} t^{cdkl} &= B_{abij}(\bar{t}). \end{aligned} \tag{6.10}$$

With orthogonal orbitals, Kronecker deltas would replace the metrics and we'd need only pseudocanonicalize the orbitals to uncouple the amplitude equations. In a basis of non-canonical, non-orthogonal orbitals, our task will thus be to find a transformation that simultaneously orthogonalizes and pseudocanonicalizes the orbitals. Exploiting the direct-product

structure of eq. 6.10, we define $G_{(ia)(jb)} = g_{ij}g_{ab}$ and $D_{(ia)(jb)} = \{f_{ij}g_{ab} - f_{ab}g_{ij}\}$ for convenience and rewrite the equations combining hole-particle pairs into compound indices "(ia)". This will be useful for thinking about pairwise truncations in our model spaces later on.

$$D_{(ia)(jb)}t^{(jb)} = A_{(ai)}(\bar{t}), \{D_{(bj)(ld)}G_{(ia)(kc)} + G_{(bj)(ld)}D_{(ia)(kc)}\}t^{(kc)(ld)} = B_{(ai)(jb)}(\bar{t}). \tag{6.11}$$

Applying the transformation $T^{(ai)}_{(AI)} = G^{-\frac{1}{2}(ai)}_{(jb)}U^{(jb)}_{(AI)}$ where $U^{(jb)}_{(AI)}$ diagonalizes the energy-difference direct product, the amplitude equations assume a convenient diagonal form, $\underline{D}_p\bar{t}^p = \underline{R}_p$. Without making use of sparse linear algebra solvers, the diagonalization scales as $\mathcal{O}(P)^3$, where P is the number of correlated occupied-virtual pairs. The amplitudes must be back-transformed before updating the right-hand side and special care must be taken to ensure all contractions in $\underline{R}_P$ respect the covariant integral representation, keeping the amplitudes contravariant. Moreover, consistent formulation of truncated flavors of eq. 6.11 requires that the two-particle direct product be formed in the same basis at the outset. For example, consider the quadratic model detailed above. There, the amplitude equations take a two-body metric composed strictly from overlaps spanning up to two fragments. The scope of the correlation problem is therefore fixed at the beginning by this designation.

The left-hand problem for $\hat{\Lambda}$ is isomorphic to the right-hand projection problem and, as such, must be consistently framed, e.g., if truncations were made in $\hat{T}$, the left-hand equations must also bear them out. We begin from the natural representation and again seek to recast these in the more convenient covariant representation. Projecting the left-hand eigenvalue problem $\langle 0|\hat{L}\bar{H} = \langle 0|\hat{L}E$ onto the p-space singles and doubles, we obtain the linear equations

$$\begin{aligned} X^i_a &\equiv \langle 0|\bar{H}|^a_i\rangle + \lambda^j_b\langle^b_j|\bar{H}|^a_i\rangle + \lambda^{jk}_{bc}\langle^{bc}_{jk}|\bar{H}|^a_i\rangle = \lambda^i_a E, \text{and} \\ Y^{ij}_{ab} &\equiv \langle 0|\bar{H}|^{ab}_{ij}\rangle + \lambda^j_b\langle^b_j|\bar{H}|^{ab}_{ij}\rangle + \lambda^{jk}_{bc}\langle^{bc}_{jk}|\bar{H}|^{ab}_{ij}\rangle = \lambda^{ab}_{ij}E. \end{aligned} \tag{6.12}$$

The spin-orbital equations for the matrix elements in the *covariant* representation are given in Appendix A.1. After subtracting the diagonal and applying the virtual block metric to take λ to the contravariant space and the occupied metric to make the left-hand side covariant, we obtain the similar form

$$\begin{aligned} X_{ia} &= \lambda^{jb}\{f_{ji}g_{ab} - f_{ab}g_{ij}\}, \text{ and} \\ Y_{ijab} &= \lambda^{klcd}\Big\{\{f_{lj}g_{bd} - f_{bd}g_{jl}\}g_{ki}g_{ac} + \{f_{ik}g_{ac} - f_{ac}g_{ik}\}g_{bd}g_{jl}\Big\}. \end{aligned} \tag{6.13}$$

The same transformation as before diagonalizes the energy difference. Again, the covariant representation must be respected when updating the left-hand side and evaluating residuals.

By this point we have detailed the working equations sufficient to solve a non-orthogonal CCSD problem permitting truncations. Regarding our local infinite-order amplitudes as zeroth-order quantities, we proceed with a discussion of some features of the perturbation

theory. As in the case of the zeroth-order amplitude equations, the scope of the perturbation will be fixed by the transformation applied to bring the first-order amplitude eqs. 6.5 to diagonal form. Thus, a first-order amplitude describing an excitation across fragments, e.g., $r^{(1)\{i\}\{jab\}}$, can only be consistently determined in a basis where the corresponding direct-product elements are taken into account, which means either the full-rank two-particle metric must be constructed and diagonalized as above, or one may equivalently solve for the first-order amplitudes in the biorthogonal representation. There, the amplitude equations are uncoupled after pseudocanonicalization of the biorthogonal (non-Hermitian) Fock operator, at the risk of obtaining complex eigenvalues. Covariant spin-orbital equations for the first-order amplitudes and intermediates are given in Appendix A.1.

By our applications below, we shall ultimately hope to understand the extent to which non-local contributions will require an infinite-order treatment for prototypical interactions, or in other words, which components of the interaction are sufficiently small to be confidently relegated to a fourth-order treatment. We take the truncated and quartic models to represent upper and Hylleraas bounds to the coupled cluster energy with confidence that the components interpolating between them are not only well-defined, but contain physical content that stand to bear on our assessment of orbital reference quality and adequacy of the correlation treatment. First, we uncover general properties of our intermolecular STPT models as applied to elementary dispersion interactions, including the convergence behavior of the binding energy and terms on basis set extension, BSSE effects, and performance on application to small clusters. A discussion of intra- and intermolecular relaxations due to the interplay of orbital choice and single excitations entering in the correlation problem will follow. Next, we discuss potential tractability gains achieved on subspace orthogonalization. In a final assessment of the generality of our conclusions, we compute statistical errors on application to the A24[293] data set of various non-covalent interactions.

6.3 Applications

All models were implemented in a hacked version of Q-Chem 4.0 taking spin-orbital expressions for matrix elements of the transformed Hamiltonian generated by applying Wick's theorem in an independent Mathematica code. Scripts are available from your correspondents by request.

We have chosen the helium dimer interaction as our poster-child case to assess the performance of the our models. Given that the zeroth-order solution in any truncation scheme is exact at infinite separation, we may cleanly ascribe any binding to the effects of the perturbation theory. Moreover, the purely dispersive nature of the interaction should, in the limit of a complete one-particle basis set, remove the confound of orbital reference (any binding at the SCF level is an artifact of BSSE, while the constrained nature of the SCF-MI solution necessarily makes it an upper bound to canonical SCF) when appraising candidate models against conventional CCSD.

We plot He_2 potential curves furnished by iSTPT models with linear and quadratic doubles plus either linear or quadratic singles in Figure 6.1. Satisfying ourselves that the difference in binding on the inclusion of non-local singles is relatively small for any truncation model, we focus for the moment on differences stemming from the level of treatment of the doubles. Examining the top two curves, it is clear that augmenting the on-site model with dispersion-type amplitudes binds the complex at zeroth-order, albeit shallowly and more distantly compared to the quartic model, which overlays canonical CCSD here. Treating all non-local doubles at fourth-order in MP theory, the second-order correction to the linear model produces a bound state, but with a protracted, shallow minimum. On the other hand, an infinite-order treatment of the dispersive doubles and a fourth-order treatment of the rest propels the quadratic model to near-exactness, with any difference against the Hylleraas bound due to higher-than-fourth-order non-local effects in the doubles. We conclude that infinite-order dispersive doubles are critical to describe this interaction, while higher-order effects due to other non-local doubles are apparently negligible. Other tests shall be required to demonstrate the generality of these conclusions.

Returning to the non-local singles, it is no real surprise that they're uninteresting here, since the canonical and locally-projected SCF solutions are rapidly approaching equivalence away from the repulsive wall. Nevertheless, we should expect in this incomplete basis that an infinite-order treatment of singles should recover more of the mean-field locality error than a perturbative treatment. For this, we fix our doubles p space and compare the second-order singles contribution to eq. 6.6 garnered by the local model to the infinite-order non-Brilluoin term of eq. 6.10 garnered by the non-local model. These are plotted alongside the SCF MI error for He_2 dimer in Figure 6.2, where it is confirmed that infinite-order singles recover more of the ALMO error than their perturbative cousins across the entire coordinate. We expect this difference to play a more significant role in cases where strong inter-fragment occupied-virtual interactions and/or inadequacies in the basis set produce a poor local reference. Indeed, glancing at Table 6.2, we see the largest improvements in error due to inclusion of non-local singles at zeroth-order occurs in smaller basis sets and more dramatically when augmented functions aren't included. All errors have converged by the augmented quadruple-zeta level where non-local singles do not improve binding, irrespective of the rank of the doubles. We see that including dispersion-type doubles in the p space results in a ten-fold reduction of error relative to a second-order treatment.

How does a consideration of basis set superposition error affect our conclusions? By construction, our ALMO reference excludes BSSE, and all of our truncation models exclude from the p-space determinants coupling inter-site occupied-virtual pairs (see Table 6.1). BSSE must lurk in the non-local correction to the energy, then. We compute BSSEs by the standard Boys-Bernardi counterpoise correction[137], compiling them alongside the change in the error in Table 6.3. Holding the singles constant, we see for our truncation models that BSSE does not depend on the quality of the doubles, but does depend on the order at which the non-local singles are treated, with a non-zero contribution due to higher-order relaxation of t_1 even at the quadruple-zeta level. Taking the difference in BSSEs computed between

basis	$\{ijab\}^{(2)}$	$\{ijab\}+\{i\}\{a\}^{(2)}$	$\{ia\}\{jb\}^{(2)}$	$\{ia\}\{jb\}+\{i\}\{a\}^{(2)}$	$\{i\}\{j\}\{a\}\{b\}$	MP2	$E^{\text{bind}}_{\text{CCSD}}$
ccpvdz	0.027	0.017	0.012	0.002	0.000	0.004	-0.131
ccpvtz	0.071	0.057	0.019	0.005	0.000	0.017	-0.235
ccpvqz	0.128	0.118	0.019	0.009	0.000	0.044	-0.315
accpvdz	0.424	0.355	0.150	0.081	0.001	0.105	-1.081
accpvtz	0.344	0.340	0.039	0.035	0.000	0.167	-0.749
accpvqz	0.343	0.344	0.032	0.032	0.000	0.165	-0.763

Table 6.2: He_2 equilibrium interaction error in meV relative to canonical CCSD on extension of the basis set.

any model with non-local singles and the quartic model will give the contribution to BSSE of higher-order non-local doubles. These effects die more steeply with basis than non-local singles because their contributions are much smaller.

basis	$\{ijab\}^{(2)}$	$\{ijab\}+\{i\}\{a\}^{(2)}$	$\{ia\}\{jb\}^{(2)}$	$\{ia\}\{jb\}+\{i\}\{a\}^{(2)}$	$\{i\}\{j\}\{a\}\{b\}$	HF+CCSD
accpvdz	0.626 / -0.11	0.687 / -0.05	0.626 / -0.11	0.687 / -0.05	0.737 / 0.00	0.737 / -
accpvtz	0.109 / -0.05	0.116 / -0.00	0.109 / -0.05	0.116 / -0.00	0.119 / 0.00	0.119 / -
accpvqz	0.064 / 0.00	0.068 / -0.00	0.064 / 0.00	0.068 / -0.00	0.068 / 0.00	0.068 / -

Table 6.3: BSSE/change in binding error on counterpoise correction. BSSE and favorable error changes die as the basis set approaches completeness.

It is appropriate at this point to ask whether conclusions we've drawn pertaining to the dimer will hold for small clusters of helium. This application will serve as a test of the extent to which our local constructions can capture non-local effects coupling more than two bodies, which may seem daunting at first since, as the reader will recall, neither the linear nor quadratic model is able to couple more than two molecules explicitly at zeroth-order. We saw for the dimer that a Hilbert-space partitioning placing on-site and dispersion-type doubles in the p space and the rest in the q space proved adequate to recover the full-rank result, or in other words, that a second-order description of non-local doubles between two bodies sufficiently approximated the infinite-order description. There is no *a priori* guarantee that this should apply to larger interactions simply because the number of non-local doubles scales quartically with cluster size while the number of zeroth-order variables can only increase quadratically. Of course, one may argue on the basis of the intrinsic locality of dynamic correlations that the most important interactions in a cluster of weakly-interacting subsystems, though they may not be the most numerous, are two-body in nature, and therefore expect to have no issue relegating effects entangling more than two fragments to a perturbative treatment. If one adopts this optimistic outlook, one should expect the cluster problem to look like a collection of weakly-coupled dimeric ones, and thus expect the error to be most sensitive to two-body errors.

Our local models, by construction, put us in good position to examine higher-order effects in clusters. As we have seen, the difference in performance between the linear and quadratic models reflects higher-order dispersion-like excitations coupling two bodies, while

the difference between the quadratic and quartic models is a measure of the strength of higher-order inter-site couplings entangling up to four bodies. For the remainder of this discussion, we'll refer to these as higher-order local and non-local doubles. Taking an idealized linear cluster of helium atoms as our test application, we plot the dependence of higher-order contributions on cluster size in Fig. 6.3. In the limit of an infinite chain length, the one-dimensionality forces any two n-body interactions to be identical, and also guarantees the number of *important* n-body interactions to grow linearly, eliminating certain confounds in our benchmark. Examining the plot, we conclude that most of the higher-order contribution is in the local doubles, and moreover, that at least an infinite-order treatment there is indispensable.

We turn our attention to a set of more realistic clusters of helium, shown in Figure 6.4. Examining the models' binding errors relative to canonical CCSD in Table 6.4, we see in all cases, again, that the interaction error decreases ten-fold on the inclusion of the quadratic dispersion amplitudes. A narrow 1-3% error bracket achieved there suggests again that higher-order non-local effects on binding are small.

	$\{ijab\}$	$\{ijab\}+\{i\}\{a\}$	$\{ia\}\{jb\}$	$\{ia\}\{jb\}+\{i\}\{a\}$	$\{i\}\{j\}\{a\}\{b\}$	MP2	$E^{\text{bind}}_{\text{CCSD}}$
$D_3/n=3$	0.93	0.93	0.11	0.10	0.00	0.46	-8.70
$T_d/n=4$	1.10	1.08	0.12	0.10	0.00	0.55	-11.60
$C_{4v}/n=5$	2.68	2.58	0.33	0.24	0.00	1.30	-14.50
$D_{5h}/n=7$	5.39	5.17	0.71	0.50	0.00	2.62	-20.30

Table 6.4: kJ/mol binding errors relative to canonical CCSD computed in the aug-cc-pvtz basis. Higher-order dispersion is required. Structures are pictured in Fig. 6.4.

Studies on clusters invite the important consideration of whether further tractability gains can be achieved by simplifying the implementation and costly operations required to diagonalize eq. 6.11 and compute matrix elements, all of which require contraction with explicit overlap metrics in both subspaces (see the Appendix). Up to this point, we have taken a reference determinant of fully non-orthogonal ALMOs. It shall be useful to consider the extent to which orthogonalization of either or both orbital subspaces will distort the domain definitions implied by the iSTPT and thereby degrade performance. Ideally, we'd prefer to orthogonalize both subspaces since then we'd only have to diagonalize the occupied and virtual blocks of the covariant Fock matrix to uncouple the amplitude equations and forgo dealing with any two-particle metric altogether, not to mention all one-body overlaps in the matrix elements reduce to Kronecker deltas. This approach is, of course, not expected to work, especially with the inclusion of more diffuse AO functions, a requirement for these applications. We return to the helium dimer interaction, computing the *change* in the interaction error going to orthogonal orbitals, compiling the data in the first rows of Table 6.5. The insensitivity of the change in error to higher-order effects and a proportional increase with basis set extension reflects difficulty (and foolhardiness) in imputing orthogonalized orbitals to molecular centers, rendering a domain-definition framework ill-begotten. This is not to say that a localization technique will do nothing to improve the result insofar as

symmetric orthogonalization will treat all functions on even footing and perhaps represents limiting-case worst orthogonal functions. Glancing at the second set of rows in Table 6.5 suggests the preliminary application of a localization scheme[341] furnishing atom-centered orthogonal virtuals and Boys-localized occupieds does not help much.

One nevertheless has recourse in the argument that electing to orthogonalize the occupied space *alone* should not distort a given domain *too* much. This position is expected to be valid in the regime where inter-site overlaps are small, and in cases where it minimally damages the locality, it will still effect tractability gains. The change in error starting from this "half-non-orthogonal" set of ALMOs is given in the final rows of Table 6.5. It is curious that this procedure has no deleterious effects. Small "improvements" are likely the consequence of delocalization degrees of freedom the ALMOs enjoy on orthogonalization. We thus expect improvements conferred this way to increase in proportion to charge-transfer and BSSE effects. We shall conduct more tests below to assess whether this fortuitous result is the general case.

orthogonalization	$\{ijab\}$	$\{ijab\}+\{i\}\{a\}$	$\{ia\}\{jb\}$	$\{ia\}\{jb\}+\{i\}\{a\}$
symmetric				
accpvdz	1.79	1.82	1.80	1.83
accpvtz	2.15	2.76	2.17	2.77
accpvqz	3.20	4.10	3.23	4.13
symmetric, localized				
accpvdz	1.78	1.81	1.79	1.82
accpvtz	2.12	2.72	2.14	2.74
accpvqz	3.15	4.04	3.18	4.06
half-non-orthogonal				
accpvdz	-0.01	-0.01	-0.01	-0.01
accpvtz	-0.01	-0.01	-0.01	-0.01
accpvqz	0.00	-0.01	0.00	-0.01

Table 6.5: Change in He_2 equilibrium interaction error on orthogonalization. Energies are in meV. Orthogonalization of both subspaces destroys domain identification, whereas orthogonalization of the occupied subspace alone preserves accuracy while conferring cost-savings.

We have yet to explore any interplay between local $\hat{T}_1$ and the choice of orbital reference, e.g., whether there is a synergy or perhaps redundancy in optimizing $\hat{T}_1$ beginning from a reference of ALMOs for which an intra-fragment Brillouin condition has been satisfied, e.g., induction has been treated to infinite-order. One can also imagine beginning from an un-optimized reference determinant of "frozen" orbitals - constructed from concatenating fragment-blocked coefficient matrices determined as the SCF solutions of molecules in vacuum - and relying on the projective optimization of $\hat{T}_1$ to polarize the orbitals. Surely

the leading occupied-virtual Fock elements, which unambiguously account for mean-field polarization, will play a significant role in the optimization, but the extent to which the simultaneous optimization of correlations will influence the mean-field induction and *vice versa* is, at this point, unclear. The other question is whether neglecting $\hat{T}_1$ altogether is compensated by choosing an ALMO starting point, in which case there can be no $\hat{T}_1$-mediated mutual interaction of induction and correlation at zeroth-order. We shall have to be careful when addressing these questions to choose a test system for which the SCF-MI solution is a good approximation to Hartree-Fock, e.g., where attractions attributed to dative effects are negligible and polarizations dominate mean-field binding. To this end we have chosen the interaction of helium with lithium cation. We conclude glancing at the first column of Table 6.6 that repulsions destabilize the "frozen" wavefunction but are overridden by inductive effects described nearly perfectly going to the ALMOs, leaving a "delocalization" error relative to canonical HF of 0.3 kJ/mol. Beginning from a frozen reference, we shift the onus onto intramonomer $\hat{T}_1$ to recover mean-field polarization.

SCF model	$HeLi^+$	NH_3BH_3
FRZ	1.24	105.20
ALMO	-5.35	-44.30
HF	-5.65	-146.54

Table 6.6: Mean-field interaction aug-cc-pvdz energies for textbook inductive and dative interactions in kJ/mol. The ALMO orbitals are quantitative for the principally-inductive $HeLi^+$ interaction, but largely inadequate to describe the charge-transfer-dominated NH_3BH_3 interaction.

We apply our local models to the interaction beginning from both references, with and without explicit singles in the correlation model. Interaction errors relative to canonical CCSD are given in the first rows of Table 6.7. In stark constrast to the helium results, there is virtually no dependence of the error on higher-order doubles. Moreover, it would seem we arrive at the same error opting either to begin from ALMOs and neglecting singles altogether, or beginning from frozen orbitals and optimizing intramonomer $\hat{T}_1$. Including non-local singles in the reference, we recover most of the remaining error, concluding that infinite-order one-body effects trump infinite-order dispersion-type doubles.

Another important question to consider is the extent to which the perturbation theory is viable when the SCF-MI orbital reference is decidedly horrendous, e.g., when dative effects become important. Here, larger-magnitude intermolecular f_{ov} elements and smaller band gaps no doubt elevate intermolecular occupied-virtual rotations to such a significance that the ALMO error is no longer negligible. The reader will recall that for iSTPTs taking only on-site singles at zeroth-order, charge-transfer effects first enter at second order, so a description of dative interactions will likely be poor. We have chosen the canonical C_{3v}-symmetry ammonia-borane dative interaction to measure the extent. It represents a

wavefunction	CCD		CCSD		CCSD
truncation model	$\{iajb\}$	$\{ia\}\{jb\}$	$\{iajb\}$	$\{ia\}\{jb\}$	$\{i\}\{a\}\{j\}\{b\}$
$HeLi^+$(FRZ)	2.25	2.24	0.09	0.08	0.00
$HeLi^+$(FRZ)+{i}{a}	-	-	0.05	0.04	-
$HeLi^+$(ALMO)	0.10	0.09	0.09	0.08	0.00
$HeLi^+$(ALMO)+{i}{a}	-	-	0.05	0.04	-
NH_3BH_3(FRZ)	112.26	102.08	63.17	53.72	14.12
NH_3BH_3(FRZ)+{i}{a}	-	-	31.26	23.38	-
NH_3BH_3(ALMO)	50.71	46.83	51.06	44.94	9.62
NH_3BH_3(ALMO)+{i}{a}	-	-	23.19	17.96	-

Table 6.7: Errors relative to the canonical CCSD equilibrium binding energy computed in aug-cc-pvdz taking various zeroth-order models. "$\{i\}\{a\}$" indicate the inclusion of non-local zeroth-order singles amplitudes. $E_{\text{bind}}^{\text{CCSD}}$ (NH_3BH_3)= 177.07 kJ/mol. $E_{\text{bind}}^{\text{CCSD}}$($HeLi^+$)= 6.65 kJ/mol. Intramolecular $\hat{T}_1$ emulates the effects of ALMO optimization. Accounting for higher-order effects due to intermolecular $\hat{T}_1$ is required to describe dative interactions.

particularly challenging case for a frozen-orbital reference (see the second column of Table 6.6) where it is unstable by a walloping two-thirds of its canonical binding energy. ALMO relaxation adds some 150kJ/mol to the interaction, but it's still missing some 100kJ/mol of delocalization. Thus, a perturbative treatment taking either local reference will have a lot to clean up. Examining the second set of rows of Table 6.7, one can see again that augmenting the local models with (on-site) singles drastically improves the frozen-orbital models while scarcely affecting the relaxed-reference results. There is a similar improvement going from unrelaxed to relaxed orbitals neglecting local singles. Adding non-local singles to CCSD on top of either a frozen or relaxed orbital reference reduces the error against the quartic model most considerably, with the improvement relatively insensitive to truncation model. In view of these applications, we anticipate that the inclusion of non-local singles at zeroth-order will effect substantial accuracy gains when applied to cases where the local reference is wanting.

Until now, we have focused on exposing properties of our local theories by applying them to model interactions. It remains to be seen how general our conclusions are. To this end, we apply our standard models and half-non-orthogonal (hno) variants thereof to the A24 dataset of non-covalent interactions which includes a varied set of hydrogen-bonded (HB), mixed-character (MIX), and dispersion-dominated (DISP) interactions. root-mean-square errors (RMSE) measured against canonical CCSD are given in Table 6.8. Refer to Appendix A.1 for individual quantities.

Unsurprisingly, the quartic model furnishes energetics virtually identical to CCSD across all interactions, so we can safely eliminate any orbital-reference confound from our considerations, viewing truncation model errors as due entirely to the Hilbert space partitioning. Including all singles in the p space substantially improves the RMSE for any doubles model,

weighing most heavily on hydrogen-bond and mixed interactions, but minimally affecting dispersion, as our test cases showed. Quadratic p-space doubles, on the other hand, benefit dispersion the most. To beat MP2, these data suggest quadratic singles and doubles at zeroth-order are required in the HB and MIX categories, though any truncation model wins out for dispersion, suggesting steep improvement beyond a first-order MP treatment there. Our best truncation model incorporates quadratic singles and doubles at zeroth-order, and is superior to MP2 for all interaction types. Similar conclusions are drawn for the half-non-orthogonal models, which again show uniform improvement relative to the fully-non-orthogonal models.

	$\{ijab\}$	$\{ijab\}+\{i\}\{a\}$	$\{ijab\}+\{i\}\{a\}_{\mathrm{hno}}$	$\{ia\}\{jb\}$	$\{ia\}\{jb\}+\{i\}\{a\}$	$\{ia\}\{jb\}+\{i\}\{a\}_{\mathrm{hno}}$	$\{i\}\{j\}\{a\}\{b\}$	MP2
total	0.59	0.38	0.35	0.46	0.24	0.22	0.05	0.36
hb	0.88	0.45	0.39	0.72	0.29	0.25	0.05	0.33
mix	0.60	0.42	0.38	0.46	0.26	0.23	0.06	0.33
disp	0.26	0.27	0.26	0.16	0.17	0.16	0.04	0.41

Table 6.8: A24 statistical errors in kcal/mol relative to CCSD. All calculations were performed in aug-cc-pvdz. The "hno" designation means the occupied orbitals alone were symmetrically orthogonalized. Models taking quadratic singles and doubles at zeroth-order are nearly quantitative.

6.4 Conclusions

We have developed and applied a hierarchy of fully-non-orthogonal coupled cluster correlation models treating intermolecular interactions at second-order in Löwdin perturbation theory. Having cataloged the importance of various higher-order contributions in a host of intermolecular interactions, we have determined that non-local singles are indispensable for dative interactions, while dispersion-type doubles are required for dispersion. Benchmark computations indicate our quadratic models nearly quantitatively approximate canonical CCSD, and further cost-reduction is achieved without a loss of accuracy by orthogonalizing the occupied subspace. Future directions in the way of economization include characterization of fully-non-iterative models substituting first-order amplitudes for CCSD ones, and orbital optimization in the field of correlation to remove the singles amplitudes, as well as extended analyses of n-body effects in clusters and extension of the q space to include non-local triples and quadruple excitations.

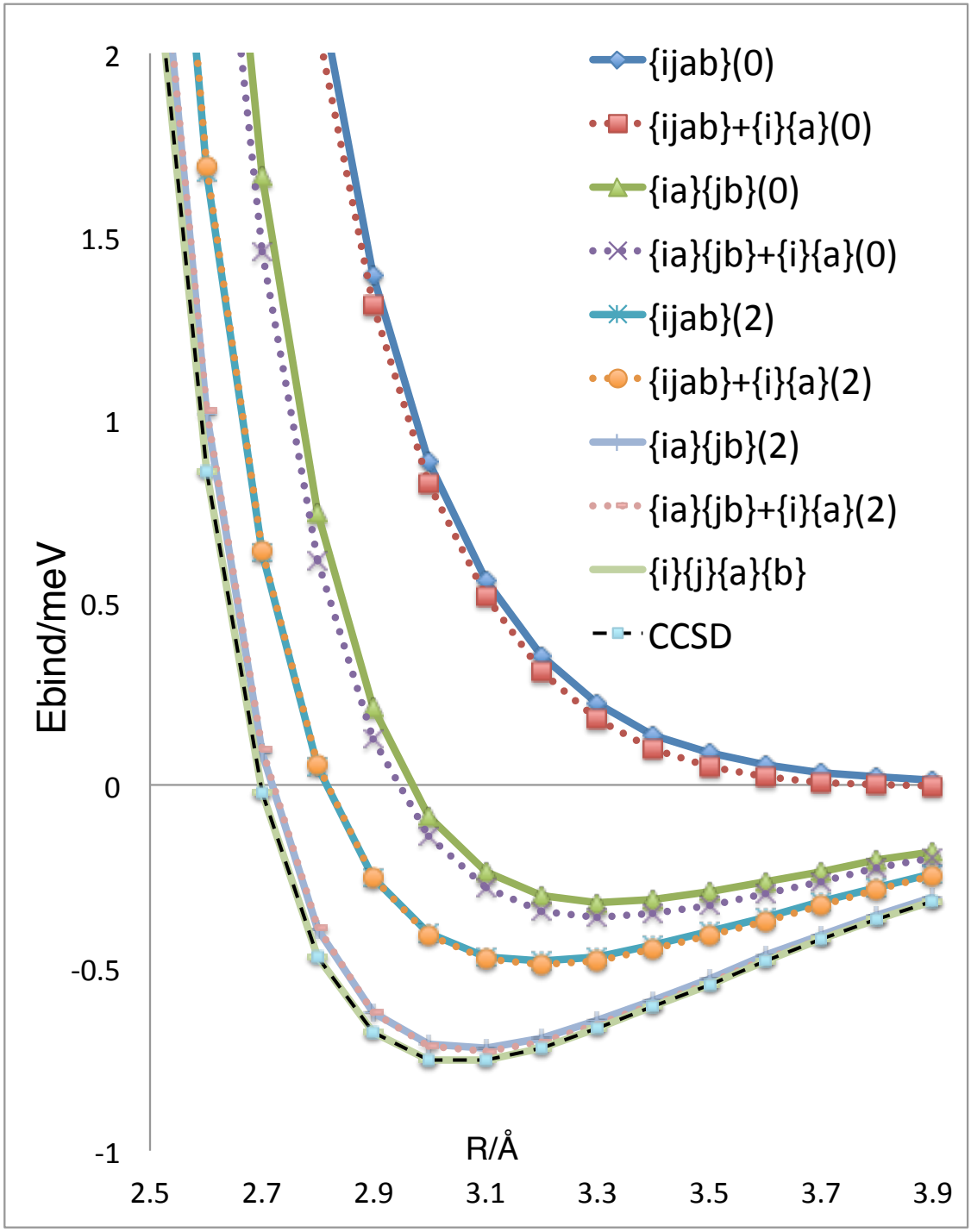

Figure 6.1: He_2 potential curve computed in aug-cc-pvtz. Energies are in meV.

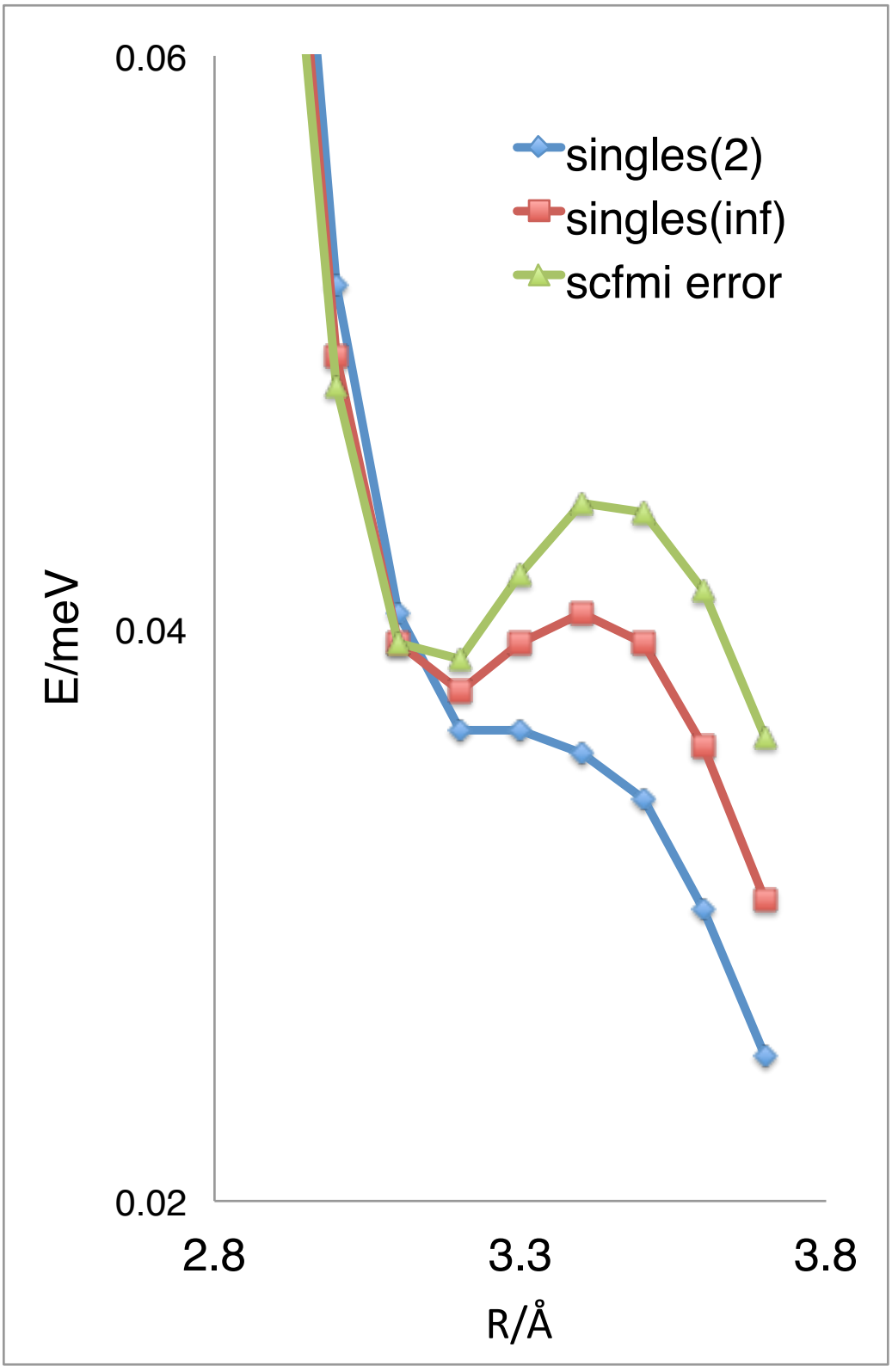

Figure 6.2: Comparison of perturbative and infinite-order recovered singles in the aug-cc-pvtz basis set.

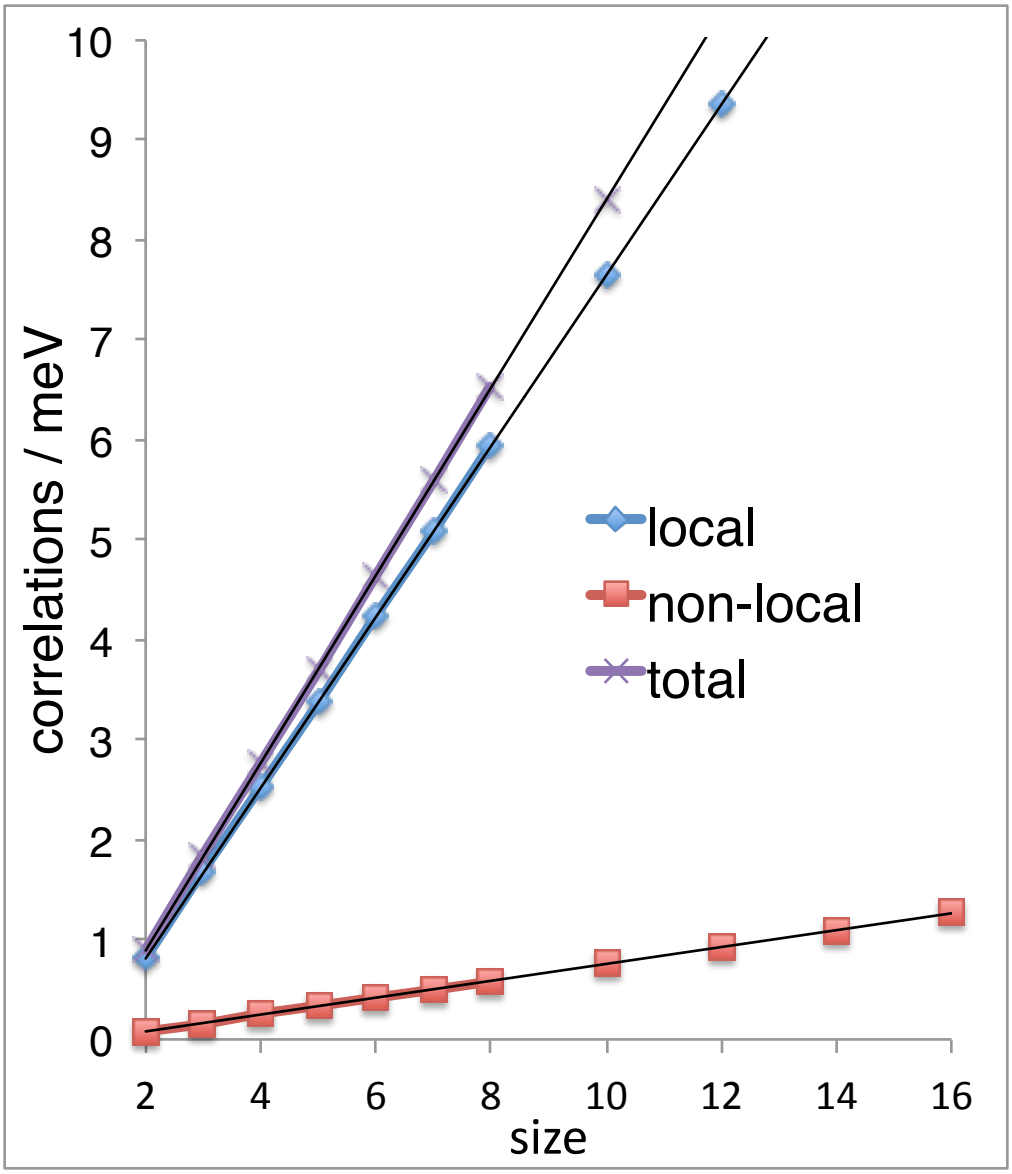

Figure 6.3: Through-infinite-order local (two-body dispersion-type) and non-local (two-through four-body charge-transfer-type) doubles contributions to the correlation binding energy computed as a function of helium chain length. Local doubles are responsible for the bulk of binding effects.

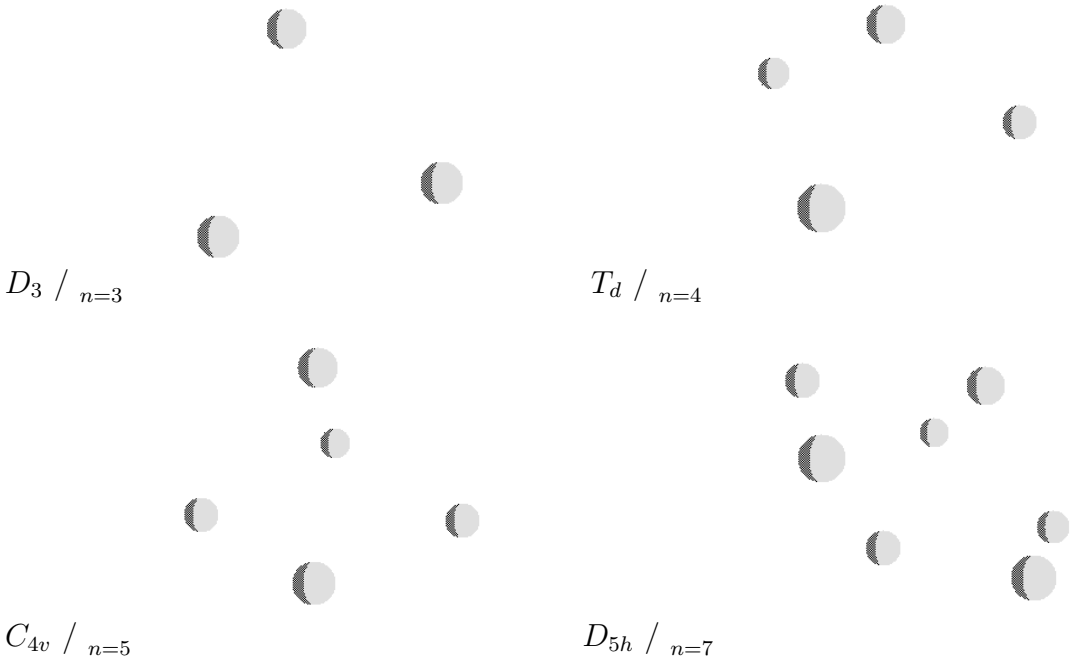

Figure 6.4: He_n clusters optimized at the CCSD/aug-cc-pvtz level.

Chapter 7

STPT(2) from first-order amplitudes

7.1 Introduction and general construction

In this Chapter, we present preliminary follow-on work to the intermolecular second-order intermolecular similarity-transformed perturbation theory (iSTPT(2)) models for local correlation models proposed in Chapter 6. Therein, we treated intermolecular interactions as perturbations to local CCSD-level zeroth-order wavefunctions centered on individual monomers in a Löwdin-style partitioning[29, 321–324] of the similarity-transformed Hamiltonian. For considerations of cost tractability and insight into the intrinsic locality of inter-electronic correlations, we enumerated a series of locally-truncated zeroth-order wavefunctions for which standard CCSD projection equations were solved in a non-orthogonal ALMO[75, 288–290] representation, and upon which a first-order correction describing non-local correlations entered at second order in the energy. Sundry applications of these upper-bound truncation models indicated that inclusion of doubles amplitudes coupling fragment-confined particle-hole excitations at zeroth-order was required to adequately approximate the lower-bound full-rank result. In other words, excitations coupling three or more bodies, or coupling two bodies, but where at least one particle-hole pair is shared between them, *and no fewer*, could be safely relegated to a perturbative description, which, as it turns out, is complete to leading order in fourth-order Møller-Plesset (MP) partitioning.

Here, we investigate the merit of a first-order approximation to the infinite-order cluster amplitudes defining our reference models, e.g., $\hat{T}^{\mathrm{CC}} = \hat{T}^{\mathrm{MP2}}$, which, aside from rendering our formulations completely non-iterative and $O(N^6)$-complex, will serve to clarify whether errors in the iterative $O(N^6)$ iSTPT(2) models developed previously are due to a low-order treatment of the missing amplitudes by PT, or to severe rank-reduction of the amplitude vector dressing the first-order Hamiltonian.

We recapitulate our iSTPT models in brief, beginning with the first few terms obtained

on expanding the expectation value for the energy $E = \langle|\mathbf{l}^\dagger\bar{\mathbf{H}}\mathbf{r}|\rangle$ in a perturbation series,

$$\begin{aligned} E^{(0)} &= \langle 0|\mathbf{l}^{(\mathbf{0})\dagger\mathbf{h}}\bar{\mathbf{H}}^{(0)}_{\mathbf{hh'}}\mathbf{r}^{(\mathbf{0})\mathbf{h'}}|0\rangle, \\ E^{(1)} &= \langle 0|\mathbf{l}^{(\mathbf{0})\dagger\mathbf{h}}\bar{\mathbf{H}}^{(1)}_{\mathbf{hh'}}\mathbf{r}^{(\mathbf{0})\mathbf{h}}|0\rangle, \quad \text{and} \\ E^{(2)} &= \langle 0|\mathbf{l}^{(\mathbf{0})\dagger\mathbf{h}}\bar{\mathbf{H}}^{(1)}_{\mathbf{hh'}}\mathbf{r}^{(\mathbf{1})\mathbf{h}}|0\rangle, \end{aligned} \tag{7.1}$$

where the operators are defined in the matrix representation of a truncated Hilbert space $|\mathbf{h}\rangle = |0\rangle + |\mathbf{s}\rangle + |\mathbf{d}\rangle$, $\bar{\mathbf{H}}_{\mathbf{hh'}} = |\mathbf{h}\rangle\bar{H}_{hh'}\langle\mathbf{h'}|$, $\mathbf{r}^{\mathbf{h'}}|0\rangle = |\mathbf{h}\rangle\mathbf{r}^{\mathbf{h}}$, and $\langle|\mathbf{l}^\dagger = \langle\mathbf{h}|\mathbf{l}^{\dagger\mathbf{h}}$, and where the Hamiltonian is dressed with first-order amplitudes, $\bar{H} = e^{-\hat{T}^{(1)}}He^{\hat{T}^{(1)}}$. Partitioning the Hilbert space $|\mathbf{h}\rangle$ into a primary space $|\mathbf{p}\rangle = |0\rangle$ and its complement $|\mathbf{q}\rangle = |\mathbf{s}\rangle + |\mathbf{d}\rangle$, and choosing $\bar{\mathbf{H}}^{(\mathbf{0})}_{\mathbf{pp}} = \bar{H}_{00}$, $\bar{\mathbf{H}}^{(\mathbf{0})}_{\mathbf{qq}} = \mathbf{F}_{\mathbf{qq}}$, $\mathbf{l}^{(\mathbf{0})\dagger} = (\mathbf{1_p} + \mathbf{T}^\dagger_{\mathbf{q}})$, and $\mathbf{r}^{(\mathbf{0})\mathbf{p}} = \mathbf{1_p}$ we obtain a zeroth-order energy complete through second-order in MP partitioning, and identical to MP2 with HF orbitals,

$$E^{(0)} = \langle 0|\mathbf{l}^{(\mathbf{0})\dagger\mathbf{p}}\bar{\mathbf{H}}^{(0)}_{\mathbf{pp'}}\mathbf{r}^{(\mathbf{0})\mathbf{p'}}|0\rangle = f_{ia}t^{ai(1)} + 0.25v_{ijab}t^{abij(1)} + 0.5v_{ijab}t^{ai(1)}t^{bj(1)}. \tag{7.2}$$

Treating the rest of the Hamiltonian as first order, the de-excitation operator in $\mathbf{l}^{(\mathbf{0})\dagger}$ causes external-space couplings giving rise to the first-order correction to the energy,

$$E^{(1)} = \langle 0|(\mathbf{1_p} + \mathbf{T}^\dagger_{\mathbf{q}})\bar{\mathbf{H}}^{(1)}_{\mathbf{qp}}\mathbf{1_p}|0\rangle = \mathbf{T}^\dagger_{\mathbf{q}}\bar{\mathbf{H}}_{\mathbf{q0}}{}^{(1)}. \tag{7.3}$$

The second-order correction is

$$E^{(2)} = \langle 0|(\mathbf{1_p} + \mathbf{T}^\dagger_{\mathbf{q}})\bar{\mathbf{H}}^{(1)}_{\mathbf{pq}}\mathbf{r}^{(\mathbf{1})\mathbf{q}}|0\rangle = \bar{\mathbf{H}}^{(1)}_{\mathbf{0q}}\mathbf{r}^{(\mathbf{1})\mathbf{q}} + \mathbf{T}^\dagger_{\mathbf{q}}\bar{\mathbf{H}}^{(\mathbf{1})}_{\mathbf{qq'}}\mathbf{r}^{(\mathbf{1})\mathbf{q'}}, \tag{7.4}$$

and takes first-order amplitudes in the q space,

$$\begin{aligned} \mathbf{D}^{(\mathbf{0})}_{\mathbf{ss}}\mathbf{r}^{\mathbf{s}(\mathbf{1})} &= \bar{\mathbf{H}}^{(1)}_{\mathbf{s0}}, \text{ and} \\ \mathbf{D}^{(\mathbf{0})}_{\mathbf{dd}}\mathbf{r}^{\mathbf{d}(\mathbf{1})} &= \bar{\mathbf{H}}^{(1)}_{\mathbf{d0}}, \end{aligned} \tag{7.5}$$

where $\mathbf{D}^{(\mathbf{0})}_{\mathbf{qq}} \equiv \{E^{(0)}\mathbf{1_q} - \bar{\mathbf{H}}^{(\mathbf{0})}_{\mathbf{qq}}\}$.

For a Hamiltonian dressed with CCSD-level amplitudes in full rank, $E^{(1)} = E^{(2)} = 0$ by the conventional projection equations and $E^{(0)} = E^{\mathrm{CC}}$. This is not true, however, for active-space models solving a subset of CC equations for a rank-reduced zeroth-order wavefunction (as in Chapter 6 where truncations were made on the basis of locality), nor is it true in full rank when first-order amplitudes dress the Hamiltonian. This invites a comparison of equivalent-rank truncation schemes employing either CC- or MP2- level amplitudes for direct assessment of *intra*monomer relaxation effects determining the total supermolecular correlation energy. Furthermore, the extent to which STPT(2) employing approximate first-order amplitudes in full-rank can adequately approximate conventional CCSD is interesting, as is the prospect of a one-to-one comparison of PTs derived from Löwdin- and MP-style

partitioning.

iSTPT truncation models developed in the previous Chapter and named for the total scaling in molecules are compiled in Table 7.1. The "linear" model restricts indices labeling doubles amplitudes to originate from a single center; the "quadratic" model augments that set with doubles coupling two bodies, but with each hole-particle pair confined to one site; the "quartic" adds back the rest of the non-local doubles and is equivalent to CCSD if $|0\rangle = |\mathrm{HF}\rangle$. This model shall serve as a useful Hylleraas bound to assess the performance of the foregoing upper-bound truncation models. All models take a quadratic number of non-local singles. General spin-orbital expressions for the PT corrections presented in the body of Chapter 6 and in full regalia in Appendix A.1 were implemented in a hacked version of Q-Chem 4.0 and derived from an independent Wick's theorem code in Mathematica. We'll compare the proposed fully-non-iterative local correlation models against their CC-reference cousins and non-iterative MP-partitioned competitors alike in the following Section. Our figure of merit will be relative errors against canonical CCSD.

model	$\|\mathbf{d}\rangle$	$\|\mathbf{s}\rangle$
linear	$\{iajb\}$	$\{i\}\{a\}$
quadratic	$\{ia\}\{jb\}$	$\{i\}\{a\}$
quartic	$\{i\}\{a\}\{j\}\{b\}$	$\{i\}\{a\}$

Table 7.1: Model specifics. The braces confine cluster amplitude indices to emanate from individual molecular subspaces.

7.2 Applications

We begin in full rank, restricting our attention to a single H_2 molecule traversing its bond-breaking coordinate to assess the differences between corrections from MP- and Löwdin-type-partitioned perturbative approximations to CCSD, which is exact for this application. Plotted in Figure 7.1 are errors relative to CCSD in the aug-cc-pvtz basis from HF orbitals. At the equilibrium separation of R(H-H)=0.7Å, the mean-field description is missing some 100mH of correlations. A second-order MP treatment (equivalent to STPT(0)) reduces this by a factor of ten, while the fourth-order MP correction (and STPT(2), similarly) confers another ten-fold improvement. Up to about R(H-H)=3*R_{eq}, STPT(1) tracks MP3 and STPT(2) tracks MP4SDQ closely, beyond which the MP-partitioned theories diverge, while STPT(2) is buffered by STPT(1)'s shallow turnabout, remaining stable out to a separation of about 6*R_{eq}, well after the first-order amplitudes give a pathological MP2 energy. The CC doubles moment, $\bar{\mathbf{H}}_{q0}$, appears in the first-order wavefunction (eq. 7.5) and in the first-order correction to the STPT energy (eq. 7.3). In addition to being complete through second-order in the MP-partitioned wavefunction, $\bar{\mathbf{H}}_{q0}$ incorporates leading third-order terms quadratic in the first-order amplitudes resulting in STPT(1)'s heightened stability relative to MP3.

The first term in the second-order correction of eq. 7.4 is identical to the first-order correction when $\hat{T} = \hat{T}^{(1)}$ and $\mathbf{l}^\dagger \leftarrow \hat{T}^{(1)\dagger}$, making our analysis easier. The second term, which is quadratic in the CC moment, is generally positive and offsets overcompensation of the linear terms. Binary contractions in $\bar{\mathbf{H}}_{qq'}$ cause the second-order energy to carry a component of the sixth-order MP contribution to the doubles space in addition to a host of fifth-order terms. It is interesting that PT from Löwdin-partitioning produces a more robust correction by introducing terms both out of order and incomplete at a given order in the MP view.

The trend is similar for the He_2 interaction, a simple dispersion model. Still in full-rank and with HF orbitals, we compile equilibrium and non-parallelity (NP) interaction errors relative to CCSD across the potential in Table 7.2. Second- and higher-order MP energies correct the unbound mean field by some ten and one hundred times at equilibrium. STPT(1) is slightly under-bound relative to MP3 due to quadratic factors in the doubles moment, and the quadratic moment in STPT(2) tempers the error while MP4SDQ overshoots. The "max" and "min" rows give a sense of an inherent error displacement, while the NPE is a measure of the error magnitude. Tracking these in the MP series, we see that the displacement goes negative, and the magnitude shrinks going to MP3, but then grows slightly at fourth order. In STPT, the displacement hovers about zero and shrinks two-fold between the first- and second-order errors, again underscoring increased stability of Löwdin-partitioned versus MP-partitioned PTs.

He_2 (in meV)	HF	MP2 = $E^{(0)}$	MP3	MP4SDQ	$E^{(1)}$	$E^{(2)}$
ΔE^{bind}_{error}	1.38	0.14	0.00	-0.06	0.04	0.01
max	12.42	0.68	0.01	0.00	0.05	0.02
min	0.08	0.01	-0.47	-0.56	-0.14	-0.07
NPE	6.17	0.33	0.24	0.28	0.09	0.04

Table 7.2: Errors against canonical CCSD/aug-cc-pvtz ($\Delta E^{bind} = 0.75\text{meV}, R_{eq} = 3.1\text{Å}$) for He_2 dissociation ($R = 0.5R_{eq}$-R_∞). Superscripts denote STPT order. With first-order amplitudes, STPT(0)=MP2.

At this point, we shall want to catalog the effects on the STPT corrections due to local approximations garnering reduced-rank zeroth-order wavefunctions of both infinite- and first-order amplitudes. Thus, applications of local models specified above in Table 7.1 employ ALMO orbitals below, while HF orbitals maintain for competitor theories and the reference CCSD numbers by which all models are appraised against. Interaction errors as a function of basis set, truncation rank, and amplitude character for He_2 are given in Table 7.3. It is immediately encouraging that only minor degradation results when first-order amplitudes are substituted for CCSD ones. The slight difference in the triple-zeta-level error garnered by the quartic model with first-order amplitudes ($\{i\}\{a\}\{j\}\{b\}^{(2)}_{t^{(1)}}$) here and the STPT(2) error from canonical orbitals above reflects effects due entirely to constrained ALMO orbitals. The same is true for non-zero errors in the $\{i\}\{a\}\{j\}\{b\}$ field. At the quadruple-zeta level,

where the errors and CCSD binding energy are arguably converged, we see improvements due to including more amplitudes at zeroth-order (whether they're CC- or MP2-level) are similar. This suggests the bulk of two-body errors depends on the number and not so much the character of the amplitudes dressing the Hamiltonian.

To see whether this the general case, we apply our models to the A24[293] data set

basis	$\{iajb\}^{(2)}_{t^{(1)}}$	inf	$\{ia\}\{jb\}^{(2)}_{t^{(1)}}$	inf	$\{i\}\{a\}\{j\}\{b\}^{(2)}_{t^{(1)}}$	inf	MP2	MP3	MP4SDQ	ΔE^{CCSD}
D	0.32	0.35	0.10	0.07	0.02	-0.01	0.11	-0.01	-0.05	-1.08
T	0.26	0.29	0.04	0.02	-0.01	0.01	0.14	0.00	-0.06	-0.75
Q	0.33	0.33	0.06	0.03	0.03	0.01	0.16	-0.01	-0.08	-0.76

Table 7.3: meV interaction errors against CCSD for He_2 from various locality and amplitude constraints as the basis set (aug-cc-pvXZ) is extended. The "$t^{(1)}$" subscript denotes first-order amplitudes were used instead of CCSD-level ones (denoted "inf") for the zeroth-order wavefunction.

of hydrogen-bonded, dispersion, and mixed-character dimeric interactions. CP-corrected errors against canonical CCSD/aug-cc-pvdz are given in Table 7.4 and computed from unprocessed quantities appearing in Table 7.5. In addition to comparing our models on the basis of truncations and amplitude character, we'll include figures obtained from a reference of symmetrically-orthogonalized occupied ALMOs and projected non-orthogonal ALMO virtuals. As discussed in Chapter 6, this so-called "half-non-orthogonal" reference not only simplifies the equations and reduces FLOPs, but also confers a small error reduction relative to its fully-non-orthogonal counterpart.

Focusing first on errors for full-rank theories in the right-most columns of Table 7.4, we remind the reader that finite errors in the $\{i\}\{a\}\{j\}\{b\}$ column stem from the upper-bound ALMO reference, and also the small difference between the error there and the preceding $\{i\}\{a\}\{j\}\{b\}^{(2)}_{t^{(1)}}$ field is due entirely to approximate amplitudes, which apparently weighs most heavily on the mixed-character subset. Of the non-iterative schemes in full rank, the STPT(2) model exhibits the smallest MSE in all categories, and the smallest RMSDs in the hydrogen-bond (HB) and dispersion (DISP) categories, though MP4SDQ achieves the smallest total RMSD overall. Of course, big improvements are expected from STPT(2) from a HF reference, viz., on the order of the $\{i\}\{a\}\{j\}\{b\}$ average error. Moving on to a discussion of the reduced-rank models toward the left side of Table 7.4, we see from a comparison of the total RMSDs within any fixed truncation model that substituting first-order amplitudes for CC-level ones only mildly affects performance. In line with the previous results, we conclude the error depends primarily on the number of amplitudes entering at zeroth-order, implying a fully-non-iterative iSTPT(2) is sufficient for a tolerated error margin in the sub-kJ regime. Moreover, non-iterative iSTPT(2) from a half-non-orthogonal orbitals uniformly reduces error relative to ALMO-reference results, and most dramatically for interactions dominated by charge-transfer effects.

RMSD	$\{iajb\}^{(2)}_{t^{(1)}}$	inf	$\{ia\}\{jb\}^{(2)}_{t^{(1)}}$	inf	$\{i\}\{a\}\{j\}\{b\}^{(2)}_{t^{(1)}}$	inf	MP2	MP3	MP4SDQ
total	1.40 , 1.22	1.34 , 1.19	0.95 , 0.78	0.75 , 0.64	0.21	0.13	1.33	0.54	0.17
hb	1.93 , 1.66	1.60 , 1.36	1.36 , 1.10	0.93 , 0.73	0.17	0.17	1.19	0.55	0.19
mix	1.42 , 1.23	1.34 , 1.21	0.99 , 0.82	0.78 , 0.68	0.30	0.15	1.20	0.58	0.17
disp	0.96 , 0.85	1.18 , 1.06	0.53 , 0.45	0.6 , 0.53	0.07	0.06	1.52	0.49	0.16
MSE	$\{iajb\}^{(2)}_{t^{(1)}}$	inf	$\{ia\}\{jb\}^{(2)}_{t^{(1)}}$	inf	$\{i\}\{a\}\{j\}\{b\}^{(2)}_{t^{(1)}}$	inf	MP2	MP3	MP4SDQ
TOTAL	1.15 , 1.01	1.19 , 1.07	0.71 , 0.58	0.64 , 0.55	-0.06	-0.06	-1.11	-0.48	-0.12
hb	1.86 , 1.61	1.53 , 1.31	1.3 , 1.05	0.88 , 0.7	0.00	-0.17	-1.08	-0.54	-0.08
mix	1.07 , 0.94	1.16 , 1.05	0.63 , 0.5	0.62 , 0.54	-0.12	-0.08	-1.06	-0.51	-0.14
disp	0.83 , 0.75	1.04 , 0.95	0.46 , 0.4	0.53 , 0.47	-0.03	0.02	-1.18	-0.41	-0.14

Table 7.4: kJ/mol root-mean-squared and mean-signed errors for CP-corrected/aug-cc-pvdz interactions from the A24[293] data set within the frozen core approximation. The second entry in a given field is the error from a half-non-orthogonal ALMO starting point (orthogonal occupieds, projected non-orthogonal virtuals). The "inf" heading denotes CCSD-quality amplitudes.

7.3 Conclusions and outlook

We have developed and applied fully-non-iterative variants of STPT(2) substituting first-order amplitudes for CC-level counterparts. By a comparison of relative and absolute energies garnered by Löwdin- and MP-partitioned PTs from canonical references, we attributed slower deterioration and generally better accuracy in the former to earlier entry of higher-order components in the latter. STPT(2) in full rank employing first-order amplitudes thus represents an attractive O(N^6) non-iterative alternative to MP-partitioned theories in the space of singles and doubles. Tests on the A24 data set of intermolecular interactions comparing rank-reduced iterative and non-iterative intermolecular STPT(2)s revealed that errors are due primarily to amplitude truncation, not amplitude character. This is of consequence in the context of large-scale tractability, where fully-non-iterative models of linearly- or quadratically-growing variables will effect immense savings without a proportional accuracy trade-off.

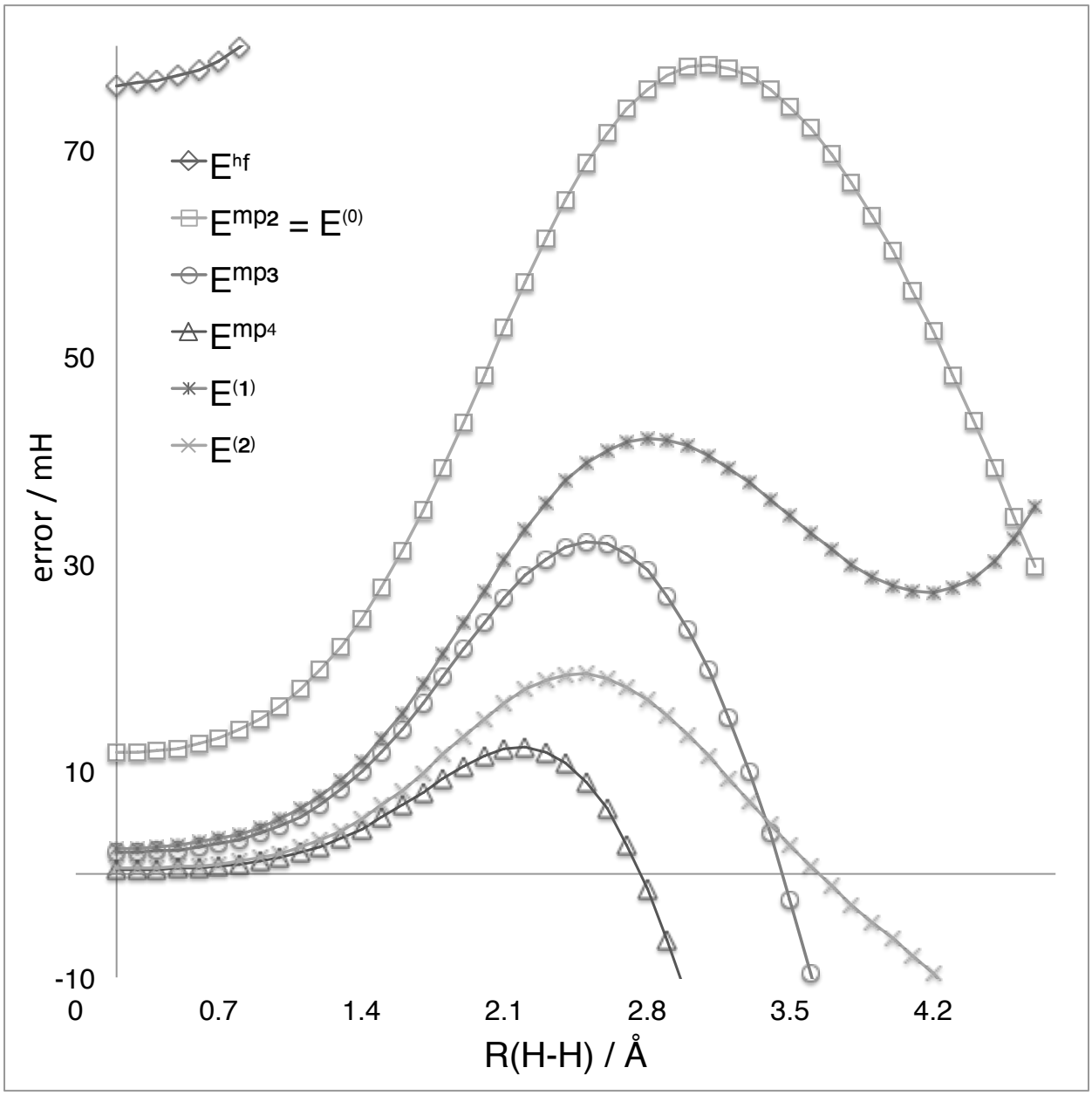

Figure 7.1: mH errors for H_2 bond dissociation ($R_{eq} = 0.7$Å) against CCSD in aug-cc-pvtz. Superscripts indicate STPT correction order.

dimer	$\{iajb\}^{(2)}_{t^{(1)}}$	inf	$\{ia\}\{jb\}^{(2)}_{t^{(1)}}$	inf	$\{i\}\{a\}\{j\}\{b\}^{(2)}_{t^{(1)}}$	inf	MP2	MP3	MP4SDQ	CCSD
01	-20.3	-20.6	-21.1	-21.5	-22.4	-22.8	-24.4	-23.3	-22.8	-22.6
02	-15.8	-16.3	-16.4	-16.9	-17.6	-17.8	-18.5	-18.2	-17.6	-17.6
03	-16.4	-16.5	-16.9	-16.9	-17.8	-17.6	-19.0	-17.8	-17.9	-17.5
04	-14.6	-15.3	-15.2	-15.8	-16.1	-16.4	-16.5	-16.8	-16.0	-16.2
05 nh_3	-9.0	-9.0	-9.5	-9.7	-10.4	-10.5	-11.3	-10.8	-10.4	-10.3
06	-2.8	-2.9	-3.3	-3.4	-3.8	-3.8	-4.4	-4.1	-3.8	-3.7
07	-1.5	-1.5	-1.8	-1.9	-2.1	-2.2	-2.4	-2.4	-2.2	-2.1
08	-1.4	-1.4	-1.6	-1.7	-1.9	-1.9	-2.1	-2.1	-1.9	-1.9
09	-10.5	-11.1	-11.3	-12.0	-13.2	-14.0	-15.4	-13.8	-13.7	-13.7
10	-6.7	-6.3	-7.2	-6.9	-8.2	-7.9	-9.3	-8.4	-7.9	-7.5
11	-3.4	-3.3	-3.9	-3.9	-4.6	-4.4	-5.6	-5.0	-4.6	-4.4
12	-3.9	-3.6	-4.2	-4.0	-4.6	-4.4	-5.6	-5.0	-4.5	-4.4
13	-3.3	-2.9	-3.6	-3.4	-4.0	-3.8	-5.1	-4.5	-4.0	-3.8
14	-1.7	-1.3	-2.2	-1.9	-2.7	-2.5	-4.2	-3.5	-2.8	-2.5
15	-0.9	-0.7	-1.1	-1.0	-1.4	-1.2	-1.8	-1.7	-1.3	-1.2
16	-0.9	-0.6	-1.8	-1.8	-2.6	-2.7	-3.7	-3.5	-3.0	-2.7
17	-1.1	-0.9	-1.6	-1.6	-2.0	-2.0	-2.6	-2.4	-2.1	-2.0
18	-0.7	-0.7	-1.2	-1.2	-1.5	-1.5	-1.8	-1.8	-1.5	-1.5
19	-0.6	-0.6	-1.0	-1.0	-1.4	-1.4	-1.5	-1.5	-1.3	-1.3
20	-0.3	-0.3	-0.5	-0.5	-0.7	-0.7	-1.1	-0.8	-0.7	-0.7
21	-0.2	-0.1	-0.3	-0.2	-0.4	-0.4	-1.0	-0.6	-0.5	-0.4
22	6.6	7.0	6.4	6.6	5.9	6.0	3.4	5.3	5.8	5.9
23	7.3	7.8	7.1	7.3	6.5	6.6	4.3	5.7	6.3	6.6
24	7.7	7.9	7.5	7.6	7.0	7.1	4.3	6.9	6.8	7.0

Table 7.5: kJ/mol A24 binding energies (CP-corrected/aug-cc-pvdz) in the frozen core approximation. Truncation model numbers reflect a half-non-orthogonal orbital reference. "inf" means CCSD amplitudes were used at zeroth-order.

Chapter 8

Iterative solutions of an effective Hamiltonian

8.1 Introduction and general construction

There has been extensive work in the past few decades[328–338] employing a Löwdin-type[29, 321–324] partitioning of the similarity-transformed Hamiltonian to garner high-accuracy so-called "(2)"-type perturbation theories on top of coupled cluster references. Here we propose to treat higher-order effects in a "perturb-then-diagonalize" approach solving an *effective* Hamiltonian problem defined in the low-dimensional space, but which folds in its Hilbert complement.

The Schrödinger equation for the wavefunction $|R\rangle = \sum_h r_h |h\rangle$ in the full Hilbert space of n-electron Slater determinants, $|\mathbf{h}\rangle = |0\rangle + |\mathbf{s}\rangle + |\mathbf{d}\rangle + ... + |\mathbf{n}\rangle$, is

$$\bar{H}|R\rangle = E|R\rangle, \tag{8.1}$$

where $\bar{H}$ is the $\hat{t_p}$-similarity-transformed Hamiltonian of CC theory, $\bar{H} = e^{-\hat{t_p}} H e^{\hat{t_p}}$ and $\{\mathbf{r_h}\}$. $\hat{R}$ and $\hat{t_p}$ are excitation operators of the form,

$$\begin{aligned} \hat{R} &= 1 + \sum_{ia} r_{ia} a_a^\dagger a_i + \sum_{i<j\ a<b} r_{ijab} a_a^\dagger a_b^\dagger a_j a_i + ..., \text{ and} \\ \hat{t} &= \sum_{ia} t_{ia} a_a^\dagger a_i + \sum_{i<j\ a<b} t_{ijab} a_a^\dagger a_b^\dagger a_j a_i + ... \ . \end{aligned} \tag{8.2}$$

Projections with the left biorthogonal state $\langle 0|\mathbf{l}^\dagger$ and $\langle \mathbf{p}'|$ give expressions for the energy and linear amplitudes $\{\mathbf{r}_{\mathbf{p}'}\}$,

$$\begin{aligned} \langle | \sum_{pp'} \mathbf{l}^\dagger_{\mathbf{p}'} \bar{\mathbf{H}}_{\mathbf{p}'\mathbf{p}} \mathbf{r}_{\mathbf{p}} | \rangle &= E, \\ \langle \mathbf{p}' | \sum_{p \neq p'} \bar{\mathbf{H}}_{\mathbf{p}'\mathbf{p}} \mathbf{r}_{\mathbf{p}'} | \mathbf{p} \rangle &= \{ E\mathbf{1}_{\mathbf{p}'\mathbf{p}'} - \bar{\mathbf{H}}_{\mathbf{p}'\mathbf{p}'} \} \mathbf{r}_{\mathbf{p}'}. \end{aligned} \tag{8.3}$$

Equations 8.3 are FCI-exact if, i) taking $\hat{t_p} = 0$, linear equations for $\mathbf{r_p}$ are solved in $|\mathbf{p}\rangle = |\mathbf{h}\rangle$, or ii) taking $\mathbf{r_p} = \mathbf{1_{pp}}$ and determining $\{t_p\}$ in $|\mathbf{p}\rangle = |\mathbf{h}\rangle$ by the nonlinear equations,

$$\langle \mathbf{p}' | \bar{\mathbf{H}}_{\mathbf{p}'\mathbf{p}} \mathbf{1}_{\mathbf{p}} | 0 \rangle = \mathbf{0}. \tag{8.4}$$

Treatment in a Hilbert space truncated at rank $U < n$ by the former gives linear, non-extensive CISD...U, and non-linear, non-variational CCSD...U by the latter.

For their individual merits, we can imagine marrying the two approaches, e.g., interacting configurations across a t_U-transformed Hamiltonian already folding in correlations coupling up to U electrons exactly. This way we account for higher-than-U-fold interactions in *linear* equations while automatically side-stepping the elephant in the room that is size-inconsistency. In the language of perturbation theory, this is equivalent to viewing the matrix elements of $\bar{\mathbf{H}}_{\mathbf{pp}'}$ determining the cluster $\{t_p\}$ in a "primary" space $|\mathbf{p}\rangle$ as zeroth-order quantities in a perturbative expansion of eq. 8.3. Identifying its Hilbert complement, $|\mathbf{q}\rangle = |\mathbf{h}\rangle - |\mathbf{p}\rangle$, we split $\bar{\mathbf{H}} = \bar{\mathbf{H}}^{(\mathbf{0})}_{\mathbf{pp}} + \bar{\mathbf{H}}^{(\mathbf{0})}_{\mathbf{qq}} + \bar{\mathbf{H}}^{(\mathbf{1})}_{\mathbf{pq}} + \bar{\mathbf{H}}^{(\mathbf{1})}_{\mathbf{qp}} + \bar{\mathbf{H}}^{(\mathbf{1})}_{\mathbf{qq}}$, $\mathbf{r}^{(\mathbf{0})} = \mathbf{1_{pp}}$, $\mathbf{l}^{\dagger(\mathbf{0})} = (\mathbf{1} + \mathbf{\Lambda})_{\mathbf{pp}}$ where $\mathbf{\Lambda}$ is the standard de-excitatory CC pseudo-lagrangian, and expand eq. 8.3 obtaining,

$$\begin{aligned} E^{(0)} = \langle 0|\mathbf{l}^{\dagger(\mathbf{0})} \bar{\mathbf{H}}^{(\mathbf{0})} \mathbf{r}^{(\mathbf{0})}|0\rangle &= \langle 0|(\mathbf{1} + \mathbf{\Lambda}_{\mathbf{pp}'}) \bar{\mathbf{H}}^{(\mathbf{0})}_{\mathbf{p}'\mathbf{p}} \mathbf{1}_{\mathbf{pp}}| \,\rangle = \bar{H}_{00} = E^{cc}, \\ E^{(1)} = \langle 0|\mathbf{l}^{\dagger(\mathbf{0})} \bar{\mathbf{H}}^{(\mathbf{1})} \mathbf{r}^{(\mathbf{0})}|0\rangle &= \langle 0|(\mathbf{1} + \mathbf{\Lambda}_{\mathbf{pp}'}) \Big(\bar{\mathbf{H}}^{(\mathbf{1})}_{\mathbf{pq}} + \bar{\mathbf{H}}^{(\mathbf{1})}_{\mathbf{qp}} + \bar{\mathbf{H}}^{(\mathbf{1})}_{\mathbf{qq}} \Big) \mathbf{1}_{\mathbf{pp}}| \,\rangle = 0, \quad \text{and} \\ E^{(2)} &= \langle 0|(\mathbf{1} + \mathbf{\Lambda}_{\mathbf{pp}'}) \bar{\mathbf{H}}^{(\mathbf{1})}_{\mathbf{pq}} \mathbf{r}^{(\mathbf{1})}_{\mathbf{q}}|0\rangle, \end{aligned} \tag{8.5}$$

noting the choice $|\mathbf{p}\rangle = |0\rangle + |\mathbf{s}\rangle + |\mathbf{d}\rangle + ... + |\mathbf{U}\rangle$ returns CCSD...U as the zeroth-order PT solution, and contributions from the complementary space debut at first-order in the wavefunction and at second-order in the energy. The solution of the amplitude eq. 8.3 requires inverting the energy difference on the right-hand side, typically approximated as the first term in a perturbation series,

$$\begin{aligned} \big\{ E\mathbf{1} - \bar{\mathbf{H}}_{\mathbf{qq}} \big\}^{-1} &= \big\{ (E^{(0)}\mathbf{1} + dE\mathbf{1}) - (\bar{\mathbf{H}}^{(\mathbf{0})}_{\mathbf{qq}} + \mathbf{d}\bar{\mathbf{H}}) \big\}^{-1} = \\ \big\{ (E^{(0)}\mathbf{1} - \bar{\mathbf{H}}^{(\mathbf{0})}_{\mathbf{qq}}) + (dE\mathbf{1} - \mathbf{d}\bar{\mathbf{H}}) \big\}^{-1} &\approx \big\{ (\mathbf{E}^{(\mathbf{0})}\mathbf{1} - \bar{\mathbf{H}}^{(\mathbf{0})}_{\mathbf{qq}}) \big\}, \end{aligned} \tag{8.6}$$

making use of the identity $\big\{\mathbf{A} - \mathbf{B}\big\}^{-1} = \mathbf{A}^{-1} + \mathbf{A}^{-1}\mathbf{B}\big\{\mathbf{A} - \mathbf{B}\big\}^{-1}$. The series is convergent provided $\mathbf{BA^{-1}} < 1$. Taking $\bar{\mathbf{H}}^{(\mathbf{0})}_{\mathbf{qq}} = \mathbf{F_{qq}}$ and shoving everything else in $\bar{\mathbf{H}}^{(\mathbf{1})}_{\mathbf{qq}}$, we define

$\mathbf{D}^{(\mathbf{0})}_{\mathbf{qq}} \equiv \{\mathbf{E}^{(\mathbf{0})}\mathbf{1}_{\mathbf{qq}} - \bar{\mathbf{H}}^{(\mathbf{0})}_{\mathbf{qq}}\}$ and proceed to enumerate the q-space amplitudes. Assuming we've solved an active-space CCSD problem treating a subset of the singles and doubles, $\{|\mathbf{s}'\rangle, |\mathbf{d}'\rangle\}$, and neglecting an inactive set $\{|\mathbf{s}\rangle, |\mathbf{d}\rangle\}$ and all higher-rank contributions $\{|\mathbf{t}\rangle, |\mathbf{q}\rangle\}$, we have $|\mathbf{p}\rangle = |0\rangle + |\mathbf{s}'\rangle + |\mathbf{d}'\rangle$ and $|\mathbf{q}\rangle = |\mathbf{s}\rangle + |\mathbf{d}\rangle + |\mathbf{t}\rangle + |\mathbf{q}\rangle$. Applying eq. 8.3, the amplitude equations in full regalia are

$$\begin{aligned}
\mathbf{D}^{(\mathbf{0})}_{\mathbf{ss}}\mathbf{r}^{(\mathbf{1})}_{\mathbf{s}} &= \bar{\mathbf{H}}^{(\mathbf{1})}_{\mathbf{s0}} + \bar{\mathbf{H}}^{(\mathbf{1})}_{\mathbf{ss'}}\mathbf{r}^{(\mathbf{0})}_{\mathbf{s'}} + \bar{\mathbf{H}}^{(\mathbf{1})}_{\mathbf{sd}}\mathbf{r}^{(\mathbf{0})}_{\mathbf{d}} + \bar{\mathbf{H}}^{(\mathbf{1})}_{\mathbf{st}}\mathbf{r}^{(\mathbf{0})}_{\mathbf{t}}, \\
\mathbf{D}^{(\mathbf{0})}_{\mathbf{dd}}\mathbf{r}^{(\mathbf{1})}_{\mathbf{d}} &= \bar{\mathbf{H}}^{(\mathbf{1})}_{\mathbf{d0}} + \bar{\mathbf{H}}^{(\mathbf{1})}_{\mathbf{ds}}\mathbf{r}^{(\mathbf{0})}_{\mathbf{s}} + \bar{\mathbf{H}}^{(\mathbf{1})}_{\mathbf{dd'}}\mathbf{r}^{(\mathbf{0})}_{\mathbf{d'}} + \bar{\mathbf{H}}^{(\mathbf{1})}_{\mathbf{dt}}\mathbf{r}^{(\mathbf{0})}_{\mathbf{t}} + \bar{\mathbf{H}}^{(\mathbf{1})}_{\mathbf{dq}}\mathbf{r}^{(\mathbf{0})}_{\mathbf{q}}, \\
\mathbf{D}^{(\mathbf{0})}_{\mathbf{tt}}\mathbf{r}^{(\mathbf{1})}_{\mathbf{t}} &= \bar{\mathbf{H}}^{(\mathbf{1})}_{\mathbf{t0}} + \bar{\mathbf{H}}^{(\mathbf{1})}_{\mathbf{ts}}\mathbf{r}^{(\mathbf{0})}_{\mathbf{s}} + \bar{\mathbf{H}}^{(\mathbf{1})}_{\mathbf{td}}\mathbf{r}^{(\mathbf{0})}_{\mathbf{d}} + \bar{\mathbf{H}}^{(\mathbf{1})}_{\mathbf{tt'}}\mathbf{r}^{(\mathbf{0})}_{\mathbf{t'}} + \bar{\mathbf{H}}^{(\mathbf{1})}_{\mathbf{tq}}\mathbf{r}^{(\mathbf{0})}_{\mathbf{q}}, \quad \text{and} \\
\mathbf{D}^{(\mathbf{0})}_{\mathbf{qq}}\mathbf{r}^{(\mathbf{1})}_{\mathbf{q}} &= \bar{\mathbf{H}}^{(\mathbf{1})}_{\mathbf{q0}} + \bar{\mathbf{H}}^{(\mathbf{1})}_{\mathbf{qd}}\mathbf{r}^{(\mathbf{0})}_{\mathbf{d}} + \bar{\mathbf{H}}^{(\mathbf{1})}_{\mathbf{qt}}\mathbf{r}^{(\mathbf{0})}_{\mathbf{d}}.
\end{aligned} \tag{8.7}$$

Various approximations to eqs. 8.7 determining the second-order correction above serve to define a suite of (2)-type perturbative schemes rivaling conventional CCSD(T). Löwdin partitioning has also found application in active space methods adding back dynamical correlations to orbital-optimized[332, 333] and pair references[334, 335], excited-state theories [336–338], and other constructions. Here we propose to treat higher-order effects in a "perturb-then-diagonalize" approach solving an *effective* Hamiltonian problem defined in the low-dimensional space $|\mathbf{p}\rangle$, but which folds in its complement $|\mathbf{q}\rangle$. Left-projecting eq. 8.1 by $\langle\mathbf{q}|$ and expanding, we obtain an equation for $\mathbf{r}_\mathbf{q}$ in terms of $\mathbf{r}_\mathbf{p}$,

$$\mathbf{r}_\mathbf{q}|0\rangle = {\mathbf{D}_\mathbf{qq}}^{-1}\bar{\mathbf{H}}_\mathbf{qp}\mathbf{r}_\mathbf{p}|0\rangle. \tag{8.8}$$

Projecting eq. 8.1 by $\langle\mathbf{p}|$ and applying eq. 8.8, we arrive at an effective eigenvalue equation in $|\mathbf{p}\rangle$:

$$\begin{aligned}
\tilde{\mathbf{H}}_\mathbf{pp}\mathbf{r}_\mathbf{p}|0\rangle &= \mathbf{r}_\mathbf{p}|0\rangle\mathbf{E}\mathbf{1}_\mathbf{pp}, \text{ with} \\
\tilde{\mathbf{H}}_\mathbf{pp} &= \bar{\mathbf{H}}_\mathbf{pp} + \bar{\mathbf{H}}_\mathbf{pq}\mathbf{D}^{-\mathbf{1}}_\mathbf{qq}\bar{\mathbf{H}}_\mathbf{qp}.
\end{aligned} \tag{8.9}$$

Again, the solution of eq. 8.9 is formally exact (and intractable) barring restrictions on $\mathbf{t}_\mathbf{p}$ and $\mathbf{r}_\mathbf{p}$ that serve to define various coupled-cluster wavefunctions and perturbative corrections discussed above and employed below. Taking $\mathbf{l}^\dagger_\mathbf{pp} = \mathbf{1}_\mathbf{pp}$, the model-space expectation value is

$$E = \langle 0|\mathbf{l}^\dagger_\mathbf{pp}\bar{\mathbf{H}}_\mathbf{pp}\mathbf{r}_\mathbf{p}|0\rangle = \bar{\mathbf{H}}_\mathbf{0p}\mathbf{r}_\mathbf{p}, \tag{8.10}$$

and biorthogonality is preserved without L-R renormalization, which would remove rigorous size-consistency. The amplitude equations for $\mathbf{r}_\mathbf{p}$ are identical to those in eq. 8.7 sans order superscripts, and shall be self-consistently determined until eq. 8.9 is satisfied. For the purpose of cataloging differential relaxation effects, we'll consider various restrictions on contributions entering the amplitude eqs. 8.7. For one, we should like to examine the effects of singles and doubles re-coupling to perturbative triples. We accomplish this by

choosing $\mathbf{r_p} = (\mathbf{1} + \mathbf{r_s} + \mathbf{r_d})$, and folding $\bar{\mathbf{H}}^{(\mathbf{1})}_{\mathbf{tp}}$ and $\bar{\mathbf{H}}^{(\mathbf{1})}_{\mathbf{pt}}\mathbf{r}^{(\mathbf{1})}_{\mathbf{t}}$ into eq. 8.9. An analogous effective-Hamiltonian construction is identified when the q space is augmented with quadruple excitations. To reduce the scaling from O(N^9) to O(N^6) there, we employ the factorization approximation introduced by Kucharski and Bartlett[342] for the $\bar{\mathbf{H}}^{(\mathbf{1})}_{\mathbf{dq}}\mathbf{r}^{(\mathbf{1})}_{\mathbf{q}}$ contraction contributing to $\mathbf{r_d}$. These are referred to as the "r$_{sd(t)}$" and "r$_{sd(tq_f)}$" models henceforth. They are on par with CCSD(T) in cost since the O(N^7) triples moment is not iteratively determined. Inclusion of the triples in $\mathbf{r_p}$ constitutes the "r$_{sdt}$" model, and amounts to infinite-order PT through triple excitations, making it a useful benchmark against which the performance of r$_{sd(t)}$ can be measured. The extended "$r_{sdt(q_f)}$" model includes excitations through triples in the p space with leading-order, factorized quadruples contributing to the doubles equation as in $r_{sd(tq_f)}$.

For the sake of completeness, we'll also want to examine our construction when the Hilbert space is restricted to singles and doubles. For a transformed Hamiltonian satisfying the CCSD equations in full rank, $\mathbf{r_s} = \mathbf{r_d} = \mathbf{0}$ trivially, and the CCSD energy is correct to infinite order in STPT, e.g., we recover the CCSD energy on diagonalization of the effective Hamiltonian of eq. 8.9 in the space of singles and doubles. If the cluster problem is solved for only a subset of singles and doubles $|\mathbf{s}'\rangle$, $|\mathbf{d}'\rangle$, on the other hand, non-zero $\mathbf{r}^{(\mathbf{1})}_{\mathbf{s}}$ and $\mathbf{r}^{(\mathbf{1})}_{\mathbf{d}}$ re-couple the active space at second order in PT. It shall thus be instructive to compare the energy obtained on diagonalization of eq. 8.9 employing a transformed Hamiltonian optimized for a subset of the singles and doubles to that obtained by CCSD in full rank. The extent to which transforming the Hamiltonian with first-order amplitudes will bear on the effective eigenvalue problem is a final curiosity to touch on. By Löwdin partitioning, such a choice returns $\mathrm{E}^{(0)} = E_{\mathrm{MP2}}$ in eq. 8.5, and $\mathbf{r}^{(\mathbf{1})}_{\mathbf{p}}$, aside from being complete through the leading-order term in fourth-order MP partitioning, resembles the amplitude update in a typical CC procedure. We'll refer to these as the "r$_{sd}$" and "$r^{t^{(1)}}_{sd}$" models below. The models are summarized in Table 8.1 and general spin-orbital equations for the amplitudes are given in Appendix B.

model	$\mathbf{r_p}$	first-order in $\tilde{\mathbf{H}}_{\mathbf{pp'}}$	scaling
r$_{sd}$	$\|\mathbf{s}'\rangle, \|\mathbf{d}'\rangle, \|\mathbf{s}\rangle, \|\mathbf{d}\rangle$	$\mathbf{H}_{(\mathbf{s'},\mathbf{d'})\mathbf{p}}$, $\mathbf{H}_{\mathbf{p}(\mathbf{s'},\mathbf{d'})}$	O(N^6)
$\mathrm{r}^{t^{(1)}}_{sd}$	$\|\mathbf{s}\rangle, \|\mathbf{d}\rangle$	$\bar{\mathbf{H}}_{\mathbf{pp'}}$	O(N^6)
r$_{sd(t)}$	$\|\mathbf{s}\rangle, \|\mathbf{d}\rangle$	$\bar{\mathbf{H}}_{\mathbf{t0}}$, $\bar{\mathbf{H}}_{\mathbf{pt}}\mathbf{r_t}$	O(N^7)
r$_{sd(tq_f)}$	$\|\mathbf{s}\rangle, \|\mathbf{d}\rangle$	$\bar{\mathbf{H}}_{\mathbf{t0}}$, $\bar{\mathbf{H}}_{\mathbf{pt}}\mathbf{r_t}$, $\bar{\mathbf{H}}_{\mathbf{dq}}\mathbf{r_q}$	O(N^7)
r$_{sdt}$	$\|\mathbf{s}\rangle, \|\mathbf{d}\rangle, \|\mathbf{t}\rangle$	$\bar{\mathbf{H}}_{\mathbf{tp}}$	O(N^8)
r$_{sdt(q_f)}$	$\|\mathbf{s}\rangle, \|\mathbf{d}\rangle, \|\mathbf{t}\rangle$	$\bar{\mathbf{H}}_{\mathbf{tp}}$, $\bar{\mathbf{H}}_{\mathbf{dq}}\mathbf{r_q}$	O(N^8)

Table 8.1: Models. $|\mathbf{s}'\rangle$ and $|\mathbf{d}'\rangle$ represent active configurations in the CCSD problem.

We apply our effective-Hamiltonian models in Section 8.2 to measure the extent to which iterative model-space solutions improve on their perturbative counterparts in situ-

ations where static correlations trump dynamic correlations and the reverse. Our figure of merit will be error against FCI or the equivalent.

8.2 Applications

Singles and doubles in the effective Hamiltonian

Confining our attention to the singles and doubles problem first, we compare STPT and traditional MP perturbation theory for H_2 dissociation, where CCSD is exact. Plotted in Figure 8.1 are errors relative to RHF-CCSD as a function of internuclear separation. Correcting HF by MP theory incrementally improves the error and non-parallelity around the equilibrium separation of 0.7Å, but divergence occurs faster with higher orders owing to compounding orbital degeneracies in the low-order wavefunction. Dressing the Hamiltonian with first-order amplitudes in the STPT corrections of eqs. 8.5 returns exactly MP2 at zeroth order. The second-order $\mathrm{r}_{sd}^{t^{(1)}}$ model and MP4SDQ behave similarly until about $2^*\mathrm{R}_{eq}$, where the latter peaks and crosses zero earlier and more steeply. Diagonalizing the effective Hamiltonian problem produces near-coincidence with CCSD up to $\sim 2^*\mathrm{R}_{eq}$ and gains against the perturbative wavefunction up to $\sim 3^*\mathrm{R}_{eq}$, where the latter has begun to turn over, thereby degrading the effective Hamiltonian conditioned on it.

Employing the same application and figure of merit, we choose a CCD reference and ask how iterative and non-iterative STPT singles and re-coupled doubles approximate CCSD. Examining Table 8.2, we note the CCD error at and around equilibrium is expectedly modest, but grows to some 9mH by $5^*\mathrm{R}_{eq}$ as the reference degrades considerably and t_1-mediated orbital relaxation is missing. Treating this defect by second-order STPT uniformly reduces the error, but the $\mathrm{r}_{sd}^{(1)}$ model starts to overcompensate past $3^*\mathrm{R}_{eq}$ and a low-order treatment of $\mathbf{r_p}$ causes the error to run negative. Infinite-order relaxation in the first-order field, on the other hand, produces an even-keeled, near-zero error and an infinite-order singles norm comparable to that of CCSD's t_1.

Triples, quadruples and re-coupled singles and doubles in the effective Hamiltonian

In this section, we examine the performance of our models compared to state-of-the-art post-CCSD methods for electron correlations. For all applications of STPT below, we transformthe Hamiltonian with CCSD-optimized t amplitudes and extend the Hilbert space to include triples and quadruples.

We begin by computing errors against FCI for BH bond dissociation, where higher-rank couplings in $\{\mathbf{r_p}\}$ describe correlations on top of the most important bond-breaking dou-

R(H-H) = x*R_{eq}	$E^{(0)}$= CCD	$r_{sd}^{(1)}$	$r_{sd}^{(i)}$	$\|t_1\|$	$\|r_s^{(1)}\|$	$\|r_s^{(i)}\|$
1.0	0.04	0.01	0.00	0.00	0.00	0.00
1.5	0.38	0.06	-0.01	0.03	0.02	0.03
2.0	1.57	0.21	-0.04	0.14	0.09	0.15
2.5	3.80	0.18	-0.07	0.40	0.25	0.41
3.0	5.78	-0.40	-0.12	0.71	0.45	0.71
3.5	7.80	-2.08	-0.16	1.12	0.77	1.13
4.0	8.56	-3.56	-0.17	1.33	0.97	1.35
5.0	8.75	-5.90	-0.13	1.46	1.19	1.48

Table 8.2: mH error against CCSD(exact) and Frobenius norms of singles amplitudes as a function of internuclear separation. Numbers were computed in 6-31G, and R_{eq}=0.7Å. The "(1)" superscript denotes a STPT second-order energy model computed from a first-order wavefunction, while a "(i)" implies an infinite-order energy from an infinite-order wavefunction.

bles amplitudes in the reference CCSD wavefunction. Examining Figure 8.2, we conclude that all methods describing triples non-iteratively perform similarly at equilibrium ($R(BH)_{eq}$ =1.4Å), with second-order $r_{sd(t)}$ and $r_{sd(tq_f)}$ models straddling CCSD(T) and beginning to turn over by 1.5*R_{eq}, and their infinite-order cousins straddling CCSD(2). Beyond 1.5*R_{eq}, a comparison of iterative and non-iterative $r_{sd(t)}$ and $r_{sd(tq_f)}$ models indicates relaxation of the singles and doubles in the field of higher-rank contributions confers significant stability, furnishing NPEs comparable to the iterative O(N^8)-scaling r_{sdt} and $r_{sdt(q_f)}$ models. A combination of

- including all terms in its triples moment (some of which are opposite in sign to binary contractions retained in CCSD(T)),
- employing optimized Λ instead of $T^\dagger$ in its left-hand eigenfunction,
- including the dressed one-body operator in the zeroth-order q space, resulting in a larger energy denominator

all cause CCSD(2) to typically underestimate correlations at equilibrium and turn over much later than CCSD(T). Since non-iterative $r_{sd(t)}$ satisfies i) but not ii) or iii) and represents a kind of middle ground, we can attribute stability in the long range to a degree of infinite-order character, be it from Λ or diagonalization of the effective Hamiltonian.

For the double-dissociation of water, the story should be similar, but we expect pathologies to bear out more quickly as the O-H bonds are stretched and four determinants begin to contribute significantly to the wavefunction. Compiled in Table 8.3 are errors against FCI for equilibrium and symmetrically-displaced geometries of water adopted from Ref. [329]. As anticipated, CCSDTQ can separate the two O-H bonds simultaneously without problem, and

R=xR_{eq}	$r^{(1)}_{sd(t)}$	$r^{(i)}_{sd(t)}$	$r^{(1)}_{sd(tq_f)}$	$r^{(i)}_{sd(tq_f)}$	$r^{(i)}_{sdt}$	$r^{(i)}_{sdt(q_f)}$	CCSD(T)	CCSD(2)	CCSDT^a	CCSDTQ^a
1	0.62	0.61	0.12	0.10	0.45	-0.06	0.53	0.16	0.45	0.01
1.5	1.56	1.79	-0.16	0.15	1.03	-0.64	1.08	0.74	1.20	0.10
2	-2.42	0.29	-3.76	-0.85	-2.29	-3.41	-6.31	0.39	-1.97	0.10

Table 8.3: mH error figures against FCI/6-31G for double dissociation of H_2O; *a*: Data are from Reference [329]. All models take $R(OH)_{eq}$=1.45Å$\angle(HOH) = 107.6°$. The "(1)" superscript denotes a STPT second-order energy model computed from a first-order wavefunction, while a "(i)" implies an infinite-order energy from an infinite-order wavefunction.

CCSDT cannot, though partial optimization of disconnected quadruples due to connected triples causes it to turn over later than CCSD(T). The same can be said of infinite-order $r_{sd(t)}$ and of r_{sdt}, while the relative stability of $r^{(1)}_{sd(t)}$ is due to an inclusion of all terms in the triples moment. The critical importance of quadruple substitutions is evinced comparing CCSDT and CCSDTQ, or similarly, $r_{sd(tq_f)}$ to $r_{sd(t)}$. Again, diagonalization of the effective Hamiltonian in the space of singles and doubles with or without quadruple substitutions reigns in runaway PTs in the multireference regime.

In a similar test, we measure the ability of the foregoing models to capture static correlations as rectangular H_4 passes through a doubly-degenerate square configuration to an identical rectangular configuration rotated 90°. We scan along the bisecting angle θ defined on the interval (0°, 90°) where 0° and 90° correspond to two different endpoints for infinitely-separated H_2 molecules, and $\theta = 45°$ to the FCI-optimized square transition state, where R(H-H)=1.3Å. We plot errors relative to FCI around the square geometry in Figure 8.3, noting a kink should exist for each of the above single-reference wavefunctions due to an inability to equally weight the degenerate configurations at the transition state. As in the symmetric stretch case, CCSD(T) represents the most dramatic failure, while neither patching with the full triples moment by perturbative $r_{sd(t)}$ nor determining r_{sdt} iteratively does much to improve the situation. The $_{sd(tq_f)}$ and $r_{sdt(q_f)}$ curves underscore the critical role of quadruples, but the most significant gains are again borne out by iterative solution of the effective Hamiltonian in the space of singles and doubles. The infinite-order $r_{sd(t)}$ and $r_{sd(tq_f)}$ models recover variationality and exhibit the smallest NPEs. CCSD(2) performs similarly due to the infinite-order character conferred by the Λ piece of its left state as well as the damping effects of a dressed one-body denominator.

8.3 Conclusions

We have compared standard post-CCSD corrections and those from second-order STPT to those obtained by diagonalizing an effective Hamiltonian in the same primary space, but which folds in its complement. Preliminary tests indicate that higher-order relaxation improves upon a first-order description of dynamical correlations near equilibrium, and also tempers ill-behaved PTs away from equilibrium where static correlations dominate. For

its infinite-order-character left state, CCSD(2) exhibits similar behavior to the effective-Hamiltonian theories introduced here.

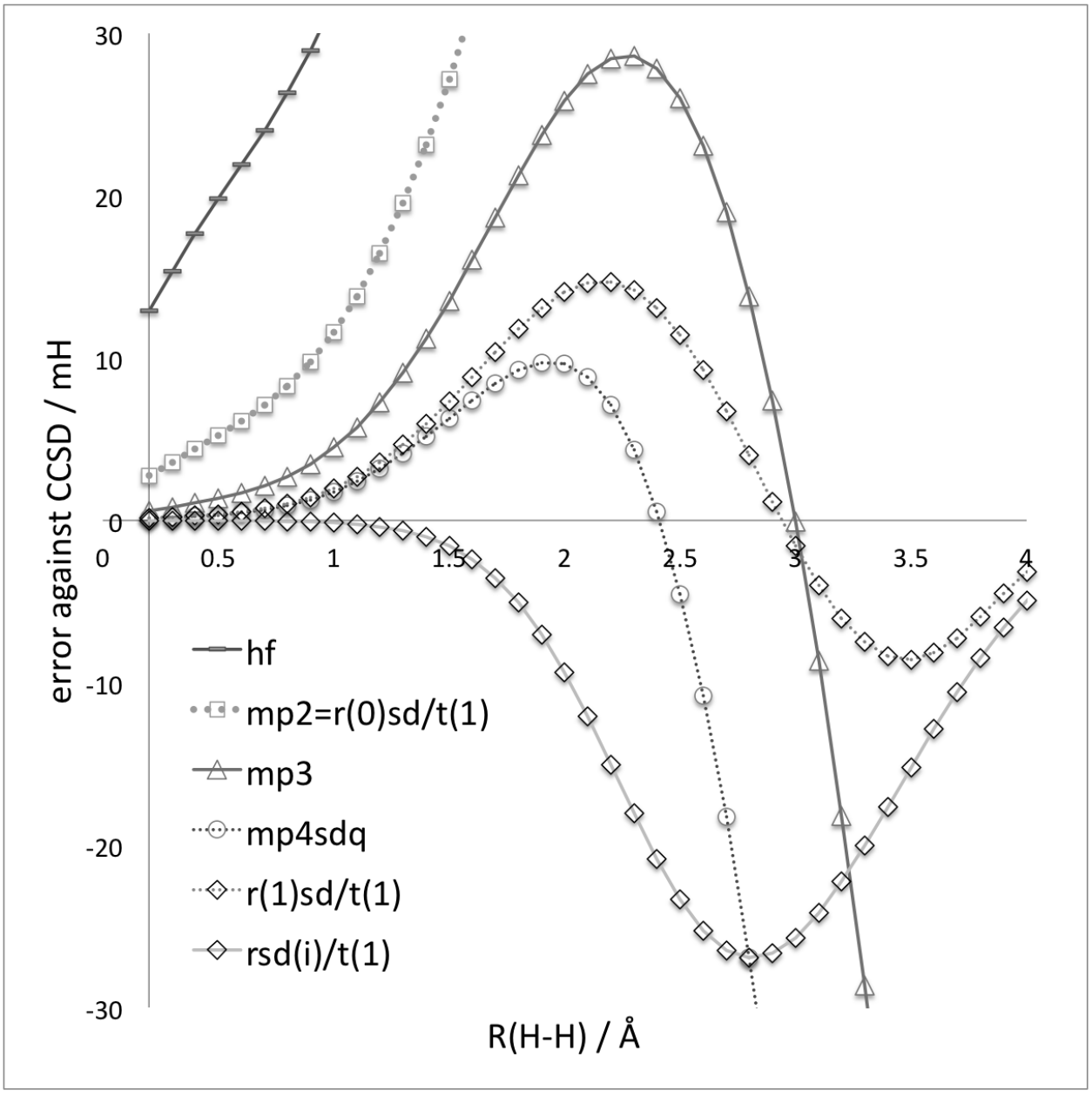

Figure 8.1: mH error relative to CCSD (FCI-equivalent) for H_2 separation in the 6-31G basis; R_{eq}=0.7Å. The "(1)" superscript denotes a STPT second-order energy model computed from a first-order wavefunction, while a "(i)" implies an infinite-order energy from an infinite-order wavefunction.

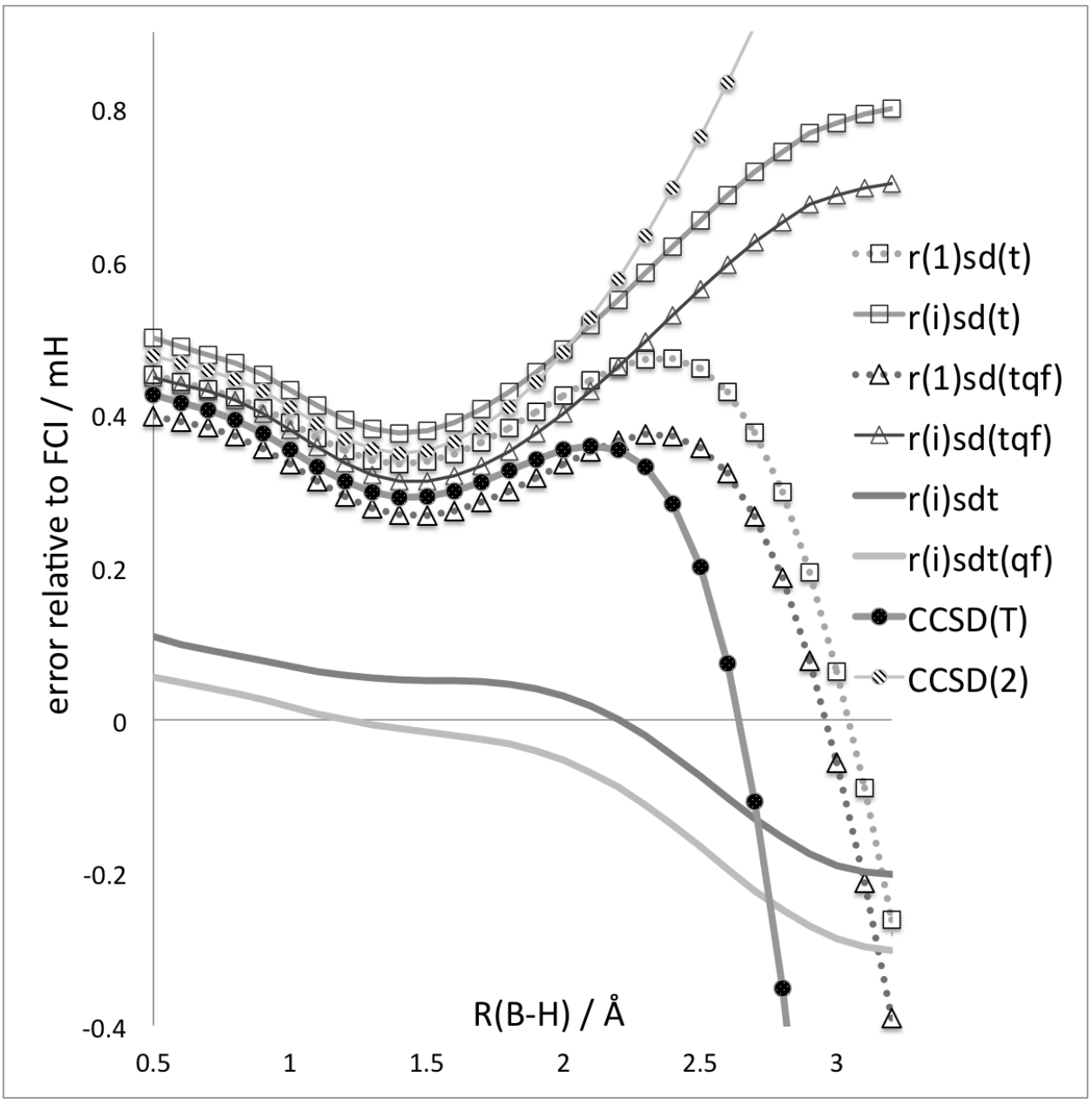

Figure 8.2: mH error relative to FCI separating B-H in 6-31G; R_{eq}=1.4Å. All electrons were correlated. The "(1)" superscript denotes a STPT second-order energy model computed from a first-order wavefunction, while a "(i)" implies an infinite-order energy from an infinite-order wavefunction.

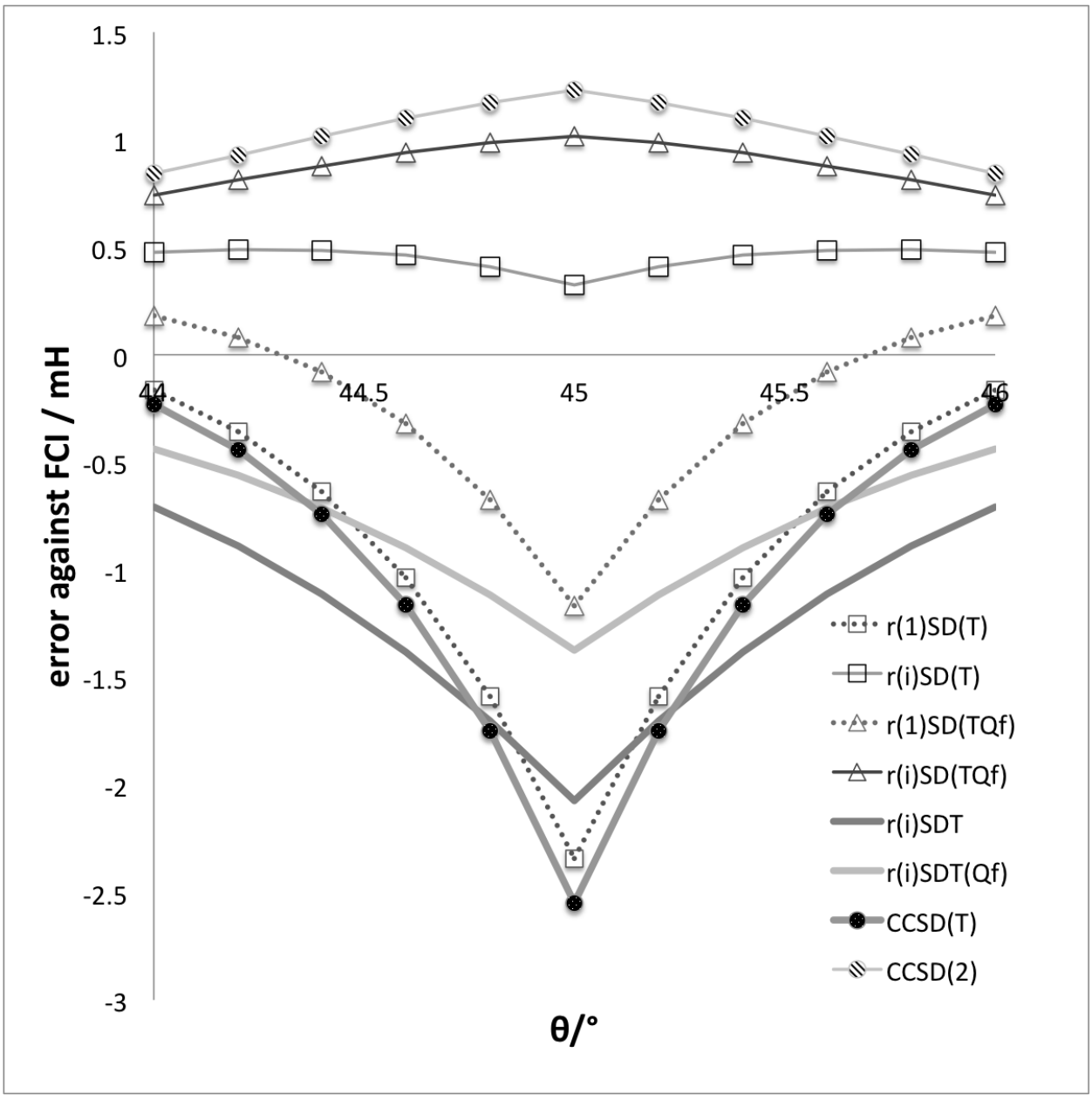

Figure 8.3: mH error relative to FCI as rectangular H_4 passes through a doubly-degenerate square geometry. All calculations were performed in 6-31G. The "(1)" superscript denotes a STPT second-order energy model computed from a first-order wavefunction, while a "(i)" implies an infinite-order energy from an infinite-order wavefunction.

Chapter 9

Outlook and concluding remarks

In the latter part of this thesis, local (2)-type correlation models and first-order approximations in full and reduced rank were considered. A continuation of this line of research might include

- *efficiency in the implementation*: While it may or may not be apparent from the Appendices, the (i)STPT computations presented herein come from a pilot implementation which enjoys only partial optimization of permutational symmetry, intermediate definitions, and integral batching. For non-orthogonal triples, this is especially limiting. Implementing more simplification rules in the generation of the spin-orbital expressions, or a diagrammatic derivation are two routes to prefactor reduction.

- *allowing orbital optimization*: In this same vein, providing an orbital basis zeroing $\hat{T}_1$ would reduce the triples prefactor there considerably. While a correct pilot implementation of non-orthogonal Brueckner orbitals determined with or without the ALMO constraint exists in the iSTPT code and has, indeed, reduced triples wall time considerably, it is inefficient in the macroiterations and arguably too "hacky".

- *quantiative many-body formulation of iSTPT*: As shown in Chapters 6 and 7, iSTPT truncation error is mostly due to rank-reduction in non-local *two-body* doubles. In the context of cluster applications, a formulation including all two-body hole-particle pairs in the two-particle metric would not only guarantee exactness for dimers by construction, but also retain quadratic scaling in fragments. It remains to be determined whether higher-than-two-body effects can be described by PT, though at least an MP4SD-level treatment there is guaranteed.

- *reformulation of existing STPTs*: The ability of STPT taking first-order amplitudes to quantitatively recover CCSD non-iteratively invites the question of whether existing active-space (2) corrections can be improved by adding back inactive doubles to the amplitude vector transforming the Hamiltonian before the PT step. This would guarantee an MP2-level treatment at zeroth-order instead of at second-order. Of course,

naive addition would no longer guarantee an active-space coupled-cluster solution at zeroth-order, so it might be more formally satisfying to parametrize the zeroth-order problem fixing them at first-order in MP theory. PP(2) is a good first target.

The encouraging results of the minimal basis SCF models presented in Chapter 5 invite the prospect of improving on dual-basis corrections to SCF. Specifically, a $2N_{occ}$-rank SCF in a minimal basis determined from Roothaan or approximate Roothaan amplitudes in the "big" basis, apart from being virtually free, will provide for a variational, more accurate correction.

In the context of correlated EDAs, a non-orthogonal coupled cluster model from ALMOs correcting HF electrostatics and induction, and including effects of local triples and factorized quadruples is possible using the iSTPT codes. A comparison of interaction components predicted this way and by the orthogonal analog developed in Chapter 3 is immediately interesting.

The effective Hamiltonian models of Chapter 8 generally improve on their PT counterparts for static and dynamic correlations, at similar cost. A more efficient implementation would increase the scope of their application, of course, but these models will likely remain theoretical curiosities not only because they're among the most expensive wavefunction methods considered in modern applications.

Appendix A

iSTPT(2) singles and doubles matrix elements

A.1 Spin-orbital expressions in the covariant integral representation

Occupied and virtual orbitals are indexed $(i, j, k, l, I, J, K, L...)$ and $(a, b, c, d, A, B, C, D...)$, respectively, with upper-case indices implying external hole/particle excitations and lower-case (internal) indices implying summation. The operator $a_{\rm pq}$ is an antisymmetrizer, e.g., $a_{\rm pq}X_{pqrs} = X_{pqrs} - X_{qprs}$. The tensors f_{pq} and v_{pqrs} are the Fock and antisymmerized integrals, respectively. t, λ, r are the cluster, left, and first-order right amplitudes. The following intermediates are used in the expressions below.

$$X_h^{\rm aI} = X^{\rm aj} g_{\rm jI} \tag{A.1}$$

$$X_p^{\rm Ai} = g_{\rm Ab} X^{\rm bi} \tag{A.2}$$

$$X_h^{\rm abIJ} = g_{\rm Ij} X^{\rm abjJ} \tag{A.3}$$

$$X_{pp}^{\rm ABij} = g_{\rm Aa} g_{\rm Bb} X^{\rm abij} \tag{A.4}$$

$$X_{hp}^{\rm bBiI} = g_{\rm ij} g_{\rm bc} X^{\rm cBjI} \tag{A.5}$$

$$X_{hp'}^{\rm bBiI} = g_{\rm Ij} g_{\rm Bc} X^{\rm bcij} \tag{A.6}$$

$$X_{hph}^{\rm bcij} = g_{\rm jk} X_{hp}^{\rm bcik} \tag{A.7}$$

$$X_{hpp}^{\rm bcij} = g_{\rm ca} X_{hp}^{\rm baij} \tag{A.8}$$

CCSD amplitude equations

$A_{AI}(\bar{t}) =$

$$f_{\mathrm{AI}} \tag{A.9}$$
$$f_{\mathrm{ai}} t_{hp}^{\mathrm{aAiI}} \tag{A.10}$$
$$-1. f_{\mathrm{ai}} t_{h}^{\mathrm{aI}} t_{p}^{\mathrm{Ai}} \tag{A.11}$$
$$-0.5 g_{\mathrm{aA}} v_{\mathrm{biIj}} t^{\mathrm{abij}} \tag{A.12}$$
$$-0.5 g_{\mathrm{Ij}} v_{\mathrm{aAbi}} t^{\mathrm{abij}} \tag{A.13}$$
$$-1. t^{\mathrm{ai}} v_{\mathrm{aAiI}} \tag{A.14}$$
$$-1. t^{\mathrm{aj}} v_{\mathrm{aiIj}} t_{p}^{\mathrm{Ai}} \tag{A.15}$$
$$-0.5 g_{\mathrm{aA}} v_{\mathrm{bcij}} t^{\mathrm{acij}} t_{h}^{\mathrm{bI}} \tag{A.16}$$
$$t^{\mathrm{ai}} v_{\mathrm{abij}} t_{hp}^{\mathrm{AbIj}} \tag{A.17}$$
$$-0.5 g_{\mathrm{Ik}} v_{\mathrm{abij}} t^{\mathrm{abjk}} t_{p}^{\mathrm{Ai}} \tag{A.18}$$
$$-1. t^{\mathrm{bi}} v_{\mathrm{aAbi}} t_{h}^{\mathrm{aI}} \tag{A.19}$$
$$-1. t^{\mathrm{bj}} v_{\mathrm{abij}} t_{h}^{\mathrm{aI}} t_{p}^{\mathrm{Ai}} \tag{A.20}$$

$B_{IJ}^{AB}(\bar{t}) =$

$$-1.g_{\mathrm{aB}}a_{\mathrm{IJ}}f_{\mathrm{bi}}t_{h}^{\mathrm{bJ}}t_{hp}^{\mathrm{aAiI}} \tag{A.21}$$
$$-1.f_{\mathrm{ai}}a_{\mathrm{AB}}g_{\mathrm{jJ}}t_{p}^{\mathrm{Bi}}t_{hp}^{\mathrm{aAIj}} \tag{A.22}$$
$$v_{\mathrm{ABIJ}} \tag{A.23}$$
$$0.5v_{\mathrm{iIjJ}}t_{pp}^{\mathrm{ABij}} \tag{A.24}$$
$$-1.a_{\mathrm{AB}}a_{\mathrm{IJ}}v_{\mathrm{aAiI}}t_{hp}^{\mathrm{aBiJ}} \tag{A.25}$$
$$0.5v_{\mathrm{aAbB}}t_{h}^{\mathrm{abIJ}} \tag{A.26}$$
$$a_{\mathrm{AB}}v_{\mathrm{AiIJ}}t_{p}^{\mathrm{Bi}} \tag{A.27}$$
$$a_{\mathrm{IJ}}v_{\mathrm{aABI}}t_{h}^{\mathrm{aJ}} \tag{A.28}$$
$$-1.a_{\mathrm{AB}}v_{\mathrm{abij}}t_{hp}^{\mathrm{aBiI}}t_{hp}^{\mathrm{AbjJ}} \tag{A.29}$$
$$0.25v_{\mathrm{abij}}t_{h}^{\mathrm{abIJ}}t_{pp}^{\mathrm{ABij}} \tag{A.30}$$
$$-0.5g_{\mathrm{aB}}g_{\mathrm{Jk}}v_{\mathrm{bcij}}t^{\mathrm{bcjk}}t_{hp}^{\mathrm{aAiI}} \tag{A.31}$$
$$-0.5g_{\mathrm{aB}}a_{\mathrm{AB}}g_{\mathrm{Jk}}v_{\mathrm{bcij}}t^{\mathrm{acij}}t_{hp}^{\mathrm{AbIk}} \tag{A.32}$$
$$-0.5g_{\mathrm{aB}}g_{\mathrm{Ik}}v_{\mathrm{bcij}}t^{\mathrm{bcik}}t_{hp}^{\mathrm{aAjJ}} \tag{A.33}$$
$$v_{\mathrm{iIjJ}}t_{p}^{\mathrm{Ai}}t_{p}^{\mathrm{Bj}} \tag{A.34}$$
$$a_{\mathrm{AB}}a_{\mathrm{IJ}}v_{\mathrm{aiIj}}t_{p}^{\mathrm{Bi}}t_{hp}^{\mathrm{aAjJ}} \tag{A.35}$$
$$0.5a_{\mathrm{IJ}}v_{\mathrm{aiIj}}t_{h}^{\mathrm{aJ}}t_{pp}^{\mathrm{ABij}} \tag{A.36}$$
$$-1.g_{\mathrm{aB}}a_{\mathrm{IJ}}t^{\mathrm{bi}}v_{\mathrm{biIj}}t_{hp}^{\mathrm{aAjJ}} \tag{A.37}$$
$$a_{\mathrm{AB}}a_{\mathrm{IJ}}v_{\mathrm{aAiI}}t_{h}^{\mathrm{aJ}}t_{p}^{\mathrm{Bi}} \tag{A.38}$$
$$0.5a_{\mathrm{AB}}v_{\mathrm{aAbi}}t_{p}^{\mathrm{Bi}}t_{h}^{\mathrm{abIJ}} \tag{A.39}$$
$$a_{\mathrm{AB}}a_{\mathrm{IJ}}v_{\mathrm{aAbi}}t_{h}^{\mathrm{aJ}}t_{hp}^{\mathrm{bBiI}} \tag{A.40}$$
$$-1.a_{\mathrm{AB}}g_{\mathrm{jJ}}t^{\mathrm{ai}}v_{\mathrm{aAbi}}t_{hp}^{\mathrm{bBIj}} \tag{A.41}$$
$$v_{\mathrm{aAbB}}t_{h}^{\mathrm{aI}}t_{h}^{\mathrm{bJ}} \tag{A.42}$$
$$a_{\mathrm{IJ}}v_{\mathrm{aiIj}}t_{h}^{\mathrm{aJ}}t_{p}^{\mathrm{Ai}}t_{p}^{\mathrm{Bj}} \tag{A.43}$$
$$0.5v_{\mathrm{abij}}t_{p}^{\mathrm{Ai}}t_{p}^{\mathrm{Bj}}t_{h}^{\mathrm{abIJ}} \tag{A.44}$$
$$-1.a_{\mathrm{AB}}a_{\mathrm{IJ}}v_{\mathrm{abij}}t_{h}^{\mathrm{aJ}}t_{p}^{\mathrm{Bi}}t_{hp}^{\mathrm{AbIj}} \tag{A.45}$$
$$-1.a_{\mathrm{AB}}g_{\mathrm{Jk}}t^{\mathrm{ai}}v_{\mathrm{abij}}t_{p}^{\mathrm{Bj}}t_{hp}^{\mathrm{AbIk}} \tag{A.46}$$
$$0.5v_{\mathrm{abij}}t_{h}^{\mathrm{aI}}t_{h}^{\mathrm{bJ}}t_{pp}^{\mathrm{ABij}} \tag{A.47}$$
$$g_{\mathrm{aB}}a_{\mathrm{IJ}}t^{\mathrm{ci}}v_{\mathrm{bcij}}t_{h}^{\mathrm{bJ}}t_{hp}^{\mathrm{aAIj}} \tag{A.48}$$
$$a_{\mathrm{AB}}v_{\mathrm{aAbi}}t_{h}^{\mathrm{aI}}t_{h}^{\mathrm{bJ}}t_{p}^{\mathrm{Bi}} \tag{A.49}$$
$$v_{\mathrm{abij}}t_{h}^{\mathrm{aI}}t_{p}^{\mathrm{Ai}}t_{h}^{\mathrm{bJ}}t_{p}^{\mathrm{Bj}} \tag{A.50}$$

Left-hand singles and doubles equations

$\lambda_b^j \langle_j^b | \bar{H} |_I^A \rangle =$

$$f_{\mathrm{aA}} \lambda_h^{\mathrm{aI}} \tag{A.51}$$
$$-1. f_{\mathrm{iI}} \lambda_p^{\mathrm{Ai}} \tag{A.52}$$
$$-1. f_{\mathrm{Ai}} \lambda_h^{\mathrm{aI}} t_p^{\mathrm{ai}} \tag{A.53}$$
$$-1. f_{\mathrm{aI}} t_h^{\mathrm{ai}} \lambda_p^{\mathrm{Ai}} \tag{A.54}$$
$$-1. r^{\mathrm{ai}} v_{\mathrm{aAiI}} \tag{A.55}$$
$$-0.5 g_{\mathrm{ab}} v_{\mathrm{Acij}} t^{\mathrm{acij}} \lambda_h^{\mathrm{bI}} \tag{A.56}$$
$$r^{\mathrm{ai}} v_{\mathrm{AbIj}} t_{hp}^{\mathrm{abij}} \tag{A.57}$$
$$-0.5 g_{\mathrm{Ab}} v_{\mathrm{aciI}} t^{\mathrm{acij}} \lambda_h^{\mathrm{bj}} \tag{A.58}$$
$$r^{\mathrm{ai}} v_{\mathrm{AiIj}} t_p^{\mathrm{aj}} \tag{A.59}$$
$$-1. t^{\mathrm{aj}} v_{\mathrm{aiIj}} \lambda_p^{\mathrm{Ai}} \tag{A.60}$$
$$-1. t^{\mathrm{bi}} v_{\mathrm{aAbi}} \lambda_h^{\mathrm{aI}} \tag{A.61}$$
$$r^{\mathrm{ai}} v_{\mathrm{aAbI}} t_h^{\mathrm{bi}} \tag{A.62}$$
$$-1. t^{\mathrm{bj}} v_{\mathrm{Abij}} \lambda_h^{\mathrm{aI}} t_p^{\mathrm{ai}} \tag{A.63}$$
$$-1. r^{\mathrm{ai}} v_{\mathrm{AbIj}} t_p^{\mathrm{aj}} t_h^{\mathrm{bi}} \tag{A.64}$$
$$-1. t^{\mathrm{bj}} v_{\mathrm{abIj}} t_h^{\mathrm{ai}} \lambda_p^{\mathrm{Ai}} \tag{A.65}$$

$\lambda^{jk}_{bc}\langle^{bc}_{jk}|\bar{H}|^{A}_{I}\rangle =$

$$1.f_{\mathrm{ai}}\lambda^{\mathrm{aAiI}}_{hp} \tag{A.66}$$
$$1.f_{\mathrm{bj}}\lambda^{\mathrm{aAiI}}_{hp}t^{\mathrm{abij}}_{hp} \tag{A.67}$$
$$0.5f_{\mathrm{Aj}}g_{\mathrm{bc}}g_{\mathrm{ik}}t^{\mathrm{acjk}}\lambda^{\mathrm{abiI}}_{hp} \tag{A.68}$$
$$0.5g_{\mathrm{ab}}f_{\mathrm{cI}}g_{\mathrm{jk}}t^{\mathrm{acij}}\lambda^{\mathrm{Abik}}_{hp} \tag{A.69}$$
$$-1.f_{\mathrm{ij}}t^{\mathrm{aj}}_{p}\lambda^{\mathrm{aAiI}}_{hp} \tag{A.70}$$
$$1.f_{\mathrm{ab}}t^{\mathrm{bi}}_{h}\lambda^{\mathrm{aAiI}}_{hp} \tag{A.71}$$
$$-1.f_{\mathrm{bj}}t^{\mathrm{aj}}_{p}t^{\mathrm{bi}}_{h}\lambda^{\mathrm{aAiI}}_{hp} \tag{A.72}$$
$$-0.5g_{\mathrm{Ab}}v_{\mathrm{aiIj}}r^{\mathrm{abij}} \tag{A.73}$$
$$-0.5g_{\mathrm{iI}}v_{\mathrm{aAbj}}r^{\mathrm{abij}} \tag{A.74}$$
$$-0.25g_{\mathrm{bc}}v_{\mathrm{Aijk}}t^{\mathrm{acjk}}\lambda^{\mathrm{abiI}}_{hp} \tag{A.75}$$
$$-0.25g_{\mathrm{ab}}v_{\mathrm{AiIj}}t^{\mathrm{acjk}}\lambda^{\mathrm{bcik}}_{hp'} \tag{A.76}$$
$$-0.5g_{\mathrm{ab}}v_{\mathrm{cijk}}t^{\mathrm{acjk}}\lambda^{\mathrm{AbiI}}_{hp} \tag{A.77}$$
$$-0.5g_{\mathrm{Ab}}v_{\mathrm{ciIj}}t^{\mathrm{acjk}}\lambda^{\mathrm{abik}}_{hp'} \tag{A.78}$$
$$0.25g_{\mathrm{bc}}v_{\mathrm{AiIk}}t^{\mathrm{acij}}\lambda^{\mathrm{abjk}}_{hp} \tag{A.79}$$
$$0.5g_{\mathrm{ab}}v_{\mathrm{ciIk}}t^{\mathrm{acij}}\lambda^{\mathrm{Abjk}}_{hp} \tag{A.80}$$
$$0.5g_{\mathrm{ik}}v_{\mathrm{Abcj}}t^{\mathrm{acjk}}\lambda^{\mathrm{abiI}}_{hp} \tag{A.81}$$
$$-0.5g_{\mathrm{iI}}v_{\mathrm{aAcj}}t^{\mathrm{bcjk}}\lambda^{\mathrm{abik}}_{hp'} \tag{A.82}$$
$$0.25g_{\mathrm{jk}}v_{\mathrm{AbcI}}t^{\mathrm{acij}}\lambda^{\mathrm{abik}}_{hp} \tag{A.83}$$
$$-0.25g_{\mathrm{ij}}v_{\mathrm{aAcI}}t^{\mathrm{bcjk}}\lambda^{\mathrm{abik}}_{hp'} \tag{A.84}$$
$$-0.5g_{\mathrm{ik}}v_{\mathrm{abcj}}t^{\mathrm{bcjk}}\lambda^{\mathrm{aAiI}}_{hp} \tag{A.85}$$
$$-0.25g_{\mathrm{jk}}v_{\mathrm{abcI}}t^{\mathrm{bcij}}\lambda^{\mathrm{aAik}}_{hp} \tag{A.86}$$

$$0.5 g_{\mathrm{aA}} v_{\mathrm{iIjk}} r^{\mathrm{abik}} t_p^{\mathrm{bj}} \tag{A.87}$$
$$0.5 t^{\mathrm{aj}} v_{\mathrm{Abij}} \lambda_{hp}^{\mathrm{abiI}} \tag{A.88}$$
$$-0.5 g_{\mathrm{iI}} v_{\mathrm{aAjk}} r^{\mathrm{abij}} t_p^{\mathrm{bk}} \tag{A.89}$$
$$-1. t^{\mathrm{bj}} v_{\mathrm{abij}} \lambda_{hp}^{\mathrm{aAiI}} \tag{A.90}$$
$$-0.5 g_{\mathrm{Ab}} v_{\mathrm{aciI}} r^{\mathrm{abij}} t_h^{\mathrm{cj}} \tag{A.91}$$
$$0.5 t^{\mathrm{bi}} v_{\mathrm{abIj}} \lambda_{hp}^{\mathrm{aAij}} \tag{A.92}$$
$$0.5 g_{\mathrm{iI}} v_{\mathrm{aAbc}} r^{\mathrm{abij}} t_h^{\mathrm{cj}} \tag{A.93}$$
$$-0.5 t^{\mathrm{aj}} v_{\mathrm{Aijk}} t_p^{\mathrm{bk}} \lambda_{hp}^{\mathrm{abiI}} \tag{A.94}$$
$$-1. t^{\mathrm{bk}} v_{\mathrm{bijk}} t_p^{\mathrm{aj}} \lambda_{hp}^{\mathrm{aAiI}} \tag{A.95}$$
$$0.5 g_{\mathrm{Ab}} t^{\mathrm{aj}} t^{\mathrm{ck}} v_{\mathrm{ciIj}} \lambda_{hp'}^{\mathrm{abik}} \tag{A.96}$$
$$-0.5 t^{\mathrm{bj}} v_{\mathrm{biIk}} t_p^{\mathrm{ai}} \lambda_{hp}^{\mathrm{aAjk}} \tag{A.97}$$
$$0.25 g_{\mathrm{bc}} v_{\mathrm{Adjk}} t^{\mathrm{acjk}} t_h^{\mathrm{di}} \lambda_{hp}^{\mathrm{abiI}} \tag{A.98}$$
$$-0.5 g_{\mathrm{bc}} g_{\mathrm{il}} t^{\mathrm{dj}} v_{\mathrm{Adjk}} t^{\mathrm{ackl}} \lambda_{hp}^{\mathrm{abiI}} \tag{A.99}$$
$$-0.25 g_{\mathrm{bc}} v_{\mathrm{AdiI}} t^{\mathrm{acij}} t_h^{\mathrm{dk}} \lambda_{hp}^{\mathrm{abjk}} \tag{A.100}$$
$$0.25 g_{\mathrm{bc}} g_{\mathrm{kl}} t^{\mathrm{dj}} v_{\mathrm{AdiI}} t^{\mathrm{acik}} \lambda_{hp}^{\mathrm{abjl}} \tag{A.101}$$
$$0.5 g_{\mathrm{il}} v_{\mathrm{Acjk}} t^{\mathrm{ackl}} t_p^{\mathrm{bj}} \lambda_{hp}^{\mathrm{abiI}} \tag{A.102}$$
$$-0.5 t^{\mathrm{aj}} v_{\mathrm{Acjk}} \lambda_{hp}^{\mathrm{abiI}} t_{hp}^{\mathrm{bcik}} \tag{A.103}$$
$$-0.25 g_{\mathrm{kl}} v_{\mathrm{AciI}} t^{\mathrm{acjk}} t_p^{\mathrm{bi}} \lambda_{hp}^{\mathrm{abjl}} \tag{A.104}$$
$$0.25 g_{\mathrm{bc}} g_{\mathrm{kl}} t^{\mathrm{ai}} v_{\mathrm{AdiI}} t^{\mathrm{cdjk}} \lambda_{hp}^{\mathrm{abjl}} \tag{A.105}$$
$$-0.5 g_{\mathrm{ab}} v_{\mathrm{cdjk}} t^{\mathrm{adjk}} t_h^{\mathrm{ci}} \lambda_{hp}^{\mathrm{AbiI}} \tag{A.106}$$
$$1. t^{\mathrm{bj}} v_{\mathrm{bcjk}} \lambda_{hp}^{\mathrm{aAiI}} t_{hp}^{\mathrm{acik}} \tag{A.107}$$
$$0.5 g_{\mathrm{ab}} v_{\mathrm{cdiI}} t^{\mathrm{adij}} t_h^{\mathrm{ck}} \lambda_{hp}^{\mathrm{Abjk}} \tag{A.108}$$
$$-0.5 t^{\mathrm{bj}} v_{\mathrm{bciI}} \lambda_{hp}^{\mathrm{aAjk}} t_{hp}^{\mathrm{acik}} \tag{A.109}$$
$$-0.5 g_{\mathrm{il}} v_{\mathrm{bcjk}} t_p^{\mathrm{aj}} t^{\mathrm{bckl}} \lambda_{hp}^{\mathrm{aAiI}} \tag{A.110}$$
$$-0.5 g_{\mathrm{ab}} g_{\mathrm{kl}} t^{\mathrm{ci}} v_{\mathrm{cdiI}} t^{\mathrm{adjk}} \lambda_{hp}^{\mathrm{Abjl}} \tag{A.111}$$
$$0.25 g_{\mathrm{kl}} v_{\mathrm{bciI}} t_p^{\mathrm{ai}} t^{\mathrm{bcjk}} \lambda_{hp}^{\mathrm{aAjl}} \tag{A.112}$$
$$-0.5 t^{\mathrm{aj}} v_{\mathrm{Abcj}} t_h^{\mathrm{ci}} \lambda_{hp}^{\mathrm{abiI}} \tag{A.113}$$
$$0.5 g_{\mathrm{iI}} t^{\mathrm{bj}} t^{\mathrm{ck}} v_{\mathrm{aAcj}} \lambda_{hp'}^{\mathrm{abik}} \tag{A.114}$$
$$-1. t^{\mathrm{cj}} v_{\mathrm{abcj}} t_h^{\mathrm{bi}} \lambda_{hp}^{\mathrm{aAiI}} \tag{A.115}$$
$$-0.5 t^{\mathrm{bi}} v_{\mathrm{abcI}} t_h^{\mathrm{cj}} \lambda_{hp}^{\mathrm{aAij}} \tag{A.116}$$
$$0.5 t^{\mathrm{aj}} v_{\mathrm{Acjk}} t_p^{\mathrm{bk}} t_h^{\mathrm{ci}} \lambda_{hp}^{\mathrm{abiI}} \tag{A.117}$$
$$-1. t^{\mathrm{ck}} v_{\mathrm{bcjk}} t_p^{\mathrm{aj}} t_h^{\mathrm{bi}} \lambda_{hp}^{\mathrm{aAiI}} \tag{A.118}$$
$$0.5 t^{\mathrm{bj}} v_{\mathrm{bciI}} t_p^{\mathrm{ai}} t_h^{\mathrm{ck}} \lambda_{hp}^{\mathrm{aAjk}} \tag{A.119}$$

$\lambda_b^j \langle {}_j^b | \bar{H} | {}_{IJ}^{AB} \rangle =$

$$-1.v_{\mathrm{aABJ}}\lambda_h^{\mathrm{aI}} \tag{A.120}$$
$$v_{\mathrm{aABI}}\lambda_h^{\mathrm{aJ}} \tag{A.121}$$
$$v_{\mathrm{AiIJ}}\lambda_p^{\mathrm{Bi}} \tag{A.122}$$
$$-1.v_{\mathrm{BiIJ}}\lambda_p^{\mathrm{Ai}} \tag{A.123}$$
$$v_{\mathrm{ABiJ}}\lambda_h^{\mathrm{aI}}t_p^{\mathrm{ai}} \tag{A.124}$$
$$-1.v_{\mathrm{ABiI}}\lambda_h^{\mathrm{aJ}}t_p^{\mathrm{ai}} \tag{A.125}$$
$$-1.v_{\mathrm{aAIJ}}t_h^{\mathrm{ai}}\lambda_p^{\mathrm{Bi}} \tag{A.126}$$
$$v_{\mathrm{aBIJ}}t_h^{\mathrm{ai}}\lambda_p^{\mathrm{Ai}} \tag{A.127}$$

$\lambda^{jk}_{bc}\langle^{bc}_{jk}|\bar{H}|^{AB}_{IJ}\rangle =$

$$1.f_{\mathrm{aB}}g_{\mathrm{iJ}}\lambda^{\mathrm{aAiI}}_{hp} \tag{A.128}$$
$$-1.f_{\mathrm{aA}}g_{\mathrm{iJ}}\lambda^{\mathrm{aBiI}}_{hp} \tag{A.129}$$
$$-1.g_{\mathrm{aB}}f_{\mathrm{iJ}}\lambda^{\mathrm{aAiI}}_{hp} \tag{A.130}$$
$$1.g_{\mathrm{aB}}f_{\mathrm{iI}}\lambda^{\mathrm{aAiJ}}_{hp} \tag{A.131}$$
$$-1.f_{\mathrm{Bj}}g_{\mathrm{iJ}}t^{\mathrm{aj}}_{p}\lambda^{\mathrm{aAiI}}_{hp} \tag{A.132}$$
$$1.f_{\mathrm{Aj}}g_{\mathrm{iJ}}t^{\mathrm{aj}}_{p}\lambda^{\mathrm{aBiI}}_{hp} \tag{A.133}$$
$$-1.f_{\mathrm{aJ}}g_{\mathrm{bB}}t^{\mathrm{ai}}_{h}\lambda^{\mathrm{AbiI}}_{hp} \tag{A.134}$$
$$1.f_{\mathrm{aI}}g_{\mathrm{bB}}t^{\mathrm{ai}}_{h}\lambda^{\mathrm{AbiJ}}_{hp} \tag{A.135}$$
$$0.5g_{\mathrm{aA}}g_{\mathrm{bB}}v_{\mathrm{iIjJ}}r^{\mathrm{abij}} \tag{A.136}$$
$$1.v_{\mathrm{aAiJ}}\lambda^{\mathrm{aBiI}}_{hp} \tag{A.137}$$
$$-1.v_{\mathrm{aAiI}}\lambda^{\mathrm{aBiJ}}_{hp} \tag{A.138}$$
$$-1.v_{\mathrm{aBiJ}}\lambda^{\mathrm{aAiI}}_{hp} \tag{A.139}$$
$$1.v_{\mathrm{aBiI}}\lambda^{\mathrm{aAiJ}}_{hp} \tag{A.140}$$
$$0.5g_{\mathrm{iI}}g_{\mathrm{jJ}}v_{\mathrm{aAbB}}r^{\mathrm{abij}} \tag{A.141}$$
$$0.25g_{\mathrm{bc}}g_{\mathrm{iJ}}v_{\mathrm{ABjk}}t^{\mathrm{acjk}}\lambda^{\mathrm{abiI}}_{hp} \tag{A.142}$$
$$-0.5g_{\mathrm{bc}}g_{\mathrm{ik}}v_{\mathrm{ABjJ}}t^{\mathrm{acjk}}\lambda^{\mathrm{abiI}}_{hp} \tag{A.143}$$
$$0.5g_{\mathrm{bc}}g_{\mathrm{ik}}v_{\mathrm{ABIj}}t^{\mathrm{acjk}}\lambda^{\mathrm{abiJ}}_{hp} \tag{A.144}$$
$$0.5g_{\mathrm{ab}}g_{\mathrm{iJ}}v_{\mathrm{Acjk}}t^{\mathrm{acjk}}\lambda^{\mathrm{bBiI}}_{hp} \tag{A.145}$$
$$-1.v_{\mathrm{AbjJ}}t^{\mathrm{abij}}_{hp}\lambda^{\mathrm{aBiI}}_{hp} \tag{A.146}$$
$$1.v_{\mathrm{AbIj}}t^{\mathrm{abij}}_{hp}\lambda^{\mathrm{aBiJ}}_{hp} \tag{A.147}$$
$$0.5g_{\mathrm{ab}}g_{\mathrm{jk}}v_{\mathrm{AcIJ}}t^{\mathrm{acij}}\lambda^{\mathrm{bBik}}_{hp} \tag{A.148}$$
$$-0.5g_{\mathrm{ab}}g_{\mathrm{iJ}}v_{\mathrm{Bcjk}}t^{\mathrm{acjk}}\lambda^{\mathrm{AbiI}}_{hp} \tag{A.149}$$
$$1.v_{\mathrm{bBjJ}}\lambda^{\mathrm{aAiI}}_{hp}t^{\mathrm{abij}}_{hp} \tag{A.150}$$
$$-1.v_{\mathrm{bBIj}}\lambda^{\mathrm{aAiJ}}_{hp}t^{\mathrm{abij}}_{hp} \tag{A.151}$$
$$-0.5g_{\mathrm{ab}}g_{\mathrm{jk}}v_{\mathrm{BcIJ}}t^{\mathrm{acij}}\lambda^{\mathrm{Abik}}_{hp} \tag{A.152}$$
$$-0.5g_{\mathrm{bB}}g_{\mathrm{ik}}v_{\mathrm{acjJ}}t^{\mathrm{acjk}}\lambda^{\mathrm{AbiI}}_{hp} \tag{A.153}$$
$$0.5g_{\mathrm{bB}}g_{\mathrm{ik}}v_{\mathrm{acIj}}t^{\mathrm{acjk}}\lambda^{\mathrm{AbiJ}}_{hp} \tag{A.154}$$

$$0.25 g_{\mathrm{bB}} g_{\mathrm{jk}} v_{\mathrm{acIJ}} t^{\mathrm{acij}} \lambda_{hp}^{\mathrm{Abik}} \tag{A.155}$$
$$-1. v_{\mathrm{AijJ}} t_{p}^{\mathrm{aj}} \lambda_{hp}^{\mathrm{aBiI}} \tag{A.156}$$
$$1. v_{\mathrm{AiIj}} t_{p}^{\mathrm{aj}} \lambda_{hp}^{\mathrm{aBiJ}} \tag{A.157}$$
$$1. v_{\mathrm{BijJ}} t_{p}^{\mathrm{aj}} \lambda_{hp}^{\mathrm{aAiI}} \tag{A.158}$$
$$-1. v_{\mathrm{BiIj}} t_{p}^{\mathrm{aj}} \lambda_{hp}^{\mathrm{aAiJ}} \tag{A.159}$$
$$-1. g_{\mathrm{bB}} t^{\mathrm{aj}} v_{\mathrm{aijJ}} \lambda_{hp}^{\mathrm{AbiI}} \tag{A.160}$$
$$1. g_{\mathrm{bB}} t^{\mathrm{aj}} v_{\mathrm{aiIj}} \lambda_{hp}^{\mathrm{AbiJ}} \tag{A.161}$$
$$0.5 g_{\mathrm{Ab}} t^{\mathrm{aj}} v_{\mathrm{aiIJ}} \lambda_{hp'}^{\mathrm{bBij}} \tag{A.162}$$
$$-0.5 g_{\mathrm{bB}} t^{\mathrm{ai}} v_{\mathrm{aIjJ}} \lambda_{hp}^{\mathrm{Abij}} \tag{A.163}$$
$$-0.5 g_{\mathrm{iJ}} t^{\mathrm{aj}} v_{\mathrm{AbBj}} \lambda_{hp}^{\mathrm{abiI}} \tag{A.164}$$
$$0.5 g_{\mathrm{iI}} t^{\mathrm{bj}} v_{\mathrm{aABj}} \lambda_{hp'}^{\mathrm{abiJ}} \tag{A.165}$$
$$1. g_{\mathrm{iJ}} t^{\mathrm{bj}} v_{\mathrm{aAbj}} \lambda_{hp}^{\mathrm{aBiI}} \tag{A.166}$$
$$-1. v_{\mathrm{aAbJ}} t_{h}^{\mathrm{bi}} \lambda_{hp}^{\mathrm{aBiI}} \tag{A.167}$$
$$1. v_{\mathrm{aAbI}} t_{h}^{\mathrm{bi}} \lambda_{hp}^{\mathrm{aBiJ}} \tag{A.168}$$
$$-1. g_{\mathrm{iJ}} t^{\mathrm{bj}} v_{\mathrm{abBj}} \lambda_{hp}^{\mathrm{aAiI}} \tag{A.169}$$
$$1. v_{\mathrm{abBJ}} t_{h}^{\mathrm{bi}} \lambda_{hp}^{\mathrm{aAiI}} \tag{A.170}$$
$$-1. v_{\mathrm{abBI}} t_{h}^{\mathrm{bi}} \lambda_{hp}^{\mathrm{aAiJ}} \tag{A.171}$$
$$0.5 g_{\mathrm{iJ}} t^{\mathrm{aj}} v_{\mathrm{ABjk}} t_{p}^{\mathrm{bk}} \lambda_{hp}^{\mathrm{abiI}} \tag{A.172}$$
$$1. g_{\mathrm{iJ}} t^{\mathrm{bk}} v_{\mathrm{Abjk}} t_{p}^{\mathrm{aj}} \lambda_{hp}^{\mathrm{aBiI}} \tag{A.173}$$
$$1. v_{\mathrm{AbjJ}} t_{p}^{\mathrm{aj}} t_{h}^{\mathrm{bi}} \lambda_{hp}^{\mathrm{aBiI}} \tag{A.174}$$
$$-1. v_{\mathrm{AbIj}} t_{p}^{\mathrm{aj}} t_{h}^{\mathrm{bi}} \lambda_{hp}^{\mathrm{aBiJ}} \tag{A.175}$$
$$-1. g_{\mathrm{iJ}} t^{\mathrm{bk}} v_{\mathrm{bBjk}} t_{p}^{\mathrm{aj}} \lambda_{hp}^{\mathrm{aAiI}} \tag{A.176}$$
$$-1. v_{\mathrm{bBjJ}} t_{p}^{\mathrm{aj}} t_{h}^{\mathrm{bi}} \lambda_{hp}^{\mathrm{aAiI}} \tag{A.177}$$
$$1. v_{\mathrm{bBIj}} t_{p}^{\mathrm{aj}} t_{h}^{\mathrm{bi}} \lambda_{hp}^{\mathrm{aAiJ}} \tag{A.178}$$
$$-1. g_{\mathrm{bB}} t^{\mathrm{cj}} v_{\mathrm{acjJ}} t_{h}^{\mathrm{ai}} \lambda_{hp}^{\mathrm{AbiI}} \tag{A.179}$$
$$1. g_{\mathrm{bB}} t^{\mathrm{cj}} v_{\mathrm{acIj}} t_{h}^{\mathrm{ai}} \lambda_{hp}^{\mathrm{AbiJ}} \tag{A.180}$$
$$0.5 g_{\mathrm{bB}} t^{\mathrm{ai}} v_{\mathrm{acIJ}} t_{h}^{\mathrm{cj}} \lambda_{hp}^{\mathrm{Abij}} \tag{A.181}$$

$r^{(1)}$ equations and intermediates

$\mathbf{H^{q0}_{AI}} =$

$$f_{\mathrm{AI}} \tag{A.182}$$
$$f_{\mathrm{ai}} t^{\mathrm{aAiI}}_{hp} \tag{A.183}$$
$$-1. f_{\mathrm{ai}} t^{\mathrm{aI}}_{h} t^{\mathrm{Ai}}_{p} \tag{A.184}$$
$$-0.5 g_{\mathrm{aA}} v_{\mathrm{biIj}} t^{\mathrm{abij}} \tag{A.185}$$
$$-0.5 g_{\mathrm{Ij}} v_{\mathrm{aAbi}} t^{\mathrm{abij}} \tag{A.186}$$
$$-1. t^{\mathrm{ai}} v_{\mathrm{aAiI}} \tag{A.187}$$
$$-1. t^{\mathrm{aj}} v_{\mathrm{aiIj}} t^{\mathrm{Ai}}_{p} \tag{A.188}$$
$$-0.5 g_{\mathrm{aA}} v_{\mathrm{bcij}} t^{\mathrm{acij}} t^{\mathrm{bI}}_{h} \tag{A.189}$$
$$t^{\mathrm{ai}} v_{\mathrm{abij}} t^{\mathrm{AbIj}}_{hp} \tag{A.190}$$
$$-0.5 g_{\mathrm{Ik}} v_{\mathrm{abij}} t^{\mathrm{abjk}} t^{\mathrm{Ai}}_{p} \tag{A.191}$$
$$-1. t^{\mathrm{bi}} v_{\mathrm{aAbi}} t^{\mathrm{aI}}_{h} \tag{A.192}$$
$$-1. t^{\mathrm{bj}} v_{\mathrm{abij}} t^{\mathrm{aI}}_{h} t^{\mathrm{Ai}}_{p} \tag{A.193}$$

$\mathbf{H^{q0}_{ABIJ}} =$

$$-1.g_{\mathrm{aB}}a_{\mathrm{IJ}}f_{\mathrm{bi}}t_{h}^{\mathrm{bJ}}t_{hp}^{\mathrm{aAiI}} \tag{A.194}$$
$$-1.f_{\mathrm{ai}}a_{\mathrm{AB}}g_{\mathrm{jJ}}t_{p}^{\mathrm{Bi}}t_{hp}^{\mathrm{aAIj}} \tag{A.195}$$
$$v_{\mathrm{ABIJ}} \tag{A.196}$$
$$0.5v_{\mathrm{iIjJ}}t_{pp}^{\mathrm{ABij}} \tag{A.197}$$
$$-1.a_{\mathrm{AB}}a_{\mathrm{IJ}}v_{\mathrm{aAiI}}t_{hp}^{\mathrm{aBiJ}} \tag{A.198}$$
$$0.5v_{\mathrm{aAbB}}t_{h}^{\mathrm{abIJ}} \tag{A.199}$$
$$a_{\mathrm{AB}}v_{\mathrm{AiIJ}}t_{p}^{\mathrm{Bi}} \tag{A.200}$$
$$a_{\mathrm{IJ}}v_{\mathrm{aABI}}t_{h}^{\mathrm{aJ}} \tag{A.201}$$
$$-1.a_{\mathrm{AB}}v_{\mathrm{abij}}t_{hp}^{\mathrm{aBiI}}t_{hp}^{\mathrm{AbjJ}} \tag{A.202}$$
$$0.25v_{\mathrm{abij}}t_{h}^{\mathrm{abIJ}}t_{pp}^{\mathrm{ABij}} \tag{A.203}$$
$$-0.5g_{\mathrm{aB}}g_{\mathrm{Jk}}v_{\mathrm{bcij}}t^{\mathrm{bcjk}}t_{hp}^{\mathrm{aAiI}} \tag{A.204}$$
$$-0.5g_{\mathrm{aB}}a_{\mathrm{AB}}g_{\mathrm{Jk}}v_{\mathrm{bcij}}t^{\mathrm{acij}}t_{hp}^{\mathrm{AbIk}} \tag{A.205}$$
$$-0.5g_{\mathrm{aB}}g_{\mathrm{Ik}}v_{\mathrm{bcij}}t^{\mathrm{bcik}}t_{hp}^{\mathrm{aAjJ}} \tag{A.206}$$
$$v_{\mathrm{iIjJ}}t_{p}^{\mathrm{Ai}}t_{p}^{\mathrm{Bj}} \tag{A.207}$$
$$a_{\mathrm{AB}}a_{\mathrm{IJ}}v_{\mathrm{aiIj}}t_{p}^{\mathrm{Bi}}t_{hp}^{\mathrm{aAjJ}} \tag{A.208}$$
$$0.5a_{\mathrm{IJ}}v_{\mathrm{aiIj}}t_{h}^{\mathrm{aJ}}t_{pp}^{\mathrm{ABij}} \tag{A.209}$$
$$-1.g_{\mathrm{aB}}a_{\mathrm{IJ}}t^{\mathrm{bi}}v_{\mathrm{biIj}}t_{hp}^{\mathrm{aAjJ}} \tag{A.210}$$
$$a_{\mathrm{AB}}a_{\mathrm{IJ}}v_{\mathrm{aAiI}}t_{h}^{\mathrm{aJ}}t_{p}^{\mathrm{Bi}} \tag{A.211}$$
$$0.5a_{\mathrm{AB}}v_{\mathrm{aAbi}}t_{p}^{\mathrm{Bi}}t_{h}^{\mathrm{abIJ}} \tag{A.212}$$
$$a_{\mathrm{AB}}a_{\mathrm{IJ}}v_{\mathrm{aAbi}}t_{h}^{\mathrm{aJ}}t_{hp}^{\mathrm{bBiI}} \tag{A.213}$$
$$-1.a_{\mathrm{AB}}g_{\mathrm{jJ}}t^{\mathrm{ai}}v_{\mathrm{aAbi}}t_{hp}^{\mathrm{bBIj}} \tag{A.214}$$
$$v_{\mathrm{aAbB}}t_{h}^{\mathrm{aI}}t_{h}^{\mathrm{bJ}} \tag{A.215}$$
$$a_{\mathrm{IJ}}v_{\mathrm{aiIj}}t_{h}^{\mathrm{aJ}}t_{p}^{\mathrm{Ai}}t_{p}^{\mathrm{Bj}} \tag{A.216}$$
$$0.5v_{\mathrm{abij}}t_{p}^{\mathrm{Ai}}t_{p}^{\mathrm{Bj}}t_{h}^{\mathrm{abIJ}} \tag{A.217}$$
$$-1.a_{\mathrm{AB}}a_{\mathrm{IJ}}v_{\mathrm{abij}}t_{h}^{\mathrm{aJ}}t_{p}^{\mathrm{Bi}}t_{hp}^{\mathrm{AbIj}} \tag{A.218}$$
$$-1.a_{\mathrm{AB}}g_{\mathrm{Jk}}t^{\mathrm{ai}}v_{\mathrm{abij}}t_{p}^{\mathrm{Bj}}t_{hp}^{\mathrm{AbIk}} \tag{A.219}$$
$$0.5v_{\mathrm{abij}}t_{h}^{\mathrm{aI}}t_{h}^{\mathrm{bJ}}t_{pp}^{\mathrm{ABij}} \tag{A.220}$$
$$g_{\mathrm{aB}}a_{\mathrm{IJ}}t^{\mathrm{ci}}v_{\mathrm{bcij}}t_{h}^{\mathrm{bJ}}t_{hp}^{\mathrm{aAIj}} \tag{A.221}$$
$$a_{\mathrm{AB}}v_{\mathrm{aAbi}}t_{h}^{\mathrm{aI}}t_{h}^{\mathrm{bJ}}t_{p}^{\mathrm{Bi}} \tag{A.222}$$
$$v_{\mathrm{abij}}t_{h}^{\mathrm{aI}}t_{p}^{\mathrm{Ai}}t_{h}^{\mathrm{bJ}}t_{p}^{\mathrm{Bj}} \tag{A.223}$$

$\langle {}^{A}_{I}|\bar{H}|{}^{a}_{i}\rangle r^{i}_{a} =$

$$f_{\mathrm{aA}} r_{h}^{\mathrm{aI}} \tag{A.224}$$
$$-1. f_{\mathrm{iI}} r_{p}^{\mathrm{Ai}} \tag{A.225}$$
$$-1. f_{\mathrm{ai}} r_{h}^{\mathrm{aI}} t_{p}^{\mathrm{Ai}} \tag{A.226}$$
$$-1. f_{\mathrm{ai}} t_{h}^{\mathrm{aI}} r_{p}^{\mathrm{Ai}} \tag{A.227}$$
$$-1. r^{\mathrm{ai}} v_{\mathrm{aAiI}} \tag{A.228}$$
$$-0.5 g_{\mathrm{aA}} v_{\mathrm{bcij}} t^{\mathrm{acij}} r_{h}^{\mathrm{bI}} \tag{A.229}$$
$$r^{\mathrm{ai}} v_{\mathrm{abij}} t_{hp}^{\mathrm{AbIj}} \tag{A.230}$$
$$-0.5 g_{\mathrm{Ik}} v_{\mathrm{abij}} t^{\mathrm{abjk}} r_{p}^{\mathrm{Ai}} \tag{A.231}$$
$$r^{\mathrm{ai}} v_{\mathrm{aiIj}} t_{p}^{\mathrm{Aj}} \tag{A.232}$$
$$-1. t^{\mathrm{aj}} v_{\mathrm{aiIj}} r_{p}^{\mathrm{Ai}} \tag{A.233}$$
$$-1. t^{\mathrm{bi}} v_{\mathrm{aAbi}} r_{h}^{\mathrm{aI}} \tag{A.234}$$
$$r^{\mathrm{ai}} v_{\mathrm{aAbi}} t_{h}^{\mathrm{bI}} \tag{A.235}$$
$$-1. t^{\mathrm{bj}} v_{\mathrm{abij}} r_{h}^{\mathrm{aI}} t_{p}^{\mathrm{Ai}} \tag{A.236}$$
$$-1. t^{\mathrm{bj}} v_{\mathrm{abij}} t_{h}^{\mathrm{aI}} r_{p}^{\mathrm{Ai}} \tag{A.237}$$
$$-1. r^{\mathrm{ai}} v_{\mathrm{abij}} t_{p}^{\mathrm{Aj}} t_{h}^{\mathrm{bI}} \tag{A.238}$$

$\langle {}^{A}_{I}|\bar{H}|{}^{bc}_{jk}\rangle r^{jk}_{bc} =$

$$1. f_{\mathrm{ai}} r_{hp}^{\mathrm{aAiI}} \tag{A.239}$$
$$-0.5 g_{\mathrm{aA}} v_{\mathrm{biIj}} r^{\mathrm{abij}} \tag{A.240}$$
$$-0.5 g_{\mathrm{Ij}} v_{\mathrm{aAbi}} r^{\mathrm{abij}} \tag{A.241}$$
$$0.5 g_{\mathrm{Ik}} v_{\mathrm{abij}} r^{\mathrm{abik}} t_{p}^{\mathrm{Aj}} \tag{A.242}$$
$$1. t^{\mathrm{bj}} v_{\mathrm{abij}} r_{hp}^{\mathrm{aAiI}} \tag{A.243}$$
$$0.5 g_{\mathrm{aA}} v_{\mathrm{bcij}} r^{\mathrm{abij}} t_{h}^{\mathrm{cI}} \tag{A.244}$$

$\langle {}^{AB}_{IJ}|\bar{H}|^{b}_{j}\rangle r^{j}_{b} =$

$$-1.g_{\mathrm{aB}}a_{\mathrm{IJ}}f_{\mathrm{bi}}r^{\mathrm{bJ}}_{h}t^{\mathrm{aAiI}}_{hp} \tag{A.245}$$
$$-1.f_{\mathrm{ai}}a_{\mathrm{AB}}g_{\mathrm{jJ}}r^{\mathrm{Bi}}_{p}t^{\mathrm{aAIj}}_{hp} \tag{A.246}$$
$$a_{\mathrm{AB}}v_{\mathrm{AiIJ}}r^{\mathrm{Bi}}_{p} \tag{A.247}$$
$$a_{\mathrm{IJ}}v_{\mathrm{aABI}}r^{\mathrm{aJ}}_{h} \tag{A.248}$$
$$a_{\mathrm{AB}}a_{\mathrm{IJ}}v_{\mathrm{aiIj}}r^{\mathrm{Bi}}_{p}t^{\mathrm{aAjJ}}_{hp} \tag{A.249}$$
$$0.5a_{\mathrm{IJ}}v_{\mathrm{aiIj}}r^{\mathrm{aJ}}_{h}t^{\mathrm{ABij}}_{pp} \tag{A.250}$$
$$-1.g_{\mathrm{aB}}a_{\mathrm{IJ}}r^{\mathrm{bi}}v_{\mathrm{biIj}}t^{\mathrm{aAjJ}}_{hp} \tag{A.251}$$
$$0.5a_{\mathrm{AB}}v_{\mathrm{aAbi}}r^{\mathrm{Bi}}_{p}t^{\mathrm{abIJ}}_{h} \tag{A.252}$$
$$a_{\mathrm{AB}}a_{\mathrm{IJ}}v_{\mathrm{aAbi}}r^{\mathrm{aJ}}_{h}t^{\mathrm{bBiI}}_{hp} \tag{A.253}$$
$$-1.a_{\mathrm{AB}}g_{\mathrm{jJ}}r^{\mathrm{ai}}v_{\mathrm{aAbi}}t^{\mathrm{bBIj}}_{hp} \tag{A.254}$$
$$-1.a_{\mathrm{AB}}v_{\mathrm{iIjJ}}t^{\mathrm{Aj}}_{p}r^{\mathrm{Bi}}_{p} \tag{A.255}$$
$$a_{\mathrm{AB}}a_{\mathrm{IJ}}v_{\mathrm{aAiI}}t^{\mathrm{aJ}}_{h}r^{\mathrm{Bi}}_{p} \tag{A.256}$$
$$a_{\mathrm{AB}}a_{\mathrm{IJ}}v_{\mathrm{aAiI}}r^{\mathrm{aJ}}_{h}t^{\mathrm{Bi}}_{p} \tag{A.257}$$
$$-1.a_{\mathrm{IJ}}v_{\mathrm{aAbB}}r^{\mathrm{aJ}}_{h}t^{\mathrm{bI}}_{h} \tag{A.258}$$
$$-1.a_{\mathrm{AB}}a_{\mathrm{IJ}}v_{\mathrm{aiIj}}t^{\mathrm{aJ}}_{h}t^{\mathrm{Aj}}_{p}r^{\mathrm{Bi}}_{p} \tag{A.259}$$
$$a_{\mathrm{IJ}}v_{\mathrm{aiIj}}r^{\mathrm{aJ}}_{h}t^{\mathrm{Ai}}_{p}t^{\mathrm{Bj}}_{p} \tag{A.260}$$
$$-0.5a_{\mathrm{AB}}v_{\mathrm{abij}}t^{\mathrm{Aj}}_{p}r^{\mathrm{Bi}}_{p}t^{\mathrm{abIJ}}_{h} \tag{A.261}$$
$$-1.a_{\mathrm{AB}}a_{\mathrm{IJ}}v_{\mathrm{abij}}t^{\mathrm{aJ}}_{h}r^{\mathrm{Bi}}_{p}t^{\mathrm{AbIj}}_{hp} \tag{A.262}$$
$$-1.a_{\mathrm{AB}}a_{\mathrm{IJ}}v_{\mathrm{abij}}r^{\mathrm{aJ}}_{h}t^{\mathrm{Bi}}_{p}t^{\mathrm{AbIj}}_{hp} \tag{A.263}$$
$$a_{\mathrm{AB}}g_{\mathrm{Jk}}t^{\mathrm{aj}}v_{\mathrm{abij}}r^{\mathrm{Bi}}_{p}t^{\mathrm{AbIk}}_{hp} \tag{A.264}$$
$$-1.a_{\mathrm{AB}}g_{\mathrm{Jk}}r^{\mathrm{ai}}v_{\mathrm{abij}}t^{\mathrm{Bj}}_{p}t^{\mathrm{AbIk}}_{hp} \tag{A.265}$$
$$-0.5a_{\mathrm{IJ}}v_{\mathrm{abij}}r^{\mathrm{aJ}}_{h}t^{\mathrm{bI}}_{h}t^{\mathrm{ABij}}_{pp} \tag{A.266}$$
$$g_{\mathrm{aB}}a_{\mathrm{IJ}}t^{\mathrm{ci}}v_{\mathrm{bcij}}r^{\mathrm{bJ}}_{h}t^{\mathrm{aAIj}}_{hp} \tag{A.267}$$
$$-1.g_{\mathrm{aB}}a_{\mathrm{IJ}}r^{\mathrm{bi}}v_{\mathrm{bcij}}t^{\mathrm{cJ}}_{h}t^{\mathrm{aAIj}}_{hp} \tag{A.268}$$
$$a_{\mathrm{AB}}v_{\mathrm{aAbi}}t^{\mathrm{aI}}_{h}t^{\mathrm{bJ}}_{h}r^{\mathrm{Bi}}_{p} \tag{A.269}$$
$$-1.a_{\mathrm{AB}}a_{\mathrm{IJ}}v_{\mathrm{aAbi}}r^{\mathrm{aJ}}_{h}t^{\mathrm{bI}}_{h}t^{\mathrm{Bi}}_{p} \tag{A.270}$$
$$-1.a_{\mathrm{AB}}v_{\mathrm{abij}}t^{\mathrm{aI}}_{h}t^{\mathrm{Aj}}_{p}t^{\mathrm{bJ}}_{h}r^{\mathrm{Bi}}_{p} \tag{A.271}$$
$$-1.a_{\mathrm{IJ}}v_{\mathrm{abij}}r^{\mathrm{aJ}}_{h}t^{\mathrm{Ai}}_{p}t^{\mathrm{bI}}_{h}t^{\mathrm{Bj}}_{p} \tag{A.272}$$

$\langle {}^{AB}_{IJ}|\bar{H}|^{bc}_{jk}\rangle r^{jk}_{bc} =$

$$-1.g_{\mathrm{aB}}a_{\mathrm{IJ}}f_{\mathrm{iJ}}r^{\mathrm{aAiI}}_{hp} \tag{A.273}$$
$$1.f_{\mathrm{aB}}a_{\mathrm{AB}}g_{\mathrm{iJ}}r^{\mathrm{aAiI}}_{hp} \tag{A.274}$$
$$1.g_{\mathrm{aB}}a_{\mathrm{IJ}}f_{\mathrm{bi}}t^{\mathrm{bI}}_{h}r^{\mathrm{aAiJ}}_{hp} \tag{A.275}$$
$$1.f_{\mathrm{ai}}a_{\mathrm{AB}}g_{\mathrm{jJ}}t^{\mathrm{Ai}}_{p}r^{\mathrm{aBIj}}_{hp} \tag{A.276}$$
$$0.5g_{\mathrm{aA}}g_{\mathrm{bB}}v_{\mathrm{iIjJ}}r^{\mathrm{abij}} \tag{A.277}$$
$$-1.a_{\mathrm{AB}}a_{\mathrm{IJ}}v_{\mathrm{aAiI}}r^{\mathrm{aBiJ}}_{hp} \tag{A.278}$$
$$0.5g_{\mathrm{iI}}g_{\mathrm{jJ}}v_{\mathrm{aAbB}}r^{\mathrm{abij}} \tag{A.279}$$
$$1.a_{\mathrm{AB}}a_{\mathrm{IJ}}v_{\mathrm{abij}}r^{\mathrm{aBiJ}}_{hp}t^{\mathrm{AbIj}}_{hp} \tag{A.280}$$
$$0.25g_{\mathrm{Ik}}g_{\mathrm{Jl}}v_{\mathrm{abij}}r^{\mathrm{abkl}}t^{\mathrm{ABij}}_{pp} \tag{A.281}$$
$$-0.5g_{\mathrm{aB}}a_{\mathrm{AB}}g_{\mathrm{Jk}}v_{\mathrm{bcij}}t^{\mathrm{acij}}r^{\mathrm{AbIk}}_{hp} \tag{A.282}$$
$$-0.5g_{\mathrm{aB}}a_{\mathrm{IJ}}g_{\mathrm{Jk}}v_{\mathrm{bcij}}t^{\mathrm{bcjk}}r^{\mathrm{aAiI}}_{hp} \tag{A.283}$$
$$0.5g_{\mathrm{aB}}a_{\mathrm{IJ}}g_{\mathrm{Jk}}v_{\mathrm{bcij}}r^{\mathrm{bcik}}t^{\mathrm{aAIj}}_{hp} \tag{A.284}$$
$$0.5g_{\mathrm{aB}}a_{\mathrm{AB}}g_{\mathrm{Jk}}v_{\mathrm{bcij}}r^{\mathrm{abij}}t^{\mathrm{AcIk}}_{hp} \tag{A.285}$$
$$0.25g_{\mathrm{aA}}g_{\mathrm{bB}}v_{\mathrm{cdij}}r^{\mathrm{abij}}t^{\mathrm{cdIJ}}_{h} \tag{A.286}$$
$$1.a_{\mathrm{AB}}a_{\mathrm{IJ}}v_{\mathrm{aiIj}}t^{\mathrm{Aj}}_{p}r^{\mathrm{aBiJ}}_{hp} \tag{A.287}$$
$$1.g_{\mathrm{aB}}a_{\mathrm{IJ}}t^{\mathrm{bj}}v_{\mathrm{biIj}}r^{\mathrm{aAiJ}}_{hp} \tag{A.288}$$
$$0.5g_{\mathrm{aA}}a_{\mathrm{IJ}}g_{\mathrm{bB}}v_{\mathrm{ciIj}}r^{\mathrm{abij}}t^{\mathrm{cJ}}_{h} \tag{A.289}$$
$$1.a_{\mathrm{AB}}g_{\mathrm{jJ}}t^{\mathrm{bi}}v_{\mathrm{aAbi}}r^{\mathrm{aBIj}}_{hp} \tag{A.290}$$
$$0.5a_{\mathrm{AB}}g_{\mathrm{Ij}}g_{\mathrm{Jk}}v_{\mathrm{aAbi}}r^{\mathrm{abjk}}t^{\mathrm{Bi}}_{p} \tag{A.291}$$
$$1.a_{\mathrm{AB}}a_{\mathrm{IJ}}v_{\mathrm{aAbi}}t^{\mathrm{bI}}_{h}r^{\mathrm{aBiJ}}_{hp} \tag{A.292}$$
$$1.a_{\mathrm{AB}}g_{\mathrm{Jk}}t^{\mathrm{bj}}v_{\mathrm{abij}}t^{\mathrm{Ai}}_{p}r^{\mathrm{aBIk}}_{hp} \tag{A.293}$$
$$-1.a_{\mathrm{AB}}a_{\mathrm{IJ}}v_{\mathrm{abij}}t^{\mathrm{Aj}}_{p}t^{\mathrm{bI}}_{h}r^{\mathrm{aBiJ}}_{hp} \tag{A.294}$$
$$0.5g_{\mathrm{Ik}}g_{\mathrm{Jl}}v_{\mathrm{abij}}r^{\mathrm{abkl}}t^{\mathrm{Ai}}_{p}t^{\mathrm{Bj}}_{p} \tag{A.295}$$
$$1.g_{\mathrm{aB}}a_{\mathrm{IJ}}t^{\mathrm{cj}}v_{\mathrm{bcij}}t^{\mathrm{bI}}_{h}r^{\mathrm{aAiJ}}_{hp} \tag{A.296}$$
$$0.5g_{\mathrm{aA}}g_{\mathrm{bB}}v_{\mathrm{cdij}}r^{\mathrm{abij}}t^{\mathrm{cI}}_{h}t^{\mathrm{dJ}}_{h} \tag{A.297}$$

A24 binding energies

complex / model	$\{ijab\}$	$\{ijab\}+\{i\}\{a\}$	$\{ia\}\{jb\}$	$\{ia\}\{jb\}+\{i\}\{a\}$	$\{i\}\{j\}\{a\}\{b\}$	MP2	CCSD
01	-5.13	-5.82	-5.34	-6.04	-6.41	-6.95	-6.47
02	-4.12	-4.56	-4.28	-4.71	-4.95	-5.24	-5.00
03	-4.63	-4.85	-4.74	-4.97	-5.16	-5.63	-5.23
04	-3.82	-4.25	-3.94	-4.37	-4.55	-4.61	-4.56
05	-2.50	-2.70	-2.66	-2.86	-3.08	-3.38	-3.09
06	-1.32	-1.40	-1.45	-1.54	-1.65	-1.86	-1.69
07	-0.75	-0.84	-0.84	-0.92	-1.03	-1.14	-1.05
08	-0.64	-0.69	-0.71	-0.75	-0.83	-0.92	-0.84
09	-3.03	-3.58	-3.25	-3.82	-4.38	-4.82	-4.37
10	-2.10	-2.30	-2.26	-2.46	-2.65	-3.21	-2.73
11	-1.42	-1.49	-1.56	-1.63	-1.84	-2.18	-1.86
12	-1.60	-1.70	-1.70	-1.80	-1.90	-2.35	-2.00
13	-1.28	-1.38	-1.40	-1.49	-1.62	-2.05	-1.69
14	-1.02	-1.09	-1.18	-1.25	-1.40	-1.97	-1.49
15	-0.60	-0.63	-0.67	-0.71	-0.82	-1.01	-0.83
16	-0.58	-0.78	-0.87	-1.08	-1.32	-1.73	-1.42
17	-0.87	-0.87	-1.03	-1.03	-1.12	-1.40	-1.20
18	-0.74	-0.74	-0.87	-0.87	-0.96	-1.11	-0.99
19	-0.64	-0.63	-0.74	-0.74	-0.83	-0.95	-0.84
20	-0.31	-0.31	-0.36	-0.37	-0.41	-0.56	-0.47
21	-0.16	-0.17	-0.20	-0.21	-0.26	-0.45	-0.30
22	1.07	1.10	0.97	1.00	0.81	0.13	0.77
23	1.10	1.13	0.97	1.00	0.76	0.14	0.73
24	1.39	1.42	1.31	1.34	1.18	0.46	1.15

Table A.1: A24 binding energies in kJ/mol for fully-non-orthogonal truncation models and canonical MP2 and CCSD computed in aug-cc-pvdz. The horizontal lines delineate hydrogen-bonded, mixed-character, and dispersion-dominated interactions.

Appendix B

STPT(2) triples and quadruples matrix elements

Occupied and virtual orbitals are indexed $(i, j, k, l, I, J, K, L...)$ and $(a, b, c, d, A, B, C, D...)$, respectively, with upper-case indices implying external hole/particle excitations and lower-case (internal) indices implying summation. The operator $a_{\rm pq}$ is an antisymmetrizer, e.g., $a_{\rm pq}X_{pqrs} = X_{pqrs} - X_{qprs}$. The tensors f_{pq} and v_{pqrs} are the Fock and antisymmerized integrals, respectively. t, λ, r are the cluster, left, and first-order right amplitudes. The following intermediates are used in the expressions below.

$$X_h^{\rm aI} = X^{\rm aj} g_{\rm jI} \tag{B.1}$$
$$X_p^{\rm Ai} = g_{\rm Ab} X^{\rm bi} \tag{B.2}$$
$$X_h^{\rm abIJ} = g_{\rm Ij} X^{\rm abjJ} \tag{B.3}$$
$$X_{pp}^{\rm ABij} = g_{\rm Aa} g_{\rm Bb} X^{\rm abij} \tag{B.4}$$
$$X_{hp}^{\rm bBiI} = g_{\rm ij} g_{\rm bc} X^{\rm cBjI} \tag{B.5}$$
$$X_{hp'}^{\rm bBiI} = g_{\rm Ij} g_{\rm Bc} X^{\rm bcij} \tag{B.6}$$
$$X_{hph}^{\rm bcij} = g_{\rm jk} X_{hp}^{\rm bcik} \tag{B.7}$$
$$X_{hpp}^{\rm bcij} = g_{\rm ca} X_{hp}^{\rm baij} \tag{B.8}$$

triples

$\langle {}_I^A | \bar{H} \hat{r}_t^{(1)} | 0 \rangle =$

$$0.25 g_{\rm Ik} v_{\rm abij} r^{\rm aAbijk} \tag{B.9}$$

$\langle {}^{AB}_{IJ}|\bar{H}\hat{r}_t^{(1)}|0\rangle =$

$$1.g_{\mathrm{aB}}f_{\mathrm{bi}}g_{\mathrm{jJ}}r_{\mathrm{hp}}^{\mathrm{aAbiIj}} \tag{B.10}$$

$$1.g_{\mathrm{aB}}f_{\mathrm{bi}}g_{\mathrm{jJ}}r_{\mathrm{hp}}^{\mathrm{aAbiIj}} \tag{B.11}$$

$$0.5g_{\mathrm{aB}}a_{\mathrm{IJ}}v_{\mathrm{biIj}}r_{\mathrm{hp}}^{\mathrm{aAbijJ}} \tag{B.12}$$

$$-0.5a_{\mathrm{AB}}g_{\mathrm{Jk}}v_{\mathrm{abij}}t_p^{\mathrm{Aj}}r_{\mathrm{hp}}^{\mathrm{abBiIk}} \tag{B.13}$$

$$1.g_{\mathrm{aB}}g_{\mathrm{Jk}}t^{\mathrm{cj}}v_{\mathrm{bcij}}r_{\mathrm{hp}}^{\mathrm{aAbiIk}} \tag{B.14}$$

$$-0.5g_{\mathrm{aB}}a_{\mathrm{IJ}}v_{\mathrm{bcij}}t_h^{\mathrm{cI}}r_{\mathrm{hp}}^{\mathrm{aAbijJ}} \tag{B.15}$$

$$0.5a_{\mathrm{AB}}g_{\mathrm{jJ}}v_{\mathrm{aAbi}}r_{\mathrm{hp}}^{\mathrm{abBiIj}} \tag{B.16}$$

$\langle {}^{ABC}_{IJK}|\bar{H}|0\rangle =$

$$f_{\mathrm{ai}} a_{\mathrm{IJ}} t_{\mathrm{hph}}^{\mathrm{aCJK}} t_{\mathrm{hpp}}^{\mathrm{ABiI}} \tag{B.17}$$
$$-1. f_{\mathrm{ai}} a_{\mathrm{AB}} a_{\mathrm{IJ}} t_{\mathrm{hph}}^{\mathrm{aBJK}} t_{\mathrm{hpp}}^{\mathrm{ACiI}} \tag{B.18}$$
$$f_{\mathrm{ai}} t_{\mathrm{hph}}^{\mathrm{aCIJ}} t_{\mathrm{hpp}}^{\mathrm{ABiK}} \tag{B.19}$$
$$-1. f_{\mathrm{ai}} a_{\mathrm{AB}} t_{\mathrm{hph}}^{\mathrm{aBIJ}} t_{\mathrm{hpp}}^{\mathrm{ACiK}} \tag{B.20}$$
$$f_{\mathrm{ai}} a_{\mathrm{IJ}} t_{\mathrm{hph}}^{\mathrm{aCJK}} t_{\mathrm{hpp}}^{\mathrm{ABiI}} \tag{B.21}$$
$$-1. f_{\mathrm{ai}} a_{\mathrm{AB}} a_{\mathrm{IJ}} t_{\mathrm{hph}}^{\mathrm{aBJK}} t_{\mathrm{hpp}}^{\mathrm{ACiI}} \tag{B.22}$$
$$f_{\mathrm{ai}} t_{\mathrm{hph}}^{\mathrm{aCIJ}} t_{\mathrm{hpp}}^{\mathrm{ABiK}} \tag{B.23}$$
$$-1. f_{\mathrm{ai}} a_{\mathrm{AB}} t_{\mathrm{hph}}^{\mathrm{aBIJ}} t_{\mathrm{hpp}}^{\mathrm{ACiK}} \tag{B.24}$$
$$-1. v_{\mathrm{iIjJ}} t_{p}^{\mathrm{Ci}} t_{\mathrm{hpp}}^{\mathrm{ABjK}} \tag{B.25}$$
$$a_{\mathrm{AB}} v_{\mathrm{iIjJ}} t_{p}^{\mathrm{Bi}} t_{\mathrm{hpp}}^{\mathrm{ACjK}} \tag{B.26}$$
$$a_{\mathrm{IJ}} v_{\mathrm{iIjK}} t_{p}^{\mathrm{Ci}} t_{\mathrm{hpp}}^{\mathrm{ABjJ}} \tag{B.27}$$
$$-1. a_{\mathrm{AB}} a_{\mathrm{IJ}} v_{\mathrm{iIjK}} t_{p}^{\mathrm{Bi}} t_{\mathrm{hpp}}^{\mathrm{ACjJ}} \tag{B.28}$$
$$-1. a_{\mathrm{AB}} a_{\mathrm{IJ}} v_{\mathrm{aiIj}} t_{p}^{\mathrm{Bi}} t_{p}^{\mathrm{Cj}} t_{\mathrm{hph}}^{\mathrm{aAJK}} \tag{B.29}$$
$$-1. a_{\mathrm{IJ}} v_{\mathrm{aiIj}} t_{p}^{\mathrm{Ai}} t_{p}^{\mathrm{Bj}} t_{\mathrm{hph}}^{\mathrm{aCJK}} \tag{B.30}$$
$$a_{\mathrm{IJ}} v_{\mathrm{aiIj}} t_{\mathrm{hp}}^{\mathrm{aCjK}} t_{\mathrm{hpp}}^{\mathrm{ABiJ}} \tag{B.31}$$
$$-1. a_{\mathrm{AB}} a_{\mathrm{IJ}} v_{\mathrm{aiIj}} t_{\mathrm{hp}}^{\mathrm{aBjK}} t_{\mathrm{hpp}}^{\mathrm{ACiJ}} \tag{B.32}$$
$$a_{\mathrm{IJ}} v_{\mathrm{aiIj}} t_{h}^{\mathrm{aK}} t_{p}^{\mathrm{Ci}} t_{\mathrm{hpp}}^{\mathrm{ABjJ}} \tag{B.33}$$
$$-1. a_{\mathrm{AB}} a_{\mathrm{IJ}} v_{\mathrm{aiIj}} t_{h}^{\mathrm{aK}} t_{p}^{\mathrm{Bi}} t_{\mathrm{hpp}}^{\mathrm{ACjJ}} \tag{B.34}$$
$$-1. a_{\mathrm{IJ}} v_{\mathrm{aiIj}} t_{h}^{\mathrm{aJ}} t_{p}^{\mathrm{Ci}} t_{\mathrm{hpp}}^{\mathrm{ABjK}} \tag{B.35}$$
$$a_{\mathrm{IJ}} v_{\mathrm{aiIj}} t_{\mathrm{hp}}^{\mathrm{aCiJ}} t_{\mathrm{hpp}}^{\mathrm{ABjK}} \tag{B.36}$$
$$a_{\mathrm{AB}} a_{\mathrm{IJ}} v_{\mathrm{aiIj}} t_{h}^{\mathrm{aJ}} t_{p}^{\mathrm{Bi}} t_{\mathrm{hpp}}^{\mathrm{ACjK}} \tag{B.37}$$
$$-1. a_{\mathrm{AB}} a_{\mathrm{IJ}} v_{\mathrm{aiIj}} t_{\mathrm{hp}}^{\mathrm{aBiJ}} t_{\mathrm{hpp}}^{\mathrm{ACjK}} \tag{B.38}$$
$$-0.5 a_{\mathrm{IJ}} v_{\mathrm{aiIj}} t_{\mathrm{hph}}^{\mathrm{aCJK}} t_{\mathrm{pp}}^{\mathrm{ABij}} \tag{B.39}$$
$$0.5 a_{\mathrm{AB}} a_{\mathrm{IJ}} v_{\mathrm{aiIj}} t_{\mathrm{hph}}^{\mathrm{aBJK}} t_{\mathrm{pp}}^{\mathrm{ACij}} \tag{B.40}$$
$$-1. a_{\mathrm{AB}} v_{\mathrm{aijK}} t_{p}^{\mathrm{Bi}} t_{p}^{\mathrm{Cj}} t_{\mathrm{hph}}^{\mathrm{aAIJ}} \tag{B.41}$$
$$-1. v_{\mathrm{aijK}} t_{p}^{\mathrm{Ai}} t_{p}^{\mathrm{Bj}} t_{\mathrm{hph}}^{\mathrm{aCIJ}} \tag{B.42}$$
$$v_{\mathrm{aijK}} t_{\mathrm{hp}}^{\mathrm{aCjJ}} t_{\mathrm{hpp}}^{\mathrm{ABiI}} \tag{B.43}$$
$$-1. a_{\mathrm{AB}} v_{\mathrm{aijK}} t_{\mathrm{hp}}^{\mathrm{aBjJ}} t_{\mathrm{hpp}}^{\mathrm{ACiI}} \tag{B.44}$$
$$a_{\mathrm{IJ}} v_{\mathrm{aijK}} t_{h}^{\mathrm{aJ}} t_{p}^{\mathrm{Ci}} t_{\mathrm{hpp}}^{\mathrm{ABIj}} \tag{B.45}$$
$$-1. a_{\mathrm{AB}} a_{\mathrm{IJ}} v_{\mathrm{aijK}} t_{h}^{\mathrm{aJ}} t_{p}^{\mathrm{Bi}} t_{\mathrm{hpp}}^{\mathrm{ACIj}} \tag{B.46}$$

$$v_{\mathrm{aijK}} t_{\mathrm{hp}}^{\mathrm{aCiI}} t_{\mathrm{hpp}}^{\mathrm{ABjJ}} \tag{B.47}$$

$$-1.a_{\mathrm{AB}} v_{\mathrm{aijK}} t_{\mathrm{hp}}^{\mathrm{aBiI}} t_{\mathrm{hpp}}^{\mathrm{ACjJ}} \tag{B.48}$$

$$-0.5 v_{\mathrm{aijK}} t_{\mathrm{hph}}^{\mathrm{aCIJ}} t_{\mathrm{pp}}^{\mathrm{ABij}} \tag{B.49}$$

$$0.5 a_{\mathrm{AB}} v_{\mathrm{aijK}} t_{\mathrm{hph}}^{\mathrm{aBIJ}} t_{\mathrm{pp}}^{\mathrm{ACij}} \tag{B.50}$$

$$a_{\mathrm{AB}} a_{\mathrm{JK}} v_{\mathrm{abij}} t_{p}^{\mathrm{Ci}} t_{\mathrm{hph}}^{\mathrm{aAIJ}} t_{\mathrm{hp}}^{\mathrm{bBjK}} \tag{B.51}$$

$$-1.a_{\mathrm{AB}} a_{\mathrm{JK}} v_{\mathrm{abij}} t_{p}^{\mathrm{Bi}} t_{\mathrm{hph}}^{\mathrm{aAIJ}} t_{\mathrm{hp}}^{\mathrm{bCjK}} \tag{B.52}$$

$$-1.a_{\mathrm{AB}} v_{\mathrm{abij}} t_{h}^{\mathrm{aK}} t_{p}^{\mathrm{Bi}} t_{p}^{\mathrm{Cj}} t_{\mathrm{hph}}^{\mathrm{AbIJ}} \tag{B.53}$$

$$a_{\mathrm{AB}} a_{\mathrm{JK}} v_{\mathrm{abij}} t_{p}^{\mathrm{Bi}} t_{\mathrm{hph}}^{\mathrm{aCIJ}} t_{\mathrm{hp}}^{\mathrm{AbjK}} \tag{B.54}$$

$$-1.v_{\mathrm{abij}} t_{h}^{\mathrm{aK}} t_{p}^{\mathrm{Ai}} t_{p}^{\mathrm{Bj}} t_{\mathrm{hph}}^{\mathrm{bCIJ}} \tag{B.55}$$

$$a_{\mathrm{AB}} a_{\mathrm{IJ}} v_{\mathrm{abij}} t_{h}^{\mathrm{aJ}} t_{p}^{\mathrm{Bi}} t_{p}^{\mathrm{Cj}} t_{\mathrm{hph}}^{\mathrm{AbIK}} \tag{B.56}$$

$$a_{\mathrm{IJ}} v_{\mathrm{abij}} t_{h}^{\mathrm{aJ}} t_{p}^{\mathrm{Ai}} t_{p}^{\mathrm{Bj}} t_{\mathrm{hph}}^{\mathrm{bCIK}} \tag{B.57}$$

$$-1.a_{\mathrm{AB}} v_{\mathrm{abij}} t_{p}^{\mathrm{Ci}} t_{\mathrm{hp}}^{\mathrm{aBIj}} t_{\mathrm{hph}}^{\mathrm{AbJK}} \tag{B.58}$$

$$a_{\mathrm{AB}} v_{\mathrm{abij}} t_{p}^{\mathrm{Bi}} t_{\mathrm{hp}}^{\mathrm{aCIj}} t_{\mathrm{hph}}^{\mathrm{AbJK}} \tag{B.59}$$

$$-1.a_{\mathrm{AB}} v_{\mathrm{abij}} t_{p}^{\mathrm{Bi}} t_{\mathrm{hp}}^{\mathrm{aAIj}} t_{\mathrm{hph}}^{\mathrm{bCJK}} \tag{B.60}$$

$$v_{\mathrm{abij}} t_{h}^{\mathrm{aK}} t_{\mathrm{hpp}}^{\mathrm{ABiI}} t_{\mathrm{hp}}^{\mathrm{bCjJ}} \tag{B.61}$$

$$-1.a_{\mathrm{IJ}} v_{\mathrm{abij}} t_{h}^{\mathrm{aJ}} t_{\mathrm{hpp}}^{\mathrm{ABiI}} t_{\mathrm{hp}}^{\mathrm{bCjK}} \tag{B.62}$$

$$-1.a_{\mathrm{AB}} v_{\mathrm{abij}} t_{h}^{\mathrm{aK}} t_{\mathrm{hpp}}^{\mathrm{ACiI}} t_{\mathrm{hp}}^{\mathrm{bBjJ}} \tag{B.63}$$

$$a_{\mathrm{AB}} a_{\mathrm{IJ}} v_{\mathrm{abij}} t_{h}^{\mathrm{aJ}} t_{\mathrm{hpp}}^{\mathrm{ACiI}} t_{\mathrm{hp}}^{\mathrm{bBjK}} \tag{B.64}$$

$$-1.a_{\mathrm{IJ}} v_{\mathrm{abij}} t_{h}^{\mathrm{aJ}} t_{h}^{\mathrm{bK}} t_{p}^{\mathrm{Ci}} t_{\mathrm{hpp}}^{\mathrm{ABIj}} \tag{B.65}$$

$$-0.5 a_{\mathrm{IJ}} v_{\mathrm{abij}} t_{p}^{\mathrm{Ci}} t_{h}^{\mathrm{abJK}} t_{\mathrm{hpp}}^{\mathrm{ABIj}} \tag{B.66}$$

$$a_{\mathrm{IJ}} t^{\mathrm{ai}} v_{\mathrm{abij}} t_{\mathrm{hpp}}^{\mathrm{ABIj}} t_{\mathrm{hph}}^{\mathrm{bCJK}} \tag{B.67}$$

$$a_{\mathrm{AB}} a_{\mathrm{IJ}} v_{\mathrm{abij}} t_{h}^{\mathrm{aJ}} t_{h}^{\mathrm{bK}} t_{p}^{\mathrm{Bi}} t_{\mathrm{hpp}}^{\mathrm{ACIj}} \tag{B.68}$$

$$0.5 a_{\mathrm{AB}} a_{\mathrm{IJ}} v_{\mathrm{abij}} t_{p}^{\mathrm{Bi}} t_{h}^{\mathrm{abJK}} t_{\mathrm{hpp}}^{\mathrm{ACIj}} \tag{B.69}$$

$$-1.a_{\mathrm{AB}} a_{\mathrm{IJ}} t^{\mathrm{ai}} v_{\mathrm{abij}} t_{\mathrm{hpp}}^{\mathrm{ACIj}} t_{\mathrm{hph}}^{\mathrm{bBJK}} \tag{B.70}$$

$$v_{\mathrm{abij}} t_{h}^{\mathrm{aK}} t_{\mathrm{hpp}}^{\mathrm{ABjJ}} t_{\mathrm{hp}}^{\mathrm{bCiI}} \tag{B.71}$$

$$-1.a_{\mathrm{AB}} v_{\mathrm{abij}} t_{h}^{\mathrm{aK}} t_{\mathrm{hpp}}^{\mathrm{ACjJ}} t_{\mathrm{hp}}^{\mathrm{bBiI}} \tag{B.72}$$

$$-1.v_{\mathrm{abij}} t_{h}^{\mathrm{aI}} t_{h}^{\mathrm{bJ}} t_{p}^{\mathrm{Ci}} t_{\mathrm{hpp}}^{\mathrm{ABjK}} \tag{B.73}$$

$$-0.5 v_{\mathrm{abij}} t_{p}^{\mathrm{Ci}} t_{h}^{\mathrm{abIJ}} t_{\mathrm{hpp}}^{\mathrm{ABjK}} \tag{B.74}$$

$$-1.a_{\mathrm{IJ}} v_{\mathrm{abij}} t_{h}^{\mathrm{aJ}} t_{\mathrm{hpp}}^{\mathrm{ABjK}} t_{\mathrm{hp}}^{\mathrm{bCiI}} \tag{B.75}$$

$$t^{\mathrm{ai}} v_{\mathrm{abij}} t_{\mathrm{hpp}}^{\mathrm{ABjK}} t_{\mathrm{hph}}^{\mathrm{bCIJ}} \tag{B.76}$$

$$a_{\mathrm{AB}} v_{\mathrm{abij}} t_{h}^{\mathrm{aI}} t_{h}^{\mathrm{bJ}} t_{p}^{\mathrm{Bi}} t_{\mathrm{hpp}}^{\mathrm{ACjK}} \tag{B.77}$$

$$0.5a_{\mathrm{AB}}v_{\mathrm{abij}}t_{p}^{\mathrm{Bi}}t_{h}^{\mathrm{abIJ}}t_{\mathrm{hpp}}^{\mathrm{ACjK}} \tag{B.78}$$

$$a_{\mathrm{AB}}a_{\mathrm{IJ}}v_{\mathrm{abij}}t_{h}^{\mathrm{aJ}}t_{\mathrm{hpp}}^{\mathrm{ACjK}}t_{\mathrm{hp}}^{\mathrm{bBiI}} \tag{B.79}$$

$$-1.a_{\mathrm{AB}}t^{\mathrm{ai}}v_{\mathrm{abij}}t_{\mathrm{hpp}}^{\mathrm{ACjK}}t_{\mathrm{hph}}^{\mathrm{bBIJ}} \tag{B.80}$$

$$-0.5v_{\mathrm{abij}}t_{h}^{\mathrm{aK}}t_{\mathrm{pp}}^{\mathrm{ABij}}t_{\mathrm{hph}}^{\mathrm{bCIJ}} \tag{B.81}$$

$$0.5a_{\mathrm{IJ}}v_{\mathrm{abij}}t_{h}^{\mathrm{aJ}}t_{\mathrm{pp}}^{\mathrm{ABij}}t_{\mathrm{hph}}^{\mathrm{bCIK}} \tag{B.82}$$

$$0.5a_{\mathrm{AB}}v_{\mathrm{abij}}t_{h}^{\mathrm{aK}}t_{\mathrm{pp}}^{\mathrm{ACij}}t_{\mathrm{hph}}^{\mathrm{bBIJ}} \tag{B.83}$$

$$-0.5a_{\mathrm{AB}}a_{\mathrm{IJ}}v_{\mathrm{abij}}t_{h}^{\mathrm{aJ}}t_{\mathrm{pp}}^{\mathrm{ACij}}t_{\mathrm{hph}}^{\mathrm{bBIK}} \tag{B.84}$$

$$-1.a_{\mathrm{AB}}v_{\mathrm{AiIJ}}t_{\mathrm{hpp}}^{\mathrm{BCiK}} \tag{B.85}$$

$$a_{\mathrm{AB}}a_{\mathrm{IJ}}v_{\mathrm{AiIK}}t_{\mathrm{hpp}}^{\mathrm{BCiJ}} \tag{B.86}$$

$$a_{\mathrm{AB}}a_{\mathrm{IJ}}v_{\mathrm{aAiI}}t_{p}^{\mathrm{Ci}}t_{\mathrm{hph}}^{\mathrm{aBJK}} \tag{B.87}$$

$$-1.a_{\mathrm{AB}}a_{\mathrm{IJ}}v_{\mathrm{aAiI}}t_{p}^{\mathrm{Bi}}t_{\mathrm{hph}}^{\mathrm{aCJK}} \tag{B.88}$$

$$a_{\mathrm{AB}}a_{\mathrm{IJ}}v_{\mathrm{aAiI}}t_{h}^{\mathrm{aK}}t_{\mathrm{hpp}}^{\mathrm{BCiJ}} \tag{B.89}$$

$$-1.a_{\mathrm{AB}}a_{\mathrm{IJ}}v_{\mathrm{aAiI}}t_{h}^{\mathrm{aJ}}t_{\mathrm{hpp}}^{\mathrm{BCiK}} \tag{B.90}$$

$$a_{\mathrm{AB}}v_{\mathrm{aAiK}}t_{p}^{\mathrm{Ci}}t_{\mathrm{hph}}^{\mathrm{aBIJ}} \tag{B.91}$$

$$-1.a_{\mathrm{AB}}v_{\mathrm{aAiK}}t_{p}^{\mathrm{Bi}}t_{\mathrm{hph}}^{\mathrm{aCIJ}} \tag{B.92}$$

$$a_{\mathrm{AB}}a_{\mathrm{IJ}}v_{\mathrm{aAiK}}t_{h}^{\mathrm{aJ}}t_{\mathrm{hpp}}^{\mathrm{BCiI}} \tag{B.93}$$

$$a_{\mathrm{AB}}a_{\mathrm{JK}}v_{\mathrm{aAbi}}t_{\mathrm{hph}}^{\mathrm{aBIJ}}t_{\mathrm{hp}}^{\mathrm{bCiK}} \tag{B.94}$$

$$a_{\mathrm{AB}}v_{\mathrm{aAbi}}t_{h}^{\mathrm{aK}}t_{p}^{\mathrm{Ci}}t_{\mathrm{hph}}^{\mathrm{bBIJ}} \tag{B.95}$$

$$-1.a_{\mathrm{AB}}a_{\mathrm{JK}}v_{\mathrm{aAbi}}t_{\mathrm{hph}}^{\mathrm{aCIJ}}t_{\mathrm{hp}}^{\mathrm{bBiK}} \tag{B.96}$$

$$-1.a_{\mathrm{AB}}v_{\mathrm{aAbi}}t_{h}^{\mathrm{aK}}t_{p}^{\mathrm{Bi}}t_{\mathrm{hph}}^{\mathrm{bCIJ}} \tag{B.97}$$

$$-1.a_{\mathrm{AB}}a_{\mathrm{IJ}}v_{\mathrm{aAbi}}t_{h}^{\mathrm{aJ}}t_{p}^{\mathrm{Ci}}t_{\mathrm{hph}}^{\mathrm{bBIK}} \tag{B.98}$$

$$a_{\mathrm{AB}}a_{\mathrm{IJ}}v_{\mathrm{aAbi}}t_{h}^{\mathrm{aJ}}t_{p}^{\mathrm{Bi}}t_{\mathrm{hph}}^{\mathrm{bCIK}} \tag{B.99}$$

$$-1.a_{\mathrm{AB}}v_{\mathrm{aAbi}}t_{\mathrm{hp}}^{\mathrm{aCiI}}t_{\mathrm{hph}}^{\mathrm{bBJK}} \tag{B.100}$$

$$a_{\mathrm{AB}}v_{\mathrm{aAbi}}t_{\mathrm{hp}}^{\mathrm{aBiI}}t_{\mathrm{hph}}^{\mathrm{bCJK}} \tag{B.101}$$

$$-1.a_{\mathrm{AB}}a_{\mathrm{IJ}}v_{\mathrm{aAbi}}t_{h}^{\mathrm{aJ}}t_{h}^{\mathrm{bK}}t_{\mathrm{hpp}}^{\mathrm{BCiI}} \tag{B.102}$$

$$-0.5a_{\mathrm{AB}}a_{\mathrm{IJ}}v_{\mathrm{aAbi}}t_{h}^{\mathrm{abJK}}t_{\mathrm{hpp}}^{\mathrm{BCiI}} \tag{B.103}$$

$$-1.a_{\mathrm{AB}}v_{\mathrm{aAbi}}t_{h}^{\mathrm{aI}}t_{h}^{\mathrm{bJ}}t_{\mathrm{hpp}}^{\mathrm{BCiK}} \tag{B.104}$$

$$-0.5a_{\mathrm{AB}}v_{\mathrm{aAbi}}t_{h}^{\mathrm{abIJ}}t_{\mathrm{hpp}}^{\mathrm{BCiK}} \tag{B.105}$$

$$-1.v_{\mathrm{CiIJ}}t_{\mathrm{hpp}}^{\mathrm{ABiK}} \tag{B.106}$$

$$a_{\mathrm{IJ}}v_{\mathrm{CiIK}}t_{\mathrm{hpp}}^{\mathrm{ABiJ}} \tag{B.107}$$

$$a_{\mathrm{AB}} a_{\mathrm{IJ}} v_{\mathrm{aCiI}} t_{p}^{\mathrm{Bi}} t_{\mathrm{hph}}^{\mathrm{aAJK}} \tag{B.108}$$

$$a_{\mathrm{IJ}} v_{\mathrm{aCiI}} t_{h}^{\mathrm{aK}} t_{\mathrm{hpp}}^{\mathrm{ABiJ}} \tag{B.109}$$

$$-1. a_{\mathrm{IJ}} v_{\mathrm{aCiI}} t_{h}^{\mathrm{aJ}} t_{\mathrm{hpp}}^{\mathrm{ABiK}} \tag{B.110}$$

$$a_{\mathrm{AB}} v_{\mathrm{aCiK}} t_{p}^{\mathrm{Bi}} t_{\mathrm{hph}}^{\mathrm{aAIJ}} \tag{B.111}$$

$$a_{\mathrm{IJ}} v_{\mathrm{aCiK}} t_{h}^{\mathrm{aJ}} t_{\mathrm{hpp}}^{\mathrm{ABiI}} \tag{B.112}$$

$$a_{\mathrm{AB}} a_{\mathrm{JK}} v_{\mathrm{abCi}} t_{\mathrm{hph}}^{\mathrm{aAIJ}} t_{\mathrm{hp}}^{\mathrm{bBiK}} \tag{B.113}$$

$$a_{\mathrm{AB}} v_{\mathrm{abCi}} t_{h}^{\mathrm{aK}} t_{p}^{\mathrm{Bi}} t_{\mathrm{hph}}^{\mathrm{AbIJ}} \tag{B.114}$$

$$-1. a_{\mathrm{AB}} a_{\mathrm{IJ}} v_{\mathrm{abCi}} t_{h}^{\mathrm{aJ}} t_{p}^{\mathrm{Bi}} t_{\mathrm{hph}}^{\mathrm{AbIK}} \tag{B.115}$$

$$-1. a_{\mathrm{AB}} v_{\mathrm{abCi}} t_{\mathrm{hp}}^{\mathrm{aBiI}} t_{\mathrm{hph}}^{\mathrm{AbJK}} \tag{B.116}$$

$$-1. a_{\mathrm{IJ}} v_{\mathrm{abCi}} t_{h}^{\mathrm{aJ}} t_{h}^{\mathrm{bK}} t_{\mathrm{hpp}}^{\mathrm{ABiI}} \tag{B.117}$$

$$-0.5 a_{\mathrm{IJ}} v_{\mathrm{abCi}} t_{h}^{\mathrm{abJK}} t_{\mathrm{hpp}}^{\mathrm{ABiI}} \tag{B.118}$$

$$-1. v_{\mathrm{abCi}} t_{h}^{\mathrm{aI}} t_{h}^{\mathrm{bJ}} t_{\mathrm{hpp}}^{\mathrm{ABiK}} \tag{B.119}$$

$$-0.5 v_{\mathrm{abCi}} t_{h}^{\mathrm{abIJ}} t_{\mathrm{hpp}}^{\mathrm{ABiK}} \tag{B.120}$$

$$-1. a_{\mathrm{IJ}} v_{\mathrm{aABI}} t_{\mathrm{hph}}^{\mathrm{aCJK}} \tag{B.121}$$

$$-1. v_{\mathrm{aABK}} t_{\mathrm{hph}}^{\mathrm{aCIJ}} \tag{B.122}$$

$$-1. v_{\mathrm{aAbB}} t_{h}^{\mathrm{aK}} t_{\mathrm{hph}}^{\mathrm{bCIJ}} \tag{B.123}$$

$$a_{\mathrm{IJ}} v_{\mathrm{aAbB}} t_{h}^{\mathrm{aJ}} t_{\mathrm{hph}}^{\mathrm{bCIK}} \tag{B.124}$$

$$a_{\mathrm{AB}} a_{\mathrm{IJ}} v_{\mathrm{aACI}} t_{\mathrm{hph}}^{\mathrm{aBJK}} \tag{B.125}$$

$$a_{\mathrm{AB}} v_{\mathrm{aACK}} t_{\mathrm{hph}}^{\mathrm{aBIJ}} \tag{B.126}$$

$$a_{\mathrm{AB}} v_{\mathrm{aAbC}} t_{h}^{\mathrm{aK}} t_{\mathrm{hph}}^{\mathrm{bBIJ}} \tag{B.127}$$

$$-1. a_{\mathrm{AB}} a_{\mathrm{IJ}} v_{\mathrm{aAbC}} t_{h}^{\mathrm{aJ}} t_{\mathrm{hph}}^{\mathrm{bBIK}} \tag{B.128}$$

$\langle {}^{ABC}_{IJK}|\bar{H}\hat{r}_t^{(1)}|0\rangle =$

$$1.g_{\mathrm{aB}}f_{\mathrm{bC}}g_{\mathrm{iJ}}g_{\mathrm{jK}}r_{\mathrm{hp}}^{\mathrm{aAbiIj}} \tag{B.129}$$
$$-1.g_{\mathrm{aC}}a_{\mathrm{AB}}f_{\mathrm{bB}}g_{\mathrm{iJ}}g_{\mathrm{jK}}r_{\mathrm{hp}}^{\mathrm{aAbiIj}} \tag{B.130}$$
$$-1.g_{\mathrm{aB}}g_{\mathrm{bC}}f_{\mathrm{iK}}g_{\mathrm{jJ}}r_{\mathrm{hp}}^{\mathrm{aAbiIj}} \tag{B.131}$$
$$1.g_{\mathrm{aB}}a_{\mathrm{IJ}}g_{\mathrm{bC}}f_{\mathrm{iJ}}g_{\mathrm{jK}}r_{\mathrm{hp}}^{\mathrm{aAbiIj}} \tag{B.132}$$
$$-1.g_{\mathrm{aB}}a_{\mathrm{IJ}}g_{\mathrm{bC}}f_{\mathrm{ci}}g_{\mathrm{jK}}t_h^{\mathrm{cI}}r_{\mathrm{hp}}^{\mathrm{aAbijJ}} \tag{B.133}$$
$$-1.g_{\mathrm{aB}}g_{\mathrm{bC}}f_{\mathrm{ci}}g_{\mathrm{jJ}}t_h^{\mathrm{cK}}r_{\mathrm{hp}}^{\mathrm{aAbiIj}} \tag{B.134}$$
$$-1.g_{\mathrm{aC}}a_{\mathrm{AB}}f_{\mathrm{bi}}g_{\mathrm{jJ}}g_{\mathrm{kK}}t_p^{\mathrm{Ai}}r_{\mathrm{hp}}^{\mathrm{abBIjk}} \tag{B.135}$$
$$-1.g_{\mathrm{aB}}f_{\mathrm{bi}}g_{\mathrm{jJ}}g_{\mathrm{kK}}t_p^{\mathrm{Ci}}r_{\mathrm{hp}}^{\mathrm{aAbIjk}} \tag{B.136}$$
$$1.g_{\mathrm{aB}}f_{\mathrm{bC}}g_{\mathrm{iJ}}g_{\mathrm{jK}}r_{\mathrm{hp}}^{\mathrm{aAbiIj}} \tag{B.137}$$
$$-1.g_{\mathrm{aC}}a_{\mathrm{AB}}f_{\mathrm{bB}}g_{\mathrm{iJ}}g_{\mathrm{jK}}r_{\mathrm{hp}}^{\mathrm{aAbiIj}} \tag{B.138}$$
$$-1.g_{\mathrm{aB}}g_{\mathrm{bC}}f_{\mathrm{iK}}g_{\mathrm{jJ}}r_{\mathrm{hp}}^{\mathrm{aAbiIj}} \tag{B.139}$$
$$1.g_{\mathrm{aB}}a_{\mathrm{IJ}}g_{\mathrm{bC}}f_{\mathrm{iJ}}g_{\mathrm{jK}}r_{\mathrm{hp}}^{\mathrm{aAbiIj}} \tag{B.140}$$
$$-1.g_{\mathrm{aB}}a_{\mathrm{IJ}}g_{\mathrm{bC}}f_{\mathrm{ci}}g_{\mathrm{jK}}t_h^{\mathrm{cI}}r_{\mathrm{hp}}^{\mathrm{aAbijJ}} \tag{B.141}$$
$$-1.g_{\mathrm{aB}}g_{\mathrm{bC}}f_{\mathrm{ci}}g_{\mathrm{jJ}}t_h^{\mathrm{cK}}r_{\mathrm{hp}}^{\mathrm{aAbiIj}} \tag{B.142}$$
$$-1.g_{\mathrm{aC}}a_{\mathrm{AB}}f_{\mathrm{bi}}g_{\mathrm{jJ}}g_{\mathrm{kK}}t_p^{\mathrm{Ai}}r_{\mathrm{hp}}^{\mathrm{abBIjk}} \tag{B.143}$$
$$-1.g_{\mathrm{aB}}f_{\mathrm{bi}}g_{\mathrm{jJ}}g_{\mathrm{kK}}t_p^{\mathrm{Ci}}r_{\mathrm{hp}}^{\mathrm{aAbIjk}} \tag{B.144}$$
$$0.5g_{\mathrm{aB}}g_{\mathrm{bC}}v_{\mathrm{iIjJ}}r_{\mathrm{hp}}^{\mathrm{aAbijK}} \tag{B.145}$$
$$-0.5g_{\mathrm{aB}}a_{\mathrm{IJ}}g_{\mathrm{bC}}v_{\mathrm{iIjK}}r_{\mathrm{hp}}^{\mathrm{aAbijJ}} \tag{B.146}$$
$$1.g_{\mathrm{aC}}a_{\mathrm{AB}}a_{\mathrm{IJ}}g_{\mathrm{kK}}v_{\mathrm{biIj}}t_p^{\mathrm{Aj}}r_{\mathrm{hp}}^{\mathrm{abBiJk}} \tag{B.147}$$
$$1.g_{\mathrm{aB}}a_{\mathrm{IJ}}g_{\mathrm{kK}}v_{\mathrm{biIj}}t_p^{\mathrm{Cj}}r_{\mathrm{hp}}^{\mathrm{aAbiJk}} \tag{B.148}$$
$$-1.g_{\mathrm{aB}}a_{\mathrm{IJ}}g_{\mathrm{bC}}g_{\mathrm{kK}}t^{\mathrm{cj}}v_{\mathrm{ciIj}}r_{\mathrm{hp}}^{\mathrm{aAbiJk}} \tag{B.149}$$
$$0.5g_{\mathrm{aB}}a_{\mathrm{IJ}}g_{\mathrm{bC}}v_{\mathrm{ciIj}}t_h^{\mathrm{cJ}}r_{\mathrm{hp}}^{\mathrm{aAbijK}} \tag{B.150}$$
$$-0.5g_{\mathrm{aB}}a_{\mathrm{IJ}}g_{\mathrm{bC}}v_{\mathrm{ciIj}}t_h^{\mathrm{cK}}r_{\mathrm{hp}}^{\mathrm{aAbijJ}} \tag{B.151}$$
$$1.g_{\mathrm{aC}}a_{\mathrm{AB}}g_{\mathrm{Jk}}v_{\mathrm{bijK}}t_p^{\mathrm{Aj}}r_{\mathrm{hp}}^{\mathrm{abBiIk}} \tag{B.152}$$
$$1.g_{\mathrm{aB}}g_{\mathrm{Jk}}v_{\mathrm{bijK}}t_p^{\mathrm{Cj}}r_{\mathrm{hp}}^{\mathrm{aAbiIk}} \tag{B.153}$$
$$-1.g_{\mathrm{aB}}g_{\mathrm{bC}}g_{\mathrm{Jk}}t^{\mathrm{cj}}v_{\mathrm{cijK}}r_{\mathrm{hp}}^{\mathrm{aAbiIk}} \tag{B.154}$$
$$0.5g_{\mathrm{aB}}a_{\mathrm{IJ}}g_{\mathrm{bC}}v_{\mathrm{cijK}}t_h^{\mathrm{cI}}r_{\mathrm{hp}}^{\mathrm{aAbijJ}} \tag{B.155}$$
$$0.5g_{\mathrm{Jk}}g_{\mathrm{Kl}}v_{\mathrm{abij}}t_p^{\mathrm{Ai}}t_p^{\mathrm{Bj}}r_{\mathrm{hp}}^{\mathrm{abCIkl}} \tag{B.156}$$
$$-0.5a_{\mathrm{AB}}g_{\mathrm{Jk}}g_{\mathrm{Kl}}v_{\mathrm{abij}}t_p^{\mathrm{Ai}}t_p^{\mathrm{Cj}}r_{\mathrm{hp}}^{\mathrm{abBIkl}} \tag{B.157}$$
$$-0.5a_{\mathrm{IJ}}g_{\mathrm{kK}}v_{\mathrm{abij}}t_{\mathrm{hpp}}^{\mathrm{ABIj}}r_{\mathrm{hp}}^{\mathrm{abCiJk}} \tag{B.158}$$

$$0.5a_{\mathrm{AB}}a_{\mathrm{IJ}}g_{\mathrm{kK}}v_{\mathrm{abij}}t_{\mathrm{hpp}}^{\mathrm{ACIj}}r_{\mathrm{hp}}^{\mathrm{abBiJk}} \tag{B.159}$$

$$-0.5g_{\mathrm{Jk}}v_{\mathrm{abij}}t_{\mathrm{hpp}}^{\mathrm{ABjK}}r_{\mathrm{hp}}^{\mathrm{abCiIk}} \tag{B.160}$$

$$0.5a_{\mathrm{AB}}g_{\mathrm{Jk}}v_{\mathrm{abij}}t_{\mathrm{hpp}}^{\mathrm{ACjK}}r_{\mathrm{hp}}^{\mathrm{abBiIk}} \tag{B.161}$$

$$0.25g_{\mathrm{Jk}}g_{\mathrm{Kl}}v_{\mathrm{abij}}t_{\mathrm{pp}}^{\mathrm{ABij}}r_{\mathrm{hp}}^{\mathrm{abCIkl}} \tag{B.162}$$

$$-0.25a_{\mathrm{AB}}g_{\mathrm{Jk}}g_{\mathrm{Kl}}v_{\mathrm{abij}}t_{\mathrm{pp}}^{\mathrm{ACij}}r_{\mathrm{hp}}^{\mathrm{abBIkl}} \tag{B.163}$$

$$-1.g_{\mathrm{aC}}a_{\mathrm{AB}}g_{\mathrm{Jk}}g_{\mathrm{Kl}}t^{\mathrm{cj}}v_{\mathrm{bcij}}t_{p}^{\mathrm{Ai}}r_{\mathrm{hp}}^{\mathrm{abBIkl}} \tag{B.164}$$

$$-1.g_{\mathrm{aC}}a_{\mathrm{AB}}a_{\mathrm{IJ}}g_{\mathrm{kK}}v_{\mathrm{bcij}}t_{p}^{\mathrm{Aj}}t_{h}^{\mathrm{cI}}r_{\mathrm{hp}}^{\mathrm{abBiJk}} \tag{B.165}$$

$$-1.g_{\mathrm{aC}}a_{\mathrm{AB}}g_{\mathrm{Jk}}v_{\mathrm{bcij}}t_{p}^{\mathrm{Aj}}t_{h}^{\mathrm{cK}}r_{\mathrm{hp}}^{\mathrm{abBiIk}} \tag{B.166}$$

$$-1.g_{\mathrm{aB}}g_{\mathrm{Jk}}g_{\mathrm{Kl}}t^{\mathrm{cj}}v_{\mathrm{bcij}}t_{p}^{\mathrm{Ci}}r_{\mathrm{hp}}^{\mathrm{aAbIkl}} \tag{B.167}$$

$$-1.g_{\mathrm{aB}}a_{\mathrm{IJ}}g_{\mathrm{kK}}v_{\mathrm{bcij}}t_{h}^{\mathrm{cI}}t_{p}^{\mathrm{Cj}}r_{\mathrm{hp}}^{\mathrm{aAbiJk}} \tag{B.168}$$

$$-1.g_{\mathrm{aB}}g_{\mathrm{Jk}}v_{\mathrm{bcij}}t_{h}^{\mathrm{cK}}t_{p}^{\mathrm{Cj}}r_{\mathrm{hp}}^{\mathrm{aAbiIk}} \tag{B.169}$$

$$1.g_{\mathrm{aC}}a_{\mathrm{AB}}a_{\mathrm{IJ}}g_{\mathrm{kK}}v_{\mathrm{bcij}}t_{\mathrm{hp}}^{\mathrm{AcIj}}r_{\mathrm{hp}}^{\mathrm{abBiJk}} \tag{B.170}$$

$$1.g_{\mathrm{aB}}a_{\mathrm{IJ}}g_{\mathrm{kK}}v_{\mathrm{bcij}}t_{\mathrm{hp}}^{\mathrm{cCIj}}r_{\mathrm{hp}}^{\mathrm{aAbiJk}} \tag{B.171}$$

$$1.g_{\mathrm{aC}}a_{\mathrm{AB}}g_{\mathrm{Jk}}v_{\mathrm{bcij}}t_{\mathrm{hp}}^{\mathrm{AcjK}}r_{\mathrm{hp}}^{\mathrm{abBiIk}} \tag{B.172}$$

$$1.g_{\mathrm{aB}}g_{\mathrm{Jk}}v_{\mathrm{bcij}}t_{\mathrm{hp}}^{\mathrm{cCjK}}r_{\mathrm{hp}}^{\mathrm{aAbiIk}} \tag{B.173}$$

$$-0.5g_{\mathrm{aC}}a_{\mathrm{AB}}v_{\mathrm{bcij}}t_{\mathrm{hph}}^{\mathrm{AcIJ}}r_{\mathrm{hp}}^{\mathrm{abBijK}} \tag{B.174}$$

$$-0.5g_{\mathrm{aB}}v_{\mathrm{bcij}}t_{\mathrm{hph}}^{\mathrm{cCIJ}}r_{\mathrm{hp}}^{\mathrm{aAbijK}} \tag{B.175}$$

$$0.5g_{\mathrm{aC}}a_{\mathrm{AB}}a_{\mathrm{IJ}}v_{\mathrm{bcij}}t_{\mathrm{hph}}^{\mathrm{AcIK}}r_{\mathrm{hp}}^{\mathrm{abBijJ}} \tag{B.176}$$

$$0.5g_{\mathrm{aB}}a_{\mathrm{IJ}}v_{\mathrm{bcij}}t_{\mathrm{hph}}^{\mathrm{cCIK}}r_{\mathrm{hp}}^{\mathrm{aAbijJ}} \tag{B.177}$$

$$-1.g_{\mathrm{aB}}a_{\mathrm{IJ}}g_{\mathrm{bC}}g_{\mathrm{kK}}t^{\mathrm{dj}}v_{\mathrm{cdij}}t_{h}^{\mathrm{cI}}r_{\mathrm{hp}}^{\mathrm{aAbiJk}} \tag{B.178}$$

$$-1.g_{\mathrm{aB}}g_{\mathrm{bC}}g_{\mathrm{Jk}}t^{\mathrm{dj}}v_{\mathrm{cdij}}t_{h}^{\mathrm{cK}}r_{\mathrm{hp}}^{\mathrm{aAbiIk}} \tag{B.179}$$

$$0.5g_{\mathrm{aB}}g_{\mathrm{bC}}v_{\mathrm{cdij}}t_{h}^{\mathrm{cI}}t_{h}^{\mathrm{dJ}}r_{\mathrm{hp}}^{\mathrm{aAbijK}} \tag{B.180}$$

$$-0.5g_{\mathrm{aB}}a_{\mathrm{IJ}}g_{\mathrm{bC}}v_{\mathrm{cdij}}t_{h}^{\mathrm{cI}}t_{h}^{\mathrm{dK}}r_{\mathrm{hp}}^{\mathrm{aAbijJ}} \tag{B.181}$$

$$0.5g_{\mathrm{aB}}a_{\mathrm{AB}}g_{\mathrm{bC}}g_{\mathrm{Jk}}g_{\mathrm{Kl}}v_{\mathrm{cdij}}t^{\mathrm{adij}}r_{\mathrm{hp}}^{\mathrm{AbcIkl}} \tag{B.182}$$

$$-0.5g_{\mathrm{aB}}g_{\mathrm{bC}}g_{\mathrm{Jk}}g_{\mathrm{Kl}}v_{\mathrm{cdij}}t^{\mathrm{bdij}}r_{\mathrm{hp}}^{\mathrm{aAcIkl}} \tag{B.183}$$

$$-0.5g_{\mathrm{aB}}g_{\mathrm{bC}}g_{\mathrm{Jl}}g_{\mathrm{kK}}v_{\mathrm{cdij}}t^{\mathrm{cdjk}}r_{\mathrm{hp}}^{\mathrm{aAbiIl}} \tag{B.184}$$

$$0.5g_{\mathrm{aB}}a_{\mathrm{IJ}}g_{\mathrm{bC}}g_{\mathrm{Jk}}g_{\mathrm{Kl}}v_{\mathrm{cdij}}t^{\mathrm{cdjk}}r_{\mathrm{hp}}^{\mathrm{aAbiIl}} \tag{B.185}$$

$$0.25g_{\mathrm{aB}}g_{\mathrm{bC}}v_{\mathrm{cdij}}t_{h}^{\mathrm{cdIJ}}r_{\mathrm{hp}}^{\mathrm{aAbijK}} \tag{B.186}$$

$$-0.25g_{\mathrm{aB}}a_{\mathrm{IJ}}g_{\mathrm{bC}}v_{\mathrm{cdij}}t_{h}^{\mathrm{cdIK}}r_{\mathrm{hp}}^{\mathrm{aAbijJ}} \tag{B.187}$$

$$-1.g_{\mathrm{aC}}a_{\mathrm{AB}}a_{\mathrm{IJ}}g_{\mathrm{jK}}v_{\mathrm{AbiI}}r_{\mathrm{hp}}^{\mathrm{abBijJ}} \tag{B.188}$$

$$-1.g_{\mathrm{aC}}a_{\mathrm{AB}}g_{\mathrm{jJ}}v_{\mathrm{AbiK}}r_{\mathrm{hp}}^{\mathrm{abBiIj}} \tag{B.189}$$

$$0.5a_{\mathrm{AB}}g_{\mathrm{jJ}}g_{\mathrm{kK}}v_{\mathrm{aAbi}}t_{p}^{\mathrm{Bi}}r_{\mathrm{hp}}^{\mathrm{abCIjk}} \tag{B.190}$$

$$-0.5a_{\mathrm{AB}}g_{\mathrm{jJ}}g_{\mathrm{kK}}v_{\mathrm{aAbi}}t_{p}^{\mathrm{Ci}}r_{\mathrm{hp}}^{\mathrm{abBIjk}} \tag{B.191}$$

$$-1.g_{\mathrm{aC}}a_{\mathrm{AB}}g_{\mathrm{jJ}}g_{\mathrm{kK}}t^{\mathrm{ci}}v_{\mathrm{Abci}}r_{\mathrm{hp}}^{\mathrm{abBIjk}} \tag{B.192}$$

$$1.g_{\mathrm{aC}}a_{\mathrm{AB}}a_{\mathrm{IJ}}g_{\mathrm{jK}}v_{\mathrm{Abci}}t_{h}^{\mathrm{cI}}r_{\mathrm{hp}}^{\mathrm{abBijJ}} \tag{B.193}$$

$$1.g_{\mathrm{aC}}a_{\mathrm{AB}}g_{\mathrm{jJ}}v_{\mathrm{Abci}}t_{h}^{\mathrm{cK}}r_{\mathrm{hp}}^{\mathrm{abBiIj}} \tag{B.194}$$

$$-1.g_{\mathrm{aB}}a_{\mathrm{IJ}}g_{\mathrm{jK}}v_{\mathrm{bCiI}}r_{\mathrm{hp}}^{\mathrm{aAbijJ}} \tag{B.195}$$

$$-1.g_{\mathrm{aB}}g_{\mathrm{jJ}}v_{\mathrm{bCiK}}r_{\mathrm{hp}}^{\mathrm{aAbiIj}} \tag{B.196}$$

$$0.5a_{\mathrm{AB}}g_{\mathrm{jJ}}g_{\mathrm{kK}}v_{\mathrm{abCi}}t_{p}^{\mathrm{Ai}}r_{\mathrm{hp}}^{\mathrm{abBIjk}} \tag{B.197}$$

$$-1.g_{\mathrm{aB}}g_{\mathrm{jJ}}g_{\mathrm{kK}}t^{\mathrm{ci}}v_{\mathrm{bcCi}}r_{\mathrm{hp}}^{\mathrm{aAbIjk}} \tag{B.198}$$

$$1.g_{\mathrm{aB}}a_{\mathrm{IJ}}g_{\mathrm{jK}}v_{\mathrm{bcCi}}t_{h}^{\mathrm{cI}}r_{\mathrm{hp}}^{\mathrm{aAbijJ}} \tag{B.199}$$

$$1.g_{\mathrm{aB}}g_{\mathrm{jJ}}v_{\mathrm{bcCi}}t_{h}^{\mathrm{cK}}r_{\mathrm{hp}}^{\mathrm{aAbiIj}} \tag{B.200}$$

$$0.5g_{\mathrm{iJ}}g_{\mathrm{jK}}v_{\mathrm{aAbB}}r_{\mathrm{hp}}^{\mathrm{abCiIj}} \tag{B.201}$$

$$-0.5a_{\mathrm{AB}}g_{\mathrm{iJ}}g_{\mathrm{jK}}v_{\mathrm{aAbC}}r_{\mathrm{hp}}^{\mathrm{abBiIj}} \tag{B.202}$$

factorized quadruples

$\langle {}^{AB}_{IJ}|\bar{H}\hat{r}_q^{(1)}|0\rangle =$

$$-0.25 v_{\mathrm{abij}} v_{\mathrm{IJkl}} t_{\mathrm{hpp}}^{\mathrm{abik}} t_{\mathrm{hpp}}^{\mathrm{ABjl}} \tag{B.203}$$

$$-0.5 a_{\mathrm{AB}} v_{\mathrm{abij}} v_{\mathrm{IJkl}} t_{\mathrm{hpp}}^{\mathrm{aBik}} t_{\mathrm{hpp}}^{\mathrm{Abjl}} \tag{B.204}$$

$$-0.25 v_{\mathrm{abij}} v_{\mathrm{IJkl}} t_{\mathrm{hpp}}^{\mathrm{abjl}} t_{\mathrm{hpp}}^{\mathrm{ABik}} \tag{B.205}$$

$$1. a_{\mathrm{AB}} a_{\mathrm{IJ}} v_{\mathrm{abij}} v_{\mathrm{iIkl}} t_{\mathrm{hpp}}^{\mathrm{aBJk}} t_{\mathrm{hpp}}^{\mathrm{Abjl}} \tag{B.206}$$

$$-0.5 a_{\mathrm{IJ}} v_{\mathrm{abij}} v_{\mathrm{Ijkl}} t_{\mathrm{hpp}}^{\mathrm{abJk}} t_{\mathrm{hpp}}^{\mathrm{ABil}} \tag{B.207}$$

$$-0.5 a_{\mathrm{IJ}} v_{\mathrm{abij}} v_{\mathrm{Ijkl}} t_{\mathrm{hpp}}^{\mathrm{abil}} t_{\mathrm{hpp}}^{\mathrm{ABJk}} \tag{B.208}$$

$$-0.5 a_{\mathrm{IJ}} v_{\mathrm{abij}} v_{\mathrm{cIkl}} t_{p}^{\mathrm{ak}} t_{\mathrm{hpp}}^{\mathrm{ABJl}} t_{\mathrm{hph}}^{\mathrm{bcij}} \tag{B.209}$$

$$0.5 a_{\mathrm{AB}} a_{\mathrm{IJ}} v_{\mathrm{abij}} v_{\mathrm{cIkl}} t_{p}^{\mathrm{Bk}} t_{\mathrm{hpp}}^{\mathrm{aAJl}} t_{\mathrm{hph}}^{\mathrm{bcij}} \tag{B.210}$$

$$0.5 a_{\mathrm{AB}} a_{\mathrm{IJ}} v_{\mathrm{abij}} v_{\mathrm{cIkl}} t_{p}^{\mathrm{ak}} t_{\mathrm{hpp}}^{\mathrm{AbJl}} t_{\mathrm{hph}}^{\mathrm{Bcij}} \tag{B.211}$$

$$0.25 a_{\mathrm{AB}} a_{\mathrm{IJ}} v_{\mathrm{abij}} v_{\mathrm{cIkl}} t_{p}^{\mathrm{Bk}} t_{\mathrm{hpp}}^{\mathrm{abJl}} t_{\mathrm{hph}}^{\mathrm{Acij}} \tag{B.212}$$

$$-0.5 a_{\mathrm{IJ}} v_{\mathrm{abij}} v_{\mathrm{cIkl}} t_{h}^{\mathrm{cj}} t_{\mathrm{hpp}}^{\mathrm{abJk}} t_{\mathrm{hpp}}^{\mathrm{ABil}} \tag{B.213}$$

$$-1. a_{\mathrm{AB}} a_{\mathrm{IJ}} v_{\mathrm{abij}} v_{\mathrm{cIkl}} t_{p}^{\mathrm{ak}} t_{\mathrm{hpp}}^{\mathrm{Abil}} t_{\mathrm{hph}}^{\mathrm{BcjJ}} \tag{B.214}$$

$$-0.5 a_{\mathrm{AB}} a_{\mathrm{IJ}} v_{\mathrm{abij}} v_{\mathrm{cIkl}} t_{p}^{\mathrm{Bk}} t_{\mathrm{hpp}}^{\mathrm{abil}} t_{\mathrm{hph}}^{\mathrm{AcjJ}} \tag{B.215}$$

$$-1. a_{\mathrm{IJ}} v_{\mathrm{abij}} v_{\mathrm{cIkl}} t_{p}^{\mathrm{ak}} t_{\mathrm{hpp}}^{\mathrm{ABjl}} t_{\mathrm{hph}}^{\mathrm{bciJ}} \tag{B.216}$$

$$-0.25 a_{\mathrm{IJ}} v_{\mathrm{abij}} v_{\mathrm{cIkl}} t_{h}^{\mathrm{cJ}} t_{\mathrm{hpp}}^{\mathrm{abik}} t_{\mathrm{hpp}}^{\mathrm{ABjl}} \tag{B.217}$$

$$1. a_{\mathrm{AB}} a_{\mathrm{IJ}} v_{\mathrm{abij}} v_{\mathrm{cIkl}} t_{p}^{\mathrm{Bk}} t_{\mathrm{hpp}}^{\mathrm{aAjl}} t_{\mathrm{hph}}^{\mathrm{bciJ}} \tag{B.218}$$

$$0.5 a_{\mathrm{AB}} a_{\mathrm{IJ}} v_{\mathrm{abij}} v_{\mathrm{cIkl}} t_{h}^{\mathrm{cJ}} t_{\mathrm{hpp}}^{\mathrm{aAjl}} t_{\mathrm{hpp}}^{\mathrm{bBik}} \tag{B.219}$$

$$1. a_{\mathrm{AB}} a_{\mathrm{IJ}} v_{\mathrm{abij}} v_{\mathrm{cIkl}} t_{h}^{\mathrm{ci}} t_{\mathrm{hpp}}^{\mathrm{aBJk}} t_{\mathrm{hpp}}^{\mathrm{Abjl}} \tag{B.220}$$

$$0.5 a_{\mathrm{IJ}} v_{\mathrm{abij}} v_{\mathrm{cIkl}} t_{h}^{\mathrm{ci}} t_{\mathrm{hpp}}^{\mathrm{abjl}} t_{\mathrm{hpp}}^{\mathrm{ABJk}} \tag{B.221}$$

$$-0.25 a_{\mathrm{IJ}} v_{\mathrm{abij}} v_{\mathrm{cIkl}} t_{h}^{\mathrm{cJ}} t_{\mathrm{hpp}}^{\mathrm{abjl}} t_{\mathrm{hpp}}^{\mathrm{ABik}} \tag{B.222}$$

$$-0.25 v_{\mathrm{abij}} v_{\mathrm{ijkl}} t_{\mathrm{hpp}}^{\mathrm{abIk}} t_{\mathrm{hpp}}^{\mathrm{ABJl}} \tag{B.223}$$

$$-0.5 a_{\mathrm{AB}} v_{\mathrm{abij}} v_{\mathrm{ijkl}} t_{\mathrm{hpp}}^{\mathrm{aBIk}} t_{\mathrm{hpp}}^{\mathrm{AbJl}} \tag{B.224}$$

$$-0.25 v_{\mathrm{abij}} v_{\mathrm{ijkl}} t_{\mathrm{hpp}}^{\mathrm{abJl}} t_{\mathrm{hpp}}^{\mathrm{ABIk}} \tag{B.225}$$

$$1. a_{\mathrm{AB}} a_{\mathrm{IJ}} v_{\mathrm{abij}} v_{\mathrm{cikl}} t_{p}^{\mathrm{Bk}} t_{\mathrm{hpp}}^{\mathrm{aAIl}} t_{\mathrm{hph}}^{\mathrm{bcjJ}} \tag{B.226}$$

$$0.5 a_{\mathrm{AB}} a_{\mathrm{IJ}} v_{\mathrm{abij}} v_{\mathrm{cikl}} t_{p}^{\mathrm{Bk}} t_{\mathrm{hpp}}^{\mathrm{abIl}} t_{\mathrm{hph}}^{\mathrm{AcjJ}} \tag{B.227}$$

$$-1. a_{\mathrm{AB}} v_{\mathrm{abij}} v_{\mathrm{cikl}} t_{h}^{\mathrm{cj}} t_{\mathrm{hpp}}^{\mathrm{aBIk}} t_{\mathrm{hpp}}^{\mathrm{AbJl}} \tag{B.228}$$

$$-1. v_{\mathrm{abij}} v_{\mathrm{cikl}} t_{p}^{\mathrm{ak}} t_{\mathrm{hpp}}^{\mathrm{ABjl}} t_{\mathrm{hph}}^{\mathrm{bcIJ}} \tag{B.229}$$

$$1.a_{\mathrm{AB}}v_{\mathrm{abij}}v_{\mathrm{cikl}}t_{p}^{\mathrm{Bk}}t_{\mathrm{hpp}}^{\mathrm{aAjl}}t_{\mathrm{hph}}^{\mathrm{bcIJ}} \tag{B.230}$$

$$1.a_{\mathrm{AB}}a_{\mathrm{IJ}}v_{\mathrm{abij}}v_{\mathrm{cikl}}t_{h}^{\mathrm{cJ}}t_{\mathrm{hpp}}^{\mathrm{aBIk}}t_{\mathrm{hpp}}^{\mathrm{Abjl}} \tag{B.231}$$

$$0.5a_{\mathrm{IJ}}v_{\mathrm{abij}}v_{\mathrm{cikl}}t_{h}^{\mathrm{cJ}}t_{\mathrm{hpp}}^{\mathrm{abjl}}t_{\mathrm{hpp}}^{\mathrm{ABIk}} \tag{B.232}$$

$$1.a_{\mathrm{IJ}}v_{\mathrm{abij}}v_{\mathrm{cjkl}}t_{p}^{\mathrm{ak}}t_{\mathrm{hpp}}^{\mathrm{ABIl}}t_{\mathrm{hph}}^{\mathrm{bciJ}} \tag{B.233}$$

$$-1.a_{\mathrm{AB}}a_{\mathrm{IJ}}v_{\mathrm{abij}}v_{\mathrm{cjkl}}t_{p}^{\mathrm{ak}}t_{\mathrm{hpp}}^{\mathrm{AbIl}}t_{\mathrm{hph}}^{\mathrm{BciJ}} \tag{B.234}$$

$$0.5v_{\mathrm{abij}}v_{\mathrm{cjkl}}t_{h}^{\mathrm{ci}}t_{\mathrm{hpp}}^{\mathrm{abIk}}t_{\mathrm{hpp}}^{\mathrm{ABJl}} \tag{B.235}$$

$$0.5v_{\mathrm{abij}}v_{\mathrm{cjkl}}t_{h}^{\mathrm{ci}}t_{\mathrm{hpp}}^{\mathrm{abJl}}t_{\mathrm{hpp}}^{\mathrm{ABIk}} \tag{B.236}$$

$$-0.5a_{\mathrm{IJ}}v_{\mathrm{abij}}v_{\mathrm{cjkl}}t_{h}^{\mathrm{cJ}}t_{\mathrm{hpp}}^{\mathrm{abIk}}t_{\mathrm{hpp}}^{\mathrm{ABil}} \tag{B.237}$$

$$-1.a_{\mathrm{AB}}v_{\mathrm{abij}}v_{\mathrm{cjkl}}t_{p}^{\mathrm{ak}}t_{\mathrm{hpp}}^{\mathrm{Abil}}t_{\mathrm{hph}}^{\mathrm{BcIJ}} \tag{B.238}$$

$$-0.5a_{\mathrm{AB}}v_{\mathrm{abij}}v_{\mathrm{cjkl}}t_{p}^{\mathrm{Bk}}t_{\mathrm{hpp}}^{\mathrm{abil}}t_{\mathrm{hph}}^{\mathrm{AcIJ}} \tag{B.239}$$

$$0.25a_{\mathrm{AB}}v_{\mathrm{abij}}v_{\mathrm{cdkl}}t_{p}^{\mathrm{ak}}t_{p}^{\mathrm{bl}}t_{\mathrm{hph}}^{\mathrm{AdiJ}}t_{\mathrm{hph}}^{\mathrm{BcIj}} \tag{B.240}$$

$$1.v_{\mathrm{abij}}v_{\mathrm{cdkl}}t_{p}^{\mathrm{Ak}}t_{p}^{\mathrm{Bl}}t_{\mathrm{hph}}^{\mathrm{adiJ}}t_{\mathrm{hph}}^{\mathrm{bcIj}} \tag{B.241}$$

$$-0.25a_{\mathrm{AB}}v_{\mathrm{abij}}v_{\mathrm{cdkl}}t_{p}^{\mathrm{ak}}t_{p}^{\mathrm{bl}}t_{\mathrm{hph}}^{\mathrm{AdjJ}}t_{\mathrm{hph}}^{\mathrm{BciI}} \tag{B.242}$$

$$-1.a_{\mathrm{AB}}v_{\mathrm{abij}}v_{\mathrm{cdkl}}t_{p}^{\mathrm{al}}t_{p}^{\mathrm{Bk}}t_{\mathrm{hph}}^{\mathrm{AdjJ}}t_{\mathrm{hph}}^{\mathrm{bciI}} \tag{B.243}$$

$$1.a_{\mathrm{AB}}v_{\mathrm{abij}}v_{\mathrm{cdkl}}t_{p}^{\mathrm{al}}t_{p}^{\mathrm{Bk}}t_{\mathrm{hph}}^{\mathrm{AciI}}t_{\mathrm{hph}}^{\mathrm{bdjJ}} \tag{B.244}$$

$$0.25a_{\mathrm{AB}}v_{\mathrm{abij}}v_{\mathrm{cdkl}}t_{p}^{\mathrm{ak}}t_{p}^{\mathrm{bl}}t_{\mathrm{hph}}^{\mathrm{Adij}}t_{\mathrm{hph}}^{\mathrm{BcIJ}} \tag{B.245}$$

$$0.5a_{\mathrm{AB}}v_{\mathrm{abij}}v_{\mathrm{cdkl}}t_{p}^{\mathrm{al}}t_{p}^{\mathrm{Bk}}t_{\mathrm{hph}}^{\mathrm{Adij}}t_{\mathrm{hph}}^{\mathrm{bcIJ}} \tag{B.246}$$

$$0.5v_{\mathrm{abij}}v_{\mathrm{cdkl}}t_{p}^{\mathrm{Ak}}t_{p}^{\mathrm{Bl}}t_{\mathrm{hph}}^{\mathrm{adij}}t_{\mathrm{hph}}^{\mathrm{bcIJ}} \tag{B.247}$$

$$-0.5a_{\mathrm{AB}}v_{\mathrm{abij}}v_{\mathrm{cdkl}}t_{p}^{\mathrm{al}}t_{p}^{\mathrm{Bk}}t_{\mathrm{hph}}^{\mathrm{AcIJ}}t_{\mathrm{hph}}^{\mathrm{bdij}} \tag{B.248}$$

$$-1.a_{\mathrm{IJ}}v_{\mathrm{abij}}v_{\mathrm{cdkl}}t_{\mathrm{hph}}^{\mathrm{acjJ}}t_{\mathrm{hpp}}^{\mathrm{ABIk}}t_{\mathrm{hp}}^{\mathrm{bdil}} \tag{B.249}$$

$$-0.5v_{\mathrm{abij}}v_{\mathrm{cdkl}}t_{\mathrm{hph}}^{\mathrm{adij}}t_{\mathrm{hpp}}^{\mathrm{ABIk}}t_{\mathrm{hp}}^{\mathrm{bcJl}} \tag{B.250}$$

$$0.75a_{\mathrm{AB}}a_{\mathrm{IJ}}v_{\mathrm{abij}}v_{\mathrm{cdkl}}t_{\mathrm{hpp}}^{\mathrm{aAIk}}t_{\mathrm{hp}}^{\mathrm{bdil}}t_{\mathrm{hph}}^{\mathrm{BcjJ}} \tag{B.251}$$

$$0.5a_{\mathrm{AB}}v_{\mathrm{abij}}v_{\mathrm{cdkl}}t_{\mathrm{hpp}}^{\mathrm{aAIk}}t_{\mathrm{hp}}^{\mathrm{bcJl}}t_{\mathrm{hph}}^{\mathrm{Bdij}} \tag{B.252}$$

$$0.25a_{\mathrm{AB}}a_{\mathrm{IJ}}v_{\mathrm{abij}}v_{\mathrm{cdkl}}t_{\mathrm{hp}}^{\mathrm{adjl}}t_{\mathrm{hpp}}^{\mathrm{AbIk}}t_{\mathrm{hph}}^{\mathrm{BciJ}} \tag{B.253}$$

$$1.a_{\mathrm{AB}}a_{\mathrm{IJ}}v_{\mathrm{abij}}v_{\mathrm{cdkl}}t_{\mathrm{hph}}^{\mathrm{acjJ}}t_{\mathrm{hpp}}^{\mathrm{AbIk}}t_{\mathrm{hp}}^{\mathrm{Bdil}} \tag{B.254}$$

$$0.5a_{\mathrm{AB}}v_{\mathrm{abij}}v_{\mathrm{cdkl}}t_{\mathrm{hph}}^{\mathrm{adij}}t_{\mathrm{hpp}}^{\mathrm{AbIk}}t_{\mathrm{hp}}^{\mathrm{BcJl}} \tag{B.255}$$

$$-0.5a_{\mathrm{AB}}a_{\mathrm{IJ}}v_{\mathrm{abij}}v_{\mathrm{cdkl}}t_{\mathrm{hpp}}^{\mathrm{abIk}}t_{\mathrm{hph}}^{\mathrm{AcjJ}}t_{\mathrm{hp}}^{\mathrm{Bdil}} \tag{B.256}$$

$$-0.25a_{\mathrm{AB}}v_{\mathrm{abij}}v_{\mathrm{cdkl}}t_{\mathrm{hpp}}^{\mathrm{abIk}}t_{\mathrm{hph}}^{\mathrm{Adij}}t_{\mathrm{hp}}^{\mathrm{BcJl}} \tag{B.257}$$

$$-1.a_{\mathrm{IJ}}v_{\mathrm{abij}}v_{\mathrm{cdkl}}t_{p}^{\mathrm{ak}}t_{h}^{\mathrm{ci}}t_{\mathrm{hpp}}^{\mathrm{ABIl}}t_{\mathrm{hph}}^{\mathrm{bdjJ}} \tag{B.258}$$

$$0.5a_{\mathrm{IJ}}v_{\mathrm{abij}}v_{\mathrm{cdkl}}t_{p}^{\mathrm{ak}}t_{h}^{\mathrm{cJ}}t_{\mathrm{hpp}}^{\mathrm{ABIl}}t_{\mathrm{hph}}^{\mathrm{bdij}} \tag{B.259}$$

$$1.a_{\mathrm{AB}}a_{\mathrm{IJ}}v_{\mathrm{abij}}v_{\mathrm{cdkl}}t_{p}^{\mathrm{Bk}}t_{h}^{\mathrm{ci}}t_{\mathrm{hpp}}^{\mathrm{aAIl}}t_{\mathrm{hph}}^{\mathrm{bdjJ}} \tag{B.260}$$

$$-0.5a_{\mathrm{AB}}a_{\mathrm{IJ}}v_{\mathrm{abij}}v_{\mathrm{cdkl}}t_{p}^{\mathrm{Bk}}t_{h}^{\mathrm{cJ}}t_{\mathrm{hpp}}^{\mathrm{aAIl}}t_{\mathrm{hph}}^{\mathrm{bdij}} \tag{B.261}$$

$$1.a_{\mathrm{AB}}a_{\mathrm{IJ}}v_{\mathrm{abij}}v_{\mathrm{cdkl}}t_{p}^{\mathrm{ak}}t_{h}^{\mathrm{ci}}t_{\mathrm{hpp}}^{\mathrm{AbIl}}t_{\mathrm{hph}}^{\mathrm{BdjJ}} \tag{B.262}$$

$$-0.5a_{\mathrm{AB}}a_{\mathrm{IJ}}v_{\mathrm{abij}}v_{\mathrm{cdkl}}t_{p}^{\mathrm{ak}}t_{h}^{\mathrm{cJ}}t_{\mathrm{hpp}}^{\mathrm{AbIl}}t_{\mathrm{hph}}^{\mathrm{Bdij}} \tag{B.263}$$

$$0.5a_{\mathrm{AB}}a_{\mathrm{IJ}}v_{\mathrm{abij}}v_{\mathrm{cdkl}}t_{p}^{\mathrm{Bk}}t_{h}^{\mathrm{ci}}t_{\mathrm{hpp}}^{\mathrm{abIl}}t_{\mathrm{hph}}^{\mathrm{AdjJ}} \tag{B.264}$$

$$-0.25a_{\mathrm{AB}}a_{\mathrm{IJ}}v_{\mathrm{abij}}v_{\mathrm{cdkl}}t_{p}^{\mathrm{Bk}}t_{h}^{\mathrm{cJ}}t_{\mathrm{hpp}}^{\mathrm{abIl}}t_{\mathrm{hph}}^{\mathrm{Adij}} \tag{B.265}$$

$$0.5v_{\mathrm{abij}}v_{\mathrm{cdkl}}t_{\mathrm{hp}}^{\mathrm{acIk}}t_{\mathrm{hpp}}^{\mathrm{ABJl}}t_{\mathrm{hph}}^{\mathrm{bdij}} \tag{B.266}$$

$$-0.25v_{\mathrm{abij}}v_{\mathrm{cdkl}}t_{h}^{\mathrm{ci}}t_{h}^{\mathrm{dj}}t_{\mathrm{hpp}}^{\mathrm{abIk}}t_{\mathrm{hpp}}^{\mathrm{ABJl}} \tag{B.267}$$

$$-0.125v_{\mathrm{abij}}v_{\mathrm{cdkl}}t_{\mathrm{hpp}}^{\mathrm{abIk}}t_{\mathrm{hpp}}^{\mathrm{ABJl}}t_{h}^{\mathrm{cdij}} \tag{B.268}$$

$$-0.5a_{\mathrm{AB}}v_{\mathrm{abij}}v_{\mathrm{cdkl}}t_{\mathrm{hpp}}^{\mathrm{aAJl}}t_{\mathrm{hph}}^{\mathrm{bdij}}t_{\mathrm{hp}}^{\mathrm{BcIk}} \tag{B.269}$$

$$0.25a_{\mathrm{AB}}v_{\mathrm{abij}}v_{\mathrm{cdkl}}t_{\mathrm{hpp}}^{\mathrm{aAJl}}t_{\mathrm{hpp}}^{\mathrm{bBIk}}t_{h}^{\mathrm{cdij}} \tag{B.270}$$

$$-0.5a_{\mathrm{AB}}v_{\mathrm{abij}}v_{\mathrm{cdkl}}t_{\mathrm{hp}}^{\mathrm{acIk}}t_{\mathrm{hpp}}^{\mathrm{AbJl}}t_{\mathrm{hph}}^{\mathrm{Bdij}} \tag{B.271}$$

$$-0.5a_{\mathrm{AB}}v_{\mathrm{abij}}v_{\mathrm{cdkl}}t_{h}^{\mathrm{ci}}t_{h}^{\mathrm{dj}}t_{\mathrm{hpp}}^{\mathrm{aBIk}}t_{\mathrm{hpp}}^{\mathrm{AbJl}} \tag{B.272}$$

$$-0.25a_{\mathrm{AB}}v_{\mathrm{abij}}v_{\mathrm{cdkl}}t_{\mathrm{hpp}}^{\mathrm{abJl}}t_{\mathrm{hph}}^{\mathrm{Adij}}t_{\mathrm{hp}}^{\mathrm{BcIk}} \tag{B.273}$$

$$-0.25v_{\mathrm{abij}}v_{\mathrm{cdkl}}t_{h}^{\mathrm{ci}}t_{h}^{\mathrm{dj}}t_{\mathrm{hpp}}^{\mathrm{abJl}}t_{\mathrm{hpp}}^{\mathrm{ABIk}} \tag{B.274}$$

$$-0.125v_{\mathrm{abij}}v_{\mathrm{cdkl}}t_{\mathrm{hpp}}^{\mathrm{abJl}}t_{\mathrm{hpp}}^{\mathrm{ABIk}}t_{h}^{\mathrm{cdij}} \tag{B.275}$$

$$-0.5v_{\mathrm{abij}}v_{\mathrm{cdkl}}t_{\mathrm{hp}}^{\mathrm{adjl}}t_{\mathrm{hpp}}^{\mathrm{ABik}}t_{\mathrm{hph}}^{\mathrm{bcIJ}} \tag{B.276}$$

$$0.5a_{\mathrm{AB}}v_{\mathrm{abij}}v_{\mathrm{cdkl}}t_{\mathrm{hpp}}^{\mathrm{aAik}}t_{\mathrm{hph}}^{\mathrm{bcIJ}}t_{\mathrm{hp}}^{\mathrm{Bdjl}} \tag{B.277}$$

$$0.5a_{\mathrm{AB}}v_{\mathrm{abij}}v_{\mathrm{cdkl}}t_{\mathrm{hp}}^{\mathrm{adjl}}t_{\mathrm{hpp}}^{\mathrm{Abik}}t_{\mathrm{hph}}^{\mathrm{BcIJ}} \tag{B.278}$$

$$0.25a_{\mathrm{AB}}v_{\mathrm{abij}}v_{\mathrm{cdkl}}t_{\mathrm{hpp}}^{\mathrm{abik}}t_{\mathrm{hph}}^{\mathrm{AcIJ}}t_{\mathrm{hp}}^{\mathrm{Bdjl}} \tag{B.279}$$

$$0.5v_{\mathrm{abij}}v_{\mathrm{cdkl}}t_{p}^{\mathrm{ak}}t_{h}^{\mathrm{cj}}t_{\mathrm{hpp}}^{\mathrm{ABil}}t_{\mathrm{hph}}^{\mathrm{bdIJ}} \tag{B.280}$$

$$0.5a_{\mathrm{IJ}}v_{\mathrm{abij}}v_{\mathrm{cdkl}}t_{p}^{\mathrm{bk}}t_{h}^{\mathrm{cJ}}t_{\mathrm{hph}}^{\mathrm{adIj}}t_{\mathrm{hpp}}^{\mathrm{ABil}} \tag{B.281}$$

$$0.5v_{\mathrm{abij}}v_{\mathrm{cdkl}}t_{\mathrm{hph}}^{\mathrm{adjJ}}t_{\mathrm{hpp}}^{\mathrm{ABil}}t_{\mathrm{hp}}^{\mathrm{bcIk}} \tag{B.282}$$

$$0.25a_{\mathrm{IJ}}v_{\mathrm{abij}}v_{\mathrm{cdkl}}t_{\mathrm{hpp}}^{\mathrm{abIk}}t_{\mathrm{hpp}}^{\mathrm{ABil}}t_{h}^{\mathrm{cdjJ}} \tag{B.283}$$

$$-1.a_{\mathrm{AB}}a_{\mathrm{IJ}}v_{\mathrm{abij}}v_{\mathrm{cdkl}}t_{p}^{\mathrm{bk}}t_{h}^{\mathrm{cJ}}t_{\mathrm{hpp}}^{\mathrm{aAil}}t_{\mathrm{hph}}^{\mathrm{BdIj}} \tag{B.284}$$

$$1.a_{\mathrm{AB}}v_{\mathrm{abij}}v_{\mathrm{cdkl}}t_{\mathrm{hpp}}^{\mathrm{aAil}}t_{\mathrm{hph}}^{\mathrm{bdjJ}}t_{\mathrm{hp}}^{\mathrm{BcIk}} \tag{B.285}$$

$$-0.5a_{\mathrm{AB}}v_{\mathrm{abij}}v_{\mathrm{cdkl}}t_{p}^{\mathrm{ak}}t_{h}^{\mathrm{cj}}t_{\mathrm{hpp}}^{\mathrm{Abil}}t_{\mathrm{hph}}^{\mathrm{BdIJ}} \tag{B.286}$$

$$-1.a_{\mathrm{AB}}v_{\mathrm{abij}}v_{\mathrm{cdkl}}t_{\mathrm{hph}}^{\mathrm{acIj}}t_{\mathrm{hpp}}^{\mathrm{Abil}}t_{\mathrm{hp}}^{\mathrm{BdJk}} \tag{B.287}$$

$$1.a_{\mathrm{AB}}a_{\mathrm{IJ}}v_{\mathrm{abij}}v_{\mathrm{cdkl}}t_{h}^{\mathrm{cJ}}t_{h}^{\mathrm{dj}}t_{\mathrm{hpp}}^{\mathrm{aBIk}}t_{\mathrm{hpp}}^{\mathrm{Abil}} \tag{B.288}$$

$$0.5a_{\mathrm{AB}}v_{\mathrm{abij}}v_{\mathrm{cdkl}}t_{\mathrm{hpp}}^{\mathrm{abil}}t_{\mathrm{hph}}^{\mathrm{AcIj}}t_{\mathrm{hp}}^{\mathrm{BdJk}} \tag{B.289}$$

$$0.5a_{\mathrm{AB}}v_{\mathrm{abij}}v_{\mathrm{cdkl}}t_{\mathrm{hpp}}^{\mathrm{abil}}t_{\mathrm{hph}}^{\mathrm{AdjJ}}t_{\mathrm{hp}}^{\mathrm{BcIk}} \tag{B.290}$$

$$0.25a_{\mathrm{IJ}}v_{\mathrm{abij}}v_{\mathrm{cdkl}}t_{\mathrm{hpp}}^{\mathrm{abil}}t_{\mathrm{hpp}}^{\mathrm{ABIk}}t_{h}^{\mathrm{cdjJ}} \tag{B.291}$$

$$0.5v_{\mathrm{abij}}v_{\mathrm{cdkl}}t_{p}^{\mathrm{bk}}t_{h}^{\mathrm{ci}}t_{\mathrm{hph}}^{\mathrm{adIJ}}t_{\mathrm{hpp}}^{\mathrm{ABjl}} \tag{B.292}$$

$$-0.5v_{\mathrm{abij}}v_{\mathrm{cdkl}}t_{\mathrm{hp}}^{\mathrm{adik}}t_{\mathrm{hpp}}^{\mathrm{ABjl}}t_{\mathrm{hph}}^{\mathrm{bcIJ}} \tag{B.293}$$

$$-0.25v_{\mathrm{abij}}v_{\mathrm{cdkl}}t_{\mathrm{hph}}^{\mathrm{aciI}}t_{\mathrm{hpp}}^{\mathrm{ABjl}}t_{\mathrm{hp}}^{\mathrm{bdJk}} \tag{B.294}$$

$$0.75v_{\mathrm{abij}}v_{\mathrm{cdkl}}t_{\mathrm{hp}}^{\mathrm{adJk}}t_{\mathrm{hpp}}^{\mathrm{ABjl}}t_{\mathrm{hph}}^{\mathrm{bciI}} \tag{B.295}$$

$$0.5a_{\mathrm{IJ}}v_{\mathrm{abij}}v_{\mathrm{cdkl}}t_{p}^{\mathrm{ak}}t_{h}^{\mathrm{cJ}}t_{\mathrm{hpp}}^{\mathrm{ABjl}}t_{\mathrm{hph}}^{\mathrm{bdiI}} \tag{B.296}$$

$$0.5v_{\mathrm{abij}}v_{\mathrm{cdkl}}t_{\mathrm{hp}}^{\mathrm{acIk}}t_{\mathrm{hpp}}^{\mathrm{ABjl}}t_{\mathrm{hph}}^{\mathrm{bdiJ}} \tag{B.297}$$

$$-0.5a_{\mathrm{IJ}}v_{\mathrm{abij}}v_{\mathrm{cdkl}}t_{h}^{\mathrm{cJ}}t_{h}^{\mathrm{di}}t_{\mathrm{hpp}}^{\mathrm{abIk}}t_{\mathrm{hpp}}^{\mathrm{ABjl}} \tag{B.298}$$

$$-0.25v_{\mathrm{abij}}v_{\mathrm{cdkl}}t_{h}^{\mathrm{cI}}t_{h}^{\mathrm{dJ}}t_{\mathrm{hpp}}^{\mathrm{abik}}t_{\mathrm{hpp}}^{\mathrm{ABjl}} \tag{B.299}$$

$$-0.125v_{\mathrm{abij}}v_{\mathrm{cdkl}}t_{\mathrm{hpp}}^{\mathrm{abik}}t_{\mathrm{hpp}}^{\mathrm{ABjl}}t_{h}^{\mathrm{cdIJ}} \tag{B.300}$$

$$-0.5a_{\mathrm{AB}}v_{\mathrm{abij}}v_{\mathrm{cdkl}}t_{p}^{\mathrm{bk}}t_{h}^{\mathrm{ci}}t_{\mathrm{hpp}}^{\mathrm{aAjl}}t_{\mathrm{hph}}^{\mathrm{BdIJ}} \tag{B.301}$$

$$1.a_{\mathrm{AB}}v_{\mathrm{abij}}v_{\mathrm{cdkl}}t_{p}^{\mathrm{Bk}}t_{h}^{\mathrm{ci}}t_{\mathrm{hpp}}^{\mathrm{aAjl}}t_{\mathrm{hph}}^{\mathrm{bdIJ}} \tag{B.302}$$

$$-1.a_{\mathrm{AB}}a_{\mathrm{IJ}}v_{\mathrm{abij}}v_{\mathrm{cdkl}}t_{p}^{\mathrm{Bk}}t_{h}^{\mathrm{cJ}}t_{\mathrm{hpp}}^{\mathrm{aAjl}}t_{\mathrm{hph}}^{\mathrm{bdiI}} \tag{B.303}$$

$$0.5a_{\mathrm{AB}}a_{\mathrm{IJ}}v_{\mathrm{abij}}v_{\mathrm{cdkl}}t_{\mathrm{hpp}}^{\mathrm{aAjl}}t_{\mathrm{hpp}}^{\mathrm{bBIk}}t_{h}^{\mathrm{cdiJ}} \tag{B.304}$$

$$0.25a_{\mathrm{AB}}v_{\mathrm{abij}}v_{\mathrm{cdkl}}t_{\mathrm{hpp}}^{\mathrm{aAjl}}t_{\mathrm{hpp}}^{\mathrm{bBik}}t_{h}^{\mathrm{cdIJ}} \tag{B.305}$$

$$0.5a_{\mathrm{AB}}v_{\mathrm{abij}}v_{\mathrm{cdkl}}t_{\mathrm{hp}}^{\mathrm{adik}}t_{\mathrm{hpp}}^{\mathrm{Abjl}}t_{\mathrm{hph}}^{\mathrm{BcIJ}} \tag{B.306}$$

$$-0.5a_{\mathrm{AB}}v_{\mathrm{abij}}v_{\mathrm{cdkl}}t_{\mathrm{hph}}^{\mathrm{acIJ}}t_{\mathrm{hpp}}^{\mathrm{Abjl}}t_{\mathrm{hp}}^{\mathrm{Bdik}} \tag{B.307}$$

$$-1.a_{\mathrm{AB}}v_{\mathrm{abij}}v_{\mathrm{cdkl}}t_{\mathrm{hp}}^{\mathrm{adJk}}t_{\mathrm{hpp}}^{\mathrm{Abjl}}t_{\mathrm{hph}}^{\mathrm{BciI}} \tag{B.308}$$

$$-1.a_{\mathrm{AB}}v_{\mathrm{abij}}v_{\mathrm{cdkl}}t_{\mathrm{hp}}^{\mathrm{acIk}}t_{\mathrm{hpp}}^{\mathrm{Abjl}}t_{\mathrm{hph}}^{\mathrm{BdiJ}} \tag{B.309}$$

$$-0.5a_{\mathrm{AB}}v_{\mathrm{abij}}v_{\mathrm{cdkl}}t_{h}^{\mathrm{cI}}t_{h}^{\mathrm{dJ}}t_{\mathrm{hpp}}^{\mathrm{aBik}}t_{\mathrm{hpp}}^{\mathrm{Abjl}} \tag{B.310}$$

$$0.25a_{\mathrm{AB}}v_{\mathrm{abij}}v_{\mathrm{cdkl}}t_{\mathrm{hpp}}^{\mathrm{abjl}}t_{\mathrm{hph}}^{\mathrm{AcIJ}}t_{\mathrm{hp}}^{\mathrm{Bdik}} \tag{B.311}$$

$$0.5a_{\mathrm{AB}}v_{\mathrm{abij}}v_{\mathrm{cdkl}}t_{p}^{\mathrm{Bk}}t_{h}^{\mathrm{ci}}t_{\mathrm{hpp}}^{\mathrm{abjl}}t_{\mathrm{hph}}^{\mathrm{AdIJ}} \tag{B.312}$$

$$-0.5a_{\mathrm{AB}}a_{\mathrm{IJ}}v_{\mathrm{abij}}v_{\mathrm{cdkl}}t_{p}^{\mathrm{Bk}}t_{h}^{\mathrm{cJ}}t_{\mathrm{hpp}}^{\mathrm{abjl}}t_{\mathrm{hph}}^{\mathrm{AdiI}} \tag{B.313}$$

$$-0.5a_{\mathrm{IJ}}v_{\mathrm{abij}}v_{\mathrm{cdkl}}t_{h}^{\mathrm{cJ}}t_{h}^{\mathrm{di}}t_{\mathrm{hpp}}^{\mathrm{abjl}}t_{\mathrm{hpp}}^{\mathrm{ABIk}} \tag{B.314}$$

$$-0.25v_{\mathrm{abij}}v_{\mathrm{cdkl}}t_{h}^{\mathrm{cI}}t_{h}^{\mathrm{dJ}}t_{\mathrm{hpp}}^{\mathrm{abjl}}t_{\mathrm{hpp}}^{\mathrm{ABik}} \tag{B.315}$$

$$-0.125v_{\mathrm{abij}}v_{\mathrm{cdkl}}t_{\mathrm{hpp}}^{\mathrm{abjl}}t_{\mathrm{hpp}}^{\mathrm{ABik}}t_{h}^{\mathrm{cdIJ}} \tag{B.316}$$

$$0.5 v_{\mathrm{abij}} v_{\mathrm{cdkl}} t_{\mathrm{hph}}^{\mathrm{aciI}} t_{\mathrm{pp}}^{\mathrm{ABkl}} t_{\mathrm{hph}}^{\mathrm{bdjJ}} \tag{B.317}$$

$$-0.25 v_{\mathrm{abij}} v_{\mathrm{cdkl}} t_{\mathrm{hph}}^{\mathrm{acIJ}} t_{\mathrm{pp}}^{\mathrm{ABkl}} t_{\mathrm{hph}}^{\mathrm{bdij}} \tag{B.318}$$

$$-0.5 a_{\mathrm{AB}} v_{\mathrm{abij}} v_{\mathrm{cdkl}} t_{\mathrm{pp}}^{\mathrm{aAkl}} t_{\mathrm{hph}}^{\mathrm{bdjJ}} t_{\mathrm{hph}}^{\mathrm{BciI}} \tag{B.319}$$

$$0.25 a_{\mathrm{AB}} v_{\mathrm{abij}} v_{\mathrm{cdkl}} t_{\mathrm{pp}}^{\mathrm{aAkl}} t_{\mathrm{hph}}^{\mathrm{bdij}} t_{\mathrm{hph}}^{\mathrm{BcIJ}} \tag{B.320}$$

$$-0.5 a_{\mathrm{AB}} v_{\mathrm{abij}} v_{\mathrm{cdkl}} t_{\mathrm{hph}}^{\mathrm{aciI}} t_{\mathrm{pp}}^{\mathrm{Abkl}} t_{\mathrm{hph}}^{\mathrm{BdjJ}} \tag{B.321}$$

$$0.25 a_{\mathrm{AB}} v_{\mathrm{abij}} v_{\mathrm{cdkl}} t_{\mathrm{hph}}^{\mathrm{acIJ}} t_{\mathrm{pp}}^{\mathrm{Abkl}} t_{\mathrm{hph}}^{\mathrm{Bdij}} \tag{B.322}$$

$$-0.25 a_{\mathrm{AB}} v_{\mathrm{abij}} v_{\mathrm{cdkl}} t_{\mathrm{pp}}^{\mathrm{abkl}} t_{\mathrm{hph}}^{\mathrm{AdjJ}} t_{\mathrm{hph}}^{\mathrm{BciI}} \tag{B.323}$$

$$0.125 a_{\mathrm{AB}} v_{\mathrm{abij}} v_{\mathrm{cdkl}} t_{\mathrm{pp}}^{\mathrm{abkl}} t_{\mathrm{hph}}^{\mathrm{Adij}} t_{\mathrm{hph}}^{\mathrm{BcIJ}} \tag{B.324}$$

$$0.5 a_{\mathrm{AB}} a_{\mathrm{IJ}} v_{\mathrm{abij}} v_{\mathrm{AcIk}} t_{\mathrm{hph}}^{\mathrm{acij}} t_{\mathrm{hpp}}^{\mathrm{bBJk}} \tag{B.325}$$

$$-0.25 a_{\mathrm{AB}} a_{\mathrm{IJ}} v_{\mathrm{abij}} v_{\mathrm{AcIk}} t_{\mathrm{hpp}}^{\mathrm{abJk}} t_{\mathrm{hph}}^{\mathrm{Bcij}} \tag{B.326}$$

$$0.5 a_{\mathrm{AB}} a_{\mathrm{IJ}} v_{\mathrm{abij}} v_{\mathrm{AcIk}} t_{\mathrm{hpp}}^{\mathrm{abik}} t_{\mathrm{hph}}^{\mathrm{BcjJ}} \tag{B.327}$$

$$1. a_{\mathrm{AB}} a_{\mathrm{IJ}} v_{\mathrm{abij}} v_{\mathrm{AcIk}} t_{\mathrm{hph}}^{\mathrm{aciJ}} t_{\mathrm{hpp}}^{\mathrm{bBjk}} \tag{B.328}$$

$$0.5 a_{\mathrm{AB}} a_{\mathrm{IJ}} v_{\mathrm{abij}} v_{\mathrm{Acik}} t_{\mathrm{hph}}^{\mathrm{acjJ}} t_{\mathrm{hpp}}^{\mathrm{bBIk}} \tag{B.329}$$

$$1. a_{\mathrm{AB}} v_{\mathrm{abij}} v_{\mathrm{Acik}} t_{\mathrm{hph}}^{\mathrm{acIJ}} t_{\mathrm{hpp}}^{\mathrm{bBjk}} \tag{B.330}$$

$$-0.5 a_{\mathrm{AB}} a_{\mathrm{IJ}} v_{\mathrm{abij}} v_{\mathrm{Acjk}} t_{\mathrm{hph}}^{\mathrm{aciJ}} t_{\mathrm{hpp}}^{\mathrm{bBIk}} \tag{B.331}$$

$$0.5 a_{\mathrm{AB}} a_{\mathrm{IJ}} v_{\mathrm{abij}} v_{\mathrm{Acjk}} t_{\mathrm{hpp}}^{\mathrm{abIk}} t_{\mathrm{hph}}^{\mathrm{BciJ}} \tag{B.332}$$

$$0.5 a_{\mathrm{AB}} v_{\mathrm{abij}} v_{\mathrm{Acjk}} t_{\mathrm{hpp}}^{\mathrm{abik}} t_{\mathrm{hph}}^{\mathrm{BcIJ}} \tag{B.333}$$

$$-0.5 a_{\mathrm{AB}} v_{\mathrm{abij}} v_{\mathrm{Acdk}} t_{p}^{\mathrm{ak}} t_{\mathrm{hph}}^{\mathrm{bcIj}} t_{\mathrm{hph}}^{\mathrm{BdiJ}} \tag{B.334}$$

$$0.5 a_{\mathrm{AB}} v_{\mathrm{abij}} v_{\mathrm{Acdk}} t_{p}^{\mathrm{Bk}} t_{\mathrm{hph}}^{\mathrm{adiJ}} t_{\mathrm{hph}}^{\mathrm{bcIj}} \tag{B.335}$$

$$-0.5 a_{\mathrm{AB}} v_{\mathrm{abij}} v_{\mathrm{Acdk}} t_{p}^{\mathrm{bk}} t_{\mathrm{hph}}^{\mathrm{aciI}} t_{\mathrm{hph}}^{\mathrm{BdjJ}} \tag{B.336}$$

$$0.25 a_{\mathrm{AB}} v_{\mathrm{abij}} v_{\mathrm{Acdk}} t_{p}^{\mathrm{bk}} t_{\mathrm{hph}}^{\mathrm{adjJ}} t_{\mathrm{hph}}^{\mathrm{BciI}} \tag{B.337}$$

$$-0.75 a_{\mathrm{AB}} v_{\mathrm{abij}} v_{\mathrm{Acdk}} t_{p}^{\mathrm{ak}} t_{\mathrm{hph}}^{\mathrm{bdjJ}} t_{\mathrm{hph}}^{\mathrm{BciI}} \tag{B.338}$$

$$0.5 a_{\mathrm{AB}} v_{\mathrm{abij}} v_{\mathrm{Acdk}} t_{p}^{\mathrm{Bk}} t_{\mathrm{hph}}^{\mathrm{aciI}} t_{\mathrm{hph}}^{\mathrm{bdjJ}} \tag{B.339}$$

$$-0.5 a_{\mathrm{AB}} v_{\mathrm{abij}} v_{\mathrm{Acdk}} t_{p}^{\mathrm{ak}} t_{\mathrm{hph}}^{\mathrm{bcIJ}} t_{\mathrm{hph}}^{\mathrm{Bdij}} \tag{B.340}$$

$$0.5 a_{\mathrm{AB}} v_{\mathrm{abij}} v_{\mathrm{Acdk}} t_{p}^{\mathrm{Bk}} t_{\mathrm{hph}}^{\mathrm{adij}} t_{\mathrm{hph}}^{\mathrm{bcIJ}} \tag{B.341}$$

$$0.5 a_{\mathrm{AB}} v_{\mathrm{abij}} v_{\mathrm{Acdk}} t_{p}^{\mathrm{ak}} t_{\mathrm{hph}}^{\mathrm{bdij}} t_{\mathrm{hph}}^{\mathrm{BcIJ}} \tag{B.342}$$

$$0.5 a_{\mathrm{AB}} a_{\mathrm{IJ}} v_{\mathrm{abij}} v_{\mathrm{Acdk}} t_{h}^{\mathrm{cj}} t_{\mathrm{hpp}}^{\mathrm{aBIk}} t_{\mathrm{hph}}^{\mathrm{bdiJ}} \tag{B.343}$$

$$0.5a_{\mathrm{AB}}a_{\mathrm{IJ}}v_{\mathrm{abij}}v_{\mathrm{Acdk}}t_{h}^{\mathrm{cJ}}t_{\mathrm{hpp}}^{\mathrm{aBIk}}t_{\mathrm{hph}}^{\mathrm{bdij}} \tag{B.344}$$

$$0.5a_{\mathrm{AB}}a_{\mathrm{IJ}}v_{\mathrm{abij}}v_{\mathrm{Acdk}}t_{h}^{\mathrm{ci}}t_{\mathrm{hph}}^{\mathrm{adjJ}}t_{\mathrm{hpp}}^{\mathrm{bBIk}} \tag{B.345}$$

$$-0.5a_{\mathrm{AB}}a_{\mathrm{IJ}}v_{\mathrm{abij}}v_{\mathrm{Acdk}}t_{h}^{\mathrm{ci}}t_{\mathrm{hpp}}^{\mathrm{abIk}}t_{\mathrm{hph}}^{\mathrm{BdjJ}} \tag{B.346}$$

$$0.25a_{\mathrm{AB}}a_{\mathrm{IJ}}v_{\mathrm{abij}}v_{\mathrm{Acdk}}t_{h}^{\mathrm{cJ}}t_{\mathrm{hpp}}^{\mathrm{abIk}}t_{\mathrm{hph}}^{\mathrm{Bdij}} \tag{B.347}$$

$$-1.a_{\mathrm{AB}}v_{\mathrm{abij}}v_{\mathrm{Acdk}}t_{h}^{\mathrm{cj}}t_{\mathrm{hph}}^{\mathrm{adIJ}}t_{\mathrm{hpp}}^{\mathrm{bBik}} \tag{B.348}$$

$$-0.5a_{\mathrm{AB}}a_{\mathrm{IJ}}v_{\mathrm{abij}}v_{\mathrm{Acdk}}t_{h}^{\mathrm{cJ}}t_{\mathrm{hpp}}^{\mathrm{abik}}t_{\mathrm{hph}}^{\mathrm{BdIj}} \tag{B.349}$$

$$1.a_{\mathrm{AB}}a_{\mathrm{IJ}}v_{\mathrm{abij}}v_{\mathrm{Acdk}}t_{h}^{\mathrm{cJ}}t_{\mathrm{hpp}}^{\mathrm{aBjk}}t_{\mathrm{hph}}^{\mathrm{bdiI}} \tag{B.350}$$

$$-0.5a_{\mathrm{AB}}v_{\mathrm{abij}}v_{\mathrm{Acdk}}t_{h}^{\mathrm{ci}}t_{\mathrm{hpp}}^{\mathrm{abjk}}t_{\mathrm{hph}}^{\mathrm{BdIJ}} \tag{B.351}$$

$$0.5a_{\mathrm{AB}}a_{\mathrm{IJ}}v_{\mathrm{abij}}v_{\mathrm{acIk}}t_{\mathrm{hpp}}^{\mathrm{AbJk}}t_{\mathrm{hph}}^{\mathrm{Bcij}} \tag{B.352}$$

$$1.a_{\mathrm{AB}}a_{\mathrm{IJ}}v_{\mathrm{abij}}v_{\mathrm{acIk}}t_{\mathrm{hpp}}^{\mathrm{Abjk}}t_{\mathrm{hph}}^{\mathrm{BciJ}} \tag{B.353}$$

$$1.a_{\mathrm{AB}}v_{\mathrm{abij}}v_{\mathrm{acik}}t_{\mathrm{hpp}}^{\mathrm{Abjk}}t_{\mathrm{hph}}^{\mathrm{BcIJ}} \tag{B.354}$$

$$-1.a_{\mathrm{AB}}a_{\mathrm{IJ}}v_{\mathrm{abij}}v_{\mathrm{acjk}}t_{\mathrm{hpp}}^{\mathrm{AbIk}}t_{\mathrm{hph}}^{\mathrm{BciJ}} \tag{B.355}$$

$$-0.5a_{\mathrm{AB}}v_{\mathrm{abij}}v_{\mathrm{acdk}}t_{p}^{\mathrm{Bk}}t_{\mathrm{hph}}^{\mathrm{AdiJ}}t_{\mathrm{hph}}^{\mathrm{bcIj}} \tag{B.356}$$

$$-0.5a_{\mathrm{AB}}v_{\mathrm{abij}}v_{\mathrm{acdk}}t_{p}^{\mathrm{bk}}t_{\mathrm{hph}}^{\mathrm{AdjJ}}t_{\mathrm{hph}}^{\mathrm{BciI}} \tag{B.357}$$

$$-0.5a_{\mathrm{AB}}v_{\mathrm{abij}}v_{\mathrm{acdk}}t_{p}^{\mathrm{Bk}}t_{\mathrm{hph}}^{\mathrm{AciI}}t_{\mathrm{hph}}^{\mathrm{bdjJ}} \tag{B.358}$$

$$-0.5a_{\mathrm{AB}}v_{\mathrm{abij}}v_{\mathrm{acdk}}t_{p}^{\mathrm{Bk}}t_{\mathrm{hph}}^{\mathrm{Adij}}t_{\mathrm{hph}}^{\mathrm{bcIJ}} \tag{B.359}$$

$$0.5a_{\mathrm{IJ}}v_{\mathrm{abij}}v_{\mathrm{acdk}}t_{h}^{\mathrm{cj}}t_{\mathrm{hpp}}^{\mathrm{ABIk}}t_{\mathrm{hph}}^{\mathrm{bdiJ}} \tag{B.360}$$

$$0.5a_{\mathrm{IJ}}v_{\mathrm{abij}}v_{\mathrm{acdk}}t_{h}^{\mathrm{cJ}}t_{\mathrm{hpp}}^{\mathrm{ABIk}}t_{\mathrm{hph}}^{\mathrm{bdij}} \tag{B.361}$$

$$0.5a_{\mathrm{AB}}a_{\mathrm{IJ}}v_{\mathrm{abij}}v_{\mathrm{acdk}}t_{h}^{\mathrm{ci}}t_{\mathrm{hpp}}^{\mathrm{AbIk}}t_{\mathrm{hph}}^{\mathrm{BdjJ}} \tag{B.362}$$

$$-1.a_{\mathrm{AB}}v_{\mathrm{abij}}v_{\mathrm{acdk}}t_{h}^{\mathrm{cj}}t_{\mathrm{hpp}}^{\mathrm{Abik}}t_{\mathrm{hph}}^{\mathrm{BdIJ}} \tag{B.363}$$

$$-1.v_{\mathrm{abij}}v_{\mathrm{acdk}}t_{h}^{\mathrm{ci}}t_{\mathrm{hpp}}^{\mathrm{ABjk}}t_{\mathrm{hph}}^{\mathrm{bdIJ}} \tag{B.364}$$

$$0.5a_{\mathrm{IJ}}v_{\mathrm{abij}}v_{\mathrm{bcIk}}t_{\mathrm{hph}}^{\mathrm{acij}}t_{\mathrm{hpp}}^{\mathrm{ABJk}} \tag{B.365}$$

$$1.a_{\mathrm{IJ}}v_{\mathrm{abij}}v_{\mathrm{bcIk}}t_{\mathrm{hph}}^{\mathrm{aciJ}}t_{\mathrm{hpp}}^{\mathrm{ABjk}} \tag{B.366}$$

$$1.v_{\mathrm{abij}}v_{\mathrm{bcik}}t_{\mathrm{hph}}^{\mathrm{acIJ}}t_{\mathrm{hpp}}^{\mathrm{ABjk}} \tag{B.367}$$

$$-1.a_{\mathrm{IJ}}v_{\mathrm{abij}}v_{\mathrm{bcjk}}t_{\mathrm{hph}}^{\mathrm{aciJ}}t_{\mathrm{hpp}}^{\mathrm{ABIk}} \tag{B.368}$$

$$-0.5a_{\mathrm{AB}}v_{\mathrm{abij}}v_{\mathrm{bcdk}}t_{p}^{\mathrm{ak}}t_{\mathrm{hph}}^{\mathrm{AdiJ}}t_{\mathrm{hph}}^{\mathrm{BcIj}} \tag{B.369}$$

$$-0.5a_{\mathrm{AB}}v_{\mathrm{abij}}v_{\mathrm{bcdk}}t_{p}^{\mathrm{Bk}}t_{\mathrm{hph}}^{\mathrm{adiJ}}t_{\mathrm{hph}}^{\mathrm{AcIj}} \tag{B.370}$$

$$-0.5a_{\mathrm{AB}}v_{\mathrm{abij}}v_{\mathrm{bcdk}}t_{p}^{\mathrm{Bk}}t_{\mathrm{hph}}^{\mathrm{aciI}}t_{\mathrm{hph}}^{\mathrm{AdjJ}} \tag{B.371}$$

$$-0.5a_{\mathrm{AB}}v_{\mathrm{abij}}v_{\mathrm{bcdk}}t_{p}^{\mathrm{ak}}t_{\mathrm{hph}}^{\mathrm{Adij}}t_{\mathrm{hph}}^{\mathrm{BcIJ}} \tag{B.372}$$

$$-0.5a_{\mathrm{AB}}v_{\mathrm{abij}}v_{\mathrm{bcdk}}t_{p}^{\mathrm{Bk}}t_{\mathrm{hph}}^{\mathrm{adij}}t_{\mathrm{hph}}^{\mathrm{AcIJ}} \tag{B.373}$$

$$0.5a_{\mathrm{IJ}}v_{\mathrm{abij}}v_{\mathrm{bcdk}}t_{h}^{\mathrm{ci}}t_{\mathrm{hph}}^{\mathrm{adjJ}}t_{\mathrm{hpp}}^{\mathrm{ABIk}} \tag{B.374}$$

$$0.5a_{\mathrm{AB}}a_{\mathrm{IJ}}v_{\mathrm{abij}}v_{\mathrm{bcdk}}t_{h}^{\mathrm{cj}}t_{\mathrm{hpp}}^{\mathrm{aAIk}}t_{\mathrm{hph}}^{\mathrm{BdiJ}} \tag{B.375}$$

$$0.5a_{\mathrm{AB}}a_{\mathrm{IJ}}v_{\mathrm{abij}}v_{\mathrm{bcdk}}t_{h}^{\mathrm{cJ}}t_{\mathrm{hpp}}^{\mathrm{aAIk}}t_{\mathrm{hph}}^{\mathrm{Bdij}} \tag{B.376}$$

$$-1.a_{\mathrm{AB}}a_{\mathrm{IJ}}v_{\mathrm{abij}}v_{\mathrm{bcdk}}t_{h}^{\mathrm{cJ}}t_{\mathrm{hpp}}^{\mathrm{aAik}}t_{\mathrm{hph}}^{\mathrm{BdIj}} \tag{B.377}$$

$$-1.a_{\mathrm{IJ}}v_{\mathrm{abij}}v_{\mathrm{bcdk}}t_{h}^{\mathrm{cJ}}t_{\mathrm{hph}}^{\mathrm{adiI}}t_{\mathrm{hpp}}^{\mathrm{ABjk}} \tag{B.378}$$

$$-1.v_{\mathrm{abij}}v_{\mathrm{ABcd}}t_{\mathrm{hph}}^{\mathrm{acIj}}t_{\mathrm{hph}}^{\mathrm{bdiJ}} \tag{B.379}$$

$$-0.5v_{\mathrm{abij}}v_{\mathrm{ABcd}}t_{\mathrm{hph}}^{\mathrm{acIJ}}t_{\mathrm{hph}}^{\mathrm{bdij}} \tag{B.380}$$

$$-1.a_{\mathrm{AB}}v_{\mathrm{aAcd}}v_{\mathrm{abij}}t_{\mathrm{hph}}^{\mathrm{bdjJ}}t_{\mathrm{hph}}^{\mathrm{BciI}} \tag{B.381}$$

$$0.5a_{\mathrm{AB}}v_{\mathrm{aAcd}}v_{\mathrm{abij}}t_{\mathrm{hph}}^{\mathrm{bdij}}t_{\mathrm{hph}}^{\mathrm{BcIJ}} \tag{B.382}$$

$$-1.a_{\mathrm{AB}}v_{\mathrm{abij}}v_{\mathrm{Abcd}}t_{\mathrm{hph}}^{\mathrm{aciI}}t_{\mathrm{hph}}^{\mathrm{BdjJ}} \tag{B.383}$$

$$0.5a_{\mathrm{AB}}v_{\mathrm{abij}}v_{\mathrm{Abcd}}t_{\mathrm{hph}}^{\mathrm{acIJ}}t_{\mathrm{hph}}^{\mathrm{Bdij}} \tag{B.384}$$

$$-0.5a_{\mathrm{AB}}v_{\mathrm{abcd}}v_{\mathrm{abij}}t_{\mathrm{hph}}^{\mathrm{AdjJ}}t_{\mathrm{hph}}^{\mathrm{BciI}} \tag{B.385}$$

$$0.25a_{\mathrm{AB}}v_{\mathrm{abcd}}v_{\mathrm{abij}}t_{\mathrm{hph}}^{\mathrm{Adij}}t_{\mathrm{hph}}^{\mathrm{BcIJ}} \tag{B.386}$$

References

(1) Heisenberg, W. Über quantentheoretische Umdeutung kinematischer und mechanischer Beziehungen. *Zeitschrift für Physik* **1925**, *33*, 879–893.

(2) Born, M.; Jordan, P. Zur Quantenmechanik. *Zeitschrift für Physik* **1925**, *34*, 858–888.

(3) Born, M.; Heisenberg, W.; Jordan, P. Zur Quantenmechanik. II. *Zeitschrift für Physik* **1926**, *35*, 557–615.

(4) Heisenberg, W. Über den anschaulichen Inhalt der quantentheoretischen Kinematik und Mechanik. *Zeitschrift für Physik* **1927**, *43*, 172–198.

(5) Schrödinger, E. Quantisierung als Eigenwertproblem. *Annalen der Physik* **1926**, *384*, 361–376.

(6) Schrödinger, E. Quantisierung als Eigenwertproblem (Zweite Mitteilung.) *Annalen der Physik* **1926**, *384*, 489–527.

(7) Schrödinger, E. Quantisierung als eigenwertproblem (Dritte Mitteilung.) *Annalen der physik* **1926**, *385*, 437–490.

(8) Schrödinger, E. Quantisierung als eigenwertproblem (Vierte Mitteilung.) *Annalen der physik* **1926**, *386*, 109–139.

(9) Dirac, P. A. M. On the Theory of Quantum Mechanics. *Proceedings of the Royal Society of London A: Mathematical, Physical and Engineering Sciences* **1926**, *112*, 661–677.

(10) Born, M.; Oppenheimer, R. Zur Quantentheorie der Molekeln. *Annalen der Physik* **1927**, *389*, 457–484.

(11) Hartree, D. R. The Wave Mechanics of an Atom with a Non-Coulomb Central Field. Part I. Theory and Methods. *Mathematical Proceedings of the Cambridge Philosophical Society* **Jan. 1928**, *24*, 89–110.

(12) Hartree, D. R. The Wave Mechanics of an Atom with a Non-Coulomb Central Field. Part II. Some Results and Discussion. *Mathematical Proceedings of the Cambridge Philosophical Society* **Jan. 1928**, *24*, 111–132.

(13) Fermi, E. Sulla quantizzazione del gas perfetto monoatomico. *Accad. Lincei, Atti* **1926**, *3*, 145–149.

(14) Slater, J. C. The Theory of Complex Spectra. *Physical Review* **1929**, *34*, 1293–1322.

(15) Slater, J. C. Note on Hartree's Method. *Phys. Rev.* **Jan. 1930**, *35*, 210–211.

(16) Fock, V. Nöherungsmethode zur Lösung des quantenmechanischen Mehrkörperproblems. *Zeitschrift für Physik* **1930**, *61*, 126–148.

(17) Dirac, P. A. M. The Quantum Theory of the Emission and Absorption of Radiation. *Proceedings of the Royal Society of London A: Mathematical, Physical and Engineering Sciences* **1927**, *114*, 243–265.

(18) Fock, V. Konfigurationsraum und zweite Quantelung. *Zeitschrift für Physik* **1932**, *75*, 622–647.

(19) Wick, G. C. The Evaluation of the Collision Matrix. *Phys. Rev.* **Oct. 1950**, *80*, 268–272.

(20) Shavitt, I. The Method of Configuration Interaction. **1977**, *3*, ed. by Schaefer HenryF., I., 189–275.

(21) Møller, C.; Plesset, M. S. Note on an approximation treatment for many-electron systems. *Physical Review* **1934**, *46*, 618.

(22) Coester, F. Bound states of a many-particle system. *Nuclear Physics* **1958**, *7*, 421–424.

(23) Čížek, J. On the Correlation Problem in Atomic and Molecular Systems. Calculation of Wavefunction Components in Ursell-Type Expansion Using Quantum-Field Theoretical Methods. *The Journal of Chemical Physics* **1966**, *45*, 4256–4266.

(24) Kümmel, H.; Lührmann, K. Equations for linked clusters and the energy variational principle. *Nuclear Physics A* **1972**, *191*, 525–534.

(25) Bartlett, R. J.; Musiał, M. Coupled-cluster theory in quantum chemistry. *Rev. Mod. Phys.* **Feb. 2007**, *79*, 291–352.

(26) Parkhill, J. A.; Lawler, K.; Head-Gordon, M. The perfect quadruples model for electron correlation in a valence active space. *The Journal of Chemical Physics* **2009**, *130*, 084101.

(27) Pople, J. A.; Head-Gordon, M.; Raghavachari, K. Quadratic configuration interaction. A general technique for determining electron correlation energies. *The Journal of chemical physics* **1987**, *87*, 5968–5975.

(28) Gwaltney, S. R.; Head-Gordon, M. A second-order perturbative correction to the coupled-cluster singles and doubles method: CCSD(2). *The Journal of Chemical Physics* **2001**, *115*, 2014–2021.

(29) Löwdin, P.-O. Studies in Perturbation Theory. IV. Solution of Eigenvalue Problem by Projection Operator Formalism. *Journal of Mathematical Physics* **1962**, *3*, 969–982.

(30) Stanton, J. F.; Bartlett, R. J. The equation of motion coupled-cluster method. A systematic biorthogonal approach to molecular excitation energies, transition probabilities, and excited state properties. *J. Chem. Phys.* **1993**, *98*, 7029–7039.

(31) Head-Gordon, M.; Rico, R. J.; Oumi, M.; Lee, T. J. A doubles correction to electronic excited states from configuration interaction in the space of single substitutions. *Chem. Phys. Lett.* **1994**, *219*, 21–29.

(32) Christiansen, O.; Koch, H.; Jørgensen, P. The second-order approximate coupled cluster singles and doubles model CC2. *Chemical Physics Letters* **1995**, *243*, 409–418.

(33) Becke, A. D. Perspective: Fifty years of density-functional theory in chemical physics. *J. Chem. Phys.* **2014**, *140*.

(34) Klimeš, J.; Michaelides, A. Perspective: Advances and challenges in treating van der Waals dispersion forces in density functional theory. *J. Chem. Phys.* **2012**, *137*, 120901.

(35) Hohenberg, P.; Kohn, W. Inhomogeneous Electron Gas. *Phys. Rev.* **Nov. 1964**, *136*, B864–B871.

(36) Kohn, W.; Sham, L. J. Self-Consistent Equations Including Exchange and Correlation Effects. *Phys. Rev.* **1965**, *140*, A1133–A1138.

(37) Dunlap, B. I.; Connolly, J. W. D.; Sabin, J. R. On some approximations in applications of XCC theory. *J. Chem. Phys.* **1979**, *71*, 3396–3402.

(38) Feyereisen, M.; Fitzgerald, G.; Komornicki, A. Use of approximate integrals in ab initio theory. An application in MP2 energy calculations. *Chem. Phys. Lett.* **1993**, *208*, 359–363.

(39) Mintmire, J. W.; Sabin, J. R.; Trickey, S. B. Local-density-functional methods in two-dimensionally periodic systems. Hydrogen and beryllium monolayers. *Phys. Rev. B* **1982**, *26*, 1743–1753.

(40) Vahtras, O.; Almlf, J.; Feyereisen, M. Integral approximations for LCAO-SCF calculations. *Chem. Phys. Lett.* **1993**, *213*, 514–518.

(41) RI-MP2: optimized auxiliary basis sets and demonstration of efficiency. *Chem. Phys. Lett.* **1998**, *294*, 143–152.

(42) Whitten, J. L. Coulombic potential energy integrals and approximations. *J. Chem. Phys.* **1973**, *58*, 4496–4501.

(43) Adler, T. B.; Werner, H.-J. Local explicitly correlated coupled-cluster methods: Efficient removal of the basis set incompleteness and domain errors. *J. Chem. Phys.* **2009**, *130*, 241101.

(44) Hylleraas, E. Über den Grundzustand des Heliumatoms. *Zeitschrift für Physik* **1928**, *48*, 469–494.

(45) Hylleraas, E. Neue Berechnung der Energie des Heliums im Grundzustande, sowie des tiefsten Terms von Ortho-Helium. *Zeitschrift für Physik* **1929**, *54*, 347–366.

(46) Klopper, W.; Kutzelnigg, W. Møller-Plesset calculations taking care of the correlation CUSP. *Chem. Phys. Lett.* **1987**, *134*, 17–22.

(47) Klopper, W.; Manby, F. R.; Ten-No, S.; Valeev, E. F. R12 methods in explicitly correlated molecular electronic structure theory. *International Reviews in Physical Chemistry* **2006**, *25*, 427–468.

(48) Kutzelnigg, W. r12-Dependent terms in the wave function as closed sums of partial wave amplitudes for large l. *Theoretica Chimica Acta* **1985**, *68*, 445–469.

(49) Noga, J.; Tunega, D.; Klopper, W.; Kutzelnigg, W. The performance of the explicitly correlated coupled cluster method. I. The four electron systems Be, Li^-, and LiH. *J. Chem. Phys.* **1995**, *103*, 309–320.

(50) Ten-no, S. Initiation of explicitly correlated Slater-type geminal theory. *Chem. Phys. Lett.* **2004**, *398*, 56–61.

(51) Valeev, E. F. Improving on the resolution of the identity in linear R12 ab initio theories. *Chem. Phys. Lett.* **2004**, *395*, 190–195.

(52) Jung, Y.; Lochan, R. C.; Dutoi, A. D.; Head-Gordon, M. Scaled opposite-spin second order Moller Plesset correlation energy: An economical electronic structure method. *J. Chem. Phys.* **2004**, *121*, 9793–9802.

(53) Lochan, R. C.; Jung, Y.; Head-Gordon, M. Scaled Opposite Spin Second Order Møller-Plesset Theory with Improved Physical Description of Long-Range Dispersion Interactions. *The Journal of Physical Chemistry A* **2005**, *109*, 7598–7605.

(54) Ahlrichs, R.; Driessler, F.; Lischka, H.; Staemmler, V.; Kutzelnigg, W. PNO-CI (pair natural orbital configuration interaction) and CEPA-PNO (coupled electron pair approximation with pair natural orbitals) calculations of molecular systems. II. The molecules BeH_2, BH, BH_3, CH_4, CH_3, NH_3 (planar and pyramidal), H_2O, OH_3^+, HF and the Ne atom. *J. Chem. Phys.* **1975**, *62*, 1235–1247.

(55) Pitoňák, M.; Neogrády, P.; Kellö, V.; Urban, M. Optimized virtual orbitals for relativistic calculations: an alternative approach to the basis set construction for correlation calculations. *Mol. Phys.* **2006**, *104*, 2277–2292.

(56) Adamowicz, L.; Bartlett, R. J. Optimized virtual orbital space for high-level correlated calculations. *J. Chem. Phys.* **1987**, *86*, 6314–6324.

(57) Adamowicz, L.; Bartlett, R. J.; Sadlej, A. J. Optimized virtual orbital space for high-level correlated calculations. II. Electric properties. *J. Chem. Phys.* **1988**, *88*, 5749–5758.

(58) Kinoshita, T.; Hino, O.; Bartlett, R. J. Singular value decomposition approach for the approximate coupled-cluster method. *J. Chem. Phys.* **2003**, *119*, 7756–7762.

(59) Hino, O.; Kinoshita, T.; Bartlett, R. J. Singular value decomposition applied to the compression of T3 amplitude for the coupled cluster method. *J. Chem. Phys.* **2004**, *121*, 1206–1213.

(60) Meyer, W. PNO-CI Studies of electron correlation effects. I. Configuration expansion by means of nonorthogonal orbitals, and application to the ground state and ionized states of methane. *J. Chem. Phys.* **1973**, *58*, 1017–1035.

(61) Neese, F.; Wennmohs, F.; Hansen, A. Efficient and accurate local approximations to coupled-electron pair approaches: An attempt to revive the pair natural orbital method. *J. Chem. Phys.* **2009**, *130*, 114108.

(62) Neese, F.; Hansen, A.; Liakos, D. G. Efficient and accurate approximations to the local coupled cluster singles doubles method using a truncated pair natural orbital basis. *J. Chem. Phys.* **2009**, *131*, 064103.

(63) Ziółkowski, M.; Jansík, B.; Kjaergaard, T.; Jørgensen, P. Linear scaling coupled cluster method with correlation energy based error control. *J. Chem. Phys.* **2010**, *133*, 014107.

(64) Kristensen, K.; Ziółkowski, M.; Jansík, B.; Kjaergaard, T.; Jørgensen, P. A Locality Analysis of the Divide-Expand-Consolidate Coupled Cluster Amplitude Equations. *Journal of Chemical Theory and Computation* **2011**, *7*, 1677–1694.

(65) Høyvik, I.-M.; Kristensen, K.; Jansik, B.; Jørgensen, P. The divide-expand-consolidate family of coupled cluster methods: Numerical illustrations using second order Møller-Plesset perturbation theory. *J. Chem. Phys.* **2012**, *136*, 014105.

(66) Flocke, N.; Bartlett, R. J. A natural linear scaling coupled-cluster method. *J. Chem. Phys.* **2004**, *121*, 10935–10944.

(67) Hughes, T. F.; Flocke, N.; Bartlett, R. J. Natural Linear-Scaled Coupled-Cluster Theory with Local Transferable Triple Excitations: Applications to Peptides. *The Journal of Physical Chemistry A* **2008**, *112*, 5994–6003.

(68) Li, W.; Piecuch, P. Improved Design of Orbital Domains within the Cluster-in-Molecule Local Correlation Framework: Single-Environment Cluster-in-Molecule Ansatz and Its Application to Local Coupled-Cluster Approach with Singles and Doubles. *The Journal of Physical Chemistry A* **2010**, *114*, 8644–8657.

(69) Li, W.; Piecuch, P.; Gour, J. R.; Li, S. Local correlation calculations using standard and renormalized coupled-cluster approaches. *J. Chem. Phys.* **2009**, *131*, 114109.

(70) Rolik, Z.; Szegedy, L.; Ladjánszki, I.; Ladóczki, B.; Kállay, M. An efficient linear-scaling CCSD(T) method based on local natural orbitals. *J. Chem. Phys.* **2013**, *139*, 094105.

(71) Rolik, Z.; Kállay, M. A general-order local coupled-cluster method based on the cluster-in-molecule approach. *J. Chem. Phys.* **2011**, *135*, 104111.

(72) Stoll, H.; Wagenblast, G.; Preuß, H. On the use of local basis sets for localized molecular orbitals. *Theoretica Chimica Acta* **1980**, *57*, 169–178.

(73) Gianinetti, E.; Raimondi, M.; Tornaghi, E. Modification of the Roothaan equations to exclude BSSE from molecular interaction calculations. *International Journal of Quantum Chemistry* **1996**, *60*, 157–166.

(74) Mo, Y.; Peyerimhoff, S. Theoretical analysis of electronic delocalization. *J. Chem. Phys.* **1998**, *109*, 1687–1697.

(75) Khaliullin, R. Z.; Head-Gordon, M.; Bell, A. T. An efficient self-consistent field method for large systems of weakly interacting components. *J. Chem. Phys.* **2006**, *124*, 204105.

(76) Khaliullin, R. Z.; Cobar, E. A.; Lochan, R. C.; Bell, A. T.; Head-Gordon, M. Unravelling the origin of intermolecular interactions using absolutely localized molecular orbitals. *J. Phys. Chem. A* **2007**, *111*, 8753–8765.

(77) Young, R. M.; Griffin, G. B.; Kammrath, A.; Ehrler, O. T.; Neumark, D. M. Time-resolved dynamics in acetonitrile cluster anions $(CH_3CN)_n^-$. *Chem. Phys. Lett.* **2010**, *485*, 59–63.

(78) Azar, J.; Kurlancheek, W.; Head-Gordon, M. Characterization of electronically excited states in anionic acetonitrile clusters. *Phys. Chem. Chem. Phys.* **2011**, *13*, 9147–9154.

(79) Young, R. M.; Azar, R. J.; Yandell, M. A.; King, S. B.; Head-Gordon, M.; Neumark, D. M. Iodide solvation in tetrahydrofuran clusters: $I^-(THF)_n$, $(1 \leq n \leq 30)$. *Mol. Phys.* **2012**, *110*, 1787–1799.

(80) Azar, R. J.; Head-Gordon, M. An energy decomposition analysis for intermolecular interactions from an absolutely localized molecular orbital reference at the coupled-cluster singles and doubles level. *J. Chem. Phys.* **2012**, *136*, 024103.

(81) Azar, R. J.; Horn, P. R.; Sundstrom, E. J.; Head-Gordon, M. Useful lower limits to polarization contributions to intermolecular interactions using a minimal basis of localized orthogonal orbitals: Theory and analysis of the water dimer. *The Journal of Chemical Physics* **2013**, *138*, 084102.

(82) Hart, E. J.; Boag, J. W. Absorption Spectrum of the Hydrated Electron in Water and in Aqueous Solutions. *Journal of the American Chemical Society* **1962**, *84*, 4090–4095.

(83) Hammer, N. I.; Shin, J.-W.; Headrick, J. M.; Diken, E. G.; Roscioli, J. R.; Weddle, G. H.; Johnson, M. A. How Do Small Water Clusters Bind an Excess Electron? *Science* **2004**, *306*, 675–679.

(84) Coe, J. Fundamental properties of bulk water from cluster ion data. *Int. Rev. Phys. Chem.* **2001**, *20*, 33–58.

(85) Coe, J. V.; Lee, G. H.; Eaton, J. G.; Arnold, S. T.; Sarkas, H. W.; Bowen, K. H.; Ludewigt, C.; Haberland, H.; Worsnop, D. R. Photoelectron spectroscopy of hydrated electron cluster anions, $(H_2O)^-_{n=2-69}$. *J. Chem. Phys.* **1990**, *92*, 3980–3982.

(86) Mitsui, M.; Ando, N.; Kokubo, S.; Nakajima, A.; Kaya, K. Coexistence of solvated electrons and solvent valence anions in negatively charged acetonitrile clusters, $(CH_3CN)^-_{(n=10-100)}$. *Phys. Rev. Lett.* **2003**, *91*, 153002.

(87) Xia, C.; Peon, J.; Kohler, B. Femtosecond electron ejection in liquid acetonitrile: Evidence for cavity electrons and solvent anions. *J. Chem. Phys.* **2002**, *117*, 8855–66.

(88) Bell, I. P.; Rodgers, M. A. J.; Burrows, H. D. Kinetic and thermodynamic character of reducing species produced on pulse radiolysis of acetonitrile. *J. Chem. Soc., Faraday Trans. 1* **1977**, *73*, 315–326.

(89) Shkrob, I.; Sauer, M. Electron localization in liquid acetonitrile. *J. Phys. Chem. A* **2002**, *106*, 9120–9131.

(90) Ehrler, O. T.; Griffin, G. B.; Young, R. M.; Neumark, D. M. Photoinduced Electron Transfer and Solvation in Iodide-doped Acetonitrile Clusters. *J. Phys. Chem. B* **2009**, *113*, 4031–4037.

(91) Takayanagi, T. Ab initio study of small acetonitrile cluster anions. *J. Chem. Phys.* **2005**, *122*, 244307.

(92) Takayanagi, T.; Hoshino, T.; Takahashi, K. Electronic structure calculations of acetonitrile cluster anions: Stabilization mechanism of molecular radical anions by solvation. *Chem. Phys.* **2006**, *324*, 679–688.

(93) Takayanagi, T. Theoretical simulations of dynamics of excess electron attachment to acetonitrile clusters. *Chem. Phys.* **2004**, *302*, 85–93.

(94) Timerghazin, Q. K.; Peslherbe, G. H. Electronic structure of the acetonitrile and acetonitrile dimer anions: A topological investigation. *J. Phys. Chem. B* **2008**, *112*, 520–528.

(95) Herbert, J.; Head-Gordon, M. Calculation of electron detachment energies for water cluster anions: An appraisal of electronic structure methods, with application to $(H2O)^-_{20}$ and $(H2O)^-_{24}$. *J. Phys. Chem. A* **2005**, *109*, 5217–5229.

(96) Stolow, A.; Bragg, A.; Neumark, D. Femtosecond time-resolved photoelectron spectroscopy. *Chem. Rev.* **2004**, *104*, 1719–1757.

(97) Adams, C. L.; Schneider, H.; Weber, J. M. Vibrational Autodetachment-Intramolecular Vibrational Relaxation Translated into Electronic Motion. *J. Phys. Chem. A* **2010**, *114*, 4017–4030.

(98) Shao, Y. et al. Advances in methods and algorithms in a modern quantum chemistry program package. *Phys. Chem. Chem. Phys.* **2006**, *8*, 3172–3191.

(99) Chai, J.-D.; Head-Gordon, M. Systematic optimization of long-range corrected hybrid density functionals. *J. Chem. Phys.* **2008**, *128*, 084106.

(100) Thomas H. Dunning, J.; McKoy, V. Nonempirical Calculations on Excited States: The Formaldehyde Molecule. *J. Chem Phys.* **1968**, *48*, 5263–5270.

(101) Dunning, T. H.; McKoy, V. Nonempirical Calculations on Excited States: The Ethylene Molecule. *J. Chem Phys.* **1967**, *47*, 1735–1747.

(102) Krylov, A. I. Equation-of-motion coupled-cluster methods for open-shell and electronically excited species: The Hitchhiker's guide to Fock space. *Annu. Rev. Phys. Chem.* **2008**, *59*, 433–462.

(103) Runge, E.; Gross, E. K. U. Density-Functional Theory for Time-Dependent Systems. *Phys. Rev. Lett.* **1984**, *52*, 997–1000.

(104) Casanova, D.; Rhee, Y. M.; Head-Gordon, M. Quasidegenerate scaled opposite spin second order perturbation corrections to single excitation configuration interaction. *J. Chem. Phys.* **2008**, *128*, 164106.

(105) WEINHOLD, F. Natural Bond Orbital Methods. *Encyclopedia of Computational Chemistry* **2002**.

(106) Reed, A. E.; Curtiss, L. A.; Weinhold, F. Intermolecular interactions from a natural bond orbital, donor-acceptor viewpoint. *Chem. Rev.* **1988**, *88*, 899–926.

(107) Herbert, J. M.; Head-Gordon, M. Charge penetration and the origin of large O-H vibrational red-shifts in hydrated-electron clusters, $(H2O)_n^-$. *J. Am. Chem. Soc.* **2006**, *128*, 13932–13939.

(108) Reisler, H.; Krylov, A. I. Interacting Rydberg and valence states in radicals and molecules: experimental and theoretical studies. *Int. Rev. Phys. Chem.* **2009**, *28*, 267–308.

(109) Heller, E. J. The semiclassical way to molecular spectroscopy. *Accounts Chem. Res.* **1981**, *14*, 368–375.

(110) Von Niessen, W.; Diercksen, G. H. F.; Cederbaum, L. S. On the accuracy of ionization potentials calculated by Green's functions. *J. Chem Phys.* **1977**, *67*, 4124–4131.

(111) Gilson, M. K.; Zhou, H.-X. Calculation of protein-ligand binding affinities. *Annu. Rev. Biophys. Biomolec. Struct.* **2007**, *36*, 21–42.

(112) Flower, D., *Molecular Collisions in the Interstellar Medium*; Cambridge University Press: Cambridge, 2007.

(113) Mandal, S.; Moudgil, M.; Mandal, S. K. Rational drug design. *European Journal of Pharmacology* **2009**, *625*, 90–100.

(114) Braga, D.; Grepioni, F. Intermolecular interactions in nonorganic crystal engineering. *Accounts Chem. Res.* **2000**, *33*, 601–608.

(115) Muthukumar, M.; Ober, C.; Thomas, E. Competing interactions and levels of ordering in self-organizing polymeric materials. *Science* **1997**, *277*, 1225–1232.

(116) Jeziorski, B.; Moszynski, R.; Szalewicz, K. Perturbation Theory Approach to Intermolecular Potential Energy Surfaces of van der Waals Complexes. *Chem. Rev.* **1994**, *94*, 1887–1930.

(117) Podeszwa, R.; Szalewicz, K. Accurate interaction energies for argon, krypton, and benzene dimers from perturbation theory based on the Kohn-Sham model. *Chem. Phys. Lett.* **2005**, *412*, 488–493.

(118) Hesselmann, A.; Jansen, G.; Schutz, M. Density-functional theory-symmetry-adapted intermolecular perturbation theory with density fitting: A new efficient method to study intermolecular interaction energies. *J. Chem. Phys.* **2005**, *122*, 014103.

(119) London, F. On the theory and system of molecular forces. *Quantum chemistry. Classic scientific papers,World Scientific, Singapore, 2000*, ed. by Hettema, H., 369–99.

(120) Korona, T.; Przybytek, M.; Jeziorski, B. Time-independent coupled cluster theory of the polarization propagator. Implementation and application of the singles and doubles model to dynamic polarizabilities and van der Waals constants. *Mol. Phys.* **2006**, *104*, 2303–2316.

(121) Korona, T. First-order exchange energy of intermolecular interactions from coupled cluster density matrices and their cumulants. *J. Chem. Phys.* **2008**, *128*, 224104.

(122) Korona, T.; Jeziorski, B. Dispersion energy from density-fitted density susceptibilities of singles and doubles coupled cluster theory. *J. Chem. Phys.* **2008**, *128*, 144107.

(123) Kitaura, K.; Morokuma, K. A new energy decomposition scheme for molecular interactions within the Hartree-Fock approximation. *International Journal of Quantum Chemistry* **1976**, *10*, 325–340.

(124) Frey, R. F.; Davidson, E. R. Energy partitioning of the self-consistent field interaction energy of ScCO. *J. Chem. Phys.* **1989**, *90*, 5555–5562.

(125) Cybulski, S. M.; Scheiner, S. Comparison of Morokuma and perturbation theory approaches to decomposition of interaction energy. $NH_4{}^+...NH_3$. *Chem. Phys. Lett.* **1990**, *166*, 57–64.

(126) Ghanty, T.; Ghosh, S. Hydrogen-bonding interactions in selected super-molecular systems: Electron density point of view. *J. Phys. Chem. A* **2003**, *107*, 7062–7067.

(127) Liu, T.; Zhu, W.; Gu, J.; Shen, J.; Luo, X.; Chen, G.; Puah, C.; Silman, I.; Chen, K.; Sussman, J.; Jiang, H. Additivity of cation-pi interactions: An ab initio computational study on pi-cation-pi sandwich complexes. *J. Phys. Chem. A* **2004**, *108*, 9400–9405.

(128) Pavelka, M.; Burda, J. Theoretical description of copper Cu(I)/Cu(II) complexes in mixed ammine-aqua environment. DFT and ab initio quantum chemical study. *Chem. Phys.* **2005**, *312*, 193–204.

(129) Glendening, E. D.; Streitwieser, A. Natural energy decomposition analysis: An energy partitioning procedure for molecular interactions with application to weak hydrogen bonding, strong ionic, and moderate donor-acceptor interactions. *J. Chem. Phys.* **1994**, *100*, 2900–2909.

(130) Foster, J.; Weinhold, F. Natural Hybrid Orbitals. *J. Am. Chem. Soc.* **1980**, *102*, 7211–7218.

(131) Stevens, W. J.; Fink, W. H. Frozen fragment reduced variational space analysis of hydrogen bonding interactions. Application to the water dimer. *Chem. Phys. Lett.* **1987**, *139*, 15–22.

(132) Bagus, P. S.; Hermann, K.; Bauschlicher, C. W. A new analysis of charge transfer and polarization for ligand-metal bonding: Model studies of Al4CO and Al4NH3. *J. Chem. Phys.* **1984**, *80*, 4378–4386.

(133) Mo, Y.; Gao, J.; Peyerimhoff, S. Energy decomposition analysis of intermolecular interactions using a block-localized wave function approach. *J. Chem. Phys.* **2000**, *112*, 5530–5538.

(134) Gianinetti, E.; Vandoni, I.; Famulari, A.; Raimondi, M. Extension of the SCF-MI Method to the Case of K Fragments one of which is an Open-Shell System. **1998**, *31*, 251–266.

(135) Nagata, T.; Takahashi, O.; Saito, K.; Iwata, S. Basis set superposition error free self-consistent field method for molecular interaction in multi-component systems: Projection operator formalism. *J. Chem. Phys.* **2001**, *115*, 3553–3560.

(136) Liu, B.; McLean, A. D. The interacting correlated fragments model for weak interactions, basis set superposition error, and the helium dimer potential. *J. Chem. Phys.* **1989**, *91*, 2348–2359.

(137) Boys, S. F.; Bernardi, F. Calculation of Small Molecular Interactions by Differences of Separate Total Energies - Some Procedures with Reduced Errors. *Mol. Phys.* **1970**, *19*, 553.

(138) Khaliullin, R. Z.; Bell, A. T.; Head-Gordon, M. Analysis of charge transfer effects in molecular complexes based on absolutely localized molecular orbitals. *J. Chem. Phys.* **2008**, *128*, 184112.

(139) Ess, D. H.; Goddard III, W. A.; Periana, R. A. Electrophilic, Ambiphilic, and Nucleophilic C-H Bond Activation: Understanding the Electronic Continuum of C-H Bond Activation Through Transition-State and Reaction Pathway Interaction Energy Decompositions. *Organometallics* **2010**, *29*, 6459–6472.

(140) Swanson, J. M. J.; Simons, J. Role of Charge Transfer in the Structure and Dynamics of the Hydrated Proton. *J. Phys. Chem. B* **2009**, *113*, 5149–5161.

(141) Ramos-Cordoba, E.; Lambrecht, D. S.; Head-Gordon, M. Charge-transfer and the hydrogen bond: Spectroscopic and structural implications from electronic structure calculations. *Faraday Disc.* **2011**, *150*, 345–362.

(142) Kristyán, S.; Pulay, P. Can (semi)local density functional theory account for the London dispersion forces? *Chem. Phys. Lett.* **1994**, *229*, 175–180.

(143) Hobza, P.; Šponer, J.; Reschel, T. Density functional theory and molecular clusters. *Journal of Computational Chemistry* **1995**, *16*, 1315–1325.

(144) Dreuw, A.; Weisman, J.; Head-Gordon, M. Long-range charge-transfer excited states in time-dependent density functional theory require non-local exchange. *J. Chem. Phys.* **2003**, *119*, 2943–2946.

(145) Moller, C.; Plesset, M. Note on an approximation treatment for many-electron systems. *Phys. Rev.* **1934**, *46*, 0618–0622.

(146) Xantheas, S. S.; Dunning, T. H. Ab initio studies of cyclic water clusters $(H2O)_n$, n=1-6. I. Optimal structures and vibrational spectra. *J. Chem. Phys.* **1993**, *99*, 8774–8792.

(147) Kim, K.; Jordan, K. D. Comparison of Density Functional and MP2 Calculations on the Water Monomer and Dimer. *The Journal of Physical Chemistry* **1994**, *98*, 10089–10094.

(148) Jurecka, P.; Sponer, J.; Cerny, J.; Hobza, P. Benchmark database of accurate (MP2 and CCSD(T) complete basis set limit) interaction energies of small model complexes, DNA base pairs, and amino acid pairs. *Phys. Chem. Chem. Phys.* **2006**, *8*, 1985–1993.

(149) Sponer, J.; Hobza, P. MP2 and CCSD(T) study on hydrogen bonding, aromatic stacking and nonaromatic stacking. *Chem. Phys. Lett.* **1997**, *267*, 263–270.

(150) Cybulski, S. M.; Lytle, M. L. The origin of deficiency of the supermolecule second-order Møller-Plesset approach for evaluating interaction energies. *J. Chem. Phys.* **2007**, *127*, 141102.

(151) Lee, M.; Maslen, P.; Head-Gordon, M. Closely approximating second-order Møller-Plesset perturbation theory with a local triatomics in molecules model. *J. Chem. Phys.* **2000**, *112*, 3592–3601.

(152) Kurlancheek, W.; Head-Gordon, M. Second order Møller-Plesset energy decomposition analysis for intermolecular interactions with applications to ehtylene dimer, He-BeO complex, and the water dimer. *A work in progress* **2011**.

(153) Purvis, G. D.; Bartlett, R. J. A full coupled-cluster singles and doubles model: The inclusion of disconnected triples. *J. Chem. Phys.* **1982**, *76*, 1910–1918.

(154) Raghavachari, K.; Trucks, G. W.; Pople, J. A.; Head-Gordon, M. A fifth-order perturbation comparison of electron correlation theories. *Chem. Phys. Lett.* **1989**, *157*, 479–483.

(155) Head-Gordon, M.; Maslen, P.; White, C. A tensor formulation of many-electron theory in a nonorthogonal single-particle basis. *J. Chem. Phys.* **1998**, *108*, 616–625.

(156) Head-Gordon, M.; Lee, M.; Maslen, P.; Van Voorhis, T.; Gwaltney, S. Tensors in Electronic Structure Theory: Basic Concepts and Applications to Electron Correlation Models. *Modern Methods and Algorithms of Quantum Chemistry* **2000**, *3*, 593–638.

(157) Subotnik, J.; Dutoi, A.; Head-Gordon, M. Fast localized orthonormal virtual orbitals which depend smoothly on nuclear coordinates. *J. Chem. Phys.* **2005**, *123*, 114108.

(158) Boys, S. F. Construction of Some Molecular Orbitals to Be Approximately Invariant for Changes from One Molecule to Another. *Rev. Mod. Phys.* **1960**, *32*, 296–299.

(159) Jurecka, P.; Sponer, J.; Cerny, J.; Hobza, P. Benchmark database of accurate (MP2 and CCSD(T) complete basis set limit) interaction energies of small model complexes, DNA base pairs, and amino acid pairs. *Phys. Chem. Chem. Phys.* **2006**, *8*, 1985–1993.

(160) Fellers, R.; Leforestier, C.; Braly, L.; Brown, M.; Saykally, R. Spectroscopic determination the water pair potential. *Science* **1999**, *284*, 945–948.

(161) Piquemal, J.; Marquez, A.; Parisel, O.; Giessner-Prettre, C. A CSOV study of the difference between HF and DFT intermolecular interaction energy values: The importance of the charge transfer contribution. *J. Comput. Chem.* **2005**, *26*, 1052–1062.

(162) Glendening, E. D. Natural energy decomposition analysis: Extension to density functional methods and analysis of cooperative effects in water clusters. *J. Phys. Chem. A* **2005**, *109*, 11936–11940.

(163) Cobar, E.; Horn, P.; Bergman, R.; Head-Gordon, M. Examination of the hydrogen-bonding networks in small water clusters (n = 2-5, 13, 17) using absolutely localized molecular orbital energy decomposition analysis. *Physical Chemistry Chemical Physics* **2012**, *14*, 15328.

(164) Dion, M.; Rydberg, H.; Schroder, E.; Langreth, D.; Lundqvist, B. Van der Waals density functional for general geometries. *Phys. Rev. Lett.* **2004**, *92*, 246401.

(165) Grimme, S. Semiempirical GGA-type density functional constructed with a long-range dispersion correction. *J. Comput. Chem.* **2006**, *27*, 1787–1799.

(166) Chai, J.-D.; Head-Gordon, M. Systematic optimization of long-range corrected hybrid density functionals. *J. Chem. Phys.* **2008**, *128*, 084106.

(167) Tkatchenko, A.; Scheffler, M. Accurate Molecular Van Der Waals Interactions from Ground-State Electron Density and Free-Atom Reference Data. *Phys. Rev. Lett.* **2009**, *102*, 073005.

(168) Tkatchenko, A.; DiStasio Jr., R. A.; Head-Gordon, M.; Scheffler, M. Dispersion-corrected Møller-Plesset second-order perturbation theory. *J. Chem. Phys.* **2009**, *131*, 094106.

(169) Pitonak, M.; Hesselmann, A. Accurate Intermolecular Interaction Energies from a Combination of MP2 and TDDFT Response Theory. *J. Chem. Theory Comput.* **2010**, *6*, 168–178.

(170) Szabo, A.; Ostlund, N. S. The correlation energy in the random phase approximation: Intermolecular forces between closed-shell systems. *J. Chem. Phys.* **1977**, *67*, 4351–4360.

(171) Tao, F. Ab initio calculation of the interaction potential for the krypton dimer: The use of bond function basis sets. *J. Chem. Phys.* **1999**, *111*, 2407–2413.

(172) Ogilvie, J.; Wang, F. Y. Potential-energy functions of diatomic molecules of the noble gases I. Like nuclear species. *Journal of Molecular Structure* **1992**, *273*, 277–290.

(173) Giese, T.; Audette, V.; York, D. Examination of the correlation energy and second virial coefficients from accurate ab initio calculations of rare-gas dimers. *J. Chem. Phys.* **2003**, *119*, 2618–2622.

(174) Woon, D. E. Benchmark calculations with correlated molecular wave functions. V. The determination of accurate ab initio intermolecular potentials for He_2, Ne_2, and Ar_2. *J. Chem. Phys.* **1994**, *100*, 2838–2850.

(175) Tsuzuki, S.; Uchimaru, T.; Tanabe, K. Intermolecular interaction potentials of methane and ethylene dimers calculated with the Møller-Plesset, coupled cluster and density functional methods. *Chem. Phys. Lett.* **1998**, *287*, 202–208.

(176) Li, A. H.-T.; Chao, S. D. Interaction energies of dispersion-bound methane dimer from coupled cluster method at complete basis set limit. *Journal of Molecular Structure* **2009**, *897*, 90–94.

(177) Craw, J. S.; de Almeida, W. B.; Hinchliffe, A. Theoretical vibrational spectra of acetylene dimer: T and cyclic configurations. *Journal of Molecular Structure* **1989**, *201*, 69–74.

(178) Karpfen, A. The dimer of acetylene and the dimer of diacetylene: A floppy and a very floppy molecule. *J. Phys. Chem. A* **1999**, *103*, 11431–11441.

(179) King, R. A. On the accuracy of spin-component-scaled perturbation theory (SCS-MP2) for the potential energy surface of the ethylene dimer. *Mol. Phys.* **2009**, *107*, 789–795.

(180) Weigend, F.; Haser, M.; Patzelt, H.; Ahlrichs, R. RI-MP2: optimized auxiliary basis sets and demonstration of efficiency. *Chem. Phys. Lett.* **1998**, *294*, 143–152.

(181) Lewis, G. Acids and bases. *J. Frankl. Inst.* **1938**, *226*, 293–313.

(182) Jagielska, A.; Moszynski, R.; Piela, L. Ab initio theoretical study of interactions in borazane molecule. *J. Chem. Phys.* **1999**, *110*, 947–954.

(183) Ha, T.-K. Ab initio SCF and CI study of the electronic structure of BH_3CO. *Journal of Molecular Structure* **1976**, *30*, 103–111.

(184) Szabo, A.; Ostlund, N. S., *Modern Quantum Chemistry*; Dover Publications: New York, 1996.

(185) Fehlner, T. P.; Mappes, G. W. Mass spectrometric investigation of the low-pressure pyrolysis of borane carbonyl. Bond dissociation energy of diborane. *The Journal of Physical Chemistry* **1969**, *73*, 873–882.

(186) Burg, A. B. The Mechanism of Decomposition of Borine Carbonyl. *Journal of the American Chemical Society* **1952**, *74*, 3482–3485.

(187) Bauer, S. H. Energetics of the Boranes. II. Kinetic Consequences of the Diborane-Borane Equilibrium. Comments on the Decomposition of OC:BH3. *Journal of the American Chemical Society* **1956**, *78*, 5775–5782.

(188) Garabedian, M. E.; Benson, S. W. The Kinetics of the Decomposition of BH_3CO and the Bond Dissociation Energy of B_2H_6. *Journal of the American Chemical Society* **1964**, *86*, 176–182.

(189) Raha, K.; Peters, M. B.; Wang, B.; Yu, N.; WollaCott, A. M.; Westerhoff, L. M.; Merz, K. M. The role of quantum mechanics in structure-based drug design. *Drug Discov. Today* **2007**, *12*, 725–731.

(190) Mandal, S.; Moudgil, M.; Mandal, S. K. Rational drug design. *Eur. J. Pharmacol.* **2009**, *625*, 90–100.

(191) Piquemal, J. P.; Perera, L.; Cisneros, G. A.; Ren, P. Y.; Pedersen, L. G.; Darden, T. A. Towards accurate solvation dynamics of divalent cations in water using the polarizable amoeba force field: From energetics to structure. *J. Chem. Phys.* **2006**, *125*, 054511.

(192) Stone, A. J., *The Theory of Intermolecular Forces*; Oxford University Press: Oxford, 1997.

(193) Jeziorski, B.; Moszynski, R.; Szalewicz, K. Perturbation-Theory Approach to Intermolecular Potential-Energy Surfaces of Van-Der-Waals Complexes. *Chem. Rev.* **1994**, *94*, 1887–1930.

(194) Szalewicz, K.; Patkowski, K.; Jeziorski, B. In *Intermolecular Forces and Clusters II*; Springer-Verlag: 2005; Vol. 116, pp 43–117.

(195) Misquitta, A. J.; Podeszwa, R.; Jeziorski, B.; Szalewicz, K. Intermolecular potentials based on symmetry-adapted perturbation theory with dispersion energies from time-dependent density-functional calculations. *J. Chem. Phys.* **2005**, *123*, 214103.

(196) Hesselmann, A.; Jansen, G.; Schutz, M. Density-functional theory-symmetry-adapted intermolecular perturbation theory with density fitting: A new efficient method to study intermolecular interaction energies. *J. Chem. Phys.* **2005**, *122*, 014103.

(197) Hankins, D.; Moskowitz, J. W.; Stillinger, F. H. Water molecule interactions. *J. Chem. Phys.* **1970**, *53*, 4544.

(198) Fedorov, D. G.; Kitaura, K. Extending the power of quantum chemistry to large systems with the fragment molecular orbital method. *J. Phys. Chem. A* **2007**, *111*, 6904–6914.

(199) Gordon, M. S.; Fedorov, D. G.; Pruitt, S. R.; Slipchenko, L. V. Fragmentation Methods: A Route to Accurate Calculations on Large Systems. *Chem. Rev.* **2012**, *112*, 632–672.

(200) Gordon, M. S.; Freitag, M. A.; Bandyopadhyay, P.; Jensen, J. H.; Kairys, V.; Stevens, W. J. The effective fragment potential method: A QM-based MM approach to modeling environmental effects in chemistry. *J. Phys. Chem. A* **2001**, *105*, 293–307.

(201) Gordon, M. S.; Mullin, J. M.; Pruitt, S. R.; Roskop, L. B.; Slipchenko, L. V.; Boatz, J. A. Accurate Methods for Large Molecular Systems. *J. Phys. Chem. B* **2009**, *113*, 9646–9663.

(202) Ren, P. Y.; Ponder, J. W. Polarizable atomic multipole water model for molecular mechanics simulation. *J. Phys. Chem. B* **2003**, *107*, 5933–5947.

(203) Ponder, J. W.; Wu, C.; Ren, P. Y.; Pande, V. S.; Chodera, J. D.; Schnieders, M. J.; Haque, I.; Mobley, D. L.; Lambrecht, D. S.; DiStasio, R. A.; Head-Gordon, M.; Clark, G. N. I.; Johnson, M. E.; Head-Gordon, T. Current Status of the AMOEBA Polarizable Force Field. *J. Phys. Chem. B* **2010**, *114*, 2549–2564.

(204) Ziegler, T.; Rauk, A. On the calculation of bonding energies by the Hartree Fock Slater method. *Theoretica Chimica Acta* **1977**, *46*, 1–10.

(205) Mitoraj, M. P.; Michalak, A.; Ziegler, T. A Combined Charge and Energy Decomposition Scheme for Bond Analysis. *J. Chem. Theor. Comput.* **2009**, *5*, 962–975.

(206) Weinhold, F.; Landis, C., *Valency and Bonding: A Natural Bond Orbital Donor-Acceptor Perspective*; Cambridge University Press: 2005, p 760.

(207) Glendening, E. D.; Landis, C. R.; Weinhold, F. Natural bond orbital methods. *Wiley Interdisciplinary Reviews: Computational Molecular Science* **2012**, *2*, 1–42.

(208) Wu, Q.; Ayers, P. W.; Zhang, Y. K. Density-based energy decomposition analysis for intermolecular interactions with variationally determined intermediate state energies. *J. Chem. Phys.* **2009**, *131*, 164112.

(209) Chen, W.; Gordon, M. S. Energy decomposition analyses for many-body interaction and applications to water complexes. *J. Phys. Chem.* **1996**, *100*, 14316–14328.

(210) Fedorov, D. G.; Kitaura, K. Pair interaction energy decomposition analysis. *J. Comput. Chem.* **2007**, *28*, 222–237.

(211) Su, P. F.; Li, H. Energy decomposition analysis of covalent bonds and intermolecular interactions. *J. Chem. Phys.* **2009**, *131*, 014102.

(212) Mo, Y. R.; Gao, J. L.; Peyerimhoff, S. D. Energy decomposition analysis of intermolecular interactions using a block-localized wave function approach. *J. Chem. Phys.* **2000**, *112*, 5530–5538.

(213) Mo, Y. R.; Bao, P.; Gao, J. L. Energy decomposition analysis based on a block-localized wavefunction and multistate density functional theory. *Phys. Chem. Chem. Phys.* **2011**, *13*, 6760–6775.

(214) Gianinetti, E.; Raimondi, M.; Tornaghi, E. Modification of the Roothaan equations to exclude BSSE from molecular interaction calculations. *Int. J. Quantum Chem.* **1996**, *60*, 157–166.

(215) Nagata, T.; Takahashi, O.; Saito, K.; Iwata, S. Basis set superposition error free self-consistent field method for molecular interaction in multi-component systems: Projection operator formalism. *J. Chem. Phys.* **2001**, *115*, 3553–3560.

(216) Lochan, R. C.; Khaliullin, R. Z.; Head-Gordon, M. Interaction of molecular hydrogen with open transition metal centers for enhanced binding in metal-organic frameworks: A computational study. *Inorg. Chem.* **2008**, *47*, 4032–4044.

(217) Swanson, J. M. J.; Simons, J. Role of Charge Transfer in the Structure and Dynamics of the Hydrated Proton. *J. Phys. Chem. B* **2009**, *113*, 5149–5161.

(218) Ess, D. H.; Gunnoe, T. B.; Cundari, T. R.; Goddard, W. A.; Periana, R. A. Ligand Lone-Pair Influence on Hydrocarbon C-H Activation A Computational Perspective. *Organometallics* **2010**, *29*, 6801–6815.

(219) Ess, D. H.; Goddard, W. A.; Periana, R. A. Electrophilic, Ambiphilic, and Nucleophilic C-H Bond Activation: Understanding the Electronic Continuum of C-H Bond Activation Through Transition-State and Reaction Pathway Interaction Energy Decompositions. *Organometallics* **2010**, *29*, 6459–6472.

(220) Ramos-Cordoba, E.; Lambrecht, D. S.; Head-Gordon, M. Charge-transfer and the hydrogen bond: Spectroscopic and structural implications from electronic structure calculations. *Faraday Disc.* **2011**, *150*, 345–362.

(221) Khaliullin, R. Z.; Bell, A. T.; Head-Gordon, M. Electron Donation in the Water-Water Hydrogen Bond. *Chem. Eur. J.* **2009**, *15*, 851–855.

(222) Martin, R. L. Natural transition orbitals. *J. Chem. Phys.* **2003**, *118*, 4775–4777.

(223) Kinoshita, T.; Hino, O.; Bartlett, R. J. Singular value decomposition approach for the approximate coupled-cluster method. *J. Chem. Phys.* **2003**, *119*, 7756–7762.

(224) Bell, F.; Lambrecht, D. S.; Head-Gordon, M. Higher order singular value decomposition in quantum chemistry. *Mol. Phys.* **2010**, *108*, 2759–2773.

(225) Boys, S. F. Construction of Some Molecular Orbitals to Be Approximately Invariant for Changes from One Molecule to Another. *Rev. Mod. Phys.* **1960**, *32*, 296.

(226) Edmiston, C.; Ruedenberg, K. Localized Atomic and Molecular Orbitals. *Rev. Mod. Phys.* **1963**, *35*, 457.

(227) Mayer, I. Towards a "Chemical" Hamiltonian. *Int. J. Quantum Chem.* **1983**, *23*, 341–363.

(228) Mayer, I.; Vibók, Á. Intermolecular SCF method without bsse: the closed-shell case. *Chem. Phys. Lett.* **1987**, *140*, 558–564.

(229) Weinhold, F.; Carpenter, J. E. Some Remarks on Nonorthogonal Orbitals in Quantum-Chemistry. *Theochem-Journal of Molecular Structure* **1988**, *42*, 189–202.

(230) Carlson, B. C.; Keller, J. M. Orthogonalization Procedures and the Localization of Wannier Functions. *Phys. Rev.* **1957**, *105*, 102–103.

(231) Löwdin, P. O. On the Non-Orthogonality Problem Connected with the Use of Atomic Wave Functions in the Theory of Molecules and Crystals. *J. Chem. Phys.* **1950**, *18*, 365–375.

(232) Liang, W. Z.; Head-Gordon, M. Approaching the basis set limit in density functional theory calculations using dual basis sets without diagonalization. *J. Phys. Chem. A* **2004**, *108*, 3206–3210.

(233) Liang, W. Z.; Head-Gordon, M. An exact reformulation of the diagonalization step in electronic structure calculations as a set of second order nonlinear equations. *J. Chem. Phys.* **2004**, *120*, 10379–10384.

(234) Weinhold, F. Resonance character of hydrogen-bonding interactions in water and other H-bonded species. *Adv. Protein Chem.* **2006**, *72*, 121.

(235) Kendall, R.; Dunning, T.; Harrison, R. Electron affinities of the first-row atoms revisited. Systematic basis sets and wave functions. *J. Chem. Phys.* **1992**, *96*, 6796–6806.

(236) Woon, D. E.; Dunning, T. H. Gaussian basis sets for use in correlated molecular calculations. IV. Calculation of static electrical response properties. *J. Chem. Phys.* **1994**, *100*, 2975–2988.

(237) Cai, Z.; Sendt, K.; Reimers, J. Failure of density-functional theory and time-dependent density-functional theory for large extended pi systems. *J. Chem. Phys.* **2002**, *117*, 5543–5549.

(238) Van Gisbergen, S.; Osinga, V.; Gritsenko, O.; van Leeuwen, R.; Snijders, J.; Baerends, E. Improved density functional theory results for frequency-dependent polarizabilities, by the use of an exchange-correlation potential with correct asymptotic behavior. *J. Chem. Phys.* **1996**, *105*, 3142–3151.

(239) Stephens, P. J.; Devlin, F. J.; Chabalowski, C. F.; Frisch, M. J. Ab Initio Calculation of Vibrational Absorption and Circular Dichroism Spectra Using Density Functional Force Fields. *The Journal of Physical Chemistry* **1994**, *98*, 11623–11627.

(240) Zhao, Y.; Truhlar, D. G. A new local density functional for main-group thermochemistry, transition metal bonding, thermochemical kinetics, and noncovalent interactions. *J. Chem. Phys.* **2006**, *125*, 194101.

(241) Zhao, Y.; Truhlar, D. G. The M06 suite of density functionals for main group thermochemistry, thermochemical kinetics, noncovalent interactions, excited states, and transition elements: two new functionals and systematic testing of four M06-class functionals and 12 other functionals. *Theoretical Chemistry Accounts* **2008**, *120*, 215–241.

(242) Perdew, J. P.; Burke, K.; Ernzerhof, M. Generalized Gradient Approximation Made Simple. *Phys. Rev. Lett.* **1996**, *77*, 3865–3868.

(243) Adamo, C.; Scuseria, G. E.; Barone, V. Accurate excitation energies from time-dependent density functional theory: Assessing the PBE0 model. *J. Chem. Phys.* **1999**, *111*, 2889–2899.

(244) Chai, J.-D.; Head-Gordon, M. Long-range corrected hybrid density functionals with damped atom-atom dispersion corrections. *Phys. Chem. Chem. Phys.* **2008**, *10*, 6615–6620.

(245) Warshel, A.; Levitt, M. Theoretical studies of enzymic reactions: Dielectric, electrostatic and steric stabilization of the carbonium ion in the reaction of lysozyme. *Journal of Molecular Biology* **1976**, *103*, 227–249.

(246) Senn, H. M.; Thiel, W. QM/MM Methods for Biomolecular Systems. *Angewandte Chemie International Edition* **2009**, *48*, 1198–1229.

(247) Saebø, S.; Pulay, P. Local configuration interaction: An efficient approach for larger molecules. *Chem. Phys. Lett.* **1985**, *113*, 13–18.

(248) Pulay, P.; Saebø, S. Orbital-invariant formulation and second-order gradient evaluation in Møller-Plesset perturbation theory. *Theoretica Chimica Acta* **1986**, *69*, 357–368.

(249) Lee, M. S.; Maslen, P. E.; Head-Gordon, M. Closely approximating second-order Møller-Plesset perturbation theory with a local triatomics in molecules model. *J. Chem. Phys.* **2000**, *112*, 3592–3601.

(250) Hampel, C.; Werner, H.-J. Local treatment of electron correlation in coupled cluster theory. *J. Chem. Phys.* **1996**, *104*, 6286–6297.

(251) Schútz, M.; Werner, H.-J. Local perturbative triples correction (T) with linear cost scaling. *Chem. Phys. Lett.* **2000**, *318*, 370–378.

(252) Schútz, M. Low-order scaling local electron correlation methods. V. Connected triples beyond (T): Linear scaling local CCSDT-1b. *J. Chem. Phys.* **2002**, *116*, 8772–8785.

(253) Ayala, P. Y.; Scuseria, G. E. Linear scaling second-order Møller-Plesset theory in the atomic orbital basis for large molecular systems. *J. Chem. Phys.* **1999**, *110*, 3660–3671.

(254) Lambrecht, D. S.; Doser, B.; Ochsenfeld, C. Rigorous integral screening for electron correlation methods. *J. Chem. Phys.* **2005**, *123*, 184102.

(255) White, C. A.; Head-Gordon, M. Rotating around the quartic angular momentum barrier in fast multipole method calculations. *J. Chem. Phys.* **1996**, *105*, 5061–5067.

(256) White, C. A.; Head-Gordon, M. A J matrix engine for density functional theory calculations. *J. Chem. Phys.* **1996**, *104*, 2620–2629.

(257) Challacombe, M.; Schwegler, E.; Almlöf, J. Fast assembly of the Coulomb matrix: A quantum chemical tree code. *J. Chem. Phys.* **1996**, *104*, 4685–4698.

(258) Greengard, L. F. The Rapid Evaluation of Potential Fields in Particle Systems., Ph.D. Thesis, New Haven, CT, USA, 1987.

(259) Greengard, L.; Rokhlin, V. A fast algorithm for particle simulations. *Journal of Computational Physics* **1987**, *73*, 325–348.

(260) White, C. A.; Head-Gordon, M. Derivation and efficient implementation of the fast multipole method. *J. Chem. Phys.* **1994**, *101*, 6593–6605.

(261) Schwegler, E.; Challacombe, M.; Head-Gordon, M. Linear scaling computation of the Fock matrix. II. Rigorous bounds on exchange integrals and incremental Fock build. *J. Chem. Phys.* **1997**, *106*, 9708–9717.

(262) Ochsenfeld, C.; White, C. A.; Head-Gordon, M. Linear and sublinear scaling formation of Hartree-Fock-type exchange matrices. *J. Chem. Phys.* **1998**, *109*, 1663–1669.

(263) Ochsenfeld, C. Linear scaling exchange gradients for Hartree-Fock and hybrid density functional theory. *Chem. Phys. Lett.* **2000**, *327*, 216–223.

(264) Chen, X.; Langlois, J.-M.; Goddard, W. Dual-space approach for density-functional calculations of two- and three-dimensional crystals using Gaussian basis functions. *Phys. Rev. B* **1995**, *52*, 2348–2361.

(265) Galli, G.; Parrinello, M. Large scale electronic structure calculations. *Phys. Rev. Lett.* **1992**, *69*, 3547–3550.

(266) Ordejón, P.; Drabold, D.; Grumbach, M.; Martin, R. Unconstrained minimization approach for electronic computations that scales linearly with system size. *Phys. Rev. B* **1993**, *48*, 14646–14649.

(267) Li, X.-P.; Nunes, R.; Vanderbilt, D. Density-matrix electronic-structure method with linear system-size scaling. *Phys. Rev. B* **1993**, *47*, 10891–10894.

(268) Millam, J. M.; Scuseria, G. E. Linear scaling conjugate gradient density matrix search as an alternative to diagonalization for first principles electronic structure calculations. *J. Chem. Phys.* **1997**, *106*, 5569–5577.

(269) Scuseria, G. E. Linear Scaling Density Functional Calculations with Gaussian Orbitals. *The Journal of Physical Chemistry A* **1999**, *103*, 4782–4790.

(270) Šimunek, J.; Noga, J. Hartree-Fock via variational coupled cluster theory: An alternative way to diagonalization free algorithm. *AIP Conference Proceedings* **2012**, *1504*, 143–151.

(271) Lee, M. S.; Head-Gordon, M. Polarized atomic orbitals for self-consistent field electronic structure calculations. *J. Chem. Phys.* **1997**, *107*, 9085–9095.

(272) Lee, M. S.; Head-Gordon, M. Absolute and relative energies from polarized atomic orbital self-consistent field calculations and a second order correction.: Convergence with size and composition of the secondary basis. *Computers & Chemistry* **2000**, *24*, 295–301.

(273) Liang; Head-Gordon, M. Approaching the Basis Set Limit in Density Functional Theory Calculations Using Dual Basis Sets without Diagonalization. *The Journal of Physical Chemistry A* **2004**, *108*, 3206–3210.

(274) Steele, R. P.; Shao, Y.; DiStasio, R. A.; Head-Gordon, M. Dual-Basis Analytic Gradients. 1. Self-Consistent Field Theory. *The Journal of Physical Chemistry A* **2006**, *110*, 13915–13922.

(275) Steele, R. P.; Head-Gordon, M. Dual-basis self-consistent field methods: 6-31G* calculations with a minimal 6-4G primary basis. *Mol. Phys.* **2007**, *105*, 2455–2473.

(276) Kobayashi, M.; Nakai, H. In *Linear-Scaling Techniques in Computational Chemistry and Physics*, Zalesny, R., Papadopoulos, M. G., Mezey, P. G., Leszczynski, J., Eds.; Challenges and Advances in Computational Chemistry and Physics, Vol. 13; Springer Netherlands: 2011, pp 97–127.

(277) Yang, W.; Lee, T.-S. A density-matrix divide-and-conquer approach for electronic structure calculations of large molecules. *J. Chem. Phys.* **1995**, *103*, 5674–5678.

(278) Kobayashi, M.; Imamura, Y.; Nakai, H. Alternative linear-scaling methodology for the second-order Møller-Plesset perturbation calculation based on the divide-and-conquer method. *J. Chem. Phys.* **2007**, *127*, 074103.

(279) Kobayashi, M.; Nakai, H. Extension of linear-scaling divide-and-conquer-based correlation method to coupled cluster theory with singles and doubles excitations. *J. Chem. Phys.* **2008**, *129*, 044103.

(280) Kobayashi, M.; Nakai, H. Divide-and-conquer-based linear-scaling approach for traditional and renormalized coupled cluster methods with single, double, and noniterative triple excitations. *J. Chem. Phys.* **2009**, *131*, 114108.

(281) Kitaura, K.; Ikeo, E.; Asada, T.; Nakano, T.; Uebayasi, M. Fragment molecular orbital method: an approximate computational method for large molecules. *Chem. Phys. Lett.* **1999**, *313*, 701–706.

(282) Fedorov, D. G.; Kitaura, K. Pair interaction energy decomposition analysis. *Journal of Computational Chemistry* **2007**, *28*, 222–237.

(283) Fedorov, D. G.; Kitaura, K. Extending the Power of Quantum Chemistry to Large Systems with the Fragment Molecular Orbital Method. *The Journal of Physical Chemistry A* **2007**, *111*, 6904–6914.

(284) Fedorov, D. G.; Nagata, T.; Kitaura, K. Exploring chemistry with the fragment molecular orbital method. *Phys. Chem. Chem. Phys.* **2012**, *14*, 7562–7577.

(285) Herbert, J. M.; Jacobson, L. D.; Un Lao, K.; Rohrdanz, M. A. Rapid computation of intermolecular interactions in molecular and ionic clusters: self-consistent polarization plus symmetry-adapted perturbation theory. *Phys. Chem. Chem. Phys.* **2012**, *14*, 7679–7699.

(286) Lao, K. U.; Herbert, J. M. Accurate Intermolecular Interactions at Dramatically Reduced Cost: XPol+SAPT with Empirical Dispersion. *The Journal of Physical Chemistry Letters* **2012**, *3*, 3241–3248.

(287) Mayhall, N. J.; Raghavachari, K. Molecules-in-Molecules: An Extrapolated Fragment-Based Approach for Accurate Calculations on Large Molecules and Materials. *Journal of Chemical Theory and Computation* **2011**, *7*, 1336–1343.

(288) Mo, Y.; Gao, J.; Peyerimhoff, S. D. Energy decomposition analysis of intermolecular interactions using a block-localized wave function approach. *J. Chem. Phys.* **2000**, *112*, 5530–5538.

(289) Mo, Y.; Bao, P.; Gao, J. Energy decomposition analysis based on a block-localized wavefunction and multistate density functional theory. *Phys. Chem. Chem. Phys.* **2011**, *13*, 6760–6775.

(290) Nagata, T.; Takahashi, O.; Saito, K.; Iwata, S. Basis set superposition error free self-consistent field method for molecular interaction in multi-component systems: Projection operator formalism. *J. Chem. Phys.* **2001**, *115*, 3553–3560.

(291) Horn, P. R.; Sundstrom, E. J.; Baker, T. A.; Head-Gordon, M. Unrestricted absolutely localized molecular orbitals for energy decomposition analysis: Theory and applications to intermolecular interactions involving radicals. *J. Chem. Phys.* **2013**, *138*, 134119.

(292) Gianinetti, E.; Raimondi, M.; Tornaghi, E. Modification of the Roothaan equations to exclude BSSE from molecular interaction calculations. *International Journal of Quantum Chemistry* **1996**, *60*, 157–166.

(293) Řezáč, J.; Hobza, P. Describing Noncovalent Interactions beyond the Common Approximations: How Accurate Is the "Gold Standard" CCSD(T) at the Complete Basis Set Limit? *Journal of Chemical Theory and Computation* **2013**, *9*, 2151–2155.

(294) Řezáč, J.; Riley, K. E.; Hobza, P. S66: A Well-balanced Database of Benchmark Interaction Energies Relevant to Biomolecular Structures. *Journal of Chemical Theory and Computation* **2011**, *7*, 2427–2438.

(295) Halgren, T. A. Merck molecular force field. I. Basis, form, scope, parameterization, and performance of MMFF94. *Journal of Computational Chemistry* **1996**, *17*, 490–519.

(296) Jeziorski, B.; Moszynski, R.; Szalewicz, K. Perturbation Theory Approach to Intermolecular Potential Energy Surfaces of van der Waals Complexes. *Chem. Rev.* **1994**, *94*, 1887–1930.

(297) Parker, T. M.; Burns, L. A.; Parrish, R. M.; Ryno, A. G.; Sherrill, C. D. Levels of symmetry adapted perturbation theory (SAPT). I. Efficiency and performance for interaction energies. *J. Chem. Phys.* **2014**, *140*, 094106.

(298) Williams, H. L.; Chabalowski, C. F. Using Kohn-Sham Orbitals in Symmetry-Adapted Perturbation Theory to Investigate Intermolecular Interactions. *The Journal of Physical Chemistry A* **2001**, *105*, 646–659.

(299) Misquitta, A. J.; Szalewicz, K. Intermolecular forces from asymptotically corrected density functional description of monomers. *Chem. Phys. Lett.* **2002**, *357*, 301–306.

(300) Lao, K. U.; Herbert, J. M. An improved treatment of empirical dispersion and a many-body energy decomposition scheme for the explicit polarization plus symmetry-adapted perturbation theory (XSAPT) method. *J. Chem. Phys.* **2013**, *139*, 034107.

(301) Jacobson, L. D.; Herbert, J. M. An efficient, fragment-based electronic structure method for molecular systems: Self-consistent polarization with perturbative two-body exchange and dispersion. *J. Chem. Phys.* **2011**, *134*, 094118.

(302) Williams, H. L.; Szalewicz, K.; Moszynski, R.; Jeziorski, B. Dispersion energy in the coupled pair approximation with noniterative inclusion of single and triple excitations. *J. Chem. Phys.* **1995**, *103*, 4586–4599.

(303) Hohenstein, E. G.; Jaeger, H. M.; Carrell, E. J.; Tschumper, G. S.; Sherrill, C. D. Accurate Interaction Energies for Problematic Dispersion-Bound Complexes: Homogeneous Dimers of NCCN, P_2, and PCCP. *Journal of Chemical Theory and Computation* **2011**, *7*, 2842–2851.

(304) Korona, T.; Jeziorski, B. Dispersion energy from density-fitted density susceptibilities of singles and doubles coupled cluster theory. *J. Chem. Phys.* **2008**, *128*, 144107.

(305) Korona, T. First-order exchange energy of intermolecular interactions from coupled cluster density matrices and their cumulants. *J. Chem. Phys.* **2008**, *128*, 224104.

(306) Korona, T. Second-order exchange-induction energy of intermolecular interactions from coupled cluster density matrices and their cumulants. *Phys. Chem. Chem. Phys.* **2008**, *10*, 6509–6519.

(307) Korona, T. Exchange-Dispersion Energy: A Formulation in Terms of Monomer Properties and Coupled Cluster Treatment of Intramonomer Correlation. *Journal of Chemical Theory and Computation* **2009**, *5*, 2663–2678.

(308) Parrish, R. M.; Hohenstein, E. G.; Sherrill, C. D. Tractability gains in symmetry-adapted perturbation theory including coupled double excitations: CCD+ST(CCD) dispersion with natural orbital truncations. *J. Chem. Phys.* **2013**, *139*, 174102.

(309) Pulay, P. Localizability of dynamic electron correlation. *Chem. Phys. Lett.* **1983**, *100*, 151–154.

(310) Saebø, S.; Pulay, P. Fourth-order Møller-Plesset perturbation theory in the local correlation treatment. I. Method. *J. Chem. Phys.* **1987**, *86*, 914–922.

(311) Saebø, S.; Pulay, P. The local correlation treatment. II. Implementation and tests. *J. Chem. Phys.* **1988**, *88*, 1884–1890.

(312) Maslen, P.; Lee, M.; Head-Gordon, M. An accurate local model for triple substitutions in fourth order Møller-Plesset theory and in perturbative corrections to singles and doubles coupled cluster methods. *Chem. Phys. Lett.* **2000**, *319*, 205–212.

(313) Schútz, M. Low-order scaling local electron correlation methods. III. Linear scaling local perturbative triples correction (T). *J. Chem. Phys.* **2000**, *113*, 9986–10001.

(314) Schútz, M.; Werner, H.-J. Low-order scaling local electron correlation methods. IV. Linear scaling local coupled-cluster (LCCSD). *J. Chem. Phys.* **2001**, *114*, 661–681.

(315) Werner, H.-J.; Schútz, M. An efficient local coupled cluster method for accurate thermochemistry of large systems. *J. Chem. Phys.* **2011**, *135*, 144116.

(316) Doser, B.; Lambrecht, D. S.; Kussmann, J.; Ochsenfeld, C. Linear-scaling atomic orbital-based second-order Møller-Plesset perturbation theory by rigorous integral screening criteria. *J. Chem. Phys.* **2009**, *130*, 064107.

(317) Maurer, S. A.; Lambrecht, D. S.; Kussmann, J.; Ochsenfeld, C. Efficient distance-including integral screening in linear-scaling Møller-Plesset perturbation theory. *J. Chem. Phys.* **2013**, *138*, 014101.

(318) Auer, A. A.; Nooijen, M. Dynamically screened local correlation method using enveloping localized orbitals. *J. Chem. Phys.* **2006**, *125*, 024104.

(319) Subotnik, J. E.; Sodt, A.; Head-Gordon, M. A near linear-scaling smooth local coupled cluster algorithm for electronic structure. *J. Chem. Phys.* **2006**, *125*, 074116.

(320) Subotnik, J. E.; Head-Gordon, M. A local correlation model that yields intrinsically smooth potential-energy surfaces. *J. Chem. Phys.* **2005**, *123*, 064108.

(321) Stanton, J. F.; Gauss, J. Perturbative treatment of the similarity transformed Hamiltonian in equation-of-motion coupled-cluster approximations. *J. Chem. Phys.* **1995**, *103*, 1064–1076.

(322) Stanton, J.; Gauss, J. A simple correction to final state energies of doublet radicals described by equation-of-motion coupled cluster theory in the singles and doubles approximation. *Theoretica Chimica Acta* **1996**, *93*, 303–313.

(323) Crawford, T. D.; Stanton, J. F. Investigation of an asymmetric triple-excitation correction for coupled-cluster energies. *International Journal of Quantum Chemistry* **1998**, *70*, 601–611.

(324) Stanton, J. F. Why CCSD(T) works: a different perspective. *Chem. Phys. Lett.* **1997**, *281*, 130–134.

(325) Adamowicz, L.; Laidig, W. D.; Bartlett, R. J. Analytical gradients for the coupled-cluster method. *International Journal of Quantum Chemistry* **1984**, *26*, 245–254.

(326) Arponen, J. S.; Bishop, R. F.; Pajanne, E. Extended coupled-cluster method. I. Generalized coherent bosonization as a mapping of quantum theory into classical Hamiltonian mechanics. *Phys. Rev. A* **1987**, *36*, 2519–2538.

(327) Koch, H.; Jørgensen, P. Coupled cluster response functions. *J. Chem. Phys.* **1990**, *93*, 3333–3344.

(328) Gwaltney, S. R.; Head-Gordon, M. A second-order perturbative correction to the coupled-cluster singles and doubles method: CCSD(2). *J. Chem. Phys.* **2001**, *115*, 2014–2021.

(329) Hirata, S.; Nooijen, M.; Grabowski, I.; Bartlett, R. J. Perturbative corrections to coupled-cluster and equation-of-motion coupled-cluster energies: A determinantal analysis. *J. Chem. Phys.* **2001**, *114*, 3919–3928.

(330) Hirata, S.; Nooijen, M.; Grabowski, I.; Bartlett, R. J. Erratum: "Perturbative corrections to coupled-cluster and equation-of-motion coupled-cluster energies: A determinantal analysis" [J. Chem. Phys. 114, 3919 (2001)]. *J. Chem. Phys.* **2001**, *115*, 3967–3968.

(331) Hirata, S.; Fan, P.-D.; Auer, A. A.; Nooijen, M.; Piecuch, P. Combined coupled-cluster and many-body perturbation theories. *J. Chem. Phys.* **2004**, *121*, 12197–12207.

(332) Gwaltney, S. R.; Head-Gordon, M. A second-order correction to singles and doubles coupled-cluster methods based on a perturbative expansion of a similarity-transformed Hamiltonian. *Chem. Phys. Lett.* **2000**, *323*, 21–28.

(333) Gwaltney, S. R.; Sherrill, C. D.; Head-Gordon, M.; Krylov, A. I. Second-order perturbation corrections to singles and doubles coupled-cluster methods: General theory and application to the valence optimized doubles model. *J. Chem. Phys.* **2000**, *113*, 3548–3560.

(334) Beran, G. J. O.; Head-Gordon, M.; Gwaltney, S. R. Second-order correction to perfect pairing: An inexpensive electronic structure method for the treatment of strong electron-electron correlations. *J. Chem. Phys.* **2006**, *124*, 114107.

(335) Parkhill, J. A.; Azar, R. J.; Head-Gordon, M. The formulation and performance of a perturbative correction to the perfect quadruples model. *J. Chem. Phys.* **2011**, *134*, 154112.

(336) Stanton, J. F.; Gauss, J. A simple correction to final state energies of doublet radicals described by equation-of-motion coupled cluster theory in the singles and doubles approximation. *Theoretica Chimica Acta* **1996**, *93*, 303–313.

(337) Manohar, P. U.; Krylov, A. I. A noniterative perturbative triples correction for the spin-flipping and spin-conserving equation-of-motion coupled-cluster methods with single and double substitutions. *J. Chem. Phys.* **2008**, *129*, 194105.

(338) Mayhall, N. J.; Goldey, M.; Head-Gordon, M. A Quasidegenerate Second-Order Perturbation Theory Approximation to RAS-nSF for Excited States and Strong Correlations. *Journal of Chemical Theory and Computation* **2014**, *10*, 589–599.

(339) Head-Gordon, M.; Maslen, P. E.; White, C. A. A tensor formulation of many-electron theory in a nonorthogonal single-particle basis. *J. Chem. Phys.* **1998**, *108*, 616–625.

(340) White, C. A.; Maslen, P.; Lee, M. S.; Head-Gordon, M. The tensor properties of energy gradients within a non-orthogonal basis. *Chem. Phys. Lett.* **1997**, *276*, 133–138.

(341) Subotnik, J. E.; Dutoi, A. D.; Head-Gordon, M. Fast localized orthonormal virtual orbitals which depend smoothly on nuclear coordinates. *J. Chem. Phys.* **2005**, *123*, 114108.

(342) Kucharski, S. A.; Bartlett, R. J. An efficient way to include connected quadruple contributions into the coupled cluster method. *J. Chem. Phys.* **1998**, *108*, 9221–9226.